1 Well Testing Analysis

Contents

1.1 Primary Reservoir Characteristics

Flow in porous media is a very complex phenomenon and cannot be described as explicitly as flow through pipes or conduits. It is rather easy to measure the length and diameter of a pipe and compute its flow capacity as a function of pressure; however, in porous media flow is different in that there are no clear-cut flow paths which lend themselves to measurement.

The analysis of fluid flow in porous media has evolved throughout the years along two fronts: the experimental and the analytical. Physicists, engineers, hydrologists, and the like have examined experimentally the behavior of various fluids as they flow through porous media ranging from sand packs to fused Pyrex glass. On the basis of their analyses, they have attempted to formulate laws and correlations that can then be utilized to make analytical predictions for similar systems.

The main objective of this chapter is to present the mathematical relationships that are designed to describe the flow behavior of the reservoir fluids. The mathematical forms of these relationships will vary depending upon the characteristics of the reservoir. These primary reservoir characteristics that must be considered include:

- types of fluids in the reservoir;
- flow regimes;
- reservoir geometry;
- number of flowing fluids in the reservoir.

1.1.1 Types of fluids

The isothermal compressibility coefficient is essentially the controlling factor in identifying the type of the reservoir fluid. In general, reservoir fluids are classified into three groups:

(1) incompressible fluids;
(2) slightly compressible fluids;
(3) compressible fluids.

The isothermal compressibility coefficient c is described mathematically by the following two equivalent expressions:

In terms of fluid volume:

$$c = \frac{-1}{V}\frac{\partial V}{\partial p} \qquad [1.1.1]$$

In terms of fluid density:

$$c = \frac{1}{\rho}\frac{\partial \rho}{\partial p} \qquad [1.1.2]$$

where

V = fluid volume
ρ = fluid density
p = pressure, psi^{-1}
c = isothermal compressibility coefficient, Ψ^{-1}

Incompressible fluids

An incompressible fluid is defined as the fluid whose volume or density does not change with pressure. That is

$$\frac{\partial V}{\partial p} = 0 \quad \text{and} \quad \frac{\partial \rho}{\partial p} = 0$$

Incompressible fluids do not exist; however, this behavior may be assumed in some cases to simplify the derivation and the final form of many flow equations.

Slightly compressible fluids

These "slightly" compressible fluids exhibit small changes in volume, or density, with changes in pressure. Knowing the volume V_{ref} of a slightly compressible liquid at a reference (initial) pressure p_{ref}, the changes in the volumetric behavior of this fluid as a function of pressure p can be mathematically described by integrating Equation 1.1.1, to give:

$$-c\int_{p_{ref}}^{p} dp = \int_{V_{ref}}^{V} \frac{dV}{V}$$

$$\exp\left[c(p_{ref} - p)\right] = \frac{V}{V_{ref}}$$

$$V = V_{ref}\exp\left[c\,(p_{ref} - p)\right] \qquad [1.1.3]$$

where:

p = pressure, psia
V = volume at pressure p, ft^3
p_{ref} = initial (reference) pressure, psia
V_{ref} = fluid volume at initial (reference) pressure, psia

The exponential e^x may be represented by a series expansion as:

$$e^x = 1 + x + \frac{x^2}{2!} + \frac{x^2}{3!} + \cdots + \frac{x^n}{n!} \qquad [1.1.4]$$

Because the exponent x (which represents the term $c\,(p_{ref} - p)$) is very small, the e^x term can be approximated by truncating Equation 1.1.4 to:

$$e^x = 1 + x \qquad [1.1.5]$$

Combining Equation 1.1.5 with 1.1.3 gives:

$$V = V_{ref}[1 + c(p_{ref} - p)] \qquad [1.1.6]$$

A similar derivation is applied to Equation 1.1.2, to give:

$$\rho = \rho_{ref}[1 - c(p_{ref} - p)] \qquad [1.1.7]$$

where:

V = volume at pressure p
ρ = density at pressure p
V_{ref} = volume at initial (reference) pressure p_{ref}
ρ_{ref} = density at initial (reference) pressure p_{ref}

It should be pointed out that crude oil and water systems fit into this category.

Compressible fluids

These are fluids that experience large changes in volume as a function of pressure. All gases are considered compressible fluids. The truncation of the series expansion as given by Equation 1.1.5 is not valid in this category and the complete expansion as given by Equation 1.1.4 is used.

The isothermal compressibility of any compressible fluid is described by the following expression:

$$c_g = \frac{1}{p} - \frac{1}{Z}\left(\frac{\partial Z}{\partial p}\right)_T \qquad [1.1.8]$$

Figures 1.1 and 1.2 show schematic illustrations of the volume and density changes as a function of pressure for the three types of fluids.

1.1.2 Flow regimes

There are basically three types of flow regimes that must be recognized in order to describe the fluid flow behavior and reservoir pressure distribution as a function of time. These three flow regimes are:

(1) steady-state flow;
(2) unsteady-state flow;
(3) pseudosteady-state flow.

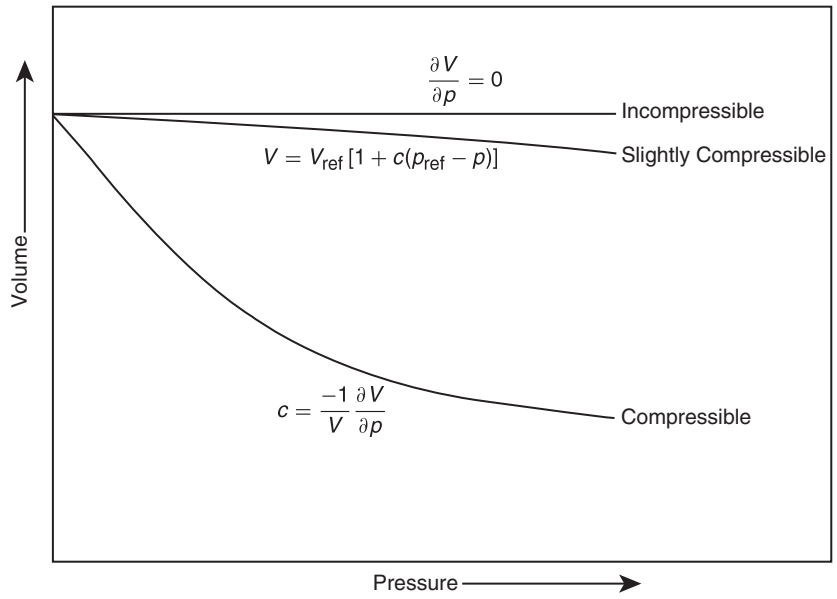

Figure 1.1 *Pressure–volume relationship.*

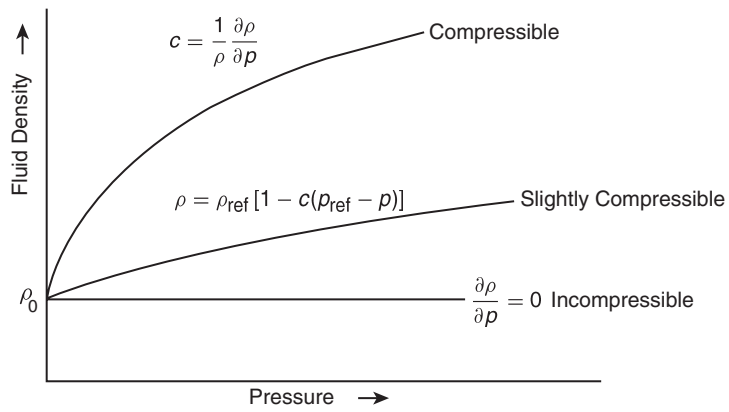

Figure 1.2 *Fluid density versus pressure for different fluid types.*

Steady-state flow

The flow regime is identified as a steady-state flow if the pressure at every location in the reservoir remains constant, i.e., does not change with time. Mathematically, this condition is expressed as:

$$\left(\frac{\partial p}{\partial t}\right)_i = 0 \qquad [1.1.9]$$

This equation states that the rate of change of pressure p with respect to time t at any location i is zero. In reservoirs, the steady-state flow condition can only occur when the reservoir is completely recharged and supported by strong aquifer or pressure maintenance operations.

Unsteady-state flow

Unsteady-state flow (frequently called transient flow) is defined as the fluid flowing condition at which the rate of change of pressure with respect to time at any position in the reservoir is not zero or constant. This definition suggests that the pressure derivative with respect to time is essentially a function of both position i and time t, thus:

$$\left(\frac{\partial p}{\partial t}\right) = f(i,t) \qquad [1.1.10]$$

Pseudosteady-state flow

When the pressure at different locations in the reservoir is declining linearly as a function of time, i.e., at a constant declining rate, the flowing condition is characterized as pseudosteady-state flow. Mathematically, this definition states that the rate of change of pressure with respect to time at every position is constant, or:

$$\left(\frac{\partial p}{\partial t}\right)_i = \text{constant} \qquad [1.1.11]$$

It should be pointed out that pseudosteady-state flow is commonly referred to as semisteady-state flow and quasisteady-state flow.

Figure 1.3 shows a schematic comparison of the pressure declines as a function of time of the three flow regimes.

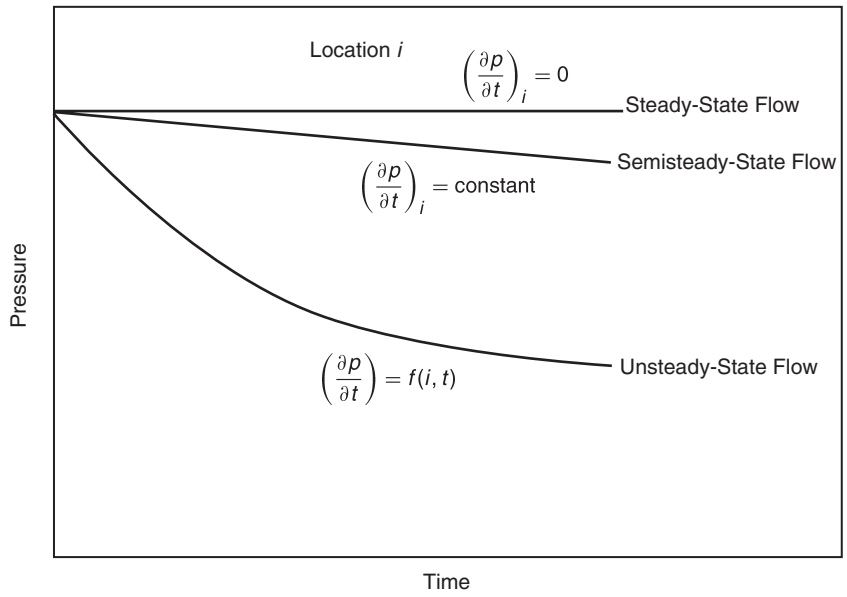

Figure 1.3 *Flow regimes.*

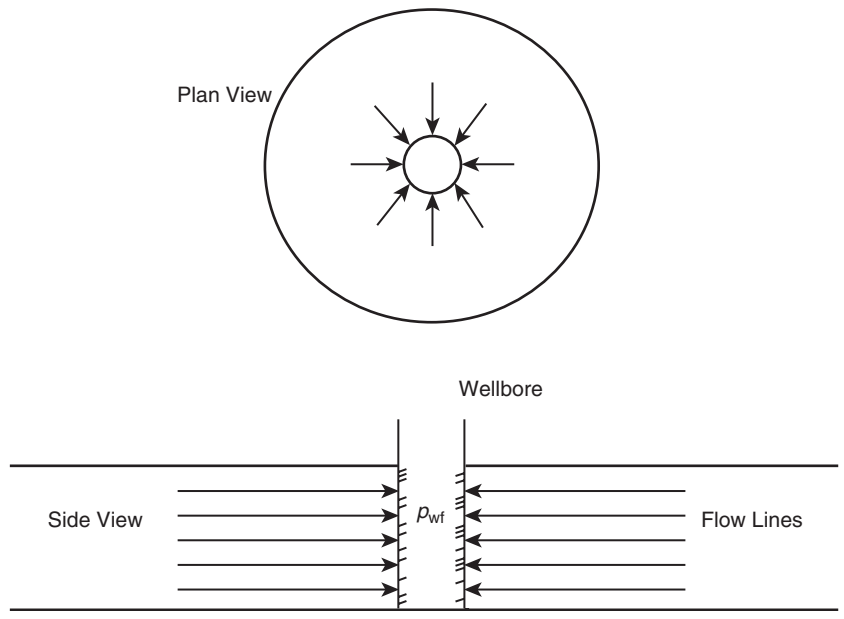

Figure 1.4 *Ideal radial flow into a wellbore.*

1.1.3 Reservoir geometry

The shape of a reservoir has a significant effect on its flow behavior. Most reservoirs have irregular boundaries and a rigorous mathematical description of their geometry is often possible only with the use of numerical simulators. However, for many engineering purposes, the actual flow geometry may be represented by one of the following flow geometries:

- radial flow;
- linear flow;
- spherical and hemispherical flow.

Radial flow

In the absence of severe reservoir heterogeneities, flow into or away from a wellbore will follow radial flow lines a substantial distance from the wellbore. Because fluids move toward the well from all directions and coverage at the wellbore, the term radial flow is used to characterize the flow of fluid into the wellbore. Figure 1.4 shows idealized flow lines and isopotential lines for a radial flow system.

Linear flow

Linear flow occurs when flow paths are parallel and the fluid flows in a single direction. In addition, the cross-sectional

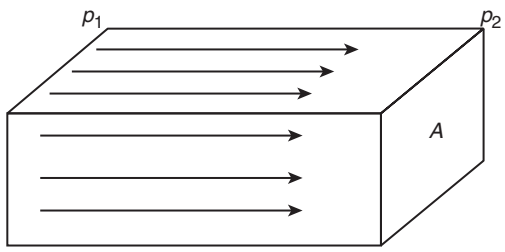

Figure 1.5 *Linear flow.*

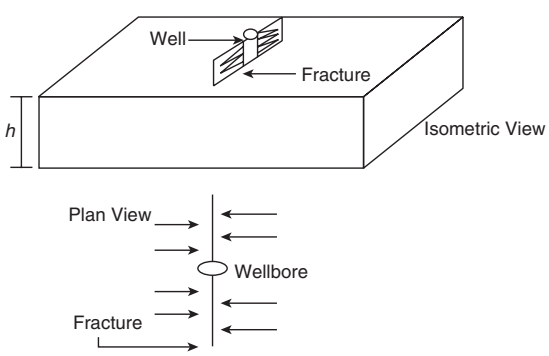

Figure 1.6 *Ideal linear flow into vertical fracture.*

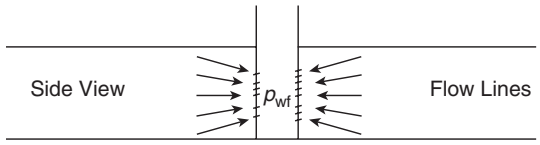

Figure 1.7 *Spherical flow due to limited entry.*

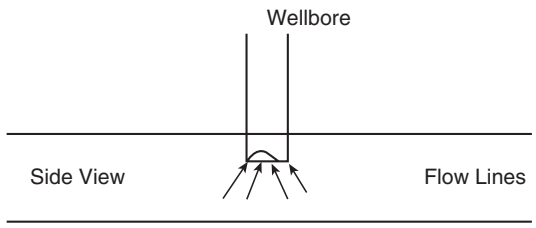

Figure 1.8 *Hemispherical flow in a partially penetrating well.*

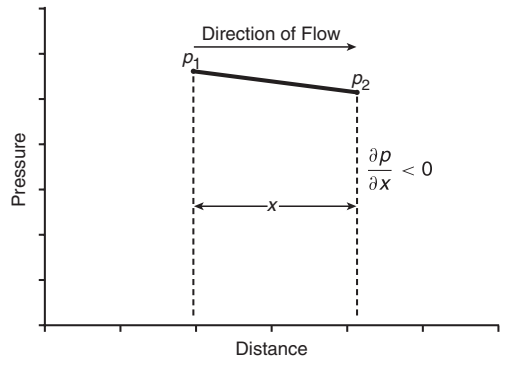

Figure 1.9 *Pressure versus distance in a linear flow.*

area to flow must be constant. Figure 1.5 shows an idealized linear flow system. A common application of linear flow equations is the fluid flow into vertical hydraulic fractures as illustrated in Figure 1.6.

Spherical and hemispherical flow

Depending upon the type of wellbore completion configuration, it is possible to have spherical or hemispherical flow near the wellbore. A well with a limited perforated interval could result in spherical flow in the vicinity of the perforations as illustrated in Figure 1.7. A well which only partially penetrates the pay zone, as shown in Figure 1.8, could result in hemispherical flow. The condition could arise where coning of bottom water is important.

1.1.4 Number of flowing fluids in the reservoir

The mathematical expressions that are used to predict the volumetric performance and pressure behavior of a reservoir vary in form and complexity depending upon the number of mobile fluids in the reservoir. There are generally three cases of flowing system:

(1) single-phase flow (oil, water, or gas);
(2) two-phase flow (oil–water, oil–gas, or gas–water);
(3) three-phase flow (oil, water, and gas).

The description of fluid flow and subsequent analysis of pressure data becomes more difficult as the number of mobile fluids increases.

1.2 Fluid Flow Equations

The fluid flow equations that are used to describe the flow behavior in a reservoir can take many forms depending upon the combination of variables presented previously (i.e., types of flow, types of fluids, etc.). By combining the conservation of mass equation with the transport equation (Darcy's equation) and various equations of state, the necessary flow equations can be developed. Since all flow equations to be considered depend on Darcy's law, it is important to consider this transport relationship first.

1.2.1 Darcy's law

The fundamental law of fluid motion in porous media is Darcy's law. The mathematical expression developed by Darcy in 1956 states that the velocity of a homogeneous fluid in a porous medium is proportional to the pressure gradient, and inversely proportional to the fluid viscosity. For a horizontal linear system, this relationship is:

$$v = \frac{q}{A} = -\frac{k}{\mu}\frac{\mathrm{d}p}{\mathrm{d}x} \qquad [1.2.1a]$$

v is the apparent velocity in centimeters per second and is equal to q/A, where q is the volumetric flow rate in cubic centimeters per second and A is the total cross-sectional area of the rock in square centimeters. In other words, A includes the area of the rock material as well as the area of the pore channels. The fluid viscosity, μ, is expressed in centipoise units, and the pressure gradient, $\mathrm{d}p/\mathrm{d}x$, is in atmospheres per centimeter, taken in the same direction as v and q. The proportionality constant, k, is the permeability of the rock expressed in Darcy units.

The negative sign in Equation 1.2.1a is added because the pressure gradient $\mathrm{d}p/\mathrm{d}x$ is negative in the direction of flow as shown in Figure 1.9.

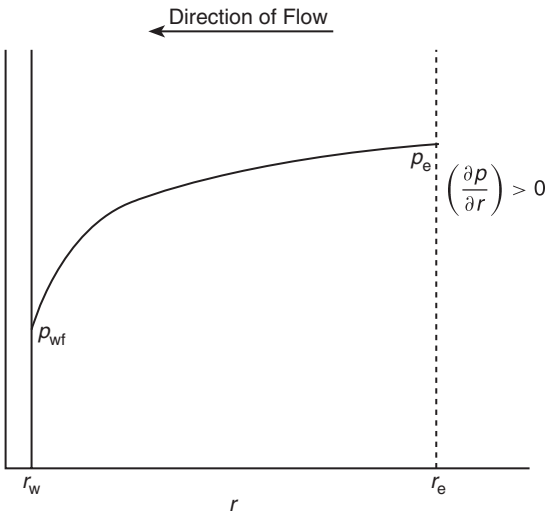

Figure 1.10 *Pressure gradient in radial flow.*

For a horizontal-radial system, the pressure gradient is positive (see Figure 1.10) and Darcy's equation can be expressed in the following generalized radial form:

$$v = \frac{q_r}{A_r} = \frac{k}{\mu}\left(\frac{\partial p}{\partial r}\right)_r \qquad [1.2.1b]$$

where:

q_r = volumetric flow rate at radius r
A_r = cross-sectional area to flow at radius r
$(\partial p/\partial r)_r$ = pressure gradient at radius r
v = apparent velocity at radius r

The cross-sectional area at radius r is essentially the surface area of a cylinder. For a fully penetrated well with a net thickness of h, the cross-sectional area A_r is given by:

$$A_r = 2\pi rh$$

Darcy's law applies only when the following conditions exist:

- laminar (viscous) flow;
- steady-state flow;
- incompressible fluids;
- homogeneous formation.

For turbulent flow, which occurs at higher velocities, the pressure gradient increases at a greater rate than does the flow rate and a special modification of Darcy's equation is needed. When turbulent flow exists, the application of Darcy's equation can result in serious errors. Modifications for turbulent flow will be discussed later in this chapter.

1.2.2 Steady-state flow

As defined previously, steady-state flow represents the condition that exists when the pressure throughout the reservoir does not change with time. The applications of steady-state flow to describe the flow behavior of several types of fluid in different reservoir geometries are presented below. These include:

- linear flow of incompressible fluids;
- linear flow of slightly compressible fluids;
- linear flow of compressible fluids;
- radial flow of incompressible fluids;
- radial flow of slightly compressible fluids;

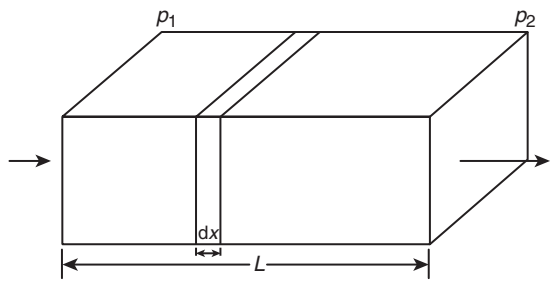

Figure 1.11 *Linear flow model.*

- radial flow of compressible fluids;
- multiphase flow.

Linear flow of incompressible fluids

In a linear system, it is assumed that the flow occurs through a constant cross-sectional area A, where both ends are entirely open to flow. It is also assumed that no flow crosses the sides, top, or bottom as shown in Figure 1.11. If an incompressible fluid is flowing across the element dx, then the fluid velocity v and the flow rate q are constants at all points. The flow behavior in this system can be expressed by the differential form of Darcy's equation, i.e., Equation 1.2.1a. Separating the variables of Equation 1.2.1a and integrating over the length of the linear system:

$$\frac{q}{A}\int_0^L \mathrm{d}x = -\frac{k}{u}\int_{p_1}^{p_2} \mathrm{d}p$$

which results in:

$$q = \frac{kA(p_1 - p_2)}{\mu L}$$

It is desirable to express the above relationship in customary field units, or:

$$q = \frac{0.001127kA(p_1 - p_2)}{\mu L} \qquad [1.2.2]$$

where:

q = flow rate, bbl/day
k = absolute permeability, md
p = pressure, psia
μ = viscosity, cp
L = distance, ft
A = cross-sectional area, ft^2

Example 1.1 An incompressible fluid flows in a linear porous media with the following properties:

$L = 2000$ ft,	$h = 20$ ft,	width = 300 ft
$k = 100$ md,	$\phi = 15\%$,	$\mu = 2$ cp
$p_1 = 2000$ psi,	$p_2 = 1990$ psi	

Calculate:

(a) flow rate in bbl/day;
(b) apparent fluid velocity in ft/day;
(c) actual fluid velocity in ft/day.

Solution Calculate the cross-sectional area A:

$$A = (h)(\text{width}) = (20)(100) = 6000 \text{ ft}^2$$

(a) Calculate the flow rate from Equation 1.2.2:

$$q = \frac{0.001127kA(p_1 - p_2)}{\mu L}$$

$$= \frac{(0.001127)(100)(6000)(2000 - 1990)}{(2)(2000)}$$

$$= 1.6905 \text{ bbl/day}$$

(b) Calculate the apparent velocity:

$$v = \frac{q}{A} = \frac{(1.6905)(5.615)}{6000} = 0.0016 \text{ ft/day}$$

(c) Calculate the actual fluid velocity:

$$v = \frac{q}{\phi A} = \frac{(1.6905)(5.615)}{(0.15)(6000)} = 0.0105 \text{ ft/day}$$

The difference in the pressure (p_1–p_2) in Equation 1.2.2 is not the only driving force in a tilted reservoir. The gravitational force is the other important driving force that must be accounted for to determine the direction and rate of flow. The fluid gradient force (gravitational force) is always directed *vertically downward* while the force that results from an applied pressure drop may be in any direction. The force causing flow would then be the *vector sum of these two*. In practice we obtain this result by introducing a new parameter, called "fluid potential," which has the same dimensions as pressure, e.g., psi. Its symbol is Φ. The fluid potential at any point in the reservoir is defined as the pressure at that point less the pressure that would be exerted by a fluid head extending to an arbitrarily assigned datum level. Letting Δz_i be the vertical distance from a point i in the reservoir to this datum level:

$$\Phi_i = p_i - \left(\frac{\rho}{144}\right)\Delta z_i \qquad [1.2.3]$$

where ρ is the density in lb/ft^3.

Expressing the fluid density in g/cm^3 in Equation 1.2.3 gives:

$$\Phi_i = p_i - 0.433\gamma\Delta z \qquad [1.2.4]$$

where:

Φ_i = fluid potential at point i, psi
p_i = pressure at point i, psi
Δz_i = vertical distance from point i to the selected datum level
ρ = fluid density under reservoir conditions, lb/ft^3
γ = *fluid density* under reservoir conditions, g/cm^3; this is *not* the fluid specific gravity

The datum is usually selected at the gas–oil contact, oil–water contact, or the highest point in formation. In using Equations 1.2.3 or 1.2.4 to calculate the fluid potential Φ_i at location i, the vertical distance z_i is assigned as a positive value when the point i is below the datum level and as a negative value when it is above the datum level. That is:

If point i is above the datum level:

$$\Phi_i = p_i + \left(\frac{\rho}{144}\right)\Delta z_i$$

and equivalently:

$$\Phi_i = p_i + 0.433\gamma\Delta z_i$$

If point i is below the datum level:

$$\Phi_i = p_i - \left(\frac{\rho}{144}\right)\Delta z_i$$

and equivalently:

$$\Phi_i = p_i - 0.433\gamma\Delta z_i$$

Applying the above-generalized concept to Darcy's equation (Equation 1.2.2) gives:

$$q = \frac{0.001127kA(\Phi_1 - \Phi_2)}{\mu L} \qquad [1.2.5]$$

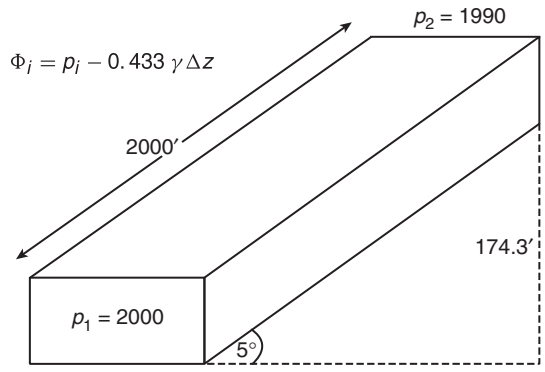

Figure 1.12 *Example of a tilted layer.*

It should be pointed out that the fluid potential drop (Φ_1–Φ_2) is equal to the pressure drop (p_1–p_2) only when the flow system is horizontal.

Example 1.2 Assume that the porous media with the properties as given in the previous example are tilted with a dip angle of 5° as shown in Figure 1.12. The incompressible fluid has a density of 42 lb/ft^3. Resolve Example 1.1 using this additional information.

Solution

Step 1. For the purpose of illustrating the concept of fluid potential, select the datum level at half the vertical distance between the two points, i.e., at 87.15 ft, as shown in Figure 1.12.

Step 2. Calculate the fluid potential at point 1 and 2. Since point 1 is below the datum level, then:

$$\Phi_1 = p_1 - \left(\frac{\rho}{144}\right)\Delta z_1 = 2000 - \left(\frac{42}{144}\right)(87.15)$$

$$= 1974.58 \text{ psi}$$

Since point 2 is above the datum level, then:

$$\Phi_2 = p_2 + \left(\frac{\rho}{144}\right)\Delta z_2 = 1990 + \left(\frac{42}{144}\right)(87.15)$$

$$= 2015.42 \text{ psi}$$

Because $\Phi_2 > \Phi_1$, the fluid flows downward from point 2 to point 1. The difference in the fluid potential is:

$$\Delta\Phi = 2015.42 - 1974.58 = 40.84 \text{ psi}$$

Notice that, if we select point 2 for the datum level, then:

$$\Phi_1 = 2000 - \left(\frac{42}{144}\right)(174.3) = 1949.16 \text{ psi}$$

$$\Phi_2 = 1990 + \left(\frac{42}{144}\right)(0) = 1990 \text{ psi}$$

The above calculations indicate that regardless of the position of the datum level, the flow is downward from point 2 to 1 with:

$$\Delta\Phi = 1990 - 1949.16 = 40.84 \text{ psi}$$

Step 3. Calculate the flow rate:

$$q = \frac{0.001127kA(\Phi_1 - \Phi_2)}{\mu L}$$

$$= \frac{(0.001127)(100)(6000)(40.84)}{(2)(2000)} = 6.9 \text{ bbl/day}$$

Step 4. Calculate the velocity:

$$\text{Apparent velocity} = \frac{(6.9)(5.615)}{6000} = 0.0065 \text{ ft/day}$$

$$\text{Actual velocity} = \frac{(6.9)(5.615)}{(0.15)(6000)} = 0.043 \text{ ft/day}$$

Linear flow of slightly compressible fluids

Equation 1.1.6 describes the relationship that exists between pressure and volume for a slightly compressible fluid, or:

$$V = V_{\text{ref}}[1 + c(p_{\text{ref}} - p)]$$

This equation can be modified and written in terms of flow rate as:

$$q = q_{\text{ref}}\,[1 + c(p_{\text{ref}} - p)] \qquad [1.2.6]$$

where q_{ref} is the flow rate at some reference pressure p_{ref}. Substituting the above relationship in Darcy's equation gives:

$$\frac{q}{A} = \frac{q_{\text{ref}}\,[1 + c(p_{\text{ref}} - p)]}{A} = -0.001127\frac{k}{\mu}\frac{\mathrm{d}p}{\mathrm{d}x}$$

Separating the variables and arranging:

$$\frac{q_{\text{ref}}}{A}\int_0^L \mathrm{d}x = -0.001127\frac{k}{\mu}\int_{p_1}^{p_2}\left[\frac{\mathrm{d}p}{1 + c(p_{\text{ref}} - p)}\right]$$

Integrating gives:

$$q_{\text{ref}} = \left[\frac{0.001127kA}{\mu cL}\right]\ln\left[\frac{1 + c(p_{\text{ref}} - p_2)}{1 + c(p_{\text{ref}} - p_1)}\right] \qquad [1.2.7]$$

where:

q_{ref} = flow rate at a reference pressure p_{ref}, bbl/day
p_1 = upstream pressure, psi
p_2 = downstream pressure, psi
k = permeability, md
μ = viscosity, cp
c = average liquid compressibility, psi^{-1}

Selecting the upstream pressure p_1 as the reference pressure p_{ref} and substituting in Equation 1.2.7 gives the flow rate at point 1 as:

$$q_1 = \left[\frac{0.001127kA}{\mu cL}\right]\ln\left[1 + c(p_1 - p_2)\right] \qquad [1.2.8]$$

Choosing the downstream pressure p_2 as the reference pressure and substituting in Equation 1.2.7 gives:

$$q_2 = \left[\frac{0.001127kA}{\mu cL}\right]\ln\left[\frac{1}{1 + c(p_2 - p_1)}\right] \qquad [1.2.9]$$

where q_1 and q_2 are the flow rates at point 1 and 2, respectively.

Example 1.3 Consider the linear system given in Example 1.1 and, assuming a slightly compressible liquid, calculate the flow rate at both ends of the linear system. The liquid has an average compressibility of 21×10^{-5} psi^{-1}.

Solution Choosing the upstream pressure as the reference pressure gives:

$$q_1 = \left[\frac{0.001127kA}{\mu cL}\right]\ln\left[1 + c(p_1 - p_2)\right]$$

$$= \left[\frac{(0.001127)(100)(6000)}{(2)(21 \times 10^{-5})(2000)}\right]$$

$$\times \ln\left[1 + 21 \times 10^{-5}(2000 - 1990)\right] = 1.689 \text{ bbl/day}$$

Choosing the downstream pressure gives

$$q_2 = \left[\frac{0.001127kA}{\mu cL}\right]\ln\left[\frac{1}{1 + c(p_2 - p_1)}\right]$$

$$= \left[\frac{(0.001127)(100)(6000)}{(2)(21 \times 10^{-5})(2000)}\right]$$

$$\times \ln\left[\frac{1}{1 + (21 \times 10^{-5})(1990 - 2000)}\right] = 1.692 \text{ bbl/day}$$

The above calculations show that q_1 and q_2 are not largely different, which is due to the fact that the liquid is slightly incompressible and its volume is not a strong function of pressure.

Linear flow of compressible fluids (gases)

For a viscous (laminar) gas flow in a homogeneous linear system, the real-gas equation of state can be applied to calculate the number of gas moles n at the pressure p, temperature T, and volume V:

$$n = \frac{pV}{ZRT}$$

At standard conditions, the volume occupied by the above n moles is given by:

$$V_{\text{sc}} = \frac{nZ_{\text{sc}}RT_{\text{sc}}}{p_{\text{sc}}}$$

Combining the above two expressions and assuming $Z_{\text{sc}} = 1$ gives:

$$\frac{pV}{ZT} = \frac{p_{\text{sc}}V_{\text{sc}}}{T_{\text{sc}}}$$

Equivalently, the above relation can be expressed in terms of the reservoir condition flow rate q, in bbl/day, and surface condition flow rate Q_{sc}, in scf/day, as:

$$\frac{p(5.615q)}{ZT} = \frac{p_{\text{sc}}Q_{\text{sc}}}{T_{\text{sc}}}$$

Rearranging:

$$\left(\frac{p_{\text{sc}}}{T_{\text{sc}}}\right)\left(\frac{ZT}{p}\right)\left(\frac{Q_{\text{sc}}}{5.615}\right) = q \qquad [1.2.10]$$

where:

q = gas flow rate at pressure p in bbl/day
Q_{sc} = gas flow rate at standard conditions, scf/day
Z = gas compressibility factor
$T_{\text{sc}}, p_{\text{sc}}$ = standard temperature and pressure in °R and psia, respectively.

Dividing both sides of the above equation by the cross-sectional area A and equating it with that of Darcy's law, i.e., Equation 1.2.1a, gives:

$$\frac{q}{A} = \left(\frac{p_{\text{sc}}}{T_{\text{sc}}}\right)\left(\frac{ZT}{p}\right)\left(\frac{Q_{\text{sc}}}{5.615}\right)\left(\frac{1}{A}\right) = -0.001127\frac{k}{\mu}\frac{\mathrm{d}p}{\mathrm{d}x}$$

The constant 0.001127 is to convert Darcy's units to field units. Separating variables and arranging yields:

$$\left[\frac{Q_{\text{sc}}p_{\text{sc}}T}{0.006328kT_{\text{sc}}A}\right]\int_0^L \mathrm{d}x = -\int_{p_1}^{p_2}\frac{p}{Z\mu_g}\mathrm{d}p$$

Assuming that the product of $Z\mu_g$ is constant over the specified pressure range between p_1 and p_2, and integrating, gives:

$$\left[\frac{Q_{\text{sc}}p_{\text{sc}}T}{0.006328kT_{\text{sc}}A}\right]\int_0^L \mathrm{d}x = -\frac{1}{Z\mu_g}\int_{p_1}^{p_2} p\,\mathrm{d}p$$

or:

$$Q_{sc} = \frac{0.003164 T_{sc} A k \left(p_1^2 - p_2^2\right)}{p_{sc} T (Z \mu_g) L}$$

where:

Q_{sc} = gas flow rate at standard conditions, scf/day
k = permeability, md
T = temperature, °R
μ_g = gas viscosity, cp
A = cross-sectional area, ft^2
L = total length of the linear system, ft

Setting $p_{sc} = 14.7$ psi and $T_{sc} = 520$°R in the above expression gives:

$$Q_{sc} = \frac{0.111924 A k (p_1^2 - p_2^2)}{TLZ\mu_g} \qquad [1.2.11]$$

It is essential to notice that those gas properties Z and μ_g are very strong functions of pressure, but they have been removed from the integral to simplify the final form of the gas flow equation. The above equation is valid for applications when the pressure is less than 2000 psi. The gas properties must be evaluated at the average pressure $\bar{p}$ as defined below:

$$\bar{p} = \sqrt{\frac{p_1^2 + p_2^2}{2}} \qquad [1.2.12]$$

Example 1.4 A natural gas with a specific gravity of 0.72 is flowing in linear porous media at 140°F. The upstream and downstream pressures are 2100 psi and 1894.73 psi, respectively. The cross-sectional area is constant at 4500 ft^2. The total length is 2500 ft with an absolute permeability of 60 md. Calculate the gas flow rate in scf/day ($p_{sc} = 14.7$ psia, $T_{sc} = 520$°R).

Solution

Step 1. Calculate average pressure by using Equation 1.2.12:

$$\bar{p} = \sqrt{\frac{2100^2 + 1894.73^2}{2}} = 2000 \text{ psi}$$

Step 2. Using the specific gravity of the gas, calculate its pseudo-critical properties by applying the following equations:

$$T_{pc} = 168 + 325\gamma_g - 12.5\gamma_g^2$$
$$= 168 + 325(0.72) - 12.5(0.72)^2 = 395.5°\text{R}$$
$$p_{pc} = 677 + 15.0\gamma_g - 37.5\gamma_g^2$$
$$= 677 + 15.0(0.72) - 37.5(0.72)^2 = 668.4 \text{ psia}$$

Step 3. Calculate the pseudo-reduced pressure and temperature:

$$p_{pr} = \frac{2000}{668.4} = 2.99$$
$$T_{pr} = \frac{600}{395.5} = 1.52$$

Step 4. Determine the Z-factor from a Standing–Katz chart to give:

$$Z = 0.78$$

Step 5. Solve for the viscosity of the gas by applying the Lee–Gonzales–Eakin method and using the following sequence of calculations:

$$M_a = 28.96\gamma_g$$
$$= 28.96(0.72) = 20.85$$
$$\rho_g = \frac{pM_a}{ZRT}$$
$$= \frac{(2000)(20.85)}{(0.78)(10.73)(600)} = 8.30 \text{ lb/ft}^3$$
$$K = \frac{(9.4 + 0.02M_a)T^{1.5}}{209 + 19M_a + T}$$
$$= \frac{\left[9.4 + 0.02(20.96)\right](600)^{1.5}}{209 + 19(20.96) + 600} = 119.72$$
$$X = 3.5 + \frac{986}{T} + 0.01M_a$$
$$= 3.5 + \frac{986}{600} + 0.01(20.85) = 5.35$$
$$Y = 2.4 - 0.2X$$
$$= 2.4 - (0.2)(5.35) = 1.33$$
$$\mu_g = 10^{-4} K \exp\left[X(\rho_g/62.4)^Y\right] = 0.0173 \text{ cp}$$
$$= 10^{-4}\left(119.72 \exp\left[5.35\left(\frac{8.3}{62.4}\right)^{1.33}\right]\right)$$
$$= 0.0173$$

Step 6. Calculate the gas flow rate by applying Equation 1.2.11:

$$Q_{sc} = \frac{0.111924 A k (p_1^2 - p_2^2)}{TLZ\mu_g}$$
$$= \frac{(0.111924)(4500)(60)(2100^2 - 1894.73^2)}{(600)(2500)(0.78)(0.0173)}$$
$$= 1\,224\,242 \text{ scf/day}$$

Radial flow of incompressible fluids

In a radial flow system, all fluids move toward the producing well from all directions. However, before flow can take place, a pressure differential must exist. Thus, if a well is to produce oil, which implies a flow of fluids through the formation to the wellbore, the pressure in the formation at the wellbore must be less than the pressure in the formation at some distance from the well.

The pressure in the formation at the wellbore of a producing well is known as the bottom-hole flowing pressure (flowing BHP, p_{wf}).

Consider Figure 1.13 which schematically illustrates the radial flow of an incompressible fluid toward a vertical well. The formation is considered to have a uniform thickness h and a constant permeability k. Because the fluid is incompressible, the flow rate q must be constant at all radii. Due to the steady-state flowing condition, the pressure profile around the wellbore is maintained constant with time.

Let p_{wf} represent the maintained bottom-hole flowing pressure at the wellbore radius r_w and p_e denotes the external pressure at the external or drainage radius. Darcy's generalized equation as described by Equation 1.2.1b can be used to determine the flow rate at any radius r:

$$v = \frac{q}{A_r} = 0.001127 \frac{k}{\mu} \frac{dp}{dr} \qquad [1.2.13]$$

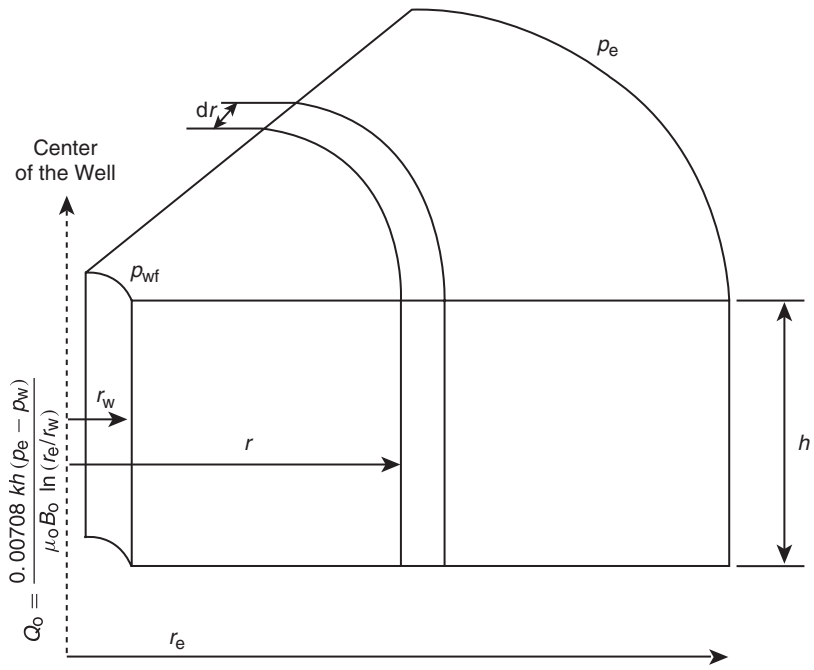

Figure 1.13 *Radial flow model.*

where:

v = apparent fluid velocity, bbl/day-ft^2
q = flow rate at radius r, bbl/day
k = permeability, md
μ = viscosity, cp
0.001127 = conversion factor to express the equation in field units
A_r = cross-sectional area at radius r

The minus sign is no longer required for the radial system shown in Figure 1.13 as the radius increases in the same direction as the pressure. In other words, as the radius increases going away from the wellbore the pressure also increases. At any point in the reservoir the cross-sectional area across which flow occurs will be the surface area of a cylinder, which is $2\pi rh$, or:

$$v = \frac{q}{A_r} = \frac{q}{2\pi rh} = 0.001127\frac{k}{\mu}\frac{dp}{dr}$$

The flow rate for a crude oil system is customarily expressed in surface units, i.e., stock-tank barrels (STB), rather than reservoir units. Using the symbol Q_o to represent the oil flow as expressed in STB/day, then:

$$q = B_o Q_o$$

where B_o is the oil formation volume factor in bbl/STB. The flow rate in Darcy's equation can be expressed in STB/day, to give:

$$\frac{Q_o B_o}{2\pi rh} = 0.001127\frac{k}{\mu_o}\frac{dp}{dr}$$

Integrating this equation between two radii, r_1 and r_2, when the pressures are p_1 and p_2, yields:

$$\int_{r_1}^{r_2}\left(\frac{Q_o}{2\pi h}\right)\frac{dr}{r} = 0.001127\int_{P_1}^{P_2}\left(\frac{k}{\mu_o B_o}\right)dp \qquad [1.2.14]$$

For an incompressible system in a uniform formation, Equation 1.2.14 can be simplified to:

$$\frac{Q_o}{2\pi h}\int_{r_1}^{r_2}\frac{dr}{r} = \frac{0.001127k}{\mu_o B_o}\int_{P_1}^{P_2}dp$$

Performing the integration gives:

$$Q_o = \frac{0.00708kh(p_2 - p_1)}{\mu_o B_o \ln(r_2/r_1)}$$

Frequently the two radii of interest are the wellbore radius r_w and the external or drainage radius r_e. Then:

$$Q_o = \frac{0.00708kh(p_e - p_w)}{\mu_o B_o \ln(r_e/r_w)} \qquad [1.2.15]$$

where:

Q_o = oil flow rate, STB/day
p_e = external pressure, psi
p_{wf} = bottom-hole flowing pressure, psi
k = permeability, md
μ_o = oil viscosity, cp
B_o = oil formation volume factor, bbl/STB
h = thickness, ft
r_e = external or drainage radius, ft
r_w = wellbore radius, ft

The external (drainage) radius r_e is usually determined from the well spacing by equating the area of the well spacing with that of a circle. That is:

$$\pi r_e^2 = 43\,560A$$

or:

$$r_e = \sqrt{\frac{43\,560A}{\pi}} \qquad [1.2.16]$$

where A is the well spacing in acres.

In practice, neither the external radius nor the wellbore radius is generally known with precision. Fortunately, they enter the equation as a logarithm, so the error in the equation will be less than the errors in the radii.

Equation 1.2.15 can be arranged to solve for the pressure p at any radius r, to give:

$$p = p_{wf} + \left[\frac{Q_o B_o \mu_o}{0.00708kh}\right] \ln\left(\frac{r}{r_w}\right) \qquad [1.2.17]$$

Example 1.5 An oil well in the Nameless Field is producing at a stabilized rate of 600 STB/day at a stabilized bottom-hole flowing pressure of 1800 psi. Analysis of the pressure buildup test data indicates that the pay zone is characterized by a permeability of 120 md and a uniform thickness of 25 ft. The well drains an area of approximately 40 acres. The following additional data is available:

$r_w = 0.25$ ft, $A = 40$ acres

$B_o = 1.25$ bbl/STB, $\mu_o = 2.5$ cp

Calculate the pressure profile (distribution) and list the pressure drop across 1 ft intervals from r_w to 1.25 ft, 4 to 5 ft, 19 to 20 ft, 99 to 100 ft, and 744 to 745 ft.

Solution

Step 1. Rearrange Equation 1.2.15 and solve for the pressure p at radius r:

$$p = p_{wf} + \left[\frac{\mu_o B_o Q_o}{0.00708kh}\right] \ln\left(\frac{r}{r_w}\right)$$

$$= 1800 + \left[\frac{(2.5)(1.25)(600)}{(0.00708)(120)(25)}\right] \ln\left(\frac{r}{0.25}\right)$$

$$= 1800 + 88.28 \ln\left(\frac{r}{0.25}\right)$$

Step 2. Calculate the pressure at the designated radii:

r (ft)	p (psi)	*Radius interval*	*Pressure drop*
0.25	1800		
1.25	1942	0.25–1.25	1942−1800 = 142 psi
4	2045		
5	2064	4–5	2064−2045 = 19 psi
19	2182		
20	2186	19–20	2186−2182 = 4 psi
99	2328		
100	2329	99–100	2329−2328 = 1 psi
744	2506.1		
745	2506.2	744–745	2506.2−2506.1 = 0.1 psi

Figure 1.14 shows the pressure profile as a function of radius for the calculated data.

Results of the above example reveal that the pressure drop just around the wellbore (i.e., 142 psi) is 7.5 times greater than at the 4 to 5 interval, 36 times greater than at 19–20 ft, and 142 times than that at the 99–100 ft interval. The reason for this large pressure drop around the wellbore is that the fluid flows in from a large drainage area of 40 acres.

The external pressure p_e used in Equation 1.2.15 cannot be measured readily, but p_e does not deviate substantially from the initial reservoir pressure if a strong and active aquifer is present.

Several authors have suggested that the average reservoir pressure p_r, which often is reported in well test results, should be used in performing material balance calculations and flow rate prediction. Craft and Hawkins (1959) showed that the average pressure is located at about 61% of the drainage radius r_e *for a steady-state flow condition.*

Substituting $0.61r_e$ in Equation 1.2.17 gives:

$$p\,(\text{at } r = 0.61r_e) = p_r = p_{wf} + \left[\frac{Q_o B_o \mu_o}{0.00708kh}\right] \ln\left(\frac{0.61r_e}{r_w}\right)$$

or in terms of flow rate:

$$Q_o = \frac{0.00708kh(p_r - p_{wf})}{\mu_o B_o \ln(0.61r_e/r_w)} \qquad [1.2.18]$$

But since $\ln(0.61r_e/r_w) = \ln(r_e/r_w) - 0.5$, then:

$$Q_o = \frac{0.00708kh(p_r - p_{wf})}{\mu_o B_o \left[\ln(r_e/r_w) - 0.5\right]} \qquad [1.2.19]$$

Golan and Whitson (1986) suggested a method for approximating the drainage area of wells producing from a common reservoir. These authors assume that the volume drained by a single well is proportional to its rate of flow. Assuming constant reservoir properties and a uniform thickness, the approximate drainage area of a single well A_w is:

$$A_w = A_T\left(\frac{q_w}{q_T}\right) \qquad [1.2.20]$$

where:

A_w = drainage area of a well
A_T = total area of the field
q_T = total flow rate of the field
q_w = well flow rate

Radial flow of slightly compressible fluids

Terry and co-authors (1991) used Equation 1.2.6 to express the dependency of the flow rate on pressure for slightly compressible fluids. If this equation is substituted into the radial form of Darcy's law, the following is obtained:

$$\frac{q}{A_r} = \frac{q_{ref}\left[1 + c(p_{ref} - p)\right]}{2\pi rh} = 0.001127\frac{k}{\mu}\frac{dp}{dr}$$

where q_{ref} is the flow rate at some reference pressure p_{ref}.

Separating the variables and assuming a constant compressibility over the entire pressure drop, and integrating over the length of the porous medium:

$$\frac{q_{ref}\mu}{2\pi kh}\int_{r_w}^{r_e}\frac{dr}{r} = 0.001127\int_{p_{wf}}^{p_e}\frac{dp}{1 + c(p_{ref} - p)}$$

gives:

$$q_{ref} = \left[\frac{0.00708kh}{\mu c \ln(r_e/r_w)}\right] \ln\left[\frac{1 + c(p_e - p_{ref})}{1 + c(p_{wf} - p_{ref})}\right]$$

where q_{ref} is the oil flow rate at a reference pressure p_{ref}. Choosing the bottom-hole flow pressure p_{wf} as the reference pressure and expressing the flow rate in STB/day gives:

$$Q_o = \left[\frac{0.00708kh}{\mu_o B_o c_o \ln(r_e/r_w)}\right] \ln\left[1 + c_o(p_e - p_{wf})\right] \qquad [1.2.21]$$

where:

c_o = isothermal compressibility coefficient, psi^{-1}
Q_o = oil flow rate, STB/day
k = permeability, md

Example 1.6 The following data is available on a well in the Red River Field:

$p_e = 2506$ psi, $p_{wf} = 1800$ psi

$r_e = 745$ ft, $r_w = 0.25$ ft

$B_o = 1.25$ bbl/STB, $\mu_o = 2.5$ cp

$k = 0.12$ darcy, $h = 25$ ft

$c_o = 25 \times 10^{-6}$ psi^{-1}

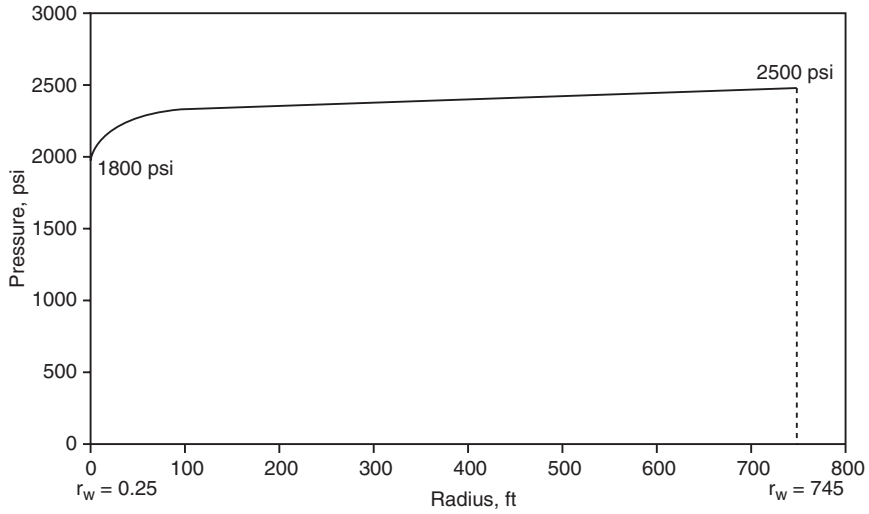

Figure 1.14 *Pressure profile around the wellbore.*

Assuming a slightly compressible fluid, calculate the oil flow rate. Compare the result with that of an incompressible fluid.

Solution For a slightly compressible fluid, the oil flow rate can be calculated by applying Equation 1.2.21:

$$Q_o = \left[\frac{0.00708kh}{\mu_o B_o c_o \ln(r_e/r_w)}\right] \ln[1 + c_o(p_e - p_{wf})]$$

$$= \left[\frac{(0.00708)\,(120)\,(25)}{(2.5)\,(1.25)\,(25 \times 10^{-6}) \ln(745/0.25)}\right]$$

$$\times \ln\left[1 + (25 \times 10^{-6})\,(2506 - 1800)\right] = 595 \text{ STB/day}$$

Assuming an incompressible fluid, the flow rate can be estimated by applying Darcy's equation, i.e., Equation 1.2.15:

$$Q_o = \frac{0.00708kh(p_e - p_w)}{\mu_o B_o \ln(r_e/r_w)}$$

$$= \frac{(0.00708)\,(120)\,(25)\,(2506 - 1800)}{(2.5)\,(1.25)\ln(745/0.25)} = 600 \text{ STB/day}$$

Radial flow of compressible gases

The basic differential form of Darcy's law for a horizontal laminar flow is valid for describing the flow of both gas and liquid systems. For a radial gas flow, Darcy's equation takes the form:

$$q_{gr} = \frac{0.001127(2\pi rh)k}{\mu_g}\frac{dp}{dr} \qquad [1.2.22]$$

where:

q_{gr} = gas flow rate at radius r, bbl/day
r = radial distance, ft
h = zone thickness, ft
μ_g = gas viscosity, cp
p = pressure, psi
0.001127 = conversion constant from Darcy units to field units

The gas flow rate is traditionally expressed in scf/day. Referring to the gas flow rate at standard (surface) condition as Q_g, the gas flow rate q_{gr} under wellbore flowing condition can be converted to that of surface condition by applying the definition of the gas formation volume factor B_g to q_{gr} as:

$$Q_g = \frac{q_{gr}}{B_g}$$

where:

$$B_g = \frac{p_{sc}}{5.615T_{sc}}\frac{ZT}{p} \text{ bbl/scf}$$

or:

$$\left(\frac{p_{sc}}{5.615T_{sc}}\right)\left(\frac{ZT}{p}\right)Q_g = q_{gr} \qquad [1.2.23]$$

where:

p_{sc} = standard pressure, psia
T_{sc} = standard temperature, °R
Q_g = gas flow rate, scf/day
q_{gr} = gas flow rate at radius r, bbl/day
p = pressure at radius r, psia
T = reservoir temperature, °R
Z = gas compressibility factor at p and T
Z_{sc} = gas compressibility factor at standard condition $\cong$ 1.0

Combining Equations 1.2.22 and 1.2.23 yields:

$$\left(\frac{p_{sc}}{5.615T_{sc}}\right)\left(\frac{ZT}{p}\right)Q_g = \frac{0.001127\,(2\pi rh)\,k}{\mu_g}\frac{dp}{dr}$$

Assuming that $T_{sc} = 520$°R and $p_{sc} = 14.7$ psia:

$$\left(\frac{TQ_g}{kh}\right)\frac{dr}{r} = 0.703\left(\frac{2p}{\mu_g Z}\right)dp \qquad [1.2.24]$$

Integrating Equation 1.2.24 from the wellbore conditions (r_w and p_{wf}) to any point in the reservoir (r and p) gives:

$$\int_{r_w}^{r}\left(\frac{TQ_g}{kh}\right)\frac{dr}{r} = 0.703\int_{p_{wf}}^{p}\left(\frac{2p}{\mu_g Z}\right)dp \qquad [1.2.25]$$

Imposing Darcy's law conditions on Equation 1.2.25, i.e., steady-state flow, which requires that Q_g is constant at all radii, and homogeneous formation, which implies that k and h are constant, gives:

$$\left(\frac{TQ_g}{kh}\right)\ln\left(\frac{r}{r_w}\right) = 0.703\int_{p_{wf}}^{p}\left(\frac{2p}{\mu_g Z}\right)dp$$

The term:

$$\int_{p_{wf}}^{p}\left(\frac{2p}{\mu_g z}\right)dp$$

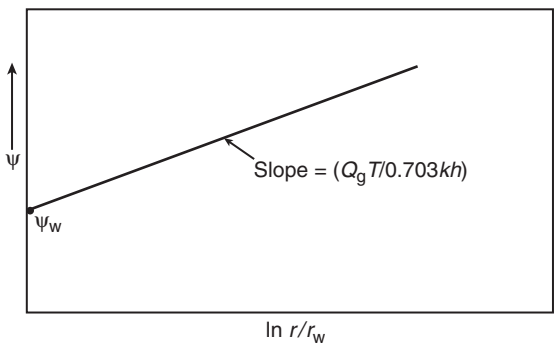

Figure 1.15 *Graph of ψ vs. $\ln(r/r_w)$.*

can be expanded to give:

$$\int_{p_{wf}}^{p}\left(\frac{2p}{\mu_g Z}\right)dp=\int_{0}^{p}\left(\frac{2p}{\mu_g Z}\right)dp-\int_{0}^{p_{wf}}\left(\frac{2p}{\mu_g Z}\right)dp$$

Replacing the integral in Equation 1.2.24 with the above expanded form yields:

$$\left(\frac{TQ_g}{kh}\right)\ln\left(\frac{r}{r_w}\right)=0.703\left[\int_{0}^{p}\left(\frac{2p}{\mu_g Z}\right)dp-\int_{0}^{p_{wf}}\left(\frac{2p}{\mu_g Z}\right)dp\right] \quad [1.2.26]$$

The integral $\int_o^p 2p/(\mu_g Z)dp$ is called the "real-gas pseudopotential" or "real-gas pseudopressure" and it is usually represented by $m(p)$ or ψ. Thus:

$$m(p)=\psi=\int_{0}^{p}\left(\frac{2p}{\mu_g Z}\right)dp \quad [1.2.27]$$

Equation 1.2.27 can be written in terms of the real-gas pseudopressure as:

$$\left(\frac{TQ_g}{kh}\right)\ln\left(\frac{r}{r_w}\right)=0.703(\psi-\psi_w)$$

or:

$$\psi=\psi_w+\frac{Q_g T}{0.703kh}\ln\left(\frac{r}{r_w}\right) \quad [1.2.28]$$

Equation 1.2.28 indicates that a graph of ψ vs. $\ln(r/r_w)$ yields a straight line with a slope of $Q_g T/0.703kh$ and an intercept value of ψ_w as shown in Figure 1.15. The exact flow rate is then given by:

$$Q_g=\frac{0.703kh(\psi-\psi_w)}{T\ln(r/r_w)} \quad [1.2.29]$$

In the particular case when $r=r_e$, then:

$$Q_g=\frac{0.703kh\,(\psi_e-\psi_w)}{T\ln(r_e/r_w)} \quad [1.2.30]$$

where:

ψ_e = real-gas pseudopressure as evaluated from 0 to p_e, psi^2/cp
ψ_w = real-gas pseudopressure as evaluated from 0 to p_{wf}, psi^2/cp
k = permeability, md
h = thickness, ft
r_e = drainage radius, ft
r_w = wellbore radius, ft
Q_g = gas flow rate, scf/day

Because the gas flow rate is commonly expressed in Mscf/day, Equation 1.2.30 can be expressed as:

$$Q_g=\frac{kh(\psi_e-\psi_w)}{1422T\ln(r_e/r_w)} \quad [1.2.31]$$

where:

Q_g = gas flow rate, Mscf/day

Equation 1.2.31 can be expressed in terms of the average reservoir pressure p_r instead of the initial reservoir pressure p_e as:

$$Q_g=\frac{kh(\psi_r-\psi_w)}{1422T\left[\ln(r_e/r_w)-0.5\right]} \quad [1.2.32]$$

To calculate the integral in Equation 1.2.31, the values of $2p/\mu_g Z$ are calculated for several values of pressure p. Then $2p/\mu_g Z$ vs. p is plotted on a Cartesian scale and the area under the curve is calculated either numerically or graphically, where the area under the curve from $p=0$ to any pressure p represents the value of ψ corresponding to p. The following example will illustrate the procedure.

Example 1.7 The *PVT* data from a gas well in the Anaconda Gas Field is given below:

p (psi)	μ_g (cp)	Z
0	0.0127	1.000
400	0.01286	0.937
800	0.01390	0.882
1200	0.01530	0.832
1600	0.01680	0.794
2000	0.01840	0.770
2400	0.02010	0.763
2800	0.02170	0.775
3200	0.02340	0.797
3600	0.02500	0.827
4000	0.02660	0.860
4400	0.02831	0.896

The well is producing at a stabilized bottom-hole flowing pressure of 3600 psi. The wellbore radius is 0.3 ft. The following additional data is available:

$k=65$ md, $h=15$ ft, $T=600°R$
$p_e=4400$ psi, $r_e=1000$ ft

Calculate the gas flow rate in Mscf/day.

Solution

Step 1. Calculate the term $2p/\mu_g Z$ for each pressure as shown below:

p (psi)	μ_g (cp)	Z	$2p/\mu_g Z$ (psia/cp)
0	0.0127	1.000	0
400	0.01286	0.937	66 391
800	0.01390	0.882	130 508
1200	0.01530	0.832	188 537
1600	0.01680	0.794	239 894
2000	0.01840	0.770	282 326
2400	0.02010	0.763	312 983
2800	0.02170	0.775	332 986
3200	0.02340	0.797	343 167

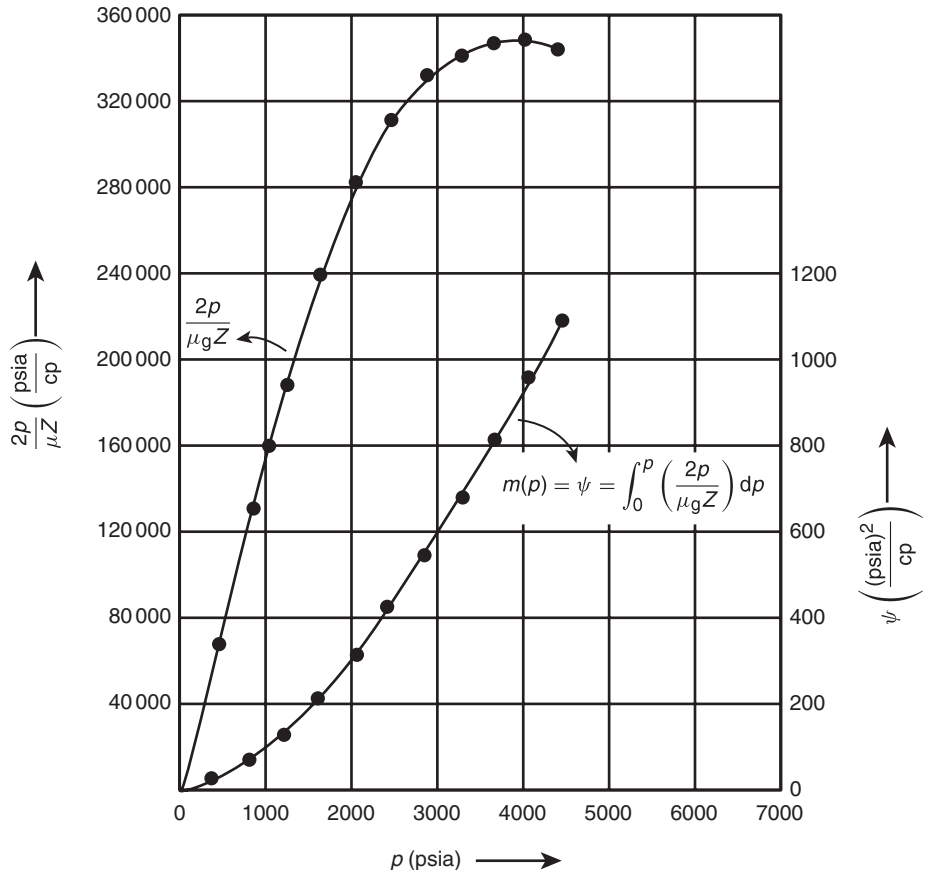

Figure 1.16 *Real-gas pseudopressure data for Example 1.7 (After Donohue and Erekin, 1982).*

p (psi)	μ_g (cp)	Z	$2p/\mu_g Z$ (psia/cp)
3600	0.02500	0.827	348 247
4000	0.02660	0.860	349 711
4400	0.02831	0.896	346 924

Step 2. Plot the term $2p/\mu_g Z$ versus pressure as shown in Figure 1.16.

Step 3. Calculate numerically the area under the curve for each value of p. These areas correspond to the real-gas pseudopressure ψ at each pressure. These ψ values are tabulated below; notice that $2p/\mu_g Z$ vs. p is also plotted in the figure.

p (psi)	ψ (psi^2/cp)
400	13.2×10^6
800	52.0×10^6
1200	113.1×10^6
1600	198.0×10^6
2000	304.0×10^6
2400	422.0×10^6
2800	542.4×10^6
3200	678.0×10^6
3600	816.0×10^6
4000	950.0×10^6
4400	1089.0×10^6

Step 4. Calculate the flow rate by applying Equation 1.2.30:

$$\text{At } p_w = 3600 \text{ psi: gives } \psi_w = 816.0 \times 10^6 \text{ psi}^2/\text{cp}$$

$$\text{At } p_e = 4400 \text{ psi: gives } \psi_e = 1089 \times 10^6 \text{ psi}^2/\text{cp}$$

$$Q_g = \frac{0.703kh(\psi_e - \psi_w)}{T \ln(r_e/r_w)}$$

$$= \frac{(65)(15)(1089 - 816)10^6}{(1422)(600)\ln(1000/0.25)}$$

$$= 37\,614 \text{ Mscf/day}$$

In the approximation of the gas flow rate, the exact gas flow rate as expressed by the different forms of Darcy's law, i.e., Equations 1.2.25 through 1.2.32, can be approximated by moving the term $2/\mu_g Z$ outside the integral as a constant. It should be pointed out that the product of $Z\mu_g$ is considered constant only under a pressure range of less than 2000 psi. Equation 1.2.31 can be rewritten as:

$$Q_g = \left[\frac{kh}{1422T \ln(r_e/r_w)}\right] \int_{p_{wf}}^{p_e} \left(\frac{2p}{\mu_g Z}\right) dp$$

Removing the term $2/\mu_g Z$ and integrating gives:

$$Q_g = \frac{kh\,(p_e^2 - p_{wf}^2)}{1422T\,(\mu_g Z)_{avg} \ln\,(r_e/r_w)} \qquad [1.2.33]$$

where:

Q_g = gas flow rate, Mscf/day
k = permeability, md

The term $(\mu_g Z)_{avg}$ is evaluated at an average pressure $\bar{p}$ that is defined by the following expression:

$$\bar{p} = \sqrt{\frac{p_{wf}^2 + p_e^2}{2}}$$

The above approximation method is called the pressure-squared method and is limited to flow calculations when the reservoir pressure is less that 2000 psi. Other approximation methods are discussed in Chapter 2.

Example 1.8 Using the data given in Example 1.7, resolve the gas flow rate by using the pressure-squared method. Compare with the exact method (i.e., real-gas pseudopressure solution).

Solution

Step 1. Calculate the arithmetic average pressure:

$$\bar{p} = \sqrt{\frac{4400^2 + 3600^2}{2}} = 4020 \text{ psi}$$

Step 2. Determine the gas viscosity and gas compressibility factor at 4020 psi:

$$\mu_g = 0.0267$$

$$Z = 0.862$$

Step 3. Apply Equation 1.2.33:

$$Q_g = \frac{kh(p_e^2 - p_{wf}^2)}{1422T(\mu_g Z)_{avg} \ln(r_e/r_w)}$$

$$= \frac{(65)(15)[4400^2 - 3600^2]}{(1422)(600)(0.0267)(0.862)\ln(1000/0.25)}$$

$$= 38\,314 \text{ Mscf/day}$$

Step 4. Results show that the pressure-squared method approximates the exact solution of 37 614 with an absolute error of 1.86%. This error is due to the limited applicability of the pressure-squared method to a pressure range of less than 2000 psi.

Horizontal multiple-phase flow

When several fluid phases are flowing simultaneously in a horizontal porous system, the concept of the effective permeability of each phase and the associated physical properties must be used in Darcy's equation. For a radial system, the generalized form of Darcy's equation can be applied to each reservoir as follows:

$$q_o = 0.001127\left(\frac{2\pi rh}{\mu_o}\right)k_o\frac{dp}{dr}$$

$$q_w = 0.001127\left(\frac{2\pi rh}{\mu_w}\right)k_w\frac{dp}{dr}$$

$$q_g = 0.001127\left(\frac{2\pi rh}{\mu_g}\right)k_g\frac{dp}{dr}$$

where:

k_o, k_w, k_g = effective permeability to oil, water, and gas, md
μ_o, μ_w, μ_g = viscosity of oil, water, and gas, cp
q_o, q_w, q_g = flow rates for oil, water, and gas, bbl/day
k = absolute permeability, md

The effective permeability can be expressed in terms of the relative and absolute permeability as:

$$k_o = k_{ro}k$$

$$k_w = k_{rw}k$$

$$k_g = k_{rg}k$$

Using the above concept in Darcy's equation and expressing the flow rate in standard conditions yields:

$$Q_o = 0.00708(rhk)\left(\frac{k_{ro}}{\mu_o B_o}\right)\frac{dp}{dr} \quad [1.2.34]$$

$$Q_w = 0.00708(rhk)\left(\frac{k_{rw}}{\mu_w B_w}\right)\frac{dp}{dr} \quad [1.2.35]$$

$$Q_g = 0.00708(rhk)\left(\frac{k_{rg}}{\mu_g B_g}\right)\frac{dp}{dr} \quad [1.2.36]$$

where:

Q_o, Q_w = oil and water flow rates, STB/day
B_o, B_w = oil and water formation volume factor, bbl/STB
Q_g = gas flow rate, scf/day
B_g = gas formation volume factor, bbl/scf
k = absolute permeability, md

The gas formation volume factor B_g is expressed by

$$B_g = 0.005035\frac{ZT}{p} \text{ bbl/scf}$$

Performing the regular integration approach on Equations, 1.2.34 through 1.2.36 yields:

Oil phase:

$$Q_o = \frac{0.00708(kh)(k_{ro})(p_e - p_{wf})}{\mu_o B_o \ln(r_e/r_w)} \quad [1.2.37]$$

Water phase:

$$Q_w = \frac{0.00708(kh)(k_{rw})(p_e - p_{wf})}{\mu_w B_w \ln(r_e/r_w)} \quad [1.2.38]$$

Gas phase:

$$Q_g = \frac{(kh)k_{rg}(\psi_e - \psi_w)}{1422T\ln(r_e/r_w)} \quad \text{in terms of the real-gas potential} \quad [1.2.39]$$

$$Q_g = \frac{(kh)k_{rg}(p_e^2 - p_{wf}^2)}{1422(\mu_g Z)_{avg}T\ln(r_e/r_w)} \quad \text{in terms of the pressure squared} \quad [1.2.40]$$

where:

Q_g = gas flow rate, Mscf/day
k = absolute permeability, md
T = temperature, °R

In numerous petroleum engineering calculations, it is convenient to express the flow rate of any phase as a ratio of other flowing phases. Two important flow ratios are the "instantaneous" water–oil ratio (WOR) and the "instantaneous" gas–oil ratio (GOR). The generalized form of Darcy's equation can be used to determine both flow ratios.

The water–oil ratio is defined as the ratio of the water flow rate to that of the oil. Both rates are expressed in stock-tank barrels per day, or:

$$\text{WOR} = \frac{Q_w}{Q_o}$$

Dividing Equation 1.2.34 by 1.2.36 gives:

$$\text{WOR} = \left(\frac{k_{rw}}{k_{ro}}\right)\left(\frac{\mu_o B_o}{\mu_w B_w}\right) \quad [1.2.41]$$

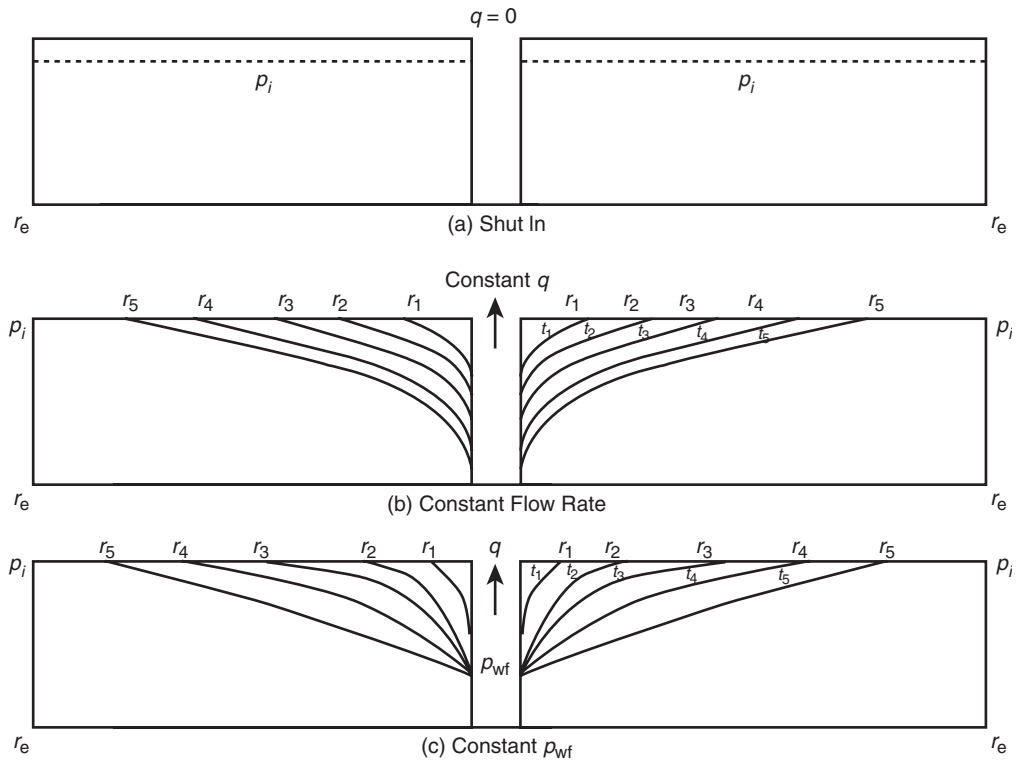

Figure 1.17 *Pressure disturbance as a function of time.*

where:

$$\text{WOR} = \text{water–oil ratio, STB/STB}$$

The instantaneous GOR, as expressed in scf/STB, is defined as the *total* gas flow rate, i.e., free gas and solution gas, divided by the oil flow rate, or:

$$\text{GOR} = \frac{Q_o R_s + Q_g}{Q_o}$$

or:

$$\text{GOR} = R_s + \frac{Q_g}{Q_o} \qquad [1.2.42]$$

where:

GOR = "instantaneous" gas–oil ratio, scf/STB
R_s = gas solubility, scf/STB
Q_g = free gas flow rate, scf/day
Q_o = oil flow rate, STB/day

Substituting Equations 1.2.34 and 1.2.36 into 1.2.42 yields:

$$\text{GOR} = R_s + \left(\frac{k_{rg}}{k_{ro}}\right)\left(\frac{\mu_o B_o}{\mu_g B_g}\right) \qquad [1.2.43]$$

where B_g is the gas formation volume factor expressed in bbl/scf.

A complete discussion of the practical applications of the WOR and GOR is given in the subsequent chapters.

1.2.3 Unsteady-state flow

Consider Figure 1.17(a) which shows a shut-in well that is centered in a homogeneous circular reservoir of radius r_e with a uniform pressure p_i throughout the reservoir. This initial reservoir condition represents the zero producing time. If the well is allowed to flow at a constant flow rate of q, a pressure disturbance will be created at the sand face. The pressure at the wellbore, i.e., p_{wf}, will drop instantaneously as the well is opened. The pressure disturbance will move away from the wellbore at a rate that is determined by:

- permeability;
- porosity;
- fluid viscosity;
- rock and fluid compressibilities.

Figure 1.17(b) shows that at time t_1, the pressure disturbance has moved a distance r_1 into the reservoir. Notice that the pressure disturbance radius is continuously increasing with time. This radius is commonly called the radius of investigation and referred to as r_{inv}. It is also important to point out that as long as the radius of investigation has not reached the reservoir boundary, i.e., r_e, the reservoir will be acting as if it is infinite in size. During this time we say that the reservoir is *infinite acting* because the outer drainage radius r_e, can be mathematically infinite, i.e., $r_e = \infty$. A similar discussion to the above can be used to describe a well that is producing at a constant bottom-hole flowing pressure. Figure 1.17(c) schematically illustrates the propagation of the radius of investigation with respect to time. At time t_4, the pressure disturbance reaches the boundary, i.e., $r_{inv} = r_e$. This causes the pressure behavior to change.

Based on the above discussion, the transient (unsteady-state) flow is defined as that time period during which the boundary has no effect on the pressure behavior in the reservoir and the reservoir will behave as if it is infinite in size. Figure 1.17(b) shows that the transient flow period occurs during the time interval $0 < t < t_t$ for the constant flow rate scenario and during the time period $0 < t < t_4$ for the constant p_{wf} scenario as depicted by Figure 1.17(c).

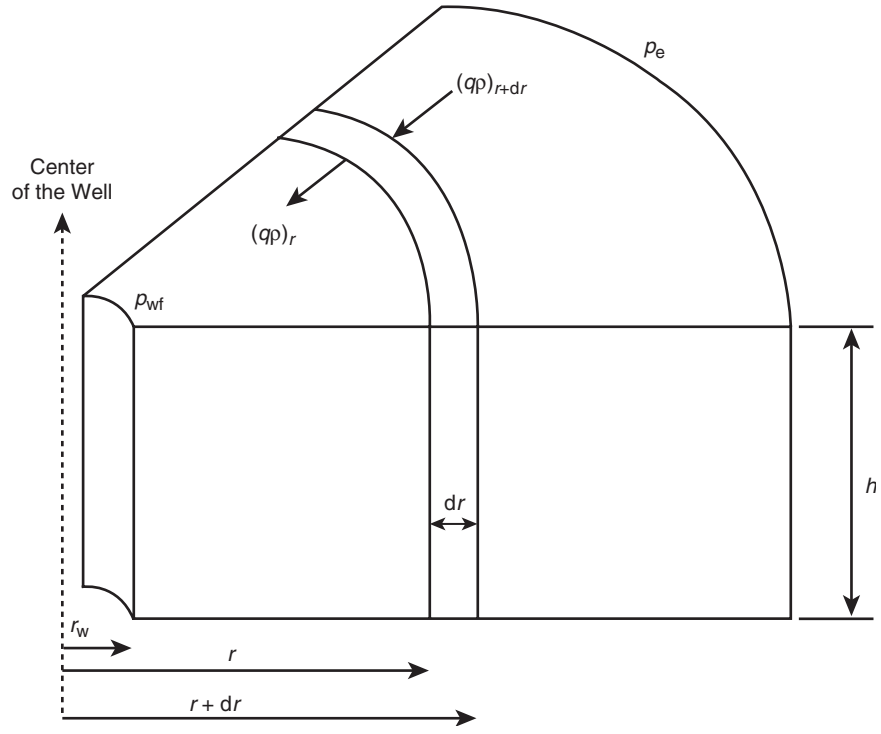

Figure 1.18 *Illustration of radial flow.*

1.2.4 Basic transient flow equation

Under the steady-state flowing condition, the same quantity of fluid enters the flow system as leaves it. In the unsteady-state flow condition, the flow rate into an element of volume of a porous medium may not be the same as the flow rate out of that element and, accordingly, the fluid content of the porous medium changes with time. The other controlling variables in unsteady-state flow *additional* to those already used for steady-state flow, therefore, become:

- time t;
- porosity ϕ;
- total compressibility c_t.

The mathematical formulation of the transient flow equation is based on combining three independent equations and a specifying set of boundary and initial conditions that constitute the unsteady-state equation. These equations and boundary conditions are briefly described below.

Continuity equation: The continuity equation is essentially a material balance equation that accounts for every pound mass of fluid produced, injected, or remaining in the reservoir.

Transport equation: The continuity equation is combined with the equation for fluid motion (transport equation) to describe the fluid flow rate "in" and "out" of the reservoir. Basically, the transport equation is Darcy's equation in its generalized differential form.

Compressibility equation: The fluid compressibility equation (expressed in terms of density or volume) is used in formulating the unsteady-state equation with the objective of describing the changes in the fluid volume as a function of pressure.

Initial and boundary conditions: There are two boundary conditions and one initial condition is required to complete the formulation and the solution of the transient flow equation. The two boundary conditions are:

(1) the formation produces at a constant rate into the wellbore;
(2) there is no flow across the outer boundary and the reservoir behaves as if it were infinite in size, i.e., $r_e = \infty$.

The initial condition simply states that the reservoir is at a uniform pressure when production begins, i.e., time = 0.

Consider the flow element shown in Figure 1.18. The element has a width of dr and is located at a distance of r from the center of the well. The porous element has a differential volume of dV. According to the concept of the material balance equation, the rate of mass flow into an element minus the rate of mass flow out of the element during a differential time Δt must be equal to the mass rate of accumulation during that time interval, or:

$$\begin{bmatrix}\text{mass entering}\\ \text{volume element}\\ \text{during interval } \Delta t\end{bmatrix} - \begin{bmatrix}\text{mass leaving}\\ \text{volume element}\\ \text{during interval } \Delta t\end{bmatrix} = \begin{bmatrix}\text{rate of mass}\\ \text{accumulation}\\ \text{during interval } \Delta t\end{bmatrix} \quad [1.2.44]$$

The individual terms of Equation 1.2.44 are described below:

Mass, entering the volume element during time interval Δt

Here:

$$(\text{Mass})_{in} = \Delta t[A v \rho]_{r+dr} \quad [1.2.45]$$

where:

v = velocity of flowing fluid, ft/day
ρ = fluid density at $(r + dr)$, lb/ft^3
A = area at $(r + dr)$
Δt = time interval, days

The area of the element at the entering side is:

$$A_{r+\mathrm{d}r} = 2\pi\,(r+\mathrm{d}r)h \qquad [1.2.46]$$

Combining Equations 1.2.46 with 1.2.35 gives:

$$[\text{Mass}]_{\text{in}} = 2\pi\,\Delta t\,(r+\mathrm{d}r)h(v\rho)_{r+\mathrm{d}r} \qquad [1.2.47]$$

Mass leaving the volume element Adopting the same approach as that of the leaving mass gives:

$$[\text{Mass}]_{\text{out}} = 2\pi\,\Delta t rh(v\rho)_r \qquad [1.2.48]$$

Total accumulation of mass The volume of some element with a radius of r is given by:

$$V = \pi r^2 h$$

Differentiating the above equation with respect to r gives:

$$\frac{\mathrm{d}V}{\mathrm{d}r} = 2\pi rh$$

or:

$$\mathrm{d}V = (2\pi rh)\,\mathrm{d}r \qquad [1.2.49]$$

Total mass accumulation during $\Delta t = \mathrm{d}V[(\phi\rho)_{t+\Delta t} - (\phi\rho)_{\mathrm{t}}]$. Substituting for $\mathrm{d}V$ yields:

$$\text{Total mass accumulation} = (2\pi rh)\mathrm{d}r[(\phi\rho)_{t+\Delta t} - (\phi\rho)_{\mathrm{t}}] \qquad [1.2.50]$$

Replacing the terms of Equation 1.2.44 with those of the calculated relationships gives:

$$2\pi h(r+\mathrm{d}r)\,\Delta t(\phi\rho)_{r+\mathrm{d}r} - 2\pi hr\,\Delta t(\phi\rho)_{\mathrm{r}} = (2\pi rh)\mathrm{d}r[(\phi\rho)_{t+\Delta t} - (\phi\rho)_{\mathrm{t}}]$$

Dividing the above equation by $(2\pi rh)\mathrm{d}r$ and simplifying gives:

$$\frac{1}{(r)\mathrm{d}r}\left[(r+\mathrm{d}r)\,(\upsilon\rho)_{r+\mathrm{d}r} - r(v\rho)_r\right] = \frac{1}{\Delta t}\left[(\phi\rho)_{t+\Delta t} - (\phi\rho)_t\right]$$

or:

$$\frac{1}{r}\frac{\partial}{\partial r}\left[r(\upsilon\rho)\right] = \frac{\partial}{\partial t}\,(\phi\rho) \qquad [1.2.51]$$

where:

ϕ = porosity
ρ = density, lb/ft^3
V = fluid velocity, ft/day

Equation 1.2.51 is called the continuity equation and it provides the principle of conservation of mass in radial coordinates.

The transport equation must be introduced into the continuity equation to relate the fluid velocity to the pressure gradient within the control volume $\mathrm{d}V$. Darcy's law is essentially the basic motion equation, which states that the velocity is proportional to the pressure gradient $\partial p/\partial r$. From Equation 1.2.13:

$$v = (5.615)\,(0.001127)\,\frac{k}{\mu}\frac{\partial p}{\partial r} = (0.006328)\,\frac{k}{\mu}\frac{\partial p}{\partial r} \qquad [1.2.52]$$

where:

k = permeability, md
v = velocity, ft/day

Combining Equation 1.2.52 with 1.2.51 results in:

$$\frac{0.006328}{r}\frac{\partial}{\partial r}\left(\frac{k}{\mu}\,(\rho r)\,\frac{\partial p}{\partial r}\right) = \frac{\partial}{\partial t}\,(\phi\rho) \qquad [1.2.53]$$

Expanding the right-hand side by taking the indicated derivatives eliminates the porosity from the partial derivative term on the right-hand side:

$$\frac{\partial}{\partial t}\,(\phi\rho) = \phi\frac{\partial\rho}{\partial t} + \rho\frac{\partial\phi}{\partial t} \qquad [1.2.54]$$

The porosity is related to the formation compressibility by the following:

$$c_{\mathrm{f}} = \frac{1}{\phi}\frac{\partial\phi}{\partial p} \qquad [1.2.55]$$

Applying the chain rule of differentiation to $\partial\phi/\partial t$:

$$\frac{\partial\phi}{\partial t} = \frac{\partial\phi}{\partial p}\frac{\partial p}{\partial t}$$

Substituting Equation 1.2.55 into this equation:

$$\frac{\partial\phi}{\partial t} = \phi c_{\mathrm{f}}\frac{\partial p}{\partial t}$$

Finally, substituting the above relation into Equation 1.2.54 and the result into Equation 1.2.53 gives:

$$\frac{0.006328}{r}\frac{\partial}{\partial r}\left(\frac{k}{\mu}\,(\rho r)\,\frac{\partial p}{\partial r}\right) = \rho\phi c_{\mathrm{f}}\frac{\partial p}{\partial t} + \phi\frac{\partial\rho}{\partial t} \qquad [1.2.56]$$

Equation 1.2.56 is the general partial differential equation used to describe the flow of any fluid flowing in a radial direction in porous media. In addition to the initial assumptions, Darcy's equation has been added, which implies that the flow is laminar. Otherwise, the equation is not restricted to any type of fluid and is equally valid for gases or liquids. However, compressible and slightly compressible fluids must be treated separately in order to develop practical equations that can be used to describe the flow behavior of these two fluids. The treatments of the following systems are discussed below:

- radial flow of slightly compressible fluids;
- radial flow of compressible fluids.

1.2.5 Radial flow of slightly compressibility fluids

To simplify Equation 1.2.56, assume that the permeability and viscosity are constant over pressure, time, and distance ranges. This leads to:

$$\left[\frac{0.006328k}{\mu r}\right]\frac{\partial}{\partial r}\left(r\rho\frac{\partial p}{\partial r}\right) = \rho\phi c_{\mathrm{f}}\frac{\partial p}{\partial t} + \phi\frac{\partial\rho}{\partial t} \qquad [1.2.57]$$

Expanding the above equation gives:

$$0.006328\left(\frac{k}{\mu}\right)\left[\frac{\rho}{r}\frac{\partial p}{\partial r} + \rho\frac{\partial^2 p}{\partial r^2} + \frac{\partial p}{\partial r}\frac{\partial\rho}{\partial r}\right] = \rho\phi c_{\mathrm{f}}\left(\frac{\partial p}{\partial t}\right) + \phi\left(\frac{\partial\rho}{\partial t}\right)$$

Using the chain rule in the above relationship yields:

$$0.006328\left(\frac{k}{\mu}\right)\left[\frac{\rho}{r}\frac{\partial p}{\partial r} + \rho\frac{\partial^2 p}{\partial r^2} + \left(\frac{\partial p}{\partial r}\right)^2\frac{\partial\rho}{\partial p}\right] = \rho\phi c_{\mathrm{f}}\left(\frac{\partial p}{\partial t}\right) + \phi\left(\frac{\partial p}{\partial t}\right)\left(\frac{\partial\rho}{\partial p}\right)$$

Dividing the above expression by the fluid density ρ gives:

$$0.006328\left(\frac{k}{u}\right)\left[\frac{1}{r}\frac{\partial p}{\partial r} + \frac{\partial^2 p}{\partial r^2} + \left(\frac{\partial p}{\partial r}\right)^2\left(\frac{1}{\rho}\frac{\partial\rho}{\partial p}\right)\right] = \phi c_{\mathrm{f}}\left(\frac{\partial p}{\partial t}\right) + \phi\frac{\partial p}{\partial t}\left(\frac{1}{\rho}\frac{\partial\rho}{\partial p}\right)$$

Recalling that the compressibility of any fluid is related to its density by:

$$c = \frac{1}{\rho}\frac{\partial\rho}{\partial p}$$

combining the above two equations gives:

$$0.006328\left(\frac{k}{\mu}\right)\left[\frac{\partial^2 p}{\partial r^2}+\frac{1}{r}\frac{\partial p}{\partial r}+c\left(\frac{\partial p}{\partial r}\right)^2\right]$$

$$=\phi c_f\left(\frac{\partial p}{\partial t}\right)+\phi c\left(\frac{\partial p}{\partial t}\right)$$

The term $c(\partial p/\partial r)^2$ is considered very small and may be ignored, which leads to:

$$0.006328\left(\frac{k}{\mu}\right)\left[\frac{\partial^2 p}{\partial r^2}+\frac{1}{r}\frac{\partial p}{\partial r}\right]=\phi\,(c_f+c)\,\frac{\partial p}{\partial t} \qquad [1.2.58]$$

Defining total compressibility, c_t, as:

$$c_t=c+c_f \qquad [1.2.59]$$

and combining Equation 1.2.57 with 1.2.58 and rearranging gives:

$$\frac{\partial^2 p}{\partial r^2}+\frac{1}{r}\frac{\partial p}{\partial r}=\frac{\phi\mu c_t}{0.006328k}\frac{\partial p}{\partial t} \qquad [1.2.60]$$

where the time t is expressed in days.

Equation 1.2.60 is called the diffusivity equation and is considered one of the most important and widely used mathematical expressions in petroleum engineering. The equation is particularly used in the analysis of well testing data where the time t is commonly reordered in hours. The equation can be rewritten as:

$$\frac{\partial^2 p}{\partial r^2}+\frac{1}{r}\frac{\partial p}{\partial r}=\frac{\phi\mu c_t}{0.0002637k}\frac{\partial p}{\partial t} \qquad [1.2.61]$$

where:

k = permeability, md
r = radial position, ft
p = pressure, psia
c_t = total compressibility, psi^{-1}
t = time, hours
ϕ = porosity, fraction
μ = viscosity, cp

When the reservoir contains more than one fluid, total compressibility should be computed as

$$c_t=c_oS_o+c_wS_w+c_gS_g+c_f \qquad [1.2.62]$$

where c_o, c_w, and c_g refer to the compressibility of oil, water, and gas, respectively, and S_o, S_w, and S_g refer to the fractional saturation of these fluids. Note that the introduction of c_t into Equation 1.2.60 does not make this equation applicable to multiphase flow; the use of c_t, as defined by Equation 1.2.61, simply accounts for the compressibility of any immobile fluids which may be in the reservoir with the fluid that is flowing.

The term $0.000264k/\phi\mu c_t$ is called the diffusivity constant and is denoted by the symbol η, or:

$$\eta=\frac{0.0002637k}{\phi\mu c_t} \qquad [1.2.63]$$

The diffusivity equation can then be written in a more convenient form as:

$$\frac{\partial^2 p}{\partial r^2}+\frac{1}{r}\frac{\partial p}{\partial r}=\frac{1}{\eta}\frac{\partial p}{\partial t} \qquad [1.2.64]$$

The diffusivity equation as represented by relationship 1.2.64 is essentially designed to determine the pressure as a function of time t and position r.

Notice that for a steady-state flow condition, the pressure at any point in the reservoir is constant and does not change with time, i.e., $\partial p/\partial t=0$, so Equation 1.2.64 reduces to:

$$\frac{\partial^2 p}{\partial r^2}+\frac{1}{r}\frac{\partial p}{\partial r}=0 \qquad [1.2.65]$$

Equation 1.2.65 is called Laplace's equation for steady-state flow.

Example 1.9 Show that the radial form of Darcy's equation is the solution to Equation 1.2.65.

Solution

Step 1. Start with Darcy's law as expressed by Equation 1.2.17:

$$p=p_{wf}+\left[\frac{Q_oB_ou_o}{0.00708kh}\right]\ln\left(\frac{r}{r_w}\right)$$

Step 2. For a steady-state incompressible flow, the term with the square brackets is constant and labeled as C, or:

$$p=p_{wf}+[C]\ln\left(\frac{r}{r_w}\right)$$

Step 3. Evaluate the above expression for the first and second derivative, to give:

$$\frac{\partial p}{\partial r}=[C]\left(\frac{1}{r}\right)$$

$$\frac{\partial^2 p}{\partial r^2}=[C]\left(\frac{-1}{r^2}\right)$$

Step 4. Substitute the above two derivatives in Equation 1.2.65:

$$\frac{-1}{r^2}[C]+\left(\frac{1}{r}\right)[C]\left(\frac{1}{r}\right)=0$$

Step 5. Results of step 4 indicate that Darcy's equation satisfies Equation 1.2.65 and is indeed the solution to Laplace's equation.

To obtain a solution to the diffusivity equation (Equation 1.2.64), it is necessary to specify an initial condition and impose two boundary conditions. The initial condition simply states that the reservoir is at a uniform pressure p_i when production begins. The two boundary conditions require that the well is producing at a constant production rate and the reservoir behaves as if it were infinite in size, i.e., $r_e=\infty$.

Based on the boundary conditions imposed on Equation 1.2.64, there are two generalized solutions to the diffusivity equation. These are:

(1) the constant-terminal-pressure solution
(2) the constant-terminal-rate solution.

The constant-terminal-pressure solution is designed to provide the cumulative flow at any particular time for a reservoir in which the pressure at one boundary of the reservoir is held constant. This technique is frequently used in water influx calculations in gas and oil reservoirs.

The constant-terminal-rate solution of the radial diffusivity equation solves for the pressure change throughout the radial system providing that the flow rate is held constant at one terminal end of the radial system, i.e., at the producing well. There are two commonly used forms of the constant-terminal-rate solution:

(1) the Ei function solution;
(2) the dimensionless pressure drop p_D solution.

Constant-terminal-pressure solution

In the constant-rate solution to the radial diffusivity equation, the flow rate is considered to be constant at certain radius (usually wellbore radius) and the pressure profile around that radius is determined as a function of time and position. In the constant-terminal-pressure solution, the pressure is known to be constant at some particular radius and the solution is designed to provide the cumulative fluid movement across the specified radius (boundary).

The constant-pressure solution is widely used in water influx calculations. A detailed description of the solution

and its practical reservoir engineering applications is appropriately discussed in the water influx chapter of the book (Chapter 5).

Constant-terminal-rate solution

The constant-terminal-rate solution is an integral part of most transient test analysis techniques, e.g., drawdown and pressure buildup analyses. Most of these tests involve producing the well at a constant flow rate and recording the flowing pressure as a function of time, i.e., $p(r_w, t)$. There are two commonly used forms of the constant-terminal-rate solution:

(1) the Ei function solution;
(2) the dimensionless pressure drop p_D solution.

These two popular forms of solution to the diffusivity equation are discussed below.

The Ei function solution

For an infinite-acting reservoir, Matthews and Russell (1967) proposed the following solution to the diffusivity equation, i.e., Equation 1.2.55:

$$p(r,\, t) = p_i + \left[\frac{70.6 Q_o \mu B_o}{kh}\right] \mathrm{Ei}\left[\frac{-948\phi\mu c_t r^2}{kt}\right] \qquad [1.2.66]$$

where:

$p(r,t)$ = pressure at radius r from the well after t hours
t = time, hours
k = permeability, md
Q_o = flow rate, STB/day

The mathematical function, Ei, is called the exponential integral and is defined by:

$$\mathrm{Ei}(-x) = -\int_x^{\infty} \frac{e^{-u}du}{u} = \left[\ln x - \frac{x}{1!} + \frac{x^2}{2\,(2!)} - \frac{x^3}{3\,(3!)} + \cdots\right] \qquad [1.2.67]$$

Craft et al. (1991) presented the values of the Ei function in tabulated and graphical forms as shown in Table 1.1 and Figure 1.19, respectively.

The Ei solution, as expressed by Equation 1.2.66, is commonly referred to as the line source solution. The exponential integral "Ei" can be approximated by the following equation when its argument x is less than 0.01:

$$\mathrm{Ei}(-x) = \ln\left(1.781x\right) \qquad [1.2.68]$$

where the argument x in this case is given by:

$$x = \frac{948\phi\mu c_t r^2}{kt}$$

Equation 1.2.68 approximates the Ei function with less than 0.25% error. Another expression that can be used to approximate the Ei function for the range of $0.01 < x < 3.0$ is given by:

$$\mathrm{Ei}(-x) = a_1 + a_2\ln(x) + a_3[\ln(x)]^2 + a_4[\ln(x)]^3 + a_5 x + a_6 x^2 + a_7 x^3 + a_8/x \qquad [1.2.69]$$

with the coefficients a_1 through a_8 having the following values:

$a_1 = -0.33153973$ $\quad a_2 = -0.81512322$

$a_3 = 5.22123384 \times 10^{-2}$ $\quad a_4 = 5.9849819 \times 10^{-3}$

$a_5 = 0.662318450$ $\quad a_6 = -0.12333524$

$a_7 = 1.0832566 \times 10^{-2}$ $\quad a_8 = 8.6709776 \times 10^{-4}$

The above relationship approximated the Ei values with an average error of 0.5%.

It should be pointed out that for $x > 10.9$, $\mathrm{Ei}(-x)$ can be considered zero for reservoir engineering calculations.

Table 1.1 *Values of* $-\mathrm{Ei}(-x)$ *as a function of* x *(After Craft et al. 1991)*

x	$-\mathrm{Ei}(-x)$	x	$-\mathrm{Ei}(-x)$	x	$-\mathrm{Ei}(-x)$
0.1	1.82292	3.5	0.00697	6.9	0.00013
0.2	1.22265	3.6	0.00616	7.0	0.00012
0.3	0.90568	3.7	0.00545	7.1	0.00010
0.4	0.70238	3.8	0.00482	7.2	0.00009
0.5	0.55977	3.9	0.00427	7.3	0.00008
0.6	0.45438	4.0	0.00378	7.4	0.00007
0.7	0.37377	4.1	0.00335	7.5	0.00007
0.8	0.31060	4.2	0.00297	7.6	0.00006
0.9	0.26018	4.3	0.00263	7.7	0.00005
1.0	0.21938	4.4	0.00234	7.8	0.00005
1.1	0.18599	4.5	0.00207	7.9	0.00004
1.2	0.15841	4.6	0.00184	8.0	0.00004
1.3	0.13545	4.7	0.00164	8.1	0.00003
1.4	0.11622	4.8	0.00145	8.2	0.00003
1.5	0.10002	4.9	0.00129	8.3	0.00003
1.6	0.08631	5.0	0.00115	8.4	0.00002
1.7	0.07465	5.1	0.00102	8.5	0.00002
1.8	0.06471	5.2	0.00091	8.6	0.00002
1.9	0.05620	5.3	0.00081	8.7	0.00002
2.0	0.04890	5.4	0.00072	8.8	0.00002
2.1	0.04261	5.5	0.00064	8.9	0.00001
2.2	0.03719	5.6	0.00057	9.0	0.00001
2.3	0.03250	5.7	0.00051	9.1	0.00001
2.4	0.02844	5.8	0.00045	9.2	0.00001
2.5	0.02491	5.9	0.00040	9.3	0.00001
2.6	0.02185	6.0	0.00036	9.4	0.00001
2.7	0.01918	6.1	0.00032	9.5	0.00001
2.8	0.01686	6.2	0.00029	9.6	0.00001
2.9	0.01482	6.3	0.00026	9.7	0.00001
3.0	0.01305	6.4	0.00023	9.8	0.00001
3.1	0.01149	6.5	0.00020	9.9	0.00000
3.2	0.01013	6.6	0.00018	10.0	0.00000
3.3	0.00894	6.7	0.00016		
3.4	0.00789	6.8	0.00014		

Example 1.10 An oil well is producing at a constant flow rate of 300 STB/day under unsteady-state flow conditions. The reservoir has the following rock and fluid properties:

$B_o = 1.25$ bbl/STB, $\quad \mu_o = 1.5$ cp, $\quad c_t = 12 \times 10^{-6}$ psi^{-1}

$k_o = 60$ md, $\quad h = 15$ ft, $\quad p_i = 4000$ psi

$\phi = 15\%$, $\quad r_w = 0.25$ ft

(1) Calculate the pressure at radii of 0.25, 5, 10, 50, 100, 500, 1000, 1500, 2000, and 2500 ft, for 1 hour. Plot the results as:
   (a) pressure versus the logarithm of radius;
   (b) pressure versus radius.

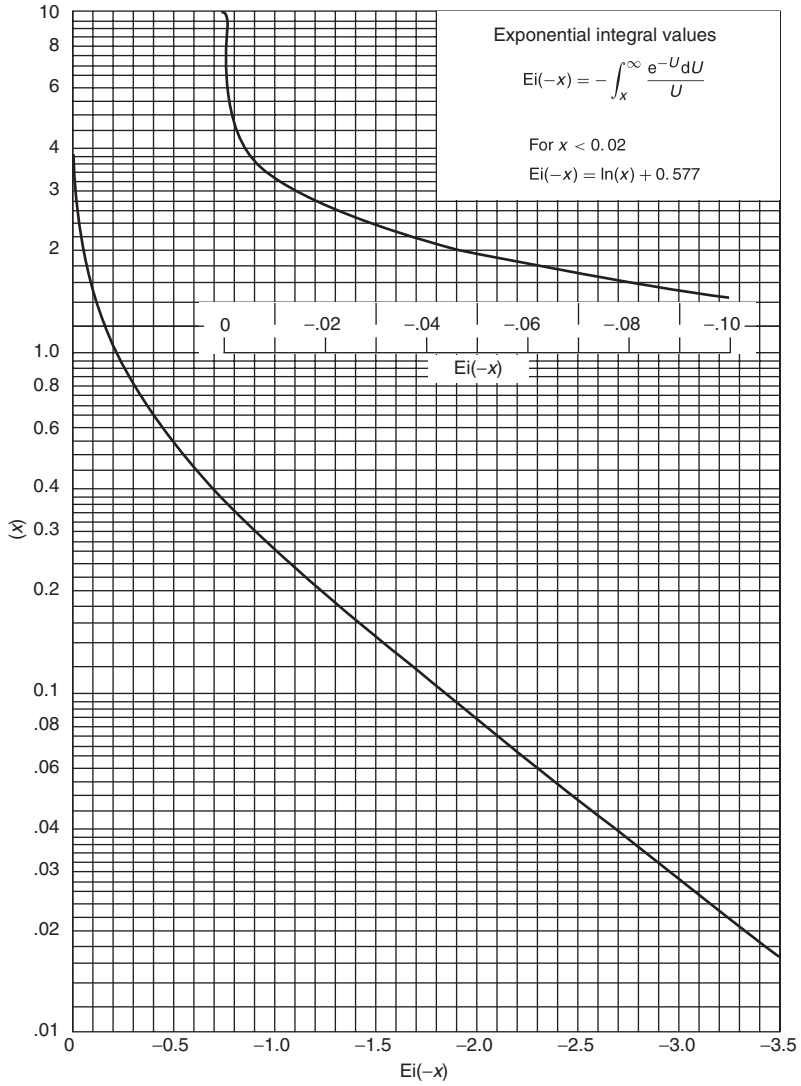

Figure 1.19 *Ei function (After Craft et al., 1991).*

(2) Repeat part 1 for $t = 12$ hours and 24 hours. Plot the results as pressure versus logarithm of radius.

Solution

Step 1. From Equation 1.2.66:

$$p(r,t) = 4000 + \left[\frac{70.6\,(300)(1.5)(1.25)}{(60)(15)}\right] \times \mathrm{Ei}\left[\frac{-948\,(1.5)(1.5)\,(12\times10^{-6})r^2}{(60)\,(t)}\right]$$

$$= 4000 + 44.125\mathrm{Ei}\left[\left(-42.6\times10^{-6}\right)\frac{r^2}{t}\right]$$

Step 2. Perform the required calculations after 1 hour in the following tabulated form:

r (ft)	$x = (-42.6\times 10^{-6})r^2/1$	Ei $(-x)$	$p(r,12) = 4000 + 44.125\,\mathrm{Ei}(-x)$
0.25	-2.6625×10^{-6}	-12.26^a	3459
5	−0.001065	-6.27^a	3723
10	−0.00426	-4.88^a	3785
50	−0.1065	-1.76^b	3922
100	−0.4260	-0.75^b	3967
500	−10.65	0	4000
1000	−42.60	0	4000
1500	−95.85	0	4000
2000	−175.40	0	4000
2500	−266.25	0	4000

[a] As calculated from Equation 1.2.17.
[b] From Figure 1.19.

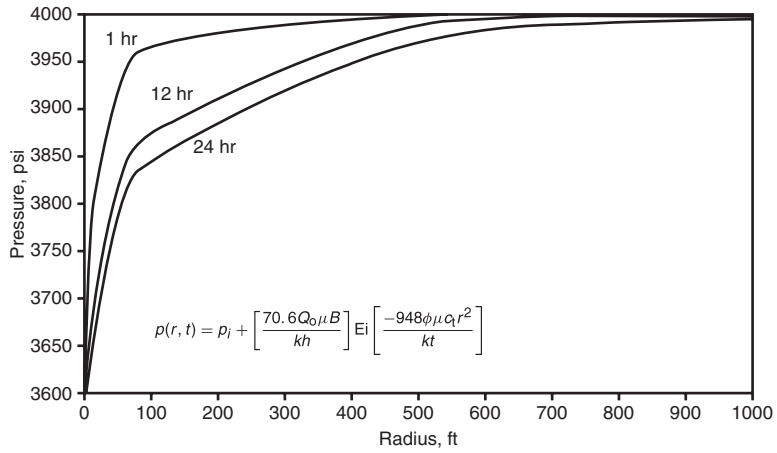

Figure 1.20 *Pressure profiles as a function of time.*

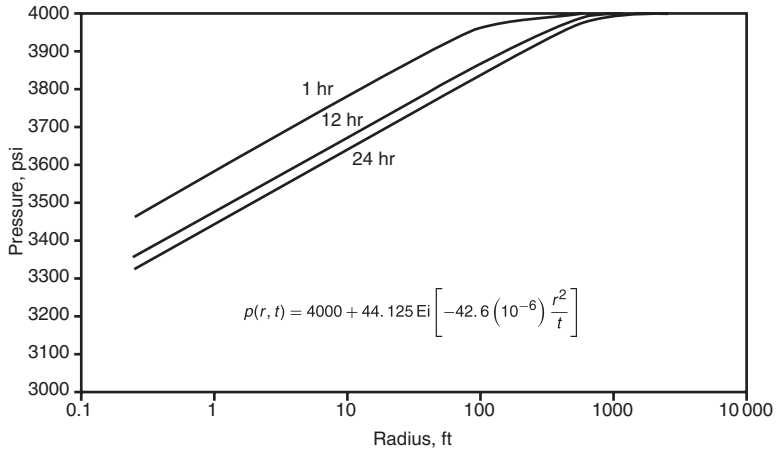

Figure 1.21 *Pressure profiles as a function of time on a semi-log scale.*

Step 3. Show the results of the calculation graphically as illustrated in Figures 1.20 and 1.21.

Step 4. Repeat the calculation for $t = 12$ and 24 hours, as in the tables below:

r (ft)	$x = (42.6\times 10^{-6})r^2/12$	$\text{Ei}(-x)$	$p(r,12) = 4000 + 44.125\ \text{Ei}(-x)$
0.25	0.222×10^{-6}	-14.74^a	3350
5	88.75×10^{-6}	-8.75^a	3614
10	355.0×10^{-6}	-7.37^a	3675
50	0.0089	-4.14^a	3817
100	0.0355	-2.81^b	3876
500	0.888	-0.269	3988
1000	3.55	-0.0069	4000
1500	7.99	-3.77×10^{-5}	4000
2000	14.62	0	4000
2500	208.3	0	4000

[a] As calculated from Equation 1.2.17.
[b] From Figure 1.19.

r (ft)	$x = (-42.6\times 10^{-6})r^2/24$	$\text{Ei}(-x)$	$p(r,24) = 4000 + 44.125\ \text{Ei}(-x)$
0.25	-0.111×10^{-6}	-15.44^a	3319
5	-44.38×10^{-6}	-9.45^a	3583
10	-177.5×10^{-6}	-8.06^a	3644
50	-0.0045	-4.83^a	3787
100	-0.0178	-8.458^b	3847
500	-0.444	-0.640	3972
1000	-1.775	-0.067	3997
1500	-3.995	-0.0427	3998
2000	-7.310	8.24×10^{-6}	4000
2500	-104.15	0	4000

[a] As calculated from Equation 1.2.17.
[b] From Figure 1.19.

Step 5. Results of step 4 are shown graphically in Figure 1.21.

Figure 1.21 indicates that as the pressure disturbance moves radially away from the wellbore, the reservoir

boundary and its configuration has no effect on the pressure behavior, which leads to the definition of transient flow as: "Transient flow is that time period during which the boundary has no effect on the pressure behavior and the well acts as if it exists in an infinite size reservoir."

Example 1.10 shows that most of the pressure loss occurs close to the wellbore; accordingly, near-wellbore conditions will exert the greatest influence on flow behavior. Figure 1.21 shows that the pressure profile and the drainage radius are continuously changing with time. It is also important to notice that the production rate of the well has no effect on the velocity or the distance of the pressure disturbance since the Ei function is independent of the flow rate.

When the Ei parameter $x < 0.01$, the log approximation of the Ei function as expressed by Equation 1.2.68 can be used in 1.2.66 to give:

$$p(r,t) = p_i - \frac{162.6 Q_o B_o \mu_o}{kh}\left[\log\left(\frac{kt}{\phi\mu c_t r^2}\right) - 3.23\right] \quad [1.2.70]$$

For most of the transient flow calculations, engineers are primarily concerned with the behavior of the bottom-hole flowing pressure at the wellbore, i.e., $r = r_w$. Equation 1.2.70 can be applied at $r = r_w$ to yield:

$$p_{wf} = p_i - \frac{162.6 Q_o B_o \mu_o}{kh}\left[\log\left(\frac{kt}{\phi\mu c_t r_w^2}\right) - 3.23\right] \quad [1.2.71]$$

where:

k = permeability, md
t = time, hours
c_t = total compressibility, psi^{-1}

It should be noted that Equations 1.2.70 and 1.2.71 cannot be used until the flow time t exceeds the limit imposed by the following constraint:

$$t > 9.48 \times 10^4 \frac{\phi\mu c_t r^2}{k} \quad [1.2.72]$$

where:

k = permeability, md
t = time, hours

Notice that when a well is producing under unsteady-state (transient) flowing conditions at a constant flow rate, Equation 1.2.71 can be expressed as the equation of a straight line by manipulating the equation to give:

$$p_{wf} = p_i - \frac{162.6 Q_o B_o \mu_o}{kh}\left[\log(t) + \log\left(\frac{k}{\phi\mu c_t r_w^2}\right) - 3.23\right]$$

or:

$$p_{wf} = a + m\log(t)$$

The above equation indicates that a plot of p_{wf} vs. t on a semilogarithmic scale would produce a straight line with an intercept of a and a slope of m as given by:

$$a = p_i - \frac{162.6 Q_o B_o \mu_o}{kh}\left[\log\left(\frac{k}{\phi\mu c_t r_w^2}\right) - 3.23\right]$$

$$m = \frac{162.6 Q_o B_o \mu_o}{kh}$$

Example 1.11 Using the data in Example 1.10, estimate the bottom-hole flowing pressure after 10 hours of production.

Solution

Step 1. Equation 1.2.71 can only be used to calculate p_{wf} at any time that exceeds the time limit imposed by Equation 1.2.72, or:

$$t > 9.48 \times 10^4 \frac{\phi\mu c_t r^2}{k}$$

$$t = 9.48\,(10^4)\,\frac{(0.15)\,(1.5)\,(12\times10^{-6})\,(0.25)^2}{60}$$

$$= 0.000267 \text{ hours}$$

$$= 0.153 \text{ seconds}$$

For all practical purposes, Equation 1.2.71 can be used anytime during the transient flow period to estimate the bottom-hole pressure.

Step 2. Since the specified time of 10 hours is greater than 0.000267 hours, the value of p_{wf} can be estimated by applying Equation 1.2.71:

$$p_{wf} = p_i - \frac{162.6 Q_o B_o \mu_o}{kh}\left[\log\left(\frac{kt}{\phi\mu c_t r_w^2}\right) - 3.23\right]$$

$$= 4000 - \frac{162.6\,(300)\,(1.25)\,(1.5)}{(60)\,(15)}$$

$$\times\left[\log\left(\frac{(60)\,(10)}{(0.15)\,(1.5)\,(12\times10^{-6})\,(0.25)^2}\right) - 3.23\right]$$

$$= 3358 \text{ psi}$$

The second form of solution to the diffusivity equation is called the dimensionless pressure drop solution and is discussed below.

The dimensionless pressure drop p_D solution

To introduce the concept of the dimensionless pressure drop solution, consider for example Darcy's equation in a radial form as given previously by Equation 1.2.15

$$Q_o = \frac{0.00708 kh\,(p_e - p_{wf})}{\mu_o B_o \ln(r_e/r_w)} = \frac{kh(p_e - p_{wf})}{141.2\mu_o B_o \ln(r_e/r_w)}$$

Rearranging the above equation gives:

$$\frac{p_e - p_{wf}}{\left(\frac{141.2 Q_o B_o \mu_o}{kh}\right)} = \ln\left(\frac{r_e}{r_w}\right) \quad [1.2.73]$$

It is obvious that the right-hand side of the above equation has no units (i.e., it is dimensionless) and, accordingly, the left-hand side must be dimensionless. Since the left-hand side is dimensionless, and $p_e - p_{wf}$ has the units of psi, it follows that the term $Q_o B_o \mu_o / 0.00708kh$ has units of pressure. In fact, any pressure difference divided by $Q_o B_o \mu_o / 0.00708kh$ is a dimensionless pressure. Therefore, Equation 1.2.73 can be written in a dimensionless form as:

$$p_D = \ln(r_{eD})$$

where:

$$p_D = \frac{p_e - p_{wf}}{\left(\frac{141.2 Q_o B_o \mu_o}{kh}\right)}$$

$$r_{eD} = \frac{r_e}{r_w}$$

The dimensionless pressure drop concept can be extended to describe the changes in the pressure during the unsteady-state flow condition where the pressure is a function of time and radius:

$$p = p(r,t)$$

Therefore, the dimensionless pressure during the unsteady-state flowing condition is defined by:

$$p_D = \frac{p_i - p(r,t)}{\left(\frac{141.2 Q_o B_o \mu_o}{kh}\right)} \quad [1.2.74]$$

Since the pressure $p(r,t)$, as expressed in a dimensionless form, varies with time and location, it is traditionally presented as a function of dimensionless time t_D and radius r_D as defined below:

$$t_D = \frac{0.0002637kt}{\phi\mu c_t r_w^2} \quad [1.2.75a]$$

Another common form of the dimensionless time t_D is based on the total drainage area A as given by:

$$t_{DA} = \frac{0.0002637kt}{\phi\mu c_t A} = t_A\left(\frac{r_w^2}{A}\right) \quad [1.2.75b]$$

$$r_D = \frac{r}{r_w} \quad [1.2.76]$$

and:

$$r_{eD} = \frac{r_e}{r_w} \quad [1.2.77]$$

where:

p_D = dimensionless pressure drop
r_{eD} = dimensionless external radius
t_D = dimensionless time based on wellbore radius r_w
t_{DA} = dimensionless time based on well drainage area A
A = well drainage area, i.e., πr_e^2, ft^2
r_D = dimensionless radius
t = time, hours
$p(r,t)$ = pressure at radius r and time t
k = permeability, md
μ = viscosity, cp

The above dimensionless groups (i.e., p_D, t_D, and r_D) can be introduced into the diffusivity equation (Equation 1.2.64) to transform the equation into the following dimensionless form:

$$\frac{\partial^2 p_D}{\partial r_D^2} + \frac{1}{r_D}\frac{\partial p_D}{\partial r_D} = \frac{\partial p_D}{\partial t_D} \quad [1.2.78]$$

Van Everdingen and Hurst (1949) proposed an analytical solution to the above equation by assuming:

- a perfectly radial reservoir system;
- the producing well is in the center and producing at a constant production rate of Q;
- uniform pressure p_i throughout the reservoir before production;
- no flow across the external radius r_e.

Van Everdingen and Hurst presented the solution to Equation 1.2.77 in a form of an infinite series of exponential terms and Bessel functions. The authors evaluated this series for several values of r_{eD} over a wide range of values for t_D and presented the solution in terms of dimensionless pressure drop p_D as a function of dimensionless radius r_{eD} and dimensionless time t_D. Chatas (1953) and Lee (1982) conveniently tabulated these solutions for the following two cases:

(1) infinite-acting reservoir $r_{eD} = \infty$;
(2) finite-radial reservoir.

Infinite-acting reservoir For an infinite-acting reservoir, i.e., $r_{eD} = \infty$, the solution to Equation 1.2.78 in terms of the dimensionless pressure drop p_D is strictly a function of the dimensionless time t_D, or:

$$p_D = f(t_D)$$

Chatas and Lee tabulated the p_D values for the infinite-acting reservoir as shown in Table 1.2. The following mathematical expressions can be used to approximate these tabulated values of p_D.

For $t_D < 0.01$:

$$p_D = 2\sqrt{\frac{t_D}{\pi}} \quad [1.2.79]$$

For $t_D > 100$:

$$p_D = 0.5[\ln(t_D) + 0.80907] \quad [1.2.80]$$

For $0.02 < t_D \leq 1000$:

$$p_D = a_1 + a_2\ln(t_D) + a_3[\ln(t_D)]^2 + a_4[\ln(t_D)]^3 + a_5 t_D + a_6(t_D)^2 + a_7(t_D)^3 + a_8/t_D \quad [1.2.81]$$

where the values of the coefficients of the above equations are:

$a_1 = 0.8085064$ $\quad a_2 = 0.29302022$

$a_3 = 3.5264177 \times 10^{-2}$ $\quad a_4 = -1.4036304 \times 10^{-3}$

$a_5 = -4.7722225 \times 10^{-4}$ $\quad a_6 = 5.1240532 \times 10^{-7}$

$a_7 = -2.3033017 \times 10^{-10}$ $\quad a_8 = -2.6723117 \times 10^{-3}$

Finite radial reservoir For a finite radial system, the solution to Equation 1.2.78 is a function of both the dimensionless time t_D and dimensionless time radius r_{eD}, or:

$$p_D = f(t_D, r_{eD})$$

Table 1.2 *p_D versus t_D—infinite radial system, constant rate at the inner boundary (After Lee, J., Well Testing, SPE Textbook Series, permission to publish by the SPE, copyright SPE, 1982)*

t_D	p_D	t_D	p_D	t_D	p_D
0	0	0.15	0.3750	60.0	2.4758
0.0005	0.0250	0.2	0.4241	70.0	2.5501
0.001	0.0352	0.3	0.5024	80.0	2.6147
0.002	0.0495	0.4	0.5645	90.0	2.6718
0.003	0.0603	0.5	0.6167	100.0	2.7233
0.004	0.0694	0.6	0.6622	150.0	2.9212
0.005	0.0774	0.7	0.7024	200.0	3.0636
0.006	0.0845	0.8	0.7387	250.0	3.1726
0.007	0.0911	0.9	0.7716	300.0	3.2630
0.008	0.0971	1.0	0.8019	350.0	3.3394
0.009	0.1028	1.2	0.8672	400.0	3.4057
0.01	0.1081	1.4	0.9160	450.0	3.4641
0.015	0.1312	2.0	1.0195	500.0	3.5164
0.02	0.1503	3.0	1.1665	550.0	3.5643
0.025	0.1669	4.0	1.2750	600.0	3.6076
0.03	0.1818	5.0	1.3625	650.0	3.6476
0.04	0.2077	6.0	1.4362	700.0	3.6842
0.05	0.2301	7.0	1.4997	750.0	3.7184
0.06	0.2500	8.0	1.5557	800.0	3.7505
0.07	0.2680	9.0	1.6057	850.0	3.7805
0.08	0.2845	10.0	1.6509	900.0	3.8088
0.09	0.2999	15.0	1.8294	950.0	3.8355
0.1	0.3144	20.0	1.9601	1000.0	3.8584
		30.0	2.1470		
		40.0	2.2824		
		50.0	2.3884		

Notes: For $t_D < 0.01$: $p_D \cong 2zt_D/x$.
For $100 < t_D < 0.25r_e^2D$: $p_D \cong 0.5(\ln t_D + 0.80907)$.

where:

$$r_{eD} = \frac{\text{external radius}}{\text{wellbore radius}} = \frac{r_e}{r_w} \qquad [1.2.82]$$

Table 1.3 presents p_D as a function of t_D for $1.5 < r_{eD} < 10$. It should be pointed out that van Everdingen and Hurst principally applied the p_D function solution to model the performance of water influx into oil reservoirs. Thus, the authors' wellbore radius r_w was in this case the external radius of the reservoir and r_e was essentially the external boundary radius of the aquifer. Therefore, the ranges of the r_{eD} values in Table 1.3 are practical for this application.

Consider the Ei function solution to the diffusivity equations as given by Equation 1.2.66:

$$p(r,t) = p_i + \left[\frac{70.6QB\mu}{kh}\right] \text{Ei}\left[\frac{-948\phi\mu c_t r^2}{kt}\right]$$

This relationship can be expressed in a dimensionless form by manipulating the expression to give:

$$\frac{p_i - p(r,t)}{\left[\dfrac{141.2Q_oB_o\mu_o}{kh}\right]} = -\frac{1}{2}\text{Ei}\left[\frac{-(r/r_w)^2}{4\left(\dfrac{0.0002637kt}{\phi\mu c_t r_w^2}\right)}\right]$$

From the definition of the dimensionless variables of Equations 1.2.74 through 1.2.77, i.e., p_D, t_D, and r_D, this relation is expressed in terms of these dimensionless variables as:

$$p_D = -\frac{1}{2}\text{Ei}\left(-\frac{r_D^2}{4t_D}\right) \qquad [1.2.83]$$

Chatas (1953) proposed the following mathematical form for calculated p_D when $25 < t_D$ and $0.25r_{eD}^2 < t_D$:

$$p_D = \frac{0.5 + 2t_D}{r_{eD}^2 - 1} - \frac{r_{eD}^4\left[3 - 4\ln(r_{eD})\right] - 2r_{eD}^2 - 1}{4\left(r_{eD}^2 - 1\right)^2}$$

There are two special cases of the above equation which arise when $r_{eD}^2 \gg 1$ or when $t_D/r_{eD}^2 > 25$:

If $r_{eD}^2 \gg 1$, then:

$$p_D = \frac{2t_D}{r_{eD}^2} + \ln(r_{eD}) - 0.75$$

If $t_D/r_{eD}^2 > 25$, then:

$$p_D = \frac{1}{2}\left[\ln\frac{t_D}{r_D^2} + 0.80907\right] \qquad [1.2.84]$$

The computational procedure of using the p_D function to determine the bottom-hole flowing pressure changing the transient flow period, i.e., during the infinite-acting behavior, is summarized in the following steps:

Step 1. Calculate the dimensionless time t_D by applying Equation 1.2.75:

$$t_D = \frac{0.0002637kt}{\phi\mu c_t r_w^2}$$

Step 2. Determine the dimensionless radius r_{eD}. Note that for an infinite-acting reservoir, the dimensionless radius $r_{eD} = \infty$.

Step 3. Using the calculated value of t_D, determine the corresponding pressure function p_D from the appropriate table or equations, e.g., Equation 1.2.80 or 1.2.84:

For an infinite-acting reservoir $p_D = 0.5[\ln(t_D) + 0.80907]$

For a finite reservoir $p_D = \frac{1}{2}[\ln(t_D/r_D^2) + 0.80907]$

Step 4. Solve for the pressure by applying Equation 1.2.74:

$$p(r_w,t) = p_i - \left(\frac{141.2Q_oB_o\mu_o}{kh}\right)p_D \qquad [1.2.85]$$

Example 1.12 A well is producing at a constant flow rate of 300 STB/day under unsteady-state flow conditions. The reservoir has the following rock and fluid properties (see Example 1.10):

$B_o = 1.25$ bbl/STB, $\mu_o = 1.5$ cp, $c_t = 12 \times 10^{-6}$ psi^{-1}

$k = 60$ md, $h = 15$ ft, $p_i = 4000$ psi

$\phi = 15\%$, $r_w = 0.25$ ft

Assuming an infinite-acting reservoir, i.e., $r_{eD} = \infty$, calculate the bottom-hole flowing pressure after 1 hour of production by using the dimensionless pressure approach.

Solution

Step 1. Calculate the dimensionless time t_D from Equation 1.2.75:

$$t_D = \frac{0.0002637kt}{\phi\mu c_t r_w^2}$$

$$= \frac{0.000264\,(60)\,(1)}{(0.15)\,(1.5)\,(12\times10^{-6})\,(0.25)^2} = 93\,866.67$$

Step 2. Since $t_D > 100$, use Equation 1.2.80 to calculate the dimensionless pressure drop function:

$$p_D = 0.5[\ln(t_D) + 0.80907]$$

$$= 0.5[\ln(93\,866.67) + 0.80907] = 6.1294$$

Step 3. Calculate the bottom-hole pressure after 1 hour by applying Equation 1.2.85:

$$p\,(r_w,t) = p_i - \left(\frac{141.2Q_oB_o\mu_o}{kh}\right)p_D$$

$$p\,(0.25,1) = 4000 - \left[\frac{141.2\,(300)\,(1.25)\,(1.5)}{(60)\,(15)}\right]$$

$$\times\,(6.1294) = 3459 \text{ psi}$$

This example shows that the solution as given by the p_D function technique is identical to that of the Ei function approach. The main difference between the two formulations is that *the p_D function can only be used to calculate the pressure at radius r when the flow rate Q is constant and known.* In that case, the p_D function application is essentially restricted to the wellbore radius because the rate is usually known. On the other hand, the Ei function approach can be used to calculate the pressure at any radius in the reservoir by using the well flow rate Q.

It should be pointed out that, for an infinite-acting reservoir with $t_D > 100$, the p_D function is related to the Ei function by the following relation:

$$p_D = 0.5\left[-\text{Ei}\left(\frac{-1}{4t_D}\right)\right] \qquad [1.2.86]$$

The previous example, i.e., Example 1.12, is not a practical problem, but it is essentially designed to show the physical significance of the p_D solution approach. In transient flow testing, we normally record the bottom-hole flowing pressure as a function of time. Therefore, the dimensionless pressure drop technique can be used to determine one or more of the reservoir properties, e.g. k or kh, as discussed later in this chapter.

1.2.6 Radial flow of compressible fluids

Gas viscosity and density vary significantly with pressure and therefore the assumptions of Equation 1.2.64 are not satisfied for gas systems, i.e., compressible fluids. In order to develop the proper mathematical function for describing

Table 1.3 *p_D vs. t_D—finite radial system, constant rate at the inner boundary (After Lee, J., Well Testing, SPE Textbook Series, permission to publish by the SPE, copyright SPE, 1982)*

$r_{eD} = 1.5$		$r_{eD} = 2.0$		$r_{eD} = 2.5$		$r_{eD} = 3.0$		$r_{eD} = 3.5$		$r_{eD} = 4.0$	
t_D	p_D	t_D	p_D	t_D	p_D	t_D	p_D	t_D	p_D	t_D	p_D
0.06	0.251	0.22	0.443	0.40	0.565	0.52	0.627	1.0	0.802	1.5	0.927
0.08	0.288	0.24	0.459	0.42	0.576	0.54	0.636	1.1	0.830	1.6	0.948
0.10	0.322	0.26	0.476	0.44	0.587	0.56	0.645	1.2	0.857	1.7	0.968
0.12	0.355	0.28	0.492	0.46	0.598	0.60	0.662	1.3	0.882	1.8	0.988
0.14	0.387	0.30	0.507	0.48	0.608	0.65	0.683	1.4	0.906	1.9	1.007
0.16	0.420	0.32	0.522	0.50	0.618	0.70	0.703	1.5	0.929	2.0	1.025
0.18	0.452	0.34	0.536	0.52	0.628	0.75	0.721	1.6	0.951	2.2	1.059
0.20	0.484	0.36	0.551	0.54	0.638	0.80	0.740	1.7	0.973	2.4	1.092
0.22	0.516	0.38	0.565	0.56	0.647	0.85	0.758	1.8	0.994	2.6	1.123
0.24	0.548	0.40	0.579	0.58	0.657	0.90	0.776	1.9	1.014	2.8	1.154
0.26	0.580	0.42	0.593	0.60	0.666	0.95	0.791	2.0	1.034	3.0	1.184
0.28	0.612	0.44	0.607	0.65	0.688	1.0	0.806	2.25	1.083	3.5	1.255
0.30	0.644	0.46	0.621	0.70	0.710	1.2	0.865	2.50	1.130	4.0	1.324
0.35	0.724	0.48	0.634	0.75	0.731	1.4	0.920	2.75	1.176	4.5	1.392
0.40	0.804	0.50	0.648	0.80	0.752	1.6	0.973	3.0	1.221	5.0	1.460
0.45	0.884	0.60	0.715	0.85	0.772	2.0	1.076	4.0	1.401	5.5	1.527
0.50	0.964	0.70	0.782	0.90	0.792	3.0	1.328	5.0	1.579	6.0	1.594
0.55	1.044	0.80	0.849	0.95	0.812	4.0	1.578	6.0	1.757	6.5	1.660
0.60	1.124	0.90	0.915	1.0	0.832	5.0	1.828			7.0	1.727
0.65	1.204	1.0	0.982	2.0	1.215					8.0	1.861
0.70	1.284	2.0	1.649	3.0	1.506					9.0	1.994
0.75	1.364	3.0	2.316	4.0	1.977					10.0	2.127
0.80	1.444	5.0	3.649	5.0	2.398						

$r_{eD} = 4.5$		$r_{eD} = 5.0$		$r_{eD} = 6.0$		$r_{eD} = 7.0$		$r_{eD} = 8.0$		$r_{eD} = 9.0$		$r_{eD} = 10.0$	
t_D	p_D	t_D	p_D	t_D	p_D	t_D	p_D	t_D	p_D	t_D	p_D	t_D	p_D
2.0	1.023	3.0	1.167	4.0	1.275	6.0	1.436	8.0	1.556	10.0	1.651	12.0	1.732
2.1	1.040	3.1	1.180	4.5	1.322	6.5	1.470	8.5	1.582	10.5	1.673	12.5	1.750
2.2	1.056	3.2	1.192	5.0	1.364	7.0	1.501	9.0	1.607	11.0	1.693	13.0	1.768
2.3	1.702	3.3	1.204	5.5	1.404	7.5	1.531	9.5	1.631	11.5	1.713	13.5	1.784
2.4	1.087	3.4	1.215	6.0	1.441	8.0	1.559	10.0	1.663	12.0	1.732	14.0	1.801
2.5	1.102	3.5	1.227	6.5	1.477	8.5	1.586	10.5	1.675	12.5	1.750	14.5	1.817
2.6	1.116	3.6	1.238	7.0	1.511	9.0	1.613	11.0	1.697	13.0	1.768	15.0	1.832
2.7	1.130	3.7	1.249	7.5	1.544	9.5	1.638	11.5	1.717	13.5	1.786	15.5	1.847
2.8	1.144	3.8	1.259	8.0	1.576	10.0	1.663	12.0	1.737	14.0	1.803	16.0	1.862
2.9	1.158	3.9	1.270	8.5	1.607	11.0	1.711	12.5	1.757	14.5	1.819	17.0	1.890
3.0	1.171	4.0	1.281	9.0	1.638	12.0	1.757	13.0	1.776	15.0	1.835	18.0	1.917
3.2	1.197	4.2	1.301	9.5	1.668	13.0	1.810	13.5	1.795	15.5	1.851	19.0	1.943
3.4	1.222	4.4	1.321	10.0	1.698	14.0	1.845	14.0	1.813	16.0	1.867	20.0	1.968
3.6	1.246	4.6	1.340	11.0	1.757	15.0	1.888	14.5	1.831	17.0	1.897	22.0	2.017
3.8	1.269	4.8	1.360	12.0	1.815	16.0	1.931	15.0	1.849	18.0	1.926	24.0	2.063
4.0	1.292	5.0	1.378	13.0	1.873	17.0	1.974	17.0	1.919	19.0	1.955	26.0	2.108
4.5	1.349	5.5	1.424	14.0	1.931	18.0	2.016	19.0	1.986	20.0	1.983	28.0	2.151
5.0	1.403	6.0	1.469	15.0	1.988	19.0	2.058	21.0	2.051	22.0	2.037	30.0	2.194
5.5	1.457	6.5	1.513	16.0	2.045	20.0	2.100	23.0	2.116	24.0	2.906	32.0	2.236
6.0	1.510	7.0	1.556	17.0	2.103	22.0	2.184	25.0	2.180	26.0	2.142	34.0	2.278
7.0	1.615	7.5	1.598	18.0	2.160	24.0	2.267	30.0	2.340	28.0	2.193	36.0	2.319
8.0	1.719	8.0	1.641	19.0	2.217	26.0	2.351	35.0	2.499	30.0	2.244	38.0	2.360
9.0	1.823	9.0	1.725	20.0	2.274	28.0	2.434	40.0	2.658	34.0	2.345	40.0	2.401
10.0	1.927	10.0	1.808	25.0	2.560	30.0	2.517	45.0	2.817	38.0	2.446	50.0	2.604
11.0	2.031	11.0	1.892	30.0	2.846					40.0	2.496	60.0	2.806
12.0	2.135	12.0	1.975							45.0	2.621	70.0	3.008
13.0	2.239	13.0	2.059							50.0	2.746	80.0	3.210
14.0	2.343	14.0	2.142							60.0	2.996	90.0	3.412
15.0	2.447	15.0	2.225							70.0	3.246	100.0	3.614

Notes: For t_D smaller than values listed in this table for a given r_{eD} reservoir is infinite acting.
Find p_D in Table 1.2.
For $25 < t_D$ and t_D larger than values in table:

$$p_D \cong \frac{(1/2+2t_D)}{r_{eD}^2} - \frac{3r_{eD}^4 - 4r_{eD}^4 \ln r_{eD} - 2r_{eD}^2 - 1}{4\left(r_{eD}^2 - 1\right)^2}$$

For wells in rebounded reservoirs with $r_{eD}^2 \gg 1$:

$$p_D \cong \frac{2t_D}{r_{eD}^2} + \ln r_{eD} - 3/4.$$

the flow of compressible fluids in the reservoir, the following two additional gas equations must be considered:

(1) Gas density equation:

$$\rho = \frac{pM}{ZRT}$$

(2) Gas compressibility equation:

$$c_g = \frac{1}{p} - \frac{1}{Z}\frac{dZ}{dp}$$

Combining the above two basic gas equations with that of Equation 1.2.56 gives:

$$\frac{1}{r}\frac{\partial}{\partial r}\left(r\frac{p}{\mu Z}\frac{\partial p}{\partial r}\right) = \frac{\phi\mu c_t}{0.000264k}\frac{p}{\mu Z}\frac{\partial p}{\partial t} \quad [1.2.87]$$

where:

t = time, hours
k = permeability, md
c_t = total isothermal compressibility, psi^{-1}
ϕ = porosity

Al-Hussainy et al. (1966) linearized the above basic flow equation by introducing the real-gas pseudopressure $m(p)$ into Equation 1.2.87. Recalling the previously defined $m(p)$ equation:

$$m(p) = \int_0^p \frac{2p}{\mu Z}\,dp \quad [1.2.88]$$

and differentiating this relation with respect to p, gives:

$$\frac{\partial m(p)}{\partial p} = \frac{2p}{\mu Z} \quad [1.2.89]$$

The following relationships are obtained by applying the chain rule:

$$\frac{\partial m(p)}{\partial r} = \frac{\partial m(p)}{\partial p}\frac{\partial p}{\partial r} \quad [1.2.90]$$

$$\frac{\partial m(p)}{\partial t} = \frac{\partial m(p)}{\partial p}\frac{\partial p}{\partial t} \quad [1.2.91]$$

Substituting Equation 1.2.89 into 1.2.90 and 1.2.91, gives:

$$\frac{\partial p}{\partial r} = \frac{\mu Z}{2p}\frac{\partial m(p)}{\partial r} \quad [1.2.92]$$

and:

$$\frac{\partial p}{\partial t} = \frac{\mu Z}{2p}\frac{\partial m(p)}{\partial t} \quad [1.2.93]$$

Combining Equations 1.2.92 and 1.2.93 with 1.2.87, yields:

$$\frac{\partial^2 m(p)}{\partial r^2} + \frac{1}{r}\frac{\partial m(p)}{\partial r} = \frac{\phi\mu c_t}{0.000264k}\frac{\partial m(p)}{\partial t} \quad [1.2.94]$$

Equation 1.2.94 is the radial diffusivity equation for compressible fluids. This differential equation relates the real-gas pseudopressure (real-gas potential) to the time t and the radius r. Al-Hussany et al. (1966) pointed out that in gas well testing analysis, the constant-rate solution has more practical applications than that provided by the constant-pressure solution. The authors provided the exact solution to Equation 1.2.94 that is commonly referred to as the $m(p)$ solution method. There are also two other solutions that approximate the exact solution. These two approximation methods are called the pressure-squared method and the pressure method. In general, there are three forms of mathematical solution to the diffusivity equation:

(1) $m(p)$ solution method (exact solution);
(2) pressure-squared method (p^2 approximation method);
(3) pressure-method (p approximation method).

These three solution methods are presented below.

First solution: m(p) method (exact solution)

Imposing the constant-rate condition as one of the boundary conditions required to solve Equation 1.2.94, Al-Hussany et al. (1966) proposed the following exact solution to the diffusivity equation:

$$m(p_{wf}) = m(p_i) - 57\,895.3\left(\frac{p_{sc}}{T_{sc}}\right)\left(\frac{Q_g T}{kh}\right) \times \left[\log\left(\frac{kt}{\phi\mu_i c_{ti} r_w^2}\right) - 3.23\right] \quad [1.2.95]$$

where:

p_{wf} = bottom-hole flowing pressure, psi
p_e = initial reservoir pressure
Q_g = gas flow rate, Mscf/day
t = time, hours
k = permeability, md
p_{sc} = standard pressure, psi
T_{sc} = standard temperature, °R
T = Reservoir temperature
r_w = wellbore radius, ft
h = thickness, ft
μ_i = gas viscosity at the initial pressure, cp
c_{ti} = total compressibility coefficient at p_i, psi^{-1}
ϕ = porosity

Setting $p_{sc} = 14.7$ psia and $T_{sc} = 520$°R, then Equation 1.2.95 reduces to:

$$m(p_{wf}) = m(p_i) - \left(\frac{1637 Q_g T}{kh}\right)\left[\log\left(\frac{kt}{\phi\mu_i c_{ti} r_w^2}\right) - 3.23\right] \quad [1.2.96]$$

The above equation can be simplified by introducing the dimensionless time (as defined previously by Equation 1.2.74) into Equation 1.2.96:

$$t_D = \frac{0.0002637\,kt}{\phi\mu_i c_{ti} r_w^2}$$

Equivalently, Equation 1.2.96 can be written in terms of the dimensionless time t_D as:

$$m(p_{wf}) = m(p_i) - \left(\frac{1637 Q_g T}{kh}\right)\left[\log\left(\frac{4t_D}{\gamma}\right)\right] \quad [1.2.97]$$

The parameter γ is called Euler's constant and is given by:

$$\gamma = e^{0.5772} = 1.781 \quad [1.2.98]$$

The solution to the diffusivity equation as given by Equations 1.2.96 and 1.2.97 expresses the bottom-hole real-gas pseudopressure as a function of the transient flow time t. The solution as expressed in terms of $m(p)$ is the recommended mathematical expression for performing gas well pressure analysis due to its applicability in all pressure ranges.

The radial gas diffusivity equation can be expressed in a dimensionless form in terms of the dimensionless real-gas pseudopressure drop ψ_D. The solution to the dimensionless equation is given by:

$$\psi_D = \frac{m(p_i) - m(p_{wf})}{(1422 Q_g T/kh)}$$

or:

$$m(p_{wf}) = m(p_i) - \left(\frac{1422 Q_g T}{kh}\right)\psi_D \quad [1.2.99]$$

where:

Q_g = gas flow rate, Mscf/day
k = permeability, md

The dimensionless pseudopressure drop ψ_D can be determined as a function of t_D by using the appropriate expression

of Equations 1.2.79 through 1.2.84. When $t_D > 100$, ψ_D can be calculated by applying Equation 1.2.70. That is:

$$\psi_D = 0.5[\ln(t_D) + 0.80907] \quad [1.2.100]$$

Example 1.13 A gas well with a wellbore radius of 0.3 ft is producing at a constant flow rate of 2000 Mscf/day under transient flow conditions. The initial reservoir pressure (shut-in pressure) is 4400 psi at 140°F. The formation permeability and thickness are 65 md and 15 ft, respectively. The porosity is recorded as 15%. Example 1.7 documents the properties of the gas as well as values of $m(p)$ as a function of pressures. The table is reproduced below for convenience:

P	μ_g(cp)	Z	$m(p)$ (psi^2/cp)
0	0.01270	1.000	0.000
400	0.01286	0.937	13.2×10^6
800	0.01390	0.882	52.0×10^6
1200	0.01530	0.832	113.1×10^6
1600	0.01680	0.794	198.0×10^6
2000	0.01840	0.770	304.0×10^6
2400	0.02010	0.763	422.0×10^6
2800	0.02170	0.775	542.4×10^6
3200	0.02340	0.797	678.0×10^6
3600	0.02500	0.827	816.0×10^6
4000	0.02660	0.860	950.0×10^6
4400	0.02831	0.896	1089.0×10^6

Assuming that the initial total isothermal compressibility is 3×10^{-4} psi^{-1}, calculate the bottom-hole flowing pressure after 1.5 hours.

Solution

Step 1. Calculate the dimensionless time t_D:

$$t_D = \frac{0.0002637kt}{\phi\mu_i c_{ti} r_w^2}$$

$$= \frac{(0.0002637)(65)(1.5)}{(0.15)(0.02831)(3 \times 10^{-4})(0.3^2)} = 224\,498.6$$

Step 2. Solve for $m(p_{wf})$ by using Equation 1.2.97:

$$m(p_{wf}) = m(p_i) - \left(\frac{1637Q_gT}{kh}\right)\left[\log\left(\frac{4t_D}{\gamma}\right)\right]$$

$$= 1089 \times 10^6 - \frac{(1637)(2000)(600)}{(65)(15)}$$

$$\times \left[\log\left(\frac{(4)224498.6}{e^{0.5772}}\right)\right] = 1077.5 \times 10^6$$

Step 3. From the given *PVT* data, interpolate using the value of $m(p_{wf})$ to give a corresponding p_{wf} of 4367 psi.

An identical solution can be obtained by applying the ψ_D approach as shown below:

Step 1. Calculate ψ_D from Equation 1.2.100:

$$\psi_D = 0.5[\ln(t_D) + 0.80907]$$

$$= 0.5[\ln(224\,498.6) + 0.8090] = 6.565$$

Step 2. Calculate m(p_{wf}) by using Equation 1.2.99:

$$m(p_{wf}) = m(p_i) - \left(\frac{1422Q_gT}{kh}\right)\psi_D$$

$$= 1089 \times 10^6 - \left(\frac{1422(2000)(600)}{(65)(15)}\right)(6.565)$$

$$= 1077.5 \times 10^6$$

By interpolation at $m(p_{wf}) = 1077.5 \times 10^6$, this gives a corresponding value of $p_{wf} = 4367$ psi.

Second solution: pressure-squared method

The first approximation to the exact solution is to move the pressure-dependent term (μZ) outside the integral that defines $m(p_{wf})$ and $m(p_i)$, to give:

$$m(p_i) - m(p_{wf}) = \frac{2}{\overline{\mu}\overline{Z}} \int_{p_{wf}}^{p_i} p \, dp \quad [1.2.101]$$

or:

$$m(p_i) - m(p_{wf}) = \frac{p_i^2 - p_{wf}^2}{\overline{\mu}\overline{Z}} \quad [1.2.102]$$

The bars over μ and Z represent the values of the gas viscosity and deviation factor as evaluated at the average pressure $\overline{p}$. This average pressure is given by:

$$\overline{p} = \sqrt{\frac{p_i^2 + p_{wf}^2}{2}} \quad [1.2.103]$$

Combining Equation 1.2.102 with 1.2.96, 1.2.97, or 1.2.99, gives:

$$p_{wf}^2 = p_i^2 - \left(\frac{1637Q_gT\overline{\mu}\overline{Z}}{kh}\right)\left[\log\left(\frac{kt}{\phi\mu_i c_{ti} r_w^2}\right) - 3.23\right] \quad [1.2.104]$$

or:

$$p_{wf}^2 = p_i^2 - \left(\frac{1637Q_gT\overline{\mu}\overline{Z}}{kh}\right)\left[\log\left(\frac{4t_D}{\gamma}\right)\right] \quad [1.2.105]$$

Equivalently:

$$p_{wf}^2 = p_i^2 - \left(\frac{1422Q_gT\overline{\mu}\overline{Z}}{kh}\right)\psi_D \quad [1.2.106]$$

The above approximation solution forms indicate that the product (μZ) is assumed constant at the average pressure $\overline{p}$. This effectively limits the applicability of the p^2 method to reservoir pressures of less than 2000. It should be pointed out that when the p^2 method is used to determine p_{wf} it is perhaps sufficient to set $\overline{\mu}\overline{Z} = \mu_i Z$.

Example 1.14 A gas well is producing at a constant rate of 7454.2 Mscf/day under transient flow conditions. The following data is available:

$k = 50$ md, $h = 10$ ft, $\phi = 20\%$, $p_i = 1600$ psi

$T = 600$°R, $r_w = 0.3$ ft, $c_{ti} = 6.25 \times 10^{-4}$ psi^{-1}

The gas properties are tabulated below:

P	μ_g (cp)	Z	$m(p)$ (psi^2/cp)
0	0.01270	1.000	0.000
400	0.01286	0.937	13.2×10^6
800	0.01390	0.882	52.0×10^6
1200	0.01530	0.832	113.1×10^6
1600	0.01680	0.794	198.0×10^6

Calculate the bottom-hole flowing pressure after 4 hours by using:

(a) the $m(p)$ method;
(b) the p^2 method.

Solution

(a) The $m(p)$ method:

Step 1. Calculate t_D:

$$t_D = \frac{0.000264\,(50)\,(4)}{(0.2)\,(0.0168)\,(6.25\times10^{-4})\,(0.3^2)}$$

$$= 279\,365.1$$

Step 2. Calculate ψ_D:

$$\psi_D = 0.5[\ln(t_D) + 0.80907]$$

$$= 0.5\left[\ln(279\,365.1) + 0.80907\right] = 6.6746$$

Step 3. Solve for $m(p_{wf})$ by applying Equation 1.2.99:

$$m(p_{wf}) = m(p_i) - \left(\frac{1422Q_gT}{kh}\right)\psi_D$$

$$= \left(198\times10^6\right) - \left[\frac{1422(7454.2)(600)}{(50)(10)}\right]6.6746$$

$$= 113.1\times10^6$$

The corresponding value of $p_{wf} = 1200$ psi.

(b) The p^2 method:

Step 1. Calculate ψ_D by applying Equation 1.2.100:

Step 2. Calculate p^2_{wf} by applying Equation 1.2.106:

$$p^2_{wf} = p^2_i - \left(\frac{1422Q_gT\overline{\mu}\overline{Z}}{kh}\right)\psi_D$$

$$= 1600^2 - \left[\frac{(1422)(7454.2)(600)(0.0168)(0.794)}{(50)(10)}\right]6.6747$$

$$= 1427491$$

$p_{wf} = 1195$ psi.

Step 3. The absolute average error is 0.4%.

Third solution: pressure approximation method

The second method of approximation to the exact solution of the radial flow of gases is to treat the gas as a pseudo-liquid. Recal that the gas formation volume factor B_g as expressed in bbl/scf is given by:

$$B_g = \left(\frac{p_{sc}}{5.615T_{sc}}\right)\left(\frac{ZT}{p}\right)$$

or:

$$B_g = 0.00504\left(\frac{ZT}{p}\right)$$

Solving the above expression for p/Z gives:

$$\frac{p}{Z} = \left(\frac{Tp_{sc}}{5.615T_{sc}}\right)\left(\frac{1}{B_g}\right)$$

The difference in the real-gas pseudopressure is given by:

$$m(p_i) - (p_{wf}) = \int_{p_{wf}}^{p_i}\frac{2p}{\mu Z}\,dp$$

Combining the above two expressions gives:

$$m(p_i) - m(p_{wf}) = \frac{2Tp_{sc}}{5.615T_{sc}}\int_{p_{wf}}^{p_i}\left(\frac{1}{\mu B_g}\right)dp \qquad [1.2.107]$$

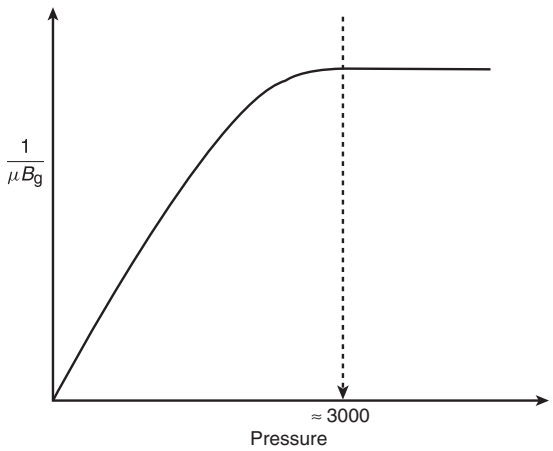

Figure 1.22 *Plot of* $1/\mu B_g$ *vs. pressure.*

Fetkovich (1973) suggested that at high pressures above 3000 psi ($p > 3000$), $1/\mu B_g$ is nearly constant as shown schematically in Figure 1.22. Imposing Fetkovich's condition on Equation 1.2.107 and integrating gives:

$$m(p_i) - m(p_{wf}) = \frac{2Tp_{sc}}{5.615T_{sc}\overline{\mu}\overline{B_g}}\left(p_i - p_{wf}\right) \qquad [1.2.108]$$

Combining Equation 1.2.108 with 1.2.96, 1.2.97, or 1.2.99 gives:

$$p_{wf} = p_i - \left(\frac{162.5\times10^3Q_g\overline{\mu}\overline{B_g}}{kh}\right)\left[\log\left(\frac{kt}{\phi\overline{\mu}\overline{c_t}r_w^2}\right) - 3.23\right] \qquad [1.2.109]$$

or:

$$p_{wf} = p_i - \left(\frac{(162.5\times10^3)Q_g\overline{\mu}\overline{B_g}}{kh}\right)\left[\log\left(\frac{4t_D}{\gamma}\right)\right] \qquad [1.2.110]$$

or, equivalently, in terms of dimensionless pressure drop:

$$p_{wf} = p_i - \left(\frac{(141.2\times10^3)Q_g\overline{\mu}\overline{B_g}}{kh}\right)p_D \qquad [1.2.111]$$

where:

Q_g = gas flow rate, Mscf/day
k = permeability, md
B_g = gas formation volume factor, bbl/scf
t = time, hours
p_D = dimensionless pressure drop
t_D = dimensionless

It should be noted that the gas properties, i.e., μ, B_g, and c_t, are evaluated at pressure $\bar{p}$ as defined below:

$$\bar{p} = \frac{p_i + p_{wf}}{2} \qquad [1.2.112]$$

Again, this method is limited only to applications above 3000 psi. When solving for p_{wf}, it might be sufficient to evaluate the gas properties at p_i.

Example 1.15 The data of Example 1.13 is repeated below for convenience.

A gas well with a wellbore radius of 0.3 ft is producing at a constant flow rate of 2000 Mscf/day under transient flow conditions. The initial reservoir pressure (shut-in pressure) is 4400 psi at 140°F. The formation permeability and thickness are 65 md and 15 ft, respectively. The porosity is recorded as 15%. The properties of the gas as well

as values of $m(p)$ as a function of pressures are tabulated below:

P	μ_g (cp)	Z	$m(p)$ (psi^2/cp)
0	0.01270	1.000	0.000
400	0.01286	0.937	13.2×10^6
800	0.01390	0.882	52.0×10^6
1200	0.01530	0.832	113.1×10^6
1600	0.01680	0.794	198.0×10^6
2000	0.01840	0.770	304.0×10^6
2400	0.02010	0.763	422.0×10^6
2800	0.02170	0.775	542.4×10^6
3200	0.02340	0.797	678.0×10^6
3600	0.02500	0.827	816.0×10^6
4000	0.02660	0.860	950.0×10^6
4400	0.02831	0.896	1089.0×10^6

Assuming that the initial total isothermal compressibility is 3×10^{-4}psi^{-1}, calculate, the bottom-hole flowing pressure after 1.5 hours by using the p approximation method and compare it with the exact solution.

Solution

Step 1. Calculate the dimensionless time t_D:

$$t_D = \frac{0.0002637kt}{\phi\mu_i c_{ti} r_w^2}$$

$$= \frac{(0.000264)(65)(1.5)}{(0.15)(0.02831)(3 \times 10^{-4})(0.3^2)} = 224\,498.6$$

Step 2. Calculate B_g at p_i:

$$B_g = 0.00504\left(\frac{Z_i T}{p_i}\right)$$

$$= 0.00504\frac{(0.896)(600)}{4400} = 0.0006158 \text{ bbl/scf}$$

Step 3. Calculate the dimensionless pressure p_D by applying Equation 1.2.80:

$$p_D = 0.5[\ln(t_D) + 0.80907]$$

$$= 0.5\left[\ln(224\,498.6) + 0.80907\right] = 6.565$$

Step 4. Approximate p_{wf} from Equation 1.2.111:

$$p_{wf} = p_i - \left(\frac{(141.210^3)Q_g\overline{\mu}\overline{B_g}}{kh}\right)p_D$$

$$= 4400 - \left[\frac{141.2 \times 10^3(2000)(0.02831)(0.0006158)}{(65)(15)}\right]6.565$$

$$= 4367 \text{ psi}$$

The solution is identical to that of the exact solution of Example 1.13.

It should be pointed out that Examples 1.10 through 1.15 are designed to illustrate the use of different solution methods. However, these examples are not practical because, in transient flow analysis, the bottom-hole flowing pressure is usually available as a function of time. All the previous methodologies are essentially used to characterize the reservoir by determining the permeability k or the permeability and thickness product (kh).

1.2.7 Pseudosteady state

In the unsteady-state flow cases discussed previously, it was assumed that a well is located in a very large reservoir and producing at a constant flow rate. This rate creates a pressure disturbance in the reservoir that travels throughout this "infinite-size reservoir." During this transient flow period, reservoir boundaries have no effect on the pressure behavior of the well. Obviously, the time period when this assumption can be imposed is often very short in length. As soon as the pressure disturbance reaches all drainage boundaries, it ends the transient (unsteady-state) flow regime and the beginning of the boundary-dominated flow condition. This different type of flow regime is called pseudosteady (semisteady)-State Flow. It is necessary at this point to impose different boundary conditions on the diffusivity equation and drive an appropriate solution to this flow regime.

Consider Figure 1.23 which shows a well in a radial system that is producing at a constant rate for a long enough period that eventually affects the entire drainage area. During this semisteady-state flow, the change in pressure with time becomes the same throughout the drainage area. Figure 1.23(b) shows that the pressure distributions become paralleled at successive time periods. Mathematically, this important condition can be expressed as:

$$\left(\frac{\partial p}{\partial t}\right)_r = \text{constant} \qquad [1.2.113]$$

The "constant" referred to in the above equation can be obtained from a simple material balance using the definition of the compressibility, assuming no free gas production, thus:

$$c = \frac{-1}{V}\frac{dV}{dp}$$

Rearranging:

$$cV\,dp = -dV$$

Differentiating with respect to time t:

$$cV\frac{dp}{dt} = -\frac{dV}{dt} = q$$

or:

$$\frac{dp}{dt} = -\frac{q}{cV}$$

Expressing the pressure decline rate dp/dt in the above relation in psi/hr gives:

$$\frac{dp}{dt} = -\frac{q}{24cV} = -\frac{Q_o B_o}{24cV} \qquad [1.2.114]$$

where:

q = flow rate, bbl/day
Q_o = flow rate, STB/day
dp/dt = pressure decline rate, psi/hr
V = pore volume, bbl

For a radial drainage system, the pore volume is given by:

$$V = \frac{\pi r_e^2 h\phi}{5.615} = \frac{Ah\phi}{5.615} \qquad [1.2.115]$$

where:

A = drainage area, ft^2

Combining Equation 1.2.115 with 1.2.114 gives:

$$\frac{dp}{dt} = -\frac{0.23396q}{c_t(\pi r_e^2)h\phi} = \frac{-0.23396q}{c_t Ah\phi} = \frac{-0.23396q}{c_t(\text{pore volume})} \qquad [1.2.116]$$

Examining Equation 1.2.116 reveals the following important characteristics of the behavior of the pressure decline rate

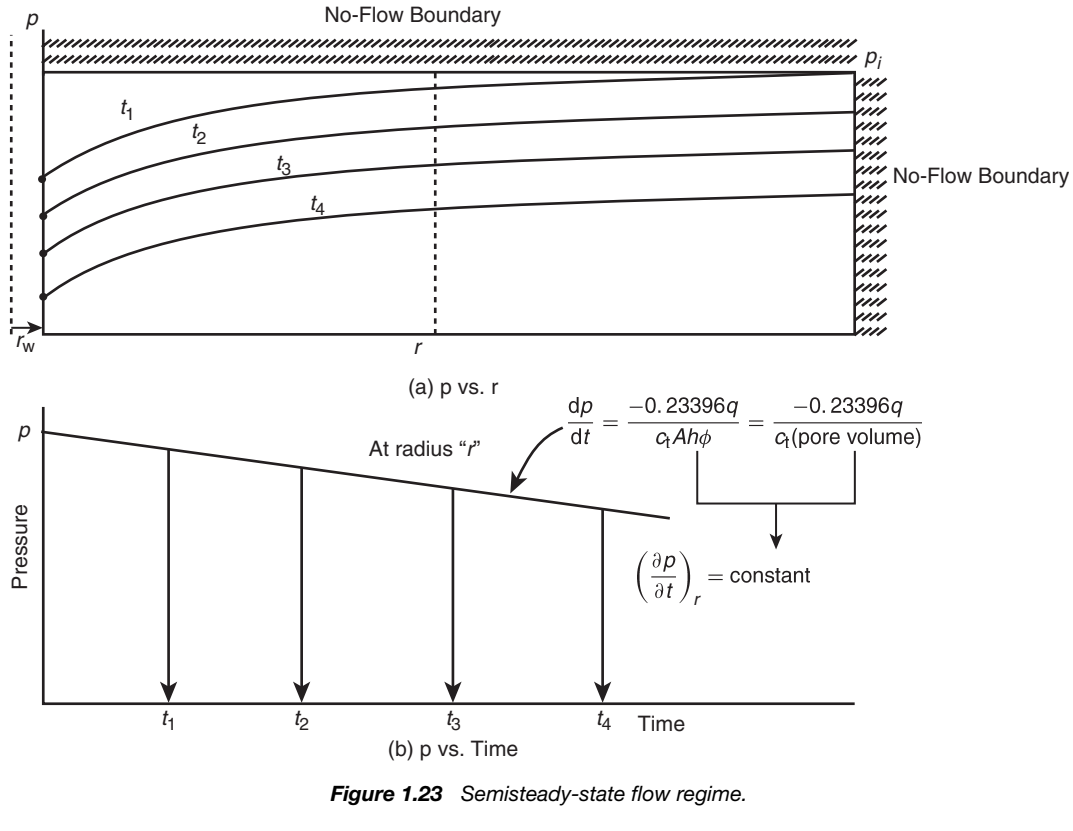

Figure 1.23 *Semisteady-state flow regime.*

dp/dt during the semisteady-state flow:

- the reservoir pressure declines at a higher rate with increasing fluid production rate;
- the reservoir pressure declines at a slower rate for reservoirs with higher total compressibility coefficients;
- the reservoir pressure declines at a lower rate for reservoirs with larger pore volumes.

And in the case of water influx with an influx rate of e_w bbl/day, the equation can be modified as:

$$\frac{dp}{dt} = \frac{-0.23396q + e_w}{c_t\,(\text{pore volume})}$$

Example 1.16 An oil well is producing at constant oil flow rate of 120 STB/day under a semisteady-state flow regime. Well testing data indicates that the pressure is declining at a constant rate of 0.04655 psi/hr. The following addition data is available:

$$h = 72 \text{ ft}, \qquad \phi = 25\%,$$
$$B_o = 1.3 \text{ bbl/STB}, \quad c_t = 25 \times 10^{-6} \text{ psi}^{-1}$$

Calculate the well drainage area.

Solution Here:

$$q = Q_o B_o = (120)(1.3) = 156 \text{ bbl/day}$$

Apply Equation 1.2.116 to solve for A:

$$\frac{dp}{dt} = -\frac{0.23396q}{c_t(\pi r_e^2)h\phi} = \frac{-0.23396q}{c_t Ah\phi} = \frac{-0.23396q}{c_t(\text{pore volume})}$$

$$-0.04655 = -\frac{0.23396(156)}{(25 \times 10^{-6})(A)(72)(0.25)}$$

$$A = 1\,742\,400 \text{ ft}^2$$

or:

$$A = 1\,742\,400/43\,560 = 40 \text{ acres}$$

Matthews et al. (1954) pointed out that once the reservoir is producing *under the semisteady-state condition*, each well will drain from within its own no-flow boundary independently of the other wells. For this condition to prevail, the pressure decline rate dp/dt must be approximately constant throughout the entire reservoir, otherwise flow would occur across the boundaries causing a readjustment in their positions. Because the pressure at every point in the reservoir is changing at the same rate, it leads to the conclusion that the average reservoir pressure is changing at the same rate. This average reservoir pressure is essentially set equal to the volumetric average reservoir pressure $\bar{p}_r$. It is the pressure that is used to perform flow calculations during the semisteady-state flowing condition. The above discussion indicates that, in principle, Equation 1.2.116 can be used to estimate the average pressure in the well drainage area $\bar{p}$ by replacing the pressure decline rate dp/dt with $(p_i - \bar{p})/t$, or:

$$p_i - \bar{p} = \frac{0.23396qt}{c_t(Ah\phi)}$$

or:

$$\bar{p} = p_i - \left[\frac{0.23396q}{c_t(Ah\phi)}\right]t \qquad [1.2.117]$$

Note that the above expression is essentially an equation of a straight line, with a slope of m\ and intercept of p_i, as

expressed by:

$$\bar{p} = a + m^{\backslash} t$$

$$m^{\backslash} = -\left[\frac{0.23396q}{c_t(Ah\phi)}\right] = -\left[\frac{0.23396q}{c_t(\text{pore volume})}\right]$$

$$a = p_i$$

Equation 1.2.117 indicates that the average reservoir pressure, after producing a cumulative oil production of N_p STB, can be roughly approximated by:

$$\bar{p} = p_i - \left[\frac{0.23396B_oN_p}{c_t(Ah\phi)}\right]$$

It should be noted that when performing material balance calculations, the volumetric average pressure of the entire reservoir is used to calculate the fluid properties. This pressure can be determined from the individual well drainage properties as follows:

$$\bar{p}_r = \frac{\sum_j (\bar{p}V)_j}{\sum_j V_j}$$

in which:

V_j = pore volume of the jth well drainage volume
$(\bar{p})_j$ = volumetric average pressure *within the jth drainage volume*

Figure 1.24 illustrates the concept of the volumetric average pressure. In practice, the V_i are difficult to determine and, therefore, it is common to use individual well flow rates q_i in determining the average reservoir pressure from individual well average drainage pressure:

$$\bar{p}_r = \frac{\sum_j (\bar{p}q)_j}{\sum_j q_j}$$

The flow rates are measured on a routing basis throughout the lifetime of the field, thus facilitating the calculation of the volumetric average reservoir pressure $\bar{p}_r$. Alternatively, the average reservoir pressure can be expressed in terms of the individual well average drainage pressure decline rates and fluid flow rates by:

$$\bar{p}_r = \frac{\sum_j [(\bar{p}q)_j/(\partial\bar{p}/\partial t)_j]}{\sum_j [q_j/(\partial\bar{p}/\partial t)_j]} \qquad [1.2.118]$$

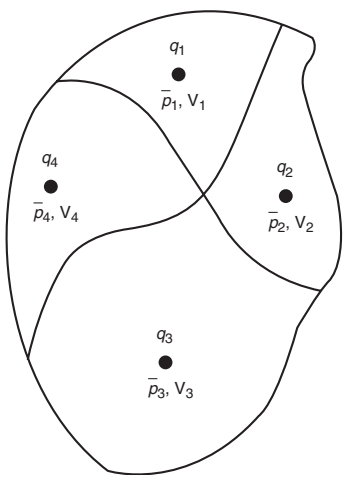

Figure 1.24 *Volumetric average reservoir pressure.*

However, since the material balance equation is usually applied at regular intervals of 3–6 months, i.e., Δt = 3–6 months, throughout the lifetime of the field, the average field pressure can be expressed in terms of the incremental net change in underground fluid withdrawal $\Delta(F)$ as:

$$\bar{p}_r = \frac{\sum_j \bar{p}_j \Delta(F)_j / \Delta\bar{p}_j}{\sum_j \Delta(F)_j / \Delta\bar{p}_j} \qquad [1.2.119]$$

where the total underground fluid withdrawal at time t and $t + \Delta t$ are given by:

$$F_t = \int_0^t [Q_oB_o + Q_wB_w + (Q_g - Q_oR_s - Q_wR_{sw})B_g]dt$$

$$F_{t+\Delta t} = \int_0^{t+\Delta t} [Q_oB_o + Q_wB_w + (Q_g - Q_oR_s - Q_wR_{sw})B_g]dt$$

with:

$$\Delta(F) = F_{t+\Delta t} - F_t$$

and where:

R_s = gas solubility, scf/STB
R_{sw} = gas solubility in the water, scf/STB
B_g = gas formation volume factor, bbl/scf
Q_o = oil flow rate, STB/day
q_o = oil flow rate, bbl/day
Q_w = water flow rate, STB/day
q_w = water flow rate, bbl/day
Q_g = gas flow rate, scf/day

The practical applications of using the pseudosteady-state flow condition to describe the flow behavior of the following two types of fluids are presented below:

(1) radial flow of slightly compressible fluids;
(2) radial flow of compressible fluids.

1.2.8 Radial flow of slightly compressible fluids

The diffusivity equation as expressed by Equation 1.2.61 for the transient flow regime is:

$$\frac{\partial^2 p}{\partial r^2} + \frac{1}{r}\frac{\partial p}{\partial r} = \left(\frac{\phi\mu c_t}{0.000264k}\right)\frac{\partial p}{\partial t}$$

For the semisteady-state flow, the term $\partial p/\partial t$ is constant and is expressed by Equation 1.2.116. Substituting Equation 1.2.116 into the diffusivity equation gives:

$$\frac{\partial^2 p}{\partial r^2} + \frac{1}{r}\frac{\partial p}{\partial r} = \left(\frac{\phi\mu c_t}{0.000264k}\right)\left(\frac{-0.23396q}{c_tAh\phi}\right)$$

or:

$$\frac{\partial^2 p}{\partial r^2} + \frac{1}{r}\frac{\partial p}{\partial r} = \frac{-887.22q\mu}{Ahk}$$

This expression can be expressed as:

$$\frac{1}{r}\frac{\partial}{\partial r}\left(r\frac{\partial p}{\partial r}\right) = -\frac{887.22q\mu}{(\pi r_e^2)hk}$$

Integrating this equation gives:

$$r\frac{\partial p}{\partial r} = -\frac{887.22q\mu}{(\pi r_e^2)hk}\left(\frac{r^2}{2}\right) + c_1$$

where c_1 is the constant of integration and can be evaluated by imposing the outer no-flow boundary condition (i.e., $(\partial p/\partial r)_{re} = 0$) on the above relation, to give:

$$c_1 = \frac{141.2q\mu}{\pi hk}$$

Combining these two expressions gives:

$$\frac{\partial p}{\partial r} = \frac{141.2q\mu}{hk}\left(\frac{1}{r} - \frac{r}{r_e^2}\right)$$

Integrating again:

$$\int_{p_{wf}}^{p_i} dp = \frac{141.2q\mu}{hk}\int_{rw}^{re}\left(\frac{1}{r}-\frac{r}{r_e^2}\right)dr$$

Performing the above integration and assuming r_w^2/r_e^2 is negligible gives:

$$(p_i - p_{wf}) = \frac{141.2q\mu}{kh}\left[\ln\left(\frac{r_e}{r_w}\right)-\frac{1}{2}\right]$$

A more appropriate form of the above is to solve for the flow rate as expressed in STB/day, to give:

$$Q = \frac{0.00708kh\,(p_i - p_{wf})}{\mu B\left[\ln\left(r_e/r_w\right)-0.5\right]} \qquad [1.2.120]$$

where:

Q = flow rate, STB/day
B = formation volume factor, bbl/STB
k = permeability, md

The volumetric average pressure in the well drainage area $\bar{p}$ is commonly used in calculating the liquid flow rate under the semisteady-state flowing condition. Introducing $\bar{p}$ into Equation 1.2.120 gives:

$$Q = \frac{0.00708kh\,(\bar{p} - p_{wf})}{\mu B\left[\ln\left(r_e/r_w\right)-0.75\right]} = \frac{(\bar{p} - p_{wf})}{141.2\mu B\left[\ln\left(r_e/r_w\right)-0.75\right]} \qquad [1.2.121]$$

Note that:

$$\ln\left(\frac{r_e}{r_w}\right) - 0.75 = \ln\left(\frac{0.471r_e}{r_w}\right)$$

The above observation suggests that the volumetric average pressure $\bar{p}$ occur at about 47% of the drainage radius during the semisteady-state condition. That is:

$$Q = \frac{0.00708kh\,(\bar{p} - p_{wf})}{\mu B\left[\ln\left(0.471r_e/r_w\right)\right]}$$

It should be pointed out that the pseudosteady-state flow occurs regardless of the geometry of the reservoir. Irregular geometries also reach this state when they have been produced long enough for the entire drainage area to be affected.

Rather than developing a separate equation for the geometry of each drainage area, Ramey and Cobb (1971) introduced a correction factor called the shape factor C_A which is designed to account for the deviation of the drainage area from the ideal circular form. The shape factor, as listed in Table 1.4, accounts also for the location of the well within the drainage area. Introducing C_A into Equation 1.2.121 and solving for p_{wf} gives the following two solutions:

(1) In terms of the volumetric average pressure $\bar{p}$:

$$p_{wf} = \bar{p} - \frac{162.6QB\mu}{kh}\log\left(\frac{2.2458A}{C_A r_w^2}\right) \qquad [1.2.122]$$

(2) In terms of the initial reservoir pressure, p_i, recall Equation 1.2.117 which shows the changes of the average reservoir pressure $\bar{p}$ as a function of time and initial reservoir pressure p_i:

$$\bar{p} = p_i - \frac{0.23396qt}{c_t Ah\phi}$$

Combining this equation with Equation 1.2.122 gives:

$$p_{wf} = \left(p_i - \frac{0.23396QBt}{Ah\phi c_t}\right) - \frac{162.6QB\mu}{kh}\log\left(\frac{2.2458A}{C_A r_w^2}\right) \qquad [1.2.123]$$

where:

k = permeability, md
A = drainage area, ft^2
C_A = shape rate
Q = flow rate, STB/day
t = time, hours
c_t = total compressibility coefficient, psi^{-1}

Equation 1.2.123 can be slightly rearranged as:

$$p_{wf} = \left[p_i - \frac{162.6QB\mu}{kh}\log\left(\frac{2.2458A}{C_A r_w^2}\right)\right] - \left(\frac{0.23396QB}{Ah\phi c_t}\right)t$$

The above expression indicates that under semisteady-state flow and constant flow rate, it can be expressed as an equation of a straight line:

$$p_{wf} = a_{pss} + m_{pss}t$$

with a_{pss} and m_{pss} as defined by:

$$a_{pss} = \left[p_i - \frac{162.6QB\mu}{kh}\log\left(\frac{2.2458A}{C_A r_w^2}\right)\right]$$

$$m_{pss} = -\left(\frac{0.23396QB}{c_t(Ah\phi)}\right) = -\left(\frac{0.23396QB}{c_t(\text{pore volume})}\right)$$

It is obvious that during the pseudosteady (semisteady)-state flow condition, a plot of the bottom-hole flowing pressure p_{wf} versus time t would produce a straight line with a negative slope of m_{pss} and intercept of a_{pss}.

A more generalized form of Darcy's equation can be developed by rearranging Equation 1.2.122 and solving for Q to give:

$$Q = \frac{kh(\bar{p} - p_{wf})}{162.6B\mu\log\left(2.2458A/C_A r_w^2\right)} \qquad [1.2.124]$$

It should be noted that if Equation 1.2.124 is applied to a circular reservoir of radius r_e, then:

$$A = \pi r_e^2$$

and the shape factor for a circular drainage area as given in Table 1.4 as:

$$C_A = 31.62$$

Substituting in Equation 1.2.124, it reduces to:

$$Q = \frac{0.00708kh(\bar{p} - p_{wf})}{B\mu[\ln(r_e/r_w) - 0.75]}$$

This equation is identical to that of Equation 1.2.123.

Example 1.17 An oil well is developed on the center of a 40 acre square-drilling pattern. The well is producing at a constant flow rate of 100 STB/day under a semisteady-state condition. The reservoir has the following properties:

$\phi = 15\%$, $h = 30$ ft, $k = 20$ md
$\mu = 1.5$ cp, $B_o = 1.2$ bbl/STB, $c_t = 25 \times 10^{-6}$ psi^{-1}
$p_i = 4500$ psi, $r_w = 0.25$ ft, $A = 40$ acres

(a) Calculate and plot the bottom-hole flowing pressure as a function of time.
(b) Based on the plot, calculate the pressure decline rate. What is the decline in the average reservoir pressure from $t = 10$ to $t = 200$ hours?

Solution

(a) For the p_{wf} calculations:

Step 1. From Table 1.4, determine C_A:

$$C_A = 30.8828$$

Table 1.4 *Shape factors for various single-well drainage areas (After Earlougher, R, Advances in Well Test Analysis, permission to publish by the SPE, copyright SPE, 1977)*

In bounded reservoirs	C_A	$\ln C_A$	$\frac{1}{2}\ln\left(\frac{2.2458}{C_A}\right)$	*Exact for* $t_{DA} >$	*Less than 1% error for* $t_{DA} >$	*Use infinite system solution with less than 1% error for* $t_{DA} >$
	31.62	3.4538	−1.3224	0.1	0.06	0.10
	31.6	3.4532	−1.3220	0.1	0.06	0.10
	27.6	3.3178	−1.2544	0.2	0.07	0.09
	27.1	3.2995	−1.2452	0.2	0.07	0.09
	21.9	3.0865	−1.1387	0.4	0.12	0.08
	0.098	−2.3227	+1.5659	0.9	0.60	0.015
	30.8828	3.4302	−1.3106	0.1	0.05	0.09
	12.9851	2.5638	−0.8774	0.7	0.25	0.03
	10132	1.5070	−0.3490	0.6	0.30 0.25	0.025 0.01
	3.3351	1.2045	−0.1977	0.7		
	21.8369	3.0836	−1.1373	0.3	0.15	0.025
	10.8374	2.3830	−0.7870	0.4	0.15	0.025
	10141	1.5072	−0.3491	1.5	0.50	0.06
	2.0769	0.7309	−0.0391	1.7	0.50	0.02
	3.1573	1.1497	−0.1703	0.4	0.15	0.005
	0.5813	−0.5425	+0.6758	2.0	0.60	0.02
	0.1109	−2.1991	+1.5041	3.0	0.60	0.005
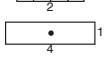	5.3790	1.6825	−0.4367	0.8	0.30	0.01
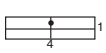	2.6896	0.9894	−0.0902	0.8	0.30	0.01
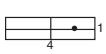	0.2318	−1.4619	+1.1355	4.0	2.00	0.03
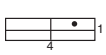	0.1155	−2.1585	+1.4838	4.0	2.00	0.01
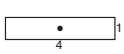	2.3606	0.8589	−0.0249	1.0	0.40	0.025
	In vertically fractured reservoirs use $(x_e/x_f)^2$ in place of A/r_w^2, for fractured systems					
	2.6541	0.9761	−0.0835	0.175	0.08	cannot use
	2.0348	0.7104	+0.0493	0.175	0.09	cannot use
	1.9986	0.6924	+0.0583	0.175	0.09	cannot use
	1.6620	0.5080	+0.1505	0.175	0.09	cannot use
	1.3127	0.2721	+0.2685	0.175	0.09	cannot use
	In water-drive reservoirs					
	0.7887	−0.2374	+0.5232	0.175	0.09	cannot use
	19.1	2.95	−1.07	–	–	–
	In reservoirs of unknown production character					
	25.0	3.22	−1.20	–	–	–

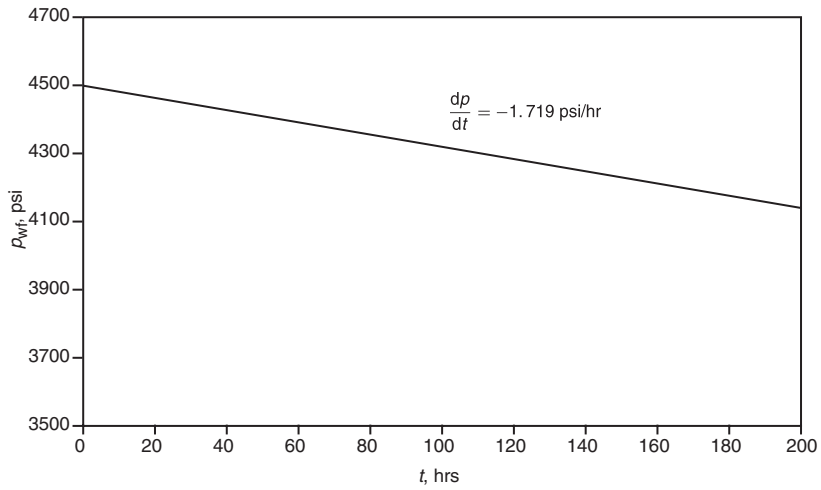

Figure 1.25 *Bottom-hole flowing pressure as a function of time.*

Step 2. Convert the area A from acres to ft^2:

$$A = (40)(43\,560) = 1\,742\,400 \text{ ft}^2$$

Step 3. Apply Equation 1.2.123:

$$p_{wf} = \left(p_i - \frac{0.23396QBt}{Ah\phi c_t}\right) - \frac{162.6QB\mu}{kh}\log\left(\frac{2.2458A}{1C_A r_w^2}\right)$$

$$= 4500 - 0.143t - 48.78\log(2\,027\,436)$$

or:

$$p_{wf} = 4192 - 0.143t$$

Step 4. Calculate p_{wf} at different assumed times, as follows:

t (hr)	$p_{wf} = 4192 - 0.143t$
10	4191
20	4189
50	4185
100	4178
200	4163

Step 5. Present the results of step 4 in graphical form as shown in Figure 1.25.

(b) It is obvious from Figure 1.25 and the above calculation that the bottom-hole flowing pressure is declining at a rate of 0.143 psi/hr, or:

$$\frac{dp}{dt} = -0.143 \text{ psi/hr}$$

The significance of this example is that the rate of pressure decline during the pseudosteady state is the same throughout the drainage area. This means that the *average reservoir pressure*, $\overline{p}_r$, is declining at the same rate of 0.143 psi/hr, therefore the change in $\overline{p}_r$ from 10 to 200 hours is:

$$\Delta\overline{p}_r = (0.143)(200 - 10) = 27.17 \text{ psi}$$

Example 1.18 An oil well is producing under a constant bottom-hole flowing pressure of 1500 psi. The current average reservoir pressure $\overline{p}_r$ is 3200 psi. The well is developed in the center of 40 acre square-drilling pattern. Given the following additional information:

$\phi = 16\%$, $h = 15$ ft, $k = 50$ md,
$\mu = 26$ cp, $B_o = 1.15$ bbl/STB,
$c_t = 10 \times 10^{-6}$ psi^{-1}, $r_w = 0.25$ ft

calculate the flow rate.

Solution

Because the volumetric average pressure is given, solve for the flow rate by applying Equation 1.2.124:

$$Q = \frac{kh(\overline{p} - p_{wf})}{162.6B\mu\log\left[\frac{2.2458A}{C_A r_w^2}\right]}$$

$$= \frac{(50)(15)(3200 - 1500)}{(162.6)(1.15)(2.6)\log\left[\frac{2.2458(40)(43\,560)}{(30.8828)(0.25^2)}\right]}$$

$$= 416 \text{ STB/day}$$

It is interesting to note that Equation 1.2.124 can also be presented in a dimensionless form by rearranging and introducing the dimensionless time t_D and dimensionless pressure drop p_D, to give:

$$p_D = 2\pi t_{DA} + \frac{1}{2}\ln\left(\frac{2.3458A}{C_A r_w^2}\right) + s \qquad [1.2.125]$$

with the dimensionless time based on the well drainage given by Equation 1.2.75a as:

$$t_{DA} = \frac{0.0002637kt}{\phi\mu c_t A} = t_A\left(\frac{r_w^2}{A}\right)$$

where:

s = skin factor (to be introduced later in the chapter)
C_A = shape factor
t_{DA} = dimensionless time based on the well drainage area πr_e^2.

Equation 1.2.125 suggests that during the *boundary-dominated flow*, i.e., pseudosteady state, a plot of p_D vs. t_{DA} on a Cartesian scale would produce a straight line with a slope of 2π. That is:

$$\frac{\partial p_D}{\partial t_{DA}} = 2\pi \qquad [1.2.126]$$

For a well located in a circular drainage area with no skin, i.e., $s = 0$, and taking the logarithm of both sides of Equation 1.2.125 gives:

$$\log(p_D) = \log(2\pi) + \log(t_{DA})$$

which indicates that a plot of p_D vs. t_{DA} on a log–log scale would produce a 45° straight line and an intercept of 2π.

1.2.9 Radial flow of compressible fluids (gases)

The radial diffusivity equation as expressed by Equation 1.2.94 was developed to study the performance of a compressible fluid under unsteady-state conditions. The equation has the following form:

$$\frac{\partial^2 m(p)}{\partial r^2} + \frac{1}{r}\frac{\partial m(p)}{\partial r} = \frac{\phi\mu c_t}{0.000264k}\frac{\partial m(p)}{\partial t}$$

For semisteady-state flow, the rate of change of the real-gas pseudopressure with respect to time is constant. That is:

$$\frac{\partial m(p)}{\partial t} = \text{constant}$$

Using the same technique identical to that described previously for liquids gives the following exact solution to the diffusivity equation:

$$Q_g = \frac{kh\left[m(\bar{p}_r) - m(p_{wf})\right]}{1422T\left[\ln\left(\dfrac{r_e}{r_w}\right) - 0.75\right]} \qquad [1.2.127]$$

where:

Q_g = gas flow rate, Mscf/day
T = temperature, °R
k = permeability, md

Two approximations to the above solution are widely used. These are:

(1) the pressure-squared approximation;
(2) the pressure approximation.

Pressure-squared method

As outlined previously, this method provides us with compatible results to that of the exact solution approach when $p < 2000$ psi. The solution has the following familiar form:

$$Q_g = \frac{kh\left(\bar{p}_r^2 - p_{wf}^2\right)}{1422T\bar{\mu}\bar{Z}\left(\ln\left(\dfrac{r_e}{r_w}\right) - 0.75\right)} \qquad [1.2.128]$$

The gas properties $\bar{Z}$ and $\bar{\mu}$ are evaluated at:

$$\bar{p} = \sqrt{\frac{\bar{p}_r^2 + p_{wf}^2}{2}}$$

where:

Q_g = gas flow rate, Mscf/day
T = temperature, °R
k = permeability, md

Pressure approximation method

This approximation method is applicable at $p > 3000$ psi and has the following mathematical form:

$$Q_g = \frac{kh\left(\bar{p}_r - p_{wf}\right)}{1422\bar{\mu}\bar{B}_g\left[\ln\left(r_e/r_w\right) - 0.75\right]} \qquad [1.2.129]$$

with the gas properties evaluated at:

$$\bar{p} = \frac{\bar{p}_r + p_{wf}}{2}$$

where:

Q_g = gas flow rate, Mscf/day
k = permeability, md
$\bar{B}_g$ = gas formation volume factor at a average pressure, bbl/scf

The gas formation volume factor is given by the following expression:

$$B_g = 0.00504\frac{\bar{Z}T}{\bar{p}}$$

In deriving the flow equations, the following two main assumptions were made:

(1) uniform permeability throughout the drainage area;
(2) laminar (viscous) flow.

Before using any of the previous mathematical solutions to the flow equations, the solution must be modified to account for the possible deviation from the above two assumptions. Introducing the following two correction factors into the solution of the flow equation can eliminate these two assumptions:

(1) skin factor;
(2) turbulent flow factor.

1.2.10 Skin factor

It is not unusual during drilling, completion, or workover operations for materials such as mud filtrate, cement slurry, or clay particles to enter the formation and reduce the permeability around the wellbore. This effect is commonly referred to as "wellbore damage" and the region of altered permeability is called the "skin zone." This zone can extend from a few inches to several feet from the wellbore. Many other wells are stimulated by acidizing or fracturing, which in effect increases the permeability near the wellbore. Thus, the permeability near the wellbore is always different from the permeability away from the well where the formation has not been affected by drilling or stimulation. A schematic illustration of the skin zone is shown in Figure 1.26.

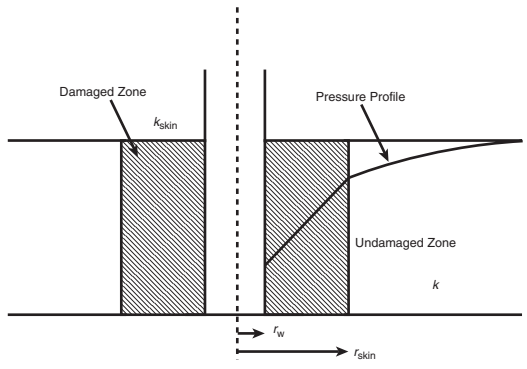

Figure 1.26 *Near-wellbore skin effect.*

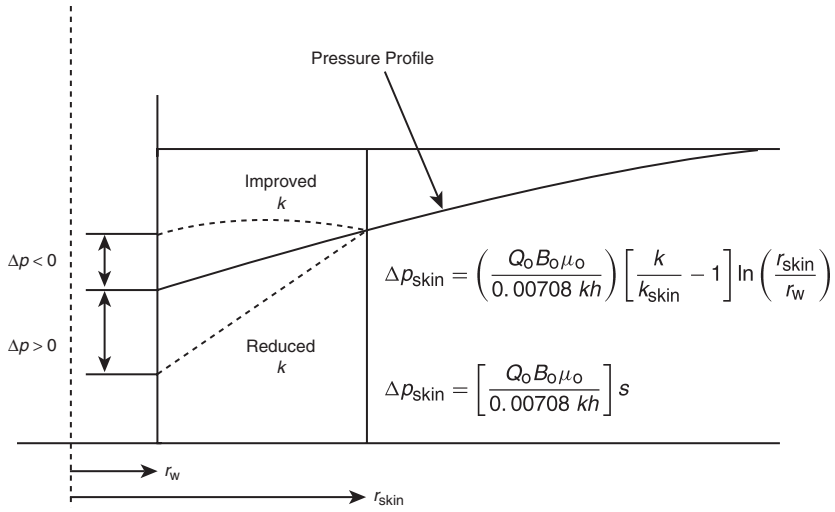

Figure 1.27 *Representation of positive and negative skin effects.*

The effect of the skin zone is to alter the pressure distribution around the wellbore. In case of wellbore damage, the skin zone causes an additional pressure loss in the formation. In case of wellbore improvement, the opposite to that of wellbore damage occurs. If we refer to the pressure drop in the skin zone as Δp_{skin}, Figure 1.27 compares the differences in the skin zone pressure drop for three possible outcomes.

- *First outcome*: $\Delta p_{skin} > 0$, which indicates an additional pressure drop due to wellbore damage, i.e., $k_{skin} < k$.
- *Second outcome*: $\Delta p_{skin} < 0$, which indicates less pressure drop due to wellbore improvement, i.e., $k_{skin} > k$.
- *Third outcome*: $\Delta p_{skin} = 0$, which indicates no changes in the wellbore condition, i.e., $k_{skin} = k$.

Hawkins (1956) suggested that the permeability in the skin zone, i.e., k_{skin}, is uniform and the pressure drop across the zone can be approximated by Darcy's equation. Hawkins proposed the following approach:

$$\Delta p_{skin} = \begin{bmatrix} \Delta p \text{ in skin zone} \\ \text{due to } k_{skin} \end{bmatrix} - \begin{bmatrix} \Delta p \text{ in the skin zone} \\ \text{due to } k \end{bmatrix}$$

Applying Darcy's equation gives:

$$(\Delta p)_{skin} = \left(\frac{Q_o B_o \mu_o}{0.00708 h k_{skin}}\right)\ln\left(\frac{r_{skin}}{r_w}\right) - \left(\frac{Q_o B_o \mu_o}{0.00708 h k}\right)\ln\left(\frac{r_{skin}}{r_w}\right)$$

or:

$$\Delta p_{skin} = \left(\frac{Q_o B_o \mu_o}{0.00708 k h}\right)\left[\frac{k}{k_{skin}} - 1\right]\ln\left(\frac{r_{skin}}{r_w}\right)$$

where:

k = permeability of the formation, md
k_{skin} = permeability of the skin zone, md

The above expression for determining the additional pressure drop in the skin zone is commonly expressed in the following form:

$$\Delta p_{skin} = \left(\frac{Q_o B_o \mu_o}{0.00708 k h}\right) s = 141.2\left(\frac{Q_o B_o \mu_o}{kh}\right) s \qquad [1.2.130]$$

where s is called the skin factor and defined as:

$$s = \left[\frac{k}{k_{skin}} - 1\right]\ln\left(\frac{r_{skin}}{r_w}\right) \qquad [1.2.131]$$

Depending on the permeability ratio k/k_{skin} and if $\ln(r_{skin}/r_w)$ is always positive, there are only three possible outcomes in evaluating the skin factor s:

(1) *Positive skin factor,* $s > 0$: When the damaged zone near the wellbore exists, k_{skin} is less than k and hence s is a positive number. The magnitude of the skin factor increases as k_{skin} decreases and as the depth of the damage r_{skin} increases.
(2) *Negative skin factor,* $s < 0$: When the permeability around the well k_{skin} is higher than that of the formation k, a negative skin factor exists. This negative factor indicates an improved wellbore condition.
(3) *Zero skin factor,* $s = 0$: Zero skin factor occurs when no alternation in the permeability around the wellbore is observed, i.e., $k_{skin} = k$.

Equation 1.2.131 indicates that a negative skin factor will result in a negative value of Δp_{skin}. This implies that a stimulated well will require less pressure drawdown to produce at rate q than an equivalent well with uniform permeability.

The proposed modification of the previous flow equation is based on the concept that the actual total pressure drawdown will increase or decrease by an amount Δp_{skin}. Assuming that $(\Delta p)_{ideal}$ represents the pressure drawdown for a drainage area with a uniform permeability k, then:

$$(\Delta p)_{actual} = (\Delta p)_{ideal} + (\Delta p)_{skin}$$

or:

$$(p_i - p_{wf})_{actual} = (p_i - p_{wf})_{ideal} + \Delta p_{skin} \qquad [1.2.132]$$

The above concept of modifying the flow equation to account for the change in the pressure drop due the wellbore skin effect can be applied to the previous three flow regimes:

(1) steady-state flow;
(2) unsteady-state (transient) flow;
(3) pseudosteady (semisteady)-state flow.

Basically, Equation 1.2.132 can be applied as follows.

Steady state radial flow (accounting for the skin factor) Substituting Equations 1.2.15 and 1.2.130 into Equation 1.2.132, gives:

$$(\Delta p)_{\text{actual}} = (\Delta p)_{\text{ideal}} + (\Delta p)_{\text{skin}}$$

$$(p_{\text{i}} - p_{\text{wf}})_{\text{actual}} = \left(\frac{Q_{\text{o}}B_{\text{o}}\mu_{\text{o}}}{0.00708kh}\right)\ln\left(\frac{r_{\text{e}}}{r_{\text{w}}}\right) + \left(\frac{Q_{\text{o}}B_{\text{o}}\mu_{\text{o}}}{0.00708kh}\right)s$$

Solving for the flow rate gives:

$$Q_{\text{o}} = \frac{0.00708kh\,(p_{\text{i}} - p_{\text{wf}})}{\mu_{\text{o}}B_{\text{o}}\left[\ln\dfrac{r_{\text{e}}}{r_{\text{w}}} + s\right]} \qquad [1.2.133]$$

where:

Q_{o} = oil flow rate, STB/day
k = permeability, md
h = thickness, ft
s = skin factor
B_{o} = oil formation volume factor, bbl/STB
μ_{o} = oil viscosity, cp
p_{i} = initial reservoir pressure, psi
p_{wf} = bottom-hole flowing pressure, psi

Unsteady-state radial flow (accounting for the skin factor)
For slightly compressible fluids Combining Equations 1.2.71 and 1.2.130 with that of 1.2.132 yields:

$$(\Delta p)_{\text{actual}} = (\Delta p)_{\text{ideal}} + (\Delta p)_{\text{skin}}$$

$$p_{\text{i}} - p_{\text{wf}} = 162.6\left(\frac{Q_{\text{o}}B_{\text{o}}\mu_{\text{o}}}{kh}\right)\left[\log\frac{kt}{\phi\mu c_{\text{t}}r_{\text{w}}^2} - 3.23\right] + 141.2\left(\frac{Q_{\text{o}}B_{\text{o}}\mu_{\text{o}}}{kh}\right)s$$

or:

$$p_{\text{i}} - p_{\text{wf}} = 162.6\left(\frac{Q_{\text{o}}B_{\text{o}}\mu_{\text{o}}}{kh}\right)\left[\log\frac{kt}{\phi\mu c_{\text{t}}r_{\text{w}}^2} - 3.23 + 0.87s\right] \qquad [1.2.134]$$

For compressible fluids A similar approach to that of the above gives:

$$m(p_{\text{i}}) - m(p_{\text{wf}}) = \frac{1637Q_{\text{g}}T}{kh}\left[\log\frac{kt}{\phi\mu c_{\text{t}_{\text{i}}}r_{\text{w}}^2} - 3.23 + 0.87s\right] \qquad [1.2.135]$$

and in terms of the pressure-squared approach, the difference $[m(p_{\text{i}}) - m(p_{\text{wf}})]$ can be replaced with:

$$m(p_{\text{i}}) - m(p_{\text{wf}}) = \int_{p_{\text{wf}}}^{p_{\text{i}}}\frac{2p}{\mu Z}\,\text{d}p = \frac{p_{\text{i}}^2 - p_{\text{wf}}^2}{\overline{\mu}\overline{Z}}$$

to give:

$$p_{\text{i}}^2 - p_{\text{wf}}^2 = \frac{1637Q_{\text{g}}T\overline{Z}\overline{\mu}}{kh}\left[\log\frac{kt}{\phi\mu_{\text{i}}c_{\text{ti}}r_{\text{w}}^2} - 3.23 + 0.87s\right] \qquad [1.2.136]$$

where:

Q_{g} = gas flow rate, Mscf/day
T = temperature, °R
k = permeability, md
t = time, hours

Pseudosteady-state flow (accounting for the skin factor)
For slightly compressible fluids Introducing the skin factor into Equation 1.2.123 gives:

$$Q_{\text{o}} = \frac{0.00708kh\,(\overline{p}_{\text{r}} - p_{\text{wf}})}{\mu_{\text{o}}B_{\text{o}}\left[\ln\left(\dfrac{r_{\text{e}}}{r_{\text{w}}}\right) - 0.75 + s\right]} \qquad [1.2.137]$$

For compressible fluids

$$Q_{\text{g}} = \frac{kh\left[m(\overline{p}_{\text{r}}) - m(p_{\text{wf}})\right]}{1422T\left[\ln\left(\dfrac{r_{\text{e}}}{r_{\text{w}}}\right) - 0.75 + s\right]} \qquad [1.2.138]$$

or in terms of the pressure-squared approximation:

$$Q_{\text{g}} = \frac{kh\left(\overline{p}_{\text{r}}^2 - p_{\text{wf}}^2\right)}{1422T\overline{\mu}\overline{Z}\left[\ln\left(\dfrac{r_{\text{e}}}{r_{\text{w}}}\right) - 0.75 + s\right]} \qquad [1.2.139]$$

where :

Q_{g} = gas flow rate, Mscf/day
k = permeability, md
T = temperature, °R
$\overline{\mu}_{\text{g}}$ = gas viscosity at average pressure $\overline{p}$, cp
$\overline{Z}_{\text{g}}$ = gas compressibility factor at average pressure $\overline{p}$

Example 1.19 Calculate the skin factor resulting from the invasion of the drilling fluid to a radius of 2 ft. The permeability of the skin zone is estimated at 20 md as compared with the unaffected formation permeability of 60 md. The wellbore radius is 0.25 ft.

Solution
Apply Equation 1.2.131 to calculate the skin factor:

$$s = \left[\frac{60}{20} - 1\right]\ln\left(\frac{2}{0.25}\right) = 4.16$$

Matthews and Russell (1967) proposed an alternative treatment to the skin effect by introducing the "effective or apparent wellbore radius" r_{wa} that accounts for the pressure drop in the skin. They define r_{wa} by the following equation:

$$r_{\text{wa}} = r_{\text{w}}\text{e}^{-s} \qquad [1.2.140]$$

All of the ideal radial flow equations can be also modified for the skin by simply replacing the wellbore radius r_{w} with that of the apparent wellbore radius r_{wa}. For example, Equation 1.2.134 can be equivalently expressed as:

$$p_{\text{i}} - p_{\text{wf}} = 162.6\left(\frac{Q_{\text{o}}B_{\text{o}}\mu_{\text{o}}}{kh}\right)\left[\log\left(\frac{kt}{\phi\mu c_{\text{t}}r_{\text{wa}}^2}\right) - 3.23\right] \qquad [1.2.141]$$

1.2.11 Turbulent flow factor

All of the mathematical formulations presented so far are based on the assumption that laminar flow conditions are observed during flow. During radial flow, the flow velocity increases as the wellbore is approached. This increase in the velocity might cause the development of turbulent flow around the wellbore. If turbulent flow does exist, it is most likely to occur with gases and causes an additional pressure drop similar to that caused by the skin effect. The term "non-Darcy flow" has been adopted by the industry to describe the additional pressure drop due to the turbulent (non-Darcy) flow.

Referring to the additional real-gas pseudopressure drop due to non-Darcy flow as $\Delta\psi_{\text{non-Darcy}}$, the total (actual) drop is given by:

$$(\Delta\psi)_{\text{actual}} = (\Delta\psi)_{\text{ideal}} + (\Delta\psi)_{\text{skin}} + (\Delta\psi)_{\text{non-Darcy}}$$

Wattenbarger and Ramey (1968) proposed the following expression for calculating $(\Delta\psi)_{\text{non-Darcy}}$:

$$(\Delta\psi)_{\text{non-Darcy}} = 3.161 \times 10^{-12}\left[\frac{\beta T\gamma_{\text{g}}}{\mu_{\text{gw}}h^2r_{\text{w}}}\right]Q_{\text{g}}^2 \qquad [1.2.142]$$

This equation can be expressed in a more convenient form as;

$$(\Delta\psi)_{\text{non-Darcy}} = FQ_{\text{g}}^2 \qquad [1.2.143]$$

where F is called the "non-Darcy flow coefficient" and given by:

$$F = 3.161 \times 10^{-12}\left[\frac{\beta T \gamma_g}{\mu_{gw} h^2 r_w}\right] \quad [1.2.144]$$

where:

Q_g = gas flow rate, Mscf/day
μ_{gw} = gas viscosity as evaluated at p_{wf}, cp
γ_g = gas specific gravity
h = thickness, ft
F = non-Darcy flow coefficient, $psi^2/cp/(Mscf/day)^2$
β = turbulence parameter

Jones (1987) proposed a mathematical expression for estimating the turbulence parameter β as:

$$\beta = 1.88(10^{-10})(k)^{-1.47}(\phi)^{-0.53} \quad [1.2.145]$$

where:

k = permeability, md
ϕ = porosity, fraction

The term FQ_g^2 can be included in all the compressible gas flow equations in the same way as the skin factor. This non-Darcy term is interpreted as a *rate-dependent skin*. The modification of the gas flow equations to account for the turbulent flow condition is given below for the three flow regimes:

(1) unsteady-state (transient) flow;
(2) semisteady-state flow;
(3) steady-state flow.

Unsteady-state radial flow

The gas flow equation for an unsteady-state flow is given by Equation 1.2.135 and can be modified to include the additional drop in the real-gas potential, as:

$$m(p_i) - m(p_{wf}) = \left(\frac{1637 Q_g T}{kh}\right)\left[\log\left(\frac{kt}{\phi\mu_i c_{ti} r_w^2}\right) - 3.23 + 0.87s\right] + FQ_g^2 \quad [1.2.146]$$

Equation 1.2.146 is commonly written in a more convenient form as:

$$m(p_i) - m(p_{wf}) = \left(\frac{1637 Q_g T}{kh}\right)\left[\log\left(\frac{kt}{\phi\mu_i c_{ti} r_w^2}\right) - 3.23 + 0.87s + 0.87DQ_g\right] \quad [1.2.147]$$

where the term DQ_g is interpreted as the rate-dependent skin factor. The coefficient D is called the "inertial or turbulent flow factor" and given by:

$$D = \frac{Fkh}{1422T} \quad [1.2.148]$$

The true skin factor s which reflects the formation damage or stimulation is usually combined with the non-Darcy rate-dependent skin and labeled as the apparent or total skin factor $s\backslash$. That is:

$$s\backslash = s + DQ_g \quad [1.2.149]$$

or:

$$m(p_i) - m(p_{wf}) = \left(\frac{1637 Q_g T}{kh}\right)\left[\log\left(\frac{kt}{\phi\mu_i c_{ti} r_w^2}\right) - 3.23 + 0.87s\backslash\right] \quad [1.2.150]$$

Equation 1.2.50 can be expressed in the pressure-squared approximation form as:

$$p_i^2 - p_{wf}^2 = \left(\frac{1637 Q_g T \overline{Z}\overline{\mu}}{kh}\right)\left[\log\frac{kt}{\phi\mu_i c_{ti} r_w^2} - 3.23 + 0.87s\backslash\right] \quad [1.2.151]$$

where:

Q_g = gas flow rate, Mscf/day
t = time, hours
k = permeability, md
μ_i = gas viscosity as evaluated at p_i, cp

Semisteady-state flow

Equation 1.2.138 and 1.2.139 can be modified to account for the non-Darcy flow as follows:

$$Q_g = \frac{kh\left[m(\bar{p}_r) - m(p_{wf})\right]}{1422T\left[\ln\left(\frac{r_e}{r_w}\right) - 0.75 + s + DQ_g\right]} \quad [1.2.152]$$

or in terms of the pressure-squared approach:

$$Q_g = \frac{kh\left(\bar{p}_r^2 - p_{wf}^2\right)}{1422T\overline{\mu}\overline{Z}\left[\ln\left(\frac{r_e}{r_w}\right) - 0.75 + s + DQ_g\right]} \quad [1.2.153]$$

where the coefficient D is defined as:

$$D = \frac{Fkh}{1422T} \quad [1.2.154]$$

Steady-state flow

Similar to the above modification procedure, Equations 1.2.32 and 1.2.33 can be expressed as:

$$Q_g = \frac{kh\left[m(p_i) - m(p_{wf})\right]}{1422T\left[\ln\left(\frac{r_e}{r_w}\right) - 0.5 + s + DQ_g\right]} \quad [1.2.155]$$

$$Q_g = \frac{kh\left(p_e^2 - p_{wf}^2\right)}{1422T\overline{\mu}\overline{Z}\left[\ln\left(\frac{r_e}{r_w}\right) - 0.5 + s + DQ_g\right]} \quad [1.2.156]$$

Example 1.20 A gas well has an estimated wellbore damage radius of 2 feet and an estimated reduced permeability of 30 md. The formation has permeability and porosity of 55 md and 12% respectively. The well is producing at a rate of 20 MMscf/day with a gas gravity of 0.6. The following additional data is available:

$$r_w = 0.25,\ h = 20 \text{ ft},\ T = 140^\circ\text{F},\ \mu_{gw} = 0.013 \text{ cp}$$

Calculate the apparent skin factor.

Solution

Step 1. Calculate skin factor from Equation 1.2.131:

$$s = \left[\frac{k}{k_{skin}} - 1\right]\ln\left(\frac{r_{skin}}{r_w}\right) = \left[\frac{55}{30} - 1\right]\ln\left(\frac{2}{0.25}\right) = 1.732$$

Step 2. Calculate the turbulence parameter β by applying Equation 1.2.145:

$$\beta = 1.88(10^{-10})(k)^{-1.47}(\phi)^{-0.53} = 1.88 \times 10^{10}(55)^{-1.47}(0.12)^{-0.53} = 159.904 \times 10^6$$

Step 3. Calculate the non-Darcy flow coefficient from Equation 1.2.144:

$$F = 3.161 \times 10^{-12}\left[\frac{\beta T \gamma_g}{\mu_{gw} h^2 r_w}\right]$$

$$= 3.1612 \times 10^{-12}\left[\frac{159.904 \times 10^6 (600)(0.6)}{(0.013)(20)^2(0.25)}\right]$$

$$= 0.14$$

Step 4. Calculate the coefficient D from Equation 1.2.148:

$$D = \frac{Fkh}{1422T}$$

$$= \frac{(0.14)(55)(20)}{(1422)(600)} = 1.805 \times 10^{-4}$$

Step 5. Estimate the apparent skin factor by applying Equation 1.2.149:

$$s^{\backslash} = s + DQ_g = 1.732 + (1.805 \times 10^{-4})(20\,000)$$

$$= 5.342$$

1.2.12 Principle of superposition

The solutions to the radial diffusivity equation as presented earlier in this chapter appear to be applicable only for describing the pressure distribution in an infinite reservoir that was caused by constant production from a single well. Since real reservoir systems usually have several wells that are operating at varying rates, a more generalized approach is needed to study the fluid flow behavior during the unsteady-state flow period.

The principle of superposition is a powerful concept that can be applied to remove the restrictions that have been imposed on various forms of solution to the transient flow equation. Mathematically the superposition theorem states that any sum of individual solutions to the diffusivity equation is also a solution to that equation. This concept can be applied to account for the following effects on the transient flow solution:

- effects of multiple wells;
- effects of rate change;
- effects of the boundary;
- effects of pressure change.

Slider (1976) presented an excellent review and discussion of the practical applications of the principle of superposition in solving a wide variety of unsteady-state flow problems.

Effects of multiple wells

Frequently, it is desired to account for the effects of more than one well on the pressure at some point in the reservoir. The superposition concept states that the total pressure drop at any point in the reservoir is the sum of the pressure changes at that point caused by the flow in each of the wells in the reservoir. In other words, we simply superimpose one effect upon another.

Consider Figure 1.28 which shows three wells that are producing at different flow rates from an infinite-acting reservoir, i.e., an unsteady-state flow reservoir. The principle of superposition states that the total pressure drop observed at any well, e.g., well 1, is:

$$(\Delta p)_{\text{total drop at well 1}} = (\Delta p)_{\text{drop due to well 1}} + (\Delta p)_{\text{drop due to well 2}} + (\Delta p)_{\text{drop due to well 3}}$$

The pressure drop at well 1 due to its own production is given by the *log approximation* to the Ei function solution

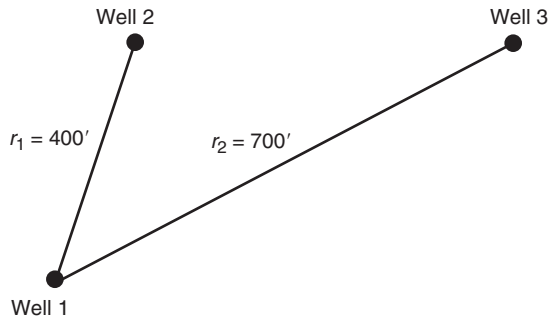

Figure 1.28 *Well layout for Example 1.21.*

presented by Equation 1.2.134, or:

$$(p_i - p_{wf}) = (\Delta p)_{well1} = \frac{162.6 Q_{o1} B_o \mu_o}{kh}\left[\log\left(\frac{kt}{\phi \mu c_t r_w^2}\right) - 3.23 + 0.87s\right]$$

where:

t = time, hours
s = skin factor
k = permeability, md
Q_{o1} = oil flow rate from well 1

The additional pressure drops at well 1 due to the production from wells 2 and 3 must be written in terms of the Ei function solution, as expressed by Equation 1.2.66, since the log approximation cannot be applied in calculating the pressure at a large distance r from the well where $x > 0.1$. Therefore:

$$p(r,t) = p_i + \left[\frac{70.6 Q_o \mu B_o}{kh}\right] \text{Ei}\left[\frac{-948\phi\mu_o c_t r^2}{kt}\right]$$

Applying the above expression to calculate the additional pressure drop due to two wells gives:

$$(\Delta p)_{\text{drop due to well 2}} = p_i - p(r_1,t) = -\left[\frac{70.6 Q_{o1} \mu_o B_o}{kh}\right] \times \text{Ei}\left[\frac{-948\phi\mu_o c_t r_1^2}{kt}\right]$$

$$(\Delta p)_{\text{drop due to well 3}} = p_i - p(r_2,t) = -\left[\frac{70.6 Q_{o2} \mu_o B_o}{kh}\right] \times \text{Ei}\left[\frac{-948\phi\mu_o c_t r_2^2}{kt}\right]$$

The total pressure drop is then given by:

$$(p_i - p_{wf})_{\text{total at well 1}} = \left(\frac{162.6 Q_{o1} B_o \mu_o}{kh}\right)\left[\log\left(\frac{kt}{\phi \mu c_t r_w^2}\right) - 3.23 + 0.87s\right] - \left(\frac{70.6 Q_{o2} B_o \mu_o}{kh}\right)\text{Ei}\left[-\frac{948\phi\mu c_t r_1^2}{kt}\right] - \left(\frac{70.6 Q_{o3} B_o \mu_o}{kh}\right)\text{Ei}\left[-\frac{948\phi\mu c_t r_2^2}{kt}\right]$$

where Q_{o1}, Q_{o2}, and Q_{o3} refer to the respective producing rates of wells 1, 2, and 3.

The above computational approach can be used to calculate the pressure at wells 2 and 3. Further, it can be extended to include any number of wells flowing under the unsteady-state flow condition. It should also be noted that if the point of interest is an operating well, the skin factor s must be included for that well only.

Example 1.21 Assume that the three wells as shown in Figure 1.28 are producing under a transient flow condition for 15 hours. The following additional data is available:

$$Q_{o1} = 100 \text{ STB/day}, \quad Q_{o2} = 160 \text{ STB/day}$$
$$Q_{o3} = 200 \text{ STB/day}, \quad p_i = 4500 \text{ psi},$$
$$B_o = 1.20 \text{ bbl/STB}, \quad c_t = 20 \times 10^{-6} \text{ psi}^{-1},$$
$$(s)_{well1} = -0.5, \quad h = 20 \text{ ft},$$
$$\phi = 15\%, \quad k = 40 \text{ md},$$
$$r_w = 0.25 \text{ ft}, \quad \mu_o = 2.0 \text{ cp},$$
$$r_1 = 400 \text{ ft}, \quad r_2 = 700 \text{ ft}.$$

If the three wells are producing at a constant flow rate, calculate the sand face flowing pressure at well 1.

Solution

Step 1. Calculate the pressure drop at well 1 caused by its own production by using Equation 1.2.134:

$$(p_i - p_{wf}) = (\Delta p)_{well\,1} = \frac{162.6 Q_{o1} B_o \mu_o}{kh} \times \left[\log\left(\frac{kt}{\phi \mu c_t r_w^2}\right) - 3.23 + 0.87s\right]$$

$$(\Delta p)_{well\,1} = \frac{(162.6)(100)(1.2)(2.0)}{(40)(20)} \times \left[\log\left(\frac{(40)(15)}{(0.15)(2)(20 \times 10^{-6})(0.25)^2}\right) - 3.23 + 0.87(0)\right] = 270.2 \text{ psi}$$

Step 2. Calculate the pressure drop at well 1 due to the production from well 2:

$$(\Delta p)_{\text{drop due to well 2}} = p_i - p(r_1, t) = -\left[\frac{70.6 Q_{o1} \mu_o B_o}{kh}\right] \text{Ei}\left[\frac{-948 \phi \mu_o c_t r_1^2}{kt}\right]$$

$$(\Delta p)_{\text{due to well 2}} = -\frac{(70.6)(160)(1.2)(2)}{(40)(20)} \times \text{Ei}\left[-\frac{(948)(0.15)(2.0)(20 \times 10^{-6})(400)^2}{(40)(15)}\right]$$
$$= 33.888\left[-\text{Ei}(-1.5168)\right]$$
$$= (33.888)(0.13) = 4.41 \text{ psi}$$

Step 3. Calculate the pressure drop due to production from well 3:

$$(\Delta p)_{\text{drop due to well 3}} = p_i - p(r_2, t) = -\left[\frac{70.6 Q_{o2} \mu_o B_o}{kh}\right] \text{Ei}\left[\frac{-948 \phi \mu_o c_t r_2^2}{kt}\right]$$

$$(\Delta p)_{\text{due to well 3}} = -\frac{(70.6)(200)(1.2)(2)}{(40)(20)} \text{Ei}\left[-\frac{(948)(0.15)(2.0)(20 \times 10^{-6})(700)^2}{(40)(15)}\right]$$
$$= (42.36)\left[-\text{Ei}(-4.645)\right]$$
$$= (42.36)(1.84 \times 10^{-3}) = 0.08 \text{ psi}$$

Step 4. Calculate the total pressure drop at well 1:

$$(\Delta p)_{\text{total at well 1}} = 270.2 + 4.41 + 0.08 = 274.69 \text{ psi}$$

Step 5. Calculate p_{wf} at well 1:

$$P_{wf} = 4500 - 274.69 = 4225.31 \text{ psi}$$

Effects of variable flow rates

All of the mathematical expressions presented previously in this chapter require that the wells produce at a constant rate during the transient flow periods. Practically all wells produce at varying rates and, therefore, it is important that we are able to predict the pressure behavior when the rate changes. For this purpose, the concept of superposition states that "Every flow rate change in a well will result in a pressure response which is independent of the pressure responses caused by the other previous rate changes." Accordingly, the total pressure drop that has occurred at any time is the summation of pressure changes caused separately by each net flow rate change.

Consider the case of a shut-in well, i.e., $Q = 0$, that was then allowed to produce at a series of constant rates for the different time periods shown in Figure 1.29. To calculate the total pressure drop at the sand face at time t_4, the composite solution is obtained by adding the individual constant-rate solutions at the specified rate-time sequence, or:

$$(\Delta p)_{total} = (\Delta p)_{\text{due to}(Q_{o1}-0)} + (\Delta p)_{\text{due to}(Q_{o2}-Q_{o1})} + (\Delta p)_{\text{due to}(Q_{o3}-Q_{o2})} + (\Delta p)_{\text{due to}(Q_{o4}-Q_{o3})}$$

The above expression indicates that there are four contributions to the total pressure drop resulting from the four individual flow rates:

The first contribution results from increasing the rate from 0 to Q_1 and is in effect over the entire time period t_4, thus:

$$(\Delta p)_{Q_1-0} = \left[\frac{162.6(Q_1 - 0)B\mu}{kh}\right] \times \left[\log\left(\frac{kt_4}{\phi \mu c_t r_w^2}\right) - 3.23 + 0.87s\right]$$

It is essential to notice the *change* in the rate, i.e., (new rate – old rate), that is used in the above equation. It is the change in the rate that causes the pressure disturbance. Further, it should be noted that the "time" in the equation represents the total elapsed time since the change in the rate has been in effect.

The second contribution results from decreasing the rate from Q_1 to Q_2 at t_1, thus:

$$(\Delta p)_{Q_2-Q_1} = \left[\frac{162.6(Q_2 - Q_1)B\mu}{kh}\right] \times \left[\log\left(\frac{k(t_4 - t_1)}{\phi \mu c_t r_w^2}\right) - 3.23 + 0.87s\right]$$

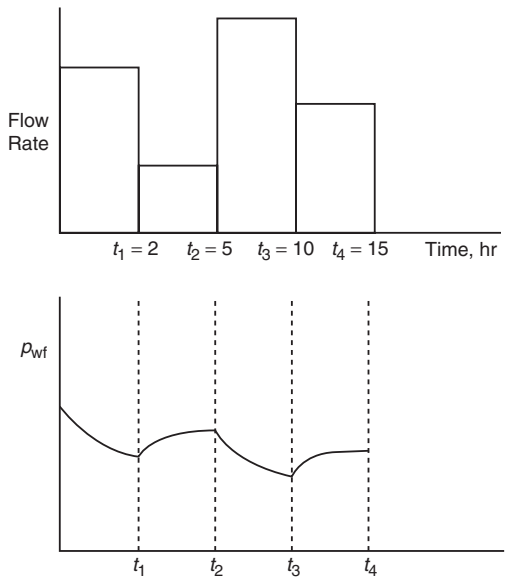

Figure 1.29 *Production and pressure history of a well.*

Using the same concept, the two other contributions from Q_2 to Q_3 and from Q_3 to Q_4 can be computed as:

$$(\Delta p)_{Q_3-Q_2} = \left[\frac{162.6\,(Q_3 - Q_2)\,B\mu}{kh}\right] \times \left[\log\left(\frac{k\,(t_4 - t_2)}{\phi\mu c_t r_w^2}\right) - 3.23 + 0.87s\right]$$

$$(\Delta p)_{Q_4-Q_3} = \left[\frac{162.6\,(Q_4 - Q_3)\,B\mu}{kh}\right] \times \left[\log\left(\frac{k\,(t_4 - t_3)}{\phi\mu c_t r_w^2}\right) - 3.23 + 0.87s\right]$$

The above approach can be extended to model a well with several rate changes. Note, however, that the above approach is valid only if the well is flowing under the unsteady state flow condition for the total time elapsed since the well began to flow at its initial rate.

Example 1.22 Figure 1.29 shows the rate history of a well that is producing under transient flow conditions for 15 hours. Given the following data:

$p_i = 5000$ psi, $h = 20$ ft, $B_o = 1.1$ bbl/STB
$\phi = 15\%$, $\mu_o = 2.5$ cp, $r_w = 0.3$ ft
$c_t = 20 \times 10^{-6}$ psi^{-1}, $s = 0$, $k = 40$ md

calculate the sand face pressure after 15 hours.

Solution

Step 1. Calculate the pressure drop due to the first flow rate for the entire flow period:

$$(\Delta p)_{Q_1-0} = \frac{(162.6)\,(100-0)\,(1.1)\,(2.5)}{(40)\,(20)} \times \left[\log\left(\frac{(40)\,(15)}{(0.15)\,(2.5)\,(20\times10^{-6})\,(0.3)^2}\right) - 3.23 + 0\right]$$

$$= 319.6 \text{ psi}$$

Step 2. Calculate the additional pressure change due to the change of the flow rate from 100 to 70 STB/day:

$$(\Delta p)_{Q_2-Q_1} = \frac{(162.6)\,(70-100)\,(1.1)\,(2.5)}{(40)\,(20)} \times \left[\log\left[\frac{(40)\,(15-2)}{(0.15)\,(2.5)\,(20\times10^{-6})\,(0.3)^2}\right] - 3.23\right]$$

$$= -94.85 \text{ psi}$$

Step 3. Calculate the additional pressure change due to the change of the flow rate from 70 to 150 STB/day:

$$(\Delta p)_{Q_3-Q_2} = \frac{(162.6)\,(150-70)\,(1.1)\,(2.5)}{(40)\,(20)} \times \left[\log\left(\frac{(40)\,(15-5)}{(0.15)\,(2.5)\,(20\times10^{-6})\,(0.3)^2}\right) - 3.23\right]$$

$$= 249.18 \text{ psi}$$

Step 4. Calculate the additional pressure change due to the change of the flow rate from 150 to 85 STB/day:

$$(\Delta p)_{Q_4-Q_3} = \frac{(162.6)\,(85-150)\,(1.1)\,(2.5)}{(40)\,(20)} \times \left[\log\left[\frac{(40)\,(15-10)}{(0.15)\,(2.5)\,(20\times10^{-6})\,(0.3)^2}\right] - 3.23\right]$$

$$= -190.44 \text{ psi}$$

Step 5. Calculate the total pressure drop:

$$(\Delta p)_{total} = 319.6 + (-94.85) + 249.18 + (-190.44) = 283.49 \text{ psi}$$

Step 6. Calculate the wellbore pressure after 15 hours of transient flow:

$$p_{wf} = 5000 - 283.49 = 4716.51 \text{ psi}$$

Effects of the reservoir boundary

The superposition theorem can also be extended to predict the pressure of a well in a bounded reservoir. Consider Figure 1.30 which shows a well that is located a distance L from the non-flow boundary, e.g., sealing fault. The no-flow boundary can be represented by the following pressure gradient expression:

$$\left(\frac{\partial p}{\partial L}\right)_{\text{Boundary}} = 0$$

Mathematically, the above boundary condition can be met by placing an *image* well, identical to that of the actual well, on the other side of the fault at exactly distance L. Consequently, the effect of the boundary on the pressure behavior of a well would be the same as the effect from an image well located a distance $2L$ from the actual well.

In accounting for the boundary effects, the superposition method is frequently called the *method of images*. Thus, for the problem of the system configuration given in Figure 1.30, the problem reduces to one of determining the effect of the image well on the actual well. The total pressure drop at the actual well will be the pressure drop due to its own production plus the additional pressure drop caused by an identical well at a distance of $2L$, or:

$$(\Delta p)_{total} = (\Delta p)_{\text{actual well}} + (\Delta p)_{\text{due to image well}}$$

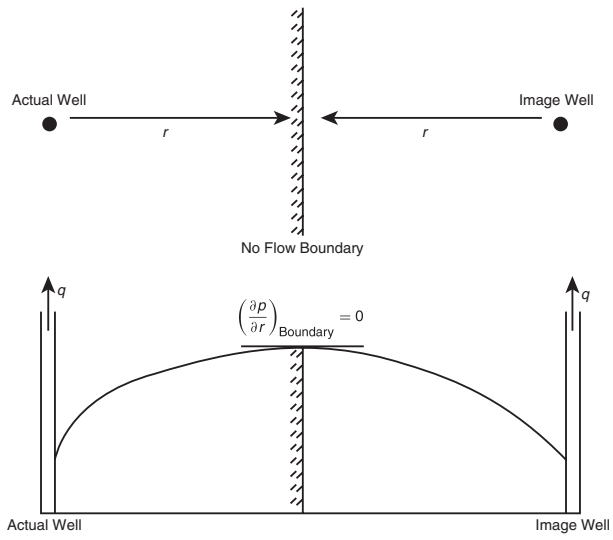

Figure 1.30 *Method of images in solving boundary problems.*

or:

$$(\Delta p)_{\text{total}} = \frac{162.6 Q_o B \mu}{kh}\left[\log\left(\frac{kt}{\phi \mu c_t r_w^2}\right) - 3.23 + 0.87s\right] - \left(\frac{70.6 Q_o B \mu}{kh}\right)\text{Ei}\left(-\frac{948\phi\mu c_t (2L)^2}{kt}\right) \quad [1.2.157]$$

Notice that this equation assumes the reservoir is infinite except for the indicated boundary. The effect of boundaries is always to cause a greater pressure drop than those calculated for infinite reservoirs.

The concept of image wells can be extended to generate the pressure behavior of a well located within a variety of boundary configurations.

Example 1.23 Figure 1.31 shows a well located between two sealing faults at 400 and 600 feet from the two faults. The well is producing under a transient flow condition at a constant flow rate of 200 STB/day. Given:

$p_i = 500$ psi, $k = 600$ md, $B_o = 1.1$ bbl/STB
$\phi = 17\%$, $\mu_o = 2.0$ cp, $h = 25$ ft
$r_w = 0.3$ ft, $s = 0$, $c_t = 25 \times 10^{-6}$ psi^{-1}

Calculate the sand face pressure after 10 hours.

Solution

Step 1. Calculate the pressure drop due to the actual well flow rate:

$$(p_i - p_{wf}) = (\Delta p)_{\text{actual}} = \frac{162.6 Q_{o1} B_o \mu_o}{kh} \times \left[\log\left(\frac{kt}{\phi \mu c_t r_w^2}\right) - 3.23 + 0.87s\right]$$

$$(\Delta p)_{\text{actual}} = \frac{(162.6)(200)(1.1)(2.0)}{(60)(25)} \times \left[\log\left(\frac{(60)(10)}{(0.17)(2)(25\times10^{-6})(0.3)^2}\right) - 3.23 + 0\right]$$

$$= 270.17$$

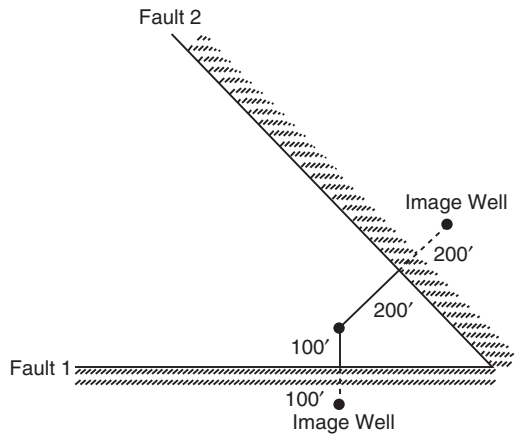

Figure 1.31 *Well layout for Example 1.23.*

Step 2. Determine the additional pressure drop due to the first fault (i.e., image well 1):

$$(\Delta p)_{\text{image well 1}} = p_i - p\,(2L_1, t) = -\left[\frac{70.6 Q_{o2} \mu_o B_o}{kh}\right]\text{Ei}\left[\frac{-948\phi\mu_o c_t (2L_1)^2}{kt}\right]$$

$$(\Delta p)_{\text{image well 1}} = -\frac{(70.6)(200)(1.1)(2.0)}{(60)(25)} \times \text{Ei}\left[-\frac{(948)(0.17)(2)(25\times10^{-6})(2\times100)^2}{(60)(10)}\right]$$

$$= 20.71\left[-\text{Ei}(-0.537)\right] = 10.64 \text{ psi}$$

Step 3. Calculate the effect of the second fault (i.e., image well 2):

$$(\Delta p)_{\text{image well 2}} = p_i - p(2L_2, t) = -\left[\frac{70.6 Q_{o2} \mu_o B_o}{kh}\right]\text{Ei}\left[\frac{-948\phi\mu_o c_t (2L_2)^2}{kt}\right]$$

$$(\Delta p)_{\text{image well 2}}$$

$$= 20.71\left[-\text{Ei}\left(\frac{-948\,(0.17)\,(2)\,(25\times10^{-6})\,(2\times200)^2}{(60)\,(10)}\right)\right]$$

$$= 20.71\left[-\text{Ei}\,(-2.15)\right] = 1.0 \text{ psi}$$

Step 4. The total pressure drop is:

$$(\Delta p)_{\text{total}} = 270.17 + 10.64 + 1.0 = 28.18 \text{ psi}$$

Step 5. $$p_{\text{wf}} = 5000 - 281.8 = 4718.2 \text{ psi}.$$

Accounting for pressure-change effects

Superposition is also used in applying the constant-pressure case. Pressure changes are accounted for in this solution in much the same way that rate changes are accounted for in the constant-rate case. The description of the superposition method to account for the pressure-change effect is fully described in Chapter 2 in this book.

1.3 Transient Well Testing

Detailed reservoir information is essential to the petroleum engineer in order to analyze the current behavior and future performance of the reservoir. Pressure transient testing is designed to provide the engineer with a quantitative analysis of the reservoir properties. A transient test is essentially conducted by creating a pressure disturbance in the reservoir and recording the pressure response at the wellbore, i.e., bottom-hole flowing pressure p_{wf}, as a function of time. The pressure transient tests most commonly used in the petroleum industry include:

- pressure drawdown;
- pressure buildup;
- multirate;
- interference;
- pulse;
- drill stem (DST);
- falloff;
- injectivity;
- step rate.

It should be pointed out that when the flow rate is changed and the pressure response is recorded in the same well, the test is called a "single-well" test. Drawdown, buildup, injectivity, falloff, and step-rate tests are examples of a single-well test. When the flow rate is changed in one well and the pressure response is measured in another well(s), the test is called a "multiple-well" test.

Several of the above listed tests are briefly described in the following sections.

It has long been recognized that the pressure behavior of a reservoir following a rate change directly reflects the geometry and flow properties of the reservoir. Some of the information that can be obtained from a well test includes:

Drawdown tests	Pressure profile
	Reservoir behavior
	Permeability
	Skin
	Fracture length
	Reservoir limit and shape
Buildup tests	Reservoir behavior
	Permeability
	Fracture length
	Skin
	Reservoir pressure
	Boundaries
DST	Reservoir behavior
	Permeability
	Skin
	Fracture length
	Reservoir limit
	Boundaries
Falloff tests	Mobility in various banks
	Skin
	Reservoir pressure
	Fracture length
	Location of front
	Boundaries
Interference and pulse tests	Communication between wells
	Reservoir-type behavior
	Porosity
	Interwell permeability
	Vertical permeability
Layered reservoir tests	Horizontal permeability
	Vertical permeability
	Skin
	Average layer pressure
	Outer boundaries
Step-rate tests	Formation parting pressure
	Permeability
	Skin

There are several excellent technical and reference books that comprehensively and thoroughly address the subject of well testing and transient flow analysis, in particular:

- C. S. Matthews and D. G. Russell, *Pressure Buildup and Flow Test in Wells* (1967);
- Energy Resources Conservation Board (ERBC), *Theory and Practice of the Testing of Gas Wells* (1975);
- Robert Earlougher, *Advances in Well Test Analysis* (1977);
- John Lee, *Well Testing* (1982);
- M. A. Sabet, *Well Test Analysis* (1991);
- Roland Horn, *Modern Well Test Analysis* (1995).

1.3.1 Drawdown test

A pressure drawdown test is simply a series of bottom-hole pressure measurements made during a period of flow at constant producing rate. Usually the well is shut in prior to the flow test for a period of time sufficient to allow the pressure to equalize throughout the formation, i.e., to reach static pressure. A schematic of the ideal flow rate and pressure history is shown in Figure 1.32.

The fundamental objectives of drawdown testing are to obtain the average permeability, k, of the reservoir rock within the drainage area of the well, and to assess the degree of damage of stimulation induced in the vicinity of the wellbore through drilling and completion practices. Other objectives are to determine the pore volume and to detect reservoir inhomogeneities within the drainage area of the well.

When a well is flowing at a constant rate of Q_{o} under the unsteady-state condition, the pressure behavior of the well will act as if it exists in an infinite-size reservoir. The pressure behavior during this period is described by Equation 1.2.134 as:

$$p_{\text{wf}} = p_{\text{i}} - \frac{162.6 Q_{\text{o}} B_{\text{o}} \mu}{kh}\left[\log\left(\frac{kt}{\phi\mu c_{\text{t}} r_{\text{w}}^2}\right) - 3.23 + 0.87s\right]$$

where:

k = permeability, md
t = time, hours
r_{w} = wellbore radius, ft
s = skin factor

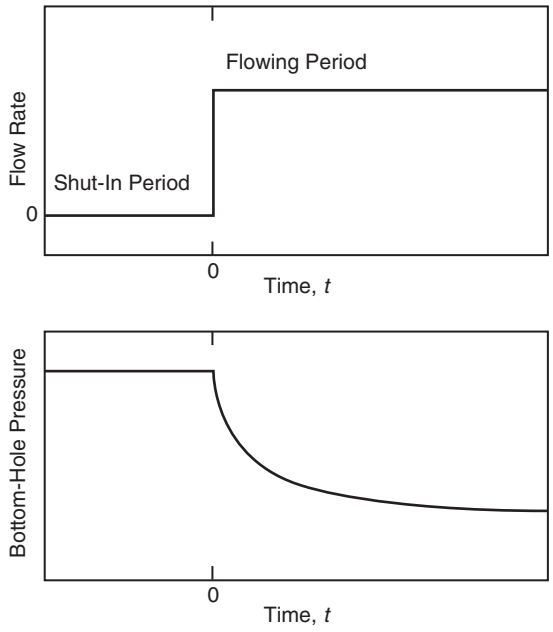

Figure 1.32 *Idealized drawdown test.*

The above expression can be written as:

$$p_{wf} = p_i - \frac{162.6 Q_o B_o \mu}{kh} \times \left[\log(t) + \log\left(\frac{k}{\phi \mu c_t r_w^2}\right) - 3.23 + 0.87s\right] \quad [1.3.1]$$

This relationship is essentially an equation of a straight line and can be expressed as:

$$p_{wf} = a + m \log(t)$$

where:

$$a = p_i - \frac{162.6 Q_o B_o \mu}{kh}\left[\log\left(\frac{k}{\phi \mu c_t r_w^2}\right) - 3.23 + 0.87s\right]$$

and the slope m is given by:

$$-m = \frac{-162.6 Q_o B_o \mu_o}{kh} \quad [1.3.2]$$

Equation 1.3.1 suggests that a plot of p_{wf} versus time t on semilog graph paper would yield a straight line with a slope m in psi/cycle. This semilog straight-line portion of the drawdown data, as shown in Figure 1.33, can also be expressed in another convenient form by employing the definition of the slope:

$$m = \frac{p_{wf} - p_{1\,hr}}{\log(t) - \log(1)} = \frac{p_{wf} - p_{1\,hr}}{\log(t) - 0}$$

or:

$$p_{wf} = m \log(t) + p_{1\,hr}$$

Notice that Equation 1.3.2 can also be rearranged to determine the capacity kh of the drainage area of the well. If the thickness is known, then the average permeability is given by:

$$k = \frac{162.6 Q_o B_o \mu_o}{|m| h}$$

where:

k = average permeability, md
$|m|$ = absolute value of slope, psi/cycle

Clearly, kh/μ or k/μ may also be estimated.

The skin effect can be obtained by rearranging Equation 1.3.1 as:

$$s = 1.151\left[\frac{p_i - p_{wf}}{|m|} - \log t - \log\left(\frac{k}{\phi \mu c_t r_w^2}\right) + 3.23\right]$$

or, more conveniently, if selecting $p_{wf} = p_{1\,hr}$ which is found on the extension of the straight line at $t = 1$ hr, then:

$$s = 1.151\left[\frac{p_i - p_{1\,hr}}{|m|} - \log\left(\frac{k}{\phi \mu c_t r_w^2}\right) + 3.23\right] \quad [1.3.3]$$

where $|m|$ is the absolute value of the slope m.

In Equation 1.2.3, $p_{1\,hr}$ must be obtained from the semilog straight line. If the pressure data measured at 1 hour does not fall on that line, the line must be extrapolated to 1 hour and the extrapolated value of $p_{1\,hr}$ must be used in Equation 1.3.3. This procedure is necessary to avoid calculating an incorrect skin by using a wellbore-storage-influenced pressure. Figure 1.33 illustrates the extrapolation to $p_{1\,hr}$.

Note that the additional pressure drop due to the skin was expressed previously by Equation 1.2.130 as:

$$\Delta p_{skin} = 141.2\left(\frac{Q_o B_o \mu_o}{kh}\right) s$$

This additional pressure drop can be equivalently written in terms of the semilog straight-line slope m by combining the above expression with that of Equation 1.3.3 to give:

$$\Delta p_{skin} = 0.87 |m| s$$

Another physically meaningful characterization of the skin factor is the flow coefficient E as defined by the ratio of the well actual or observed productivity index J_{actual} and its ideal productivity index J_{ideal}. The ideal productivity index J_{ideal} is the value obtained with no alternation of permeability around the wellbore. Mathematically, the flow coefficient is given by:

$$E = \frac{J_{actual}}{J_{ideal}} = \frac{\bar{p} - p_{wf} - \Delta p_{skin}}{\bar{p} - p_{wf}}$$

where $\bar{p}$ is the average pressure in the well drainage area.

If the drawdown test is long enough, the bottom-hole pressure will deviate from the semilog straight line and make the transition from infinite acting to pseudosteady state. The rate of pressure decline during the pseudosteady-state flow is defined by Equation 1.2.116 as:

$$\frac{dp}{dt} = -\frac{0.23396q}{c_t(\pi r_e^2)h\phi} = \frac{-0.23396q}{c_t(A)h\phi} = \frac{-0.23396q}{c_t(\text{pore volume})}$$

Under this condition, the pressure will decline at a constant rate at any point in the reservoir including the bottom-hole flowing pressure p_{wf}. That is:

$$\frac{dp_{wf}}{dt} = m' = \frac{-0.23396q}{c_t A h \phi}$$

This expression suggests that during the semisteady-state flow, a plot of p_{wf} vs. t on a Cartesian scale would produce a straight line with a negative slope of m' that is defined by:

$$-m' = \frac{-0.23396q}{c_t A h \phi}$$

where:

m' = slope of the *Cartesian straight line* during the pseudosteady state, psi/hr
q = flow rate, bbl/day
A = drainage area, ft^2

Example 1.24[a] Estimate the oil permeability and skin factor from the drawdown data of Figure 1.34.

[a]This example problem and the solution procedure are given in Earlougher, R. Advances in Well Test Analysis, Monograph Series, SPE, Dallas (1997).

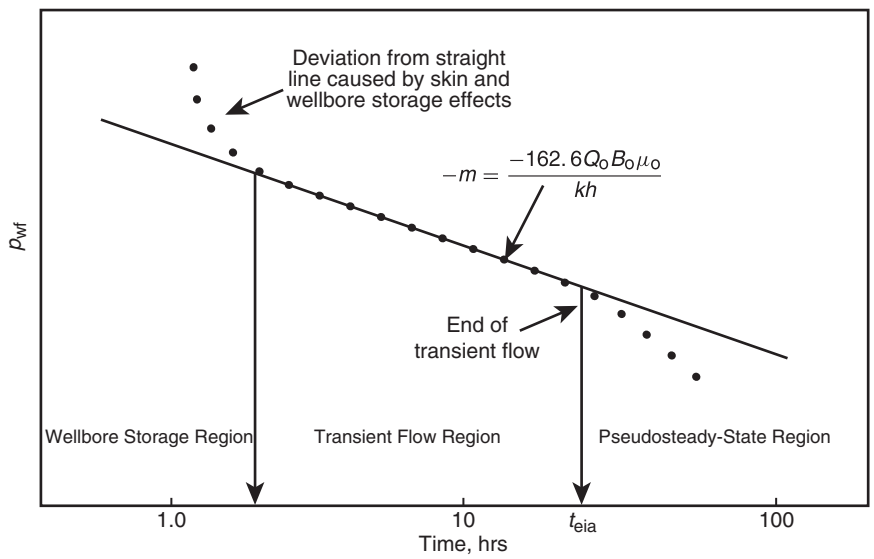

Figure 1.33 *Semilog plot of pressure drawdown data.*

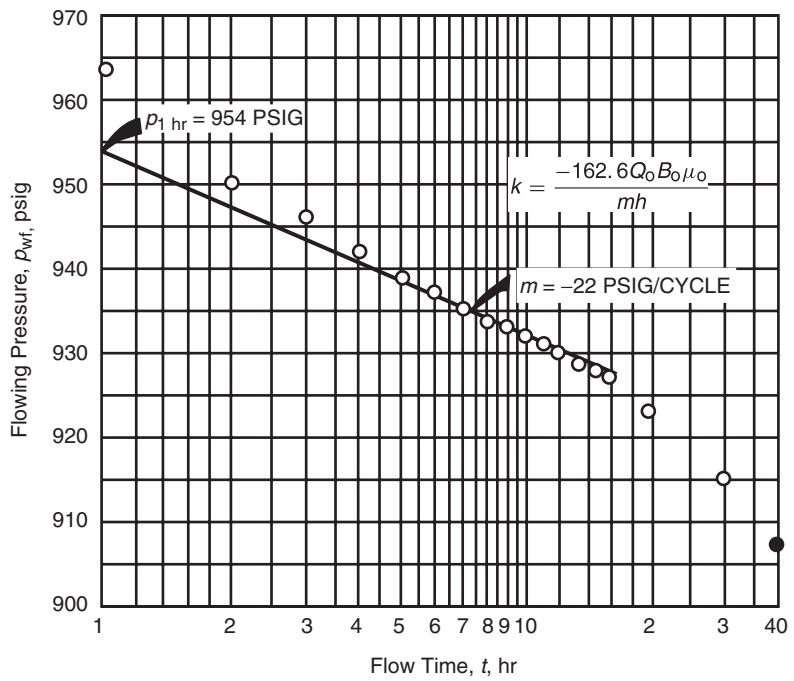

Figure 1.34 *Earlougher's semilog data plot for the drawdown test (Permission to publish by the SPE, copyright SPE, 1977).*

The following reservoir data are available:

$h = 130$ ft, $\phi = 20\,\%$, $r_w = 0.25$ ft,

$p_i = 1154$ psi, $Q_o = 348$ STB/D, $m = -22$ psi/cycle

$B_o = 1.14$ bbl/STB, $\mu_o = 3.93$ cp, $c_t = 8.74 \times 10^{-6}$ psi^{-1}

Assuming that the wellbore storage effect is not significant, calculate:

- the permeability;
- the skin factor;
- the additional pressure drop due to the skin.

Solution

Step 1. From Figure 1.34, calculate $p_{1\,hr}$:

$$p_{1\,hr} = 954 \text{ psi}$$

Step 2. Determine the slope of the transient flow line:

$$m = -22 \text{ psi/cycle}$$

Step 3. Calculate the permeability by applying Equation 1.3.2:

$$k = \frac{-162.6 Q_o B_o \mu_o}{mh}$$

$$= \frac{-(162.6)(348)(1.14)(3.93)}{(-22)(130)} = 89 \text{ md}$$

Step 4. Solve for the skin factor s by using Equation 1.3.3:

$$s = 1.151\left[\frac{p_i - p_{1\text{ hr}}}{|m|} - \log\left(\frac{k}{\phi\mu c_t r_w^2}\right) + 3.23\right]$$

$$= 1.151\left[\left(\frac{1154 - 954}{22}\right)\right.$$

$$- \log\left(\frac{89}{(0.2)(3.93)(8.74 \times 10^{-6})(0.25)^2}\right)$$

$$\left. + 3.2275\right] = 4.6$$

Step 5. Calculate the additional pressure drop:

$$\Delta p_{skin} = 0.87\,|m|\,s = 0.87(22)(4.6) = 88 \text{ psi}$$

It should be noted that for a *multiphase flow*, Equations 1.3.1 and 1.3.3 become:

$$p_{wf} = p_i - \frac{162.6 q_t}{\lambda_t h}\left[\log(t) + \log\left(\frac{\lambda_t}{\phi c_t r_w^2}\right) - 3.23 + 0.87s\right]$$

$$s = 1.151\left[\frac{p_i - p_{1\text{ hr}}}{|m|} - \log\left(\frac{\lambda_t}{\phi c_t r_w^2}\right) + 3.23\right]$$

with:

$$\lambda_t = \frac{k_o}{\mu_o} + \frac{k_w}{\mu_w} + \frac{k_g}{\mu_g}$$

$$q_t = Q_o B_o + Q_w B_w + (Q_g - Q_o R_s) B_g$$

or equivalently in terms of GOR as:

$$q_t = Q_o B_o + Q_w B_w + (GOR - R_s) Q_o B_g$$

where:

q_t = total fluid voidage rate, bbl/day
Q_o = oil flow rate, STB/day
Q_w = water flow rate, STB/day
Q_g = total gas flow rate, scf/day
R_s = gas solubility, scf/STB
B_g = gas formation volume factor, bbl/scf
λ_t = total mobility, md/cp
k_o = effective permeability to oil, md
k_w = effective permeability to water, md
k_g = effective permeability to gas, md

The above drawdown relationships indicate that a plot of p_{wf} vs. t on a semilog scale would produce a straight line with a slope m that can be used to determine the total mobility λ_t from:

$$\lambda_t = \frac{162.6 q_t}{mh}$$

Perrine (1956) showed that the effective permeability of each phase, i.e., k_o, k_w, and k_g, can be determined as:

$$k_o = \frac{162.6 Q_o B_o \mu_o}{mh}$$

$$k_w = \frac{162.6 Q_w B_w \mu_w}{mh}$$

$$k_g = \frac{162.6 (Q_g - Q_o R_s) B_g \mu_g}{mh}$$

If the drawdown pressure data is available during both the unsteady-state flow period and the pseudosteady-state flow period, it is possible to estimate the drainage shape and the drainage area of the test well. The transient semilog plot is used to determine its slope m and $p_{1\text{ hr}}$; the Cartesian straight-line plot of the pseudosteady-state data is used to determine its slope m' and its intercept p_{int}. Earlougher (1977) proposed the following expression to determine the shape factor C_A:

$$C_A = 5.456\left(\frac{m}{m'}\right)\exp\left[\frac{2.303(p_{1\text{ hr}} - p_{int})}{m}\right]$$

where:

m = slope of transient semilog straight line, psi/log cycle
m' = slope of the semisteady-state Cartesian straight line
$p_{1\text{ hr}}$ = pressure at $t = 1$ hour from transient semilog straight line, psi
p_{int} = pressure at $t = 0$ from pseudosteady-state Cartesian straight line, psi

The calculated shape factor from applying the above relationship is compared with those values listed in Table 1.4 to select the geometry of well drainage with a shape factor closest to the calculated value. When extending the drawdown test time with the objective of reaching the drainage boundary of the test well, the test is commonly called the "reservoir limit test."

The reported data of Example 1.24 was extended by Earlougher to include the pseudosteady-state flow period and used to determine the geometry of the test well drainage area as shown in the following example.

Example 1.25 Use the data in Example 1.24 and the Cartesian plot of the pseudosteady-state flow period, as shown in Figure 1.35, to determine the geometry and drainage area of the test well.

Solution

Step 1. From Figure 1.35, determine the slope m' and intercept p_{int}:

$$m' = -0.8 \text{ psi/hr}$$

$$p_{int} = 940 \text{ psi}$$

Step 2. From Example 1.24:

$$m = -22 \text{ psi/cycle}$$

$$p_{1\text{ hr}} = 954 \text{ psi}$$

Step 3. Calculate the shape factor C_A from Earlougher's equation:

$$C_A = 5.456\left(\frac{m}{m'}\right)\exp\left[\frac{2.303(p_{1\text{ hr}} - p_{int})}{m}\right]$$

$$= 5.456\left(\frac{-22}{-0.8}\right)\exp\left[\frac{2.303(954 - 940)}{-22}\right]$$

$$= 34.6$$

Step 4. From Table 1.4, $C_A = 34.6$ corresponds to a well in the center of a circle, square, or hexagon:

For a circle: $C_A = 31.62$
For a square: $C_A = 30.88$
For a hexagon: $C_A = 31.60$

Step 5. Calculate the pore volume and drainage area from Equation 1.2.116:

$$\frac{dp}{dt} = m' = \frac{-0.23396(Q_o B_o)}{c_t (A) h \phi} = \frac{-0.23396(Q_o B_o)}{c_t\,(\text{pore volume})}$$

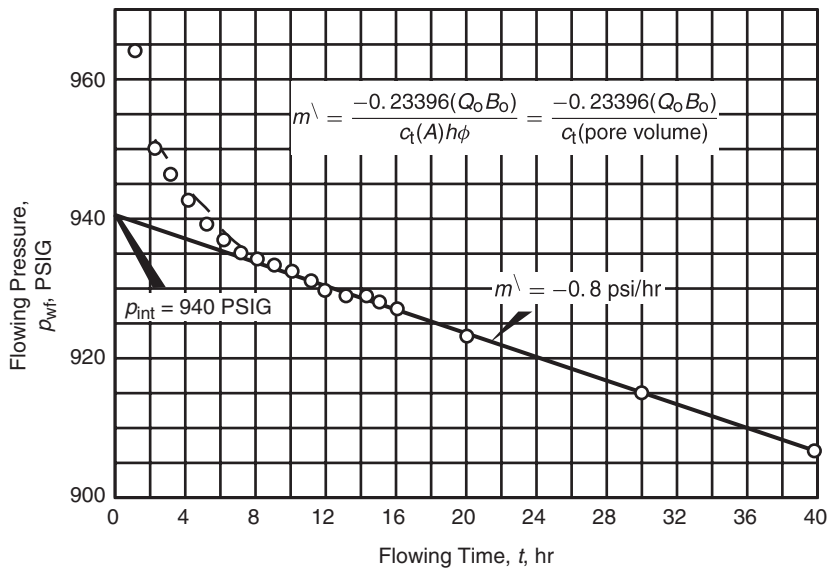

Figure 1.35 *Cartesian plot of the drawdown test data (Permission to publish by the SPE, copyright SPE, 1977).*

Solving for the pore volume gives:

$$\text{Pore volume} = \frac{-0.23396q}{c_t m^{\backslash}} = \frac{-0.23396(348)(1.4)}{(8.74 \times 10^{-6})(-0.8)}$$
$$= 2.37 \text{ MMbbl}$$

and the drainage area:

$$A = \frac{2.37 \times 10^6 (5.615)}{43460(0.2)(130)} = 11.7 \text{ acres}$$

The above example indicates that the measured bottom-hole flowing pressures are 88 psi more than they would be in the absence of the skin. However, it should be pointed out that when the concept of positive skin factor $+s$ indicates formation damage, whereas a negative skin factor $-s$ suggests formation stimulation, this is essentially a misleading interpretation of the skin factor. The skin factor as determined from any transient well testing analysis represents the composite "total" skin factor that includes the following other skin factors:

- skin due to wellbore damage or stimulation s_d;
- skin due to partial penetration and restricted entry s_r;
- skin due to perforations s_p;
- skin due to turbulence flow s_t;
- skin due to deviated well s_{dw}.

That is:

$$s = s_d + s_r + s_p + s_t + s_{dw}$$

where s is the skin factor as calculated from transient flow analysis. Therefore, to determine if the formation is damaged or stimulated from the skin factor value s obtained from well test analysis, the individual components of the skin factor in the above relationship must be known, to give:

$$s_d = s - s_r - s_p - s_t - s_{dw}$$

There are correlations that can be used to separately estimate these individual skin quantities.

Wellbore storage

Basically, well test analysis deals with the interpretation of the wellbore pressure response to a given change in the flow rate (from zero to a constant value for a drawdown test, or from a constant rate to zero for a buildup test). Unfortunately, the producing rate is controlled at the surface, not at the sand face. Because of the wellbore volume, a constant surface flow rate does not ensure that the entire rate is being produced from the formation. This effect is due to wellbore storage. Consider the case of a drawdown test. When the well is first open to flow after a shut-in period, the pressure in the wellbore drops. This drop in pressure causes the following two types of wellbore storage:

(1) a wellbore storage effect caused by fluid expansion;
(2) a wellbore storage effect caused by changing fluid level in the casing–tubing annulus.

As the bottom-hole pressure drops, the wellbore fluid expands and, thus, the initial surface flow rate is not from the formation, but basically from the fluid that had been stored in the wellbore. This is defined as the *wellbore storage due to fluid expansion*.

The second type of wellbore storage is due to a change in the annulus fluid level (falling level during a drawdown test, rising level during a drawdown test, and rising fluid level during a pressure buildup test). When the well is open to flow during a drawdown test, the reduction in pressure causes the fluid level in the annulus to fall. This annulus fluid production joins that from the formation and contributes to the total flow from the well. The falling fluid level is generally able to contribute more fluid than that by expansion.

The above discussion suggests that part of the flow will be contributed by the wellbore instead of the reservoir. That is:

$$q = q_f + q_{wb}$$

where:

q = surface flow rate, bbl/day
q_f = formation flow rate, bbl/day
q_{wb} = flow rate contributed by the wellbore, bbl/day

During this period when the flow is dominated by the wellbore storage, the measured drawdown pressures will not produce the ideal semilog straight-line behavior that is expected during transient flow. This indicates that the

pressure data collected during the duration of the wellbore storage effect cannot be analyzed by using conventional methods. As production time increases, the wellbore contribution decreases and the formation rate increases until it eventually equals the surface flow rate, i.e., $q = q_f$, which signifies the *end of the wellbore storage effect*.

The effect of fluid expansion and changing fluid level can be quantified in terms of the *wellbore storage factor C* which is defined as:

$$C = \frac{\Delta V_{wb}}{\Delta p}$$

where:

C = wellbore storage coefficient, bbl/psi
ΔV_{wb} = change in the volume of fluid in the wellbore, bbl

The above relationship can be applied to mathematically represent the individual effect of wellbore fluid expansion and falling (or rising) fluid level, to give:

Wellbore storage effect caused by fluid expansion

$$C_{FE} = V_{wb} c_{wb}$$

where:

C_{FE} = wellbore storage coefficient due to fluid expansion, bbl/psi
V_{wb} = total wellbore fluid volume, bbl
c_{wb} = average compressibility of fluid in the wellbore, psi^{-1}

Wellbore storage effect due to changing fluid level

$$C_{FL} = \frac{144 A_a}{5.615 \rho}$$

with:

$$A_a = \frac{\pi[(ID_C)^2 - (OD_T)^2]}{4(144)}$$

where:

C_{FL} = wellbore storage coefficient due to changing fluid level, bbl/psi
A_a = annulus cross-sectional area, ft^2
OD_T = outside diameter of the production tubing, inches
ID_C = inside diameter of the casing, inches
ρ = wellbore fluid density, lb/ft^3

This effect is essentially small if a packer is placed near the producing zone. The total storage effect is the sum of both coefficients. That is:

$$C = C_{FE} + C_{FL}$$

It should be noted during oil well testing that the fluid expansion is generally insignificant due to the small compressibility of liquids. For gas wells, the primary storage effect is due to gas expansion.

To determine the duration of the wellbore storage effect, it is convenient to express the wellbore storage factor in a dimensionless form as:

$$C_D = \frac{5.615 C}{2\pi h \phi c_t r_w^2} = \frac{0.8936 C}{\phi h c_t r_w^2} \qquad [1.3.4]$$

where:

C_D = dimensionless wellbore storage factor
C = wellbore storage factor, bbl/psi
c_t = total compressibility coefficient, psi^{-1}
r_w = wellbore radius, ft
h = thickness, ft

Horn (1995) and Earlougher (1977), among other authors, have indicated that the wellbore pressure is directly proportional to the time during the wellbore storage-dominated period of the test and is expressed by:

$$p_D = t_D / C_D \qquad [1.3.5]$$

where:

p_D = dimensionless pressure during wellbore storage domination time
t_D = dimensionless time

Taking the logarithm of both sides of this relationship gives:

$$\log(p_D) = \log(t_D) - \log(C_D)$$

This expression has a characteristic that is diagnostic of wellbore storage effects. It indicates that a plot of p_D vs. t_D on a log–log scale will yield a straight line of a *unit slope, i.e., a straight line with a 45° angle*, during the wellbore storage-dominated period. Since p_D is proportional to pressure drop Δp and t_D is proportional to time t, it is convenient to plot $\log(p_i - p_{wf})$ versus $\log(t)$ and observe where the plot has a slope of one cycle in pressure per cycle in time. This unit slope observation is of major value in well test analysis.

The log–log plot is a valuable aid for recognizing wellbore storage effects in transient tests (e.g., drawdown or buildup tests) when early-time pressure recorded data is available. It is recommended that this plot be made a part of the transient test analysis. As wellbore storage effects become less severe, the formation begins to influence the bottom-hole pressure more and more, and the data points on the log–log plot fall below the unit-slope straight line and signify the end of the wellbore storage effect. At this point, wellbore storage is no longer important and standard semilog data-plotting analysis techniques apply. As a rule of thumb, the time that indicates the end of the wellbore storage effect can be determined from the log–log plot by moving 1 to $1\frac{1}{2}$ cycles in time after the plot starts to deviate from the unit slop and reading the corresponding time on the x axis. This time may be estimated from:

$$t_D > (60 + 3.5s) C_D$$

or:

$$t > \frac{(200\,000 + 12\,000s) C}{(kh/\mu)}$$

where:

t = total time that marks the end of the wellbore storage effect and the beginning of the semilog straight line, hours
k = permeability, md
s = skin factor
μ = viscosity, cp
C = wellbore storage coefficient, bbl/psi

In practice, it is convenient to determine the wellbore storage coefficient C by selecting *a point on the log–log unit-slope straight line* and reading the coordinate of the point in terms of t and Δp, to give:

$$C = \frac{qt}{24\Delta p} = \frac{QBt}{24\Delta p}$$

where:

t = time, hours
Δp = pressure difference $(p_i - p_{wf})$, psi
q = flow rate, bbl/day
Q = flow rate, STB/day
B = formation volume factor, bbl/STB

It is important to note that the volume of fluids stored in the wellbore distorts the early-time pressure response and controls the duration of wellbore storage, especially in deep wells with large wellbore volumes. If the wellbore storage

effects are not minimized or if the test is not continued beyond the end of the wellbore storage-dominated period, the test data will be difficult to analyze with current conventional well testing methods. To minimize wellbore storage distortion and to keep well tests within reasonable lengths of time, it may be necessary to run tubing, packers, and bottom-hole shut-in devices.

Example 1.26 The following data is given for an oil well that is scheduled for a drawdown test:

- volume of fluid in the wellbore = 180 bbl
- tubing outside diameter = 2 inches
- production oil density in the wellbore = 7.675 inches
- average oil density in the wellbore = 45 lb/ft^3

$h = 50$ ft, $\phi = 15$ %,

$r_w = 0.25$ ft, $\mu_o = 2$ cp

$k = 30$ md, $s = 0$

$c_t = 20 \times 10^{-6}$ psi^{-1}, $c_o = 10 \times 10^{-6}$ psi^{-1}

If this well is placed under a constant production rate, calculate the dimensionless wellbore storage coefficient C_D. How long will it take for wellbore storage effects to end?

Solution

Step 1. Calculate the cross-sectional area of the annulus A_a:

$$A_a = \frac{\pi[(ID_C)^2 - (OD_T)^2]}{4(144)}$$

$$= \frac{\pi[(7.675)^2 - (2)^2]}{(4)(144)} = 0.2995 \text{ ft}^2$$

Step 2. Calculate the wellbore storage factor caused by fluid expansion:

$$C_{FE} = V_{wb} c_{wb}$$

$$= (180)(10 \times 10^{-6}) = 0.0018 \text{ bbl/psi}$$

Step 3. Determine the wellbore storage factor caused by the falling fluid level:

$$C_{FL} = \frac{144 A_a}{5.615 \rho}$$

$$= \frac{144(0.2995)}{(5.615)(45)} = 0.1707 \text{ bbl/psi}$$

Step 4. Calculate the total wellbore storage coefficient:

$$C = C_{FE} + C_{FL}$$

$$= 0.0018 + 0.1707 = 0.1725 \text{ bbl/psi}$$

The above calculations show that the effect of fluid expansion C_{FE} can generally be neglected in crude oil systems.

Step 5. Calculate the dimensionless wellbore storage coefficient from Equation 1.3.4:

$$C_D = \frac{0.8936C}{\phi h c_t r_w^2} = \frac{0.8936(0.1707)}{0.15(50)(20 \times 10^{-6})(0.25)^2}$$

$$= 16\,271$$

Step 6. Approximate the time required for wellbore storage influence to end from:

$$t = \frac{(200\,000 + 12\,000s) C\mu}{kh}$$

$$= \frac{(200\,000 + 0)(0.1725)(2)}{(30)(50)} = 46 \text{ hours}$$

The straight-line relationship as expressed by Equation 1.3.2 is only valid during the infinite-acting behavior of the well. Obviously, reservoirs are not infinite in extent, so the infinite-acting radial flow period cannot last indefinitely. Eventually the effects of the reservoir boundaries will be felt at the well being tested. The time at which the boundary effect is felt is dependent on the following factors:

- permeability k;
- total compressibility c_t;
- porosity ϕ;
- viscosity μ;
- distance to the boundary;
- shape of the drainage area.

Earlougher (1977) suggested the following mathematical expression for estimating the duration of the infinite-acting period:

$$t_{eia} = \left[\frac{\phi \mu c_t A}{0.0002637k}\right](t_{DA})_{eia}$$

where:

t_{eia} = time to the end of infinite-acting period, hours
A = well drainage area, ft^2
c_t = total compressibility, psi^{-1}
$(t_{DA})_{eia}$ = dimensionless time to the end of the infinite-acting period

This expression is designed to predict the time that marks the end of transient flow in a drainage system of any geometry by obtaining the value of t_{DA} from Table 1.4. The *last three columns* of the table provide with values of t_{DA} that allow the engineer to calculate:

- the maximum elapsed time during which a reservoir is infinite acting;
- the time required for the pseudosteady-state solution to be applied and predict pressure drawdown within 1% accuracy;
- the time required for the pseudosteady-state solution (equations) to be exact and applied.

As an example, for a well centered in a circular reservoir, the maximum time for the reservoir to remain as an infinite-acting system can be determined using the entry in the final column of Table 1.4 to give $(t_{DA})_{eia} = 0.1$, and accordingly:

$$t_{eia} = \left[\frac{\phi \mu c_t A}{0.0002637k}\right](t_{DA})_{eia} = \left[\frac{\phi \mu c_t A}{0.0002637k}\right]0.1$$

or:

$$t_{eia} = \frac{380 \phi \mu c_t A}{k}$$

For example, for a well that is located in the center of a 40 acre circular drainage area with the following properties:

$k = 60$ md, $c_t = 6 \times 10^{-6}$ psi^{-1}, $\mu = 1.5$ cp, $\phi = 0.12$

the maximum time, in hours, for the well to remain in an infinite-acting system is:

$$t_{eia} = \frac{380 \phi \mu c_t A}{k} = \frac{380(0.12)(1.4)(6 \times 10^{-6})(40 \times 43560)}{60}$$

$$= 11.1 \text{ hours}$$

Similarly, the pseudosteady-state solution can be applied any time after the semisteady-state flow begins at t_{pss} as estimated from:

$$t_{pss} = \left[\frac{\phi \mu c_t A}{0.0002637k}\right](t_{DA})_{pss}$$

where $(t_{DA})_{pss}$ can be found from the entry in the fifth column of the table.

Hence, the specific steps involved in a drawdown test analysis are:

(1) Plot $p_i - p_{wf}$ vs. t on a log–log scale.

(2) Determine the time at which the unit-slope line ends.
(3) Determine the corresponding time at $1\frac{1}{2}$ log cycle, ahead of the observed time in step 2. This is the time that marks the end of the wellbore storage effect and the start of the semilog straight line.
(4) Estimate the wellbore storage coefficient from:

$$C = \frac{qt}{24\Delta p} = \frac{QBt}{24\Delta p}$$

where t and Δp are values read from a point on the log–log unit-slope straight line and q is the flow rate in bbl/day.
(5) Plot p_{wf} vs. t on a semilog scale.
(6) Determine the start of the straight-line portion as suggested in step 3 and draw the best line through the points.
(7) Calculate the slope of the straight line and determine the permeability k and skin factor s by applying Equations 1.3.2 and 1.3.3, respectively:

$$k = \frac{-162.6 Q_o B_o \mu_o}{mh}$$

$$s = 1.151\left[\frac{p_i - p_{1\,hr}}{|m|} - \log\left(\frac{k}{\phi\mu c_t r_w^2}\right) + 3.23\right]$$

(8) Estimate the time to the end of the infinite-acting (transient flow) period, i.e., t_{eia}, which marks the beginning of the pseudosteady-state flow.
(9) Plot all the recorded pressure data after t_{eia} as a function of time on a regular Cartesian scale. This data should form a straight-line relationship.
(10) Determine the slope of the pseudosteady-state line, i.e., dp/dt (commonly referred to as m\) and use Equation 1.2.116 to solve for the drainage area A:

$$A = \frac{-0.23396 QB}{c_t h\phi (dp/dt)} = \frac{-0.23396 QB}{c_t h\phi m\backslash}$$

where:

$m\backslash$ = slope of the semisteady-state Cartesian straight line
Q = fluid flow rate, STB/day
B = formation volume factor, bbl/STB

(11) Calculate the shape factor C_A from the expression that was developed by Earlougher (1977):

$$C_A = 5.456\left(\frac{m}{m\backslash}\right)\exp\left[\frac{2.303(p_{1\,hr} - p_{int})}{m}\right]$$

where:

m = slope of transient semilog straight line, psi/log cycle
$m\backslash$ = slope of the pseudosteady-state Cartesian straight line
$p_{1\,hr}$ = pressure at $t = 1$ hour from transient semilog straight line, psi
p_{int} = pressure at $t = 0$ from semisteady-state Cartesian straight line, psi

(12) Use Table 1.4 to determine the drainage configuration of the tested well that has a value of the shape factor C_A closest to that of the calculated one, i.e., step 11.

Radius of investigation

The radius of investigation r_{inv} of a given test is the effective distance traveled by the pressure transients, as measured from the tested well. This radius depends on the speed with which the pressure waves propagate through the reservoir rock, which, in turn, is determined by the rock and fluid properties, such as:

- porosity;
- permeability;
- fluid viscosity;
- total compressibility.

As time t increases, more of the reservoir is influenced by the well and the radius of drainage, or investigation, increases as given by:

$$r_{inv} = 0.0325\sqrt{\frac{kt}{\phi\mu c_t}}$$

where:

t = time, hours
k = permeability, md
c_t = total compressibility, psi^{-1}

It should be pointed out that the equations developed for slightly compressible liquids can be extended to describe the behavior of real gases by replacing the pressure with the real-gas pseudopressure $m(p)$, as defined by:

$$m(p) = \int_0^p \frac{2p}{\mu Z}\,dp$$

with the transient pressure drawdown behavior as described by Equation 1.2.151, or:

$$m(p_{wf}) = m(p_i) - \left[\frac{1637 Q_g T}{kh}\right] \times \left[\log\left(\frac{kt}{\phi\mu_i c_{ti} r_w^2}\right) - 3.23 + 0.87 s\backslash\right]$$

Under constant gas flow rate, the above relation can be expressed in a linear form as:

$$m(p_{wf}) = \left\{m(p_i) - \left[\frac{1637 Q_g T}{kh}\right] \times \left[\log\left(\frac{k}{\phi\mu_i c_{ti} r_w^2}\right) - 3.23 + 0.87 s\backslash\right]\right\} - \left[\frac{1637 Q_g T}{kh}\right]\log(t)$$

or:

$$m(p_{wf}) = a + m\log(t)$$

which indicates that a plot of $m(p_{wf})$ vs. log(t) would produce a semilog straight line with a negative slope of:

$$m = \frac{1637 Q_g T}{kh}$$

Similarly, in terms of the pressure-squared approximation form:

$$p_{wf}^2 = p_i^2 - \left[\frac{1637 Q_g T\overline{Z}\overline{\mu}}{kh}\right] \times \left[\log\left(\frac{kt}{\phi\mu_i c_{ti} r_w^2}\right) - 3.23 + 0.87 s\backslash\right]$$

or:

$$p_{wf}^2 = \left\{p_i^2 - \left[\frac{1637 Q_g T\overline{Z}\overline{\mu}}{kh}\right] \times \left[\log\left(\frac{k}{\phi\mu_i c_{ti} r_w^2}\right) - 3.23 + 0.87 s\backslash\right]\right\} - \left[\frac{1637 Q_g T\overline{Z}\overline{\mu}}{kh}\right]\log(t)$$

This equation is an equation of a straight line that can be simplified to give:

$$p_{wf}^2 = a + m\log(t)$$

which indicates that a plot of p_{wf}^2 vs. $\log(t)$ would produce a semilog straight line with a negative slope of:

$$m = \frac{1637 Q_g T \overline{Z} \overline{\mu}}{kh}$$

The true skin factor s which reflects the formation damage or stimulation is usually combined with the non-Darcy rate-dependent skin and labeled as the apparent or total skin factor:

$$s^{\backslash} = s + DQ_g$$

with the term DQ_g interpreted as the rate-dependent skin factor. The coefficient D is called the inertial or turbulent flow factor and given by Equation 1.2.148:

$$D = \frac{Fkh}{1422T}$$

where:

Q_g = gas flow rate, Mscf/day
t = time, hours
k = permeability, md
μ_i = gas viscosity as evaluated at p_i, cp

The apparent skin factor $s^{\backslash}$ is given by:
For pseudopressure approach:

$$s^{\backslash} = 1.151\left[\frac{m(p_i) - m(p_{1\text{ hr}})}{|m|} - \log\left(\frac{k}{\phi\mu_i c_{ti} r_w^2}\right) + 3.23\right]$$

For pressure-squared approach:

$$s^{\backslash} = 1.151\left[\frac{p_i^2 - p_{1\text{ hr}}^2}{|m|} - \log\left(\frac{k}{\phi\overline{\mu c}_t r_w^2}\right) + 3.23\right]$$

If the duration of the drawdown test of the gas well is long enough to reach its boundary, the pressure behavior during the boundary-dominated period (pseudosteady-state condition) is described by an equation similar to that of Equation 1.2.125 as:
For pseudopressure approach:

$$\frac{m(p_i) - m(p_{wf})}{q} = \frac{\Delta m(p)}{q} = \frac{711T}{kh}\left(\ln\frac{4A}{1.781 C_A r_{wa}^2}\right) + \left[\frac{2.356T}{\phi(\mu_g c_g)_i Ah}\right]t$$

and as a linear equation by:

$$\frac{\Delta m(p)}{q} = b_{pss} + m^{\backslash} t$$

This relationship indicates that a plot of $\Delta m(p)/q$ vs. t will form a straight line with:

$$\text{Intercept:}\quad b_{pss} = \frac{711T}{kh}\left(\ln\frac{4A}{1.781 C_A r_{wa}^2}\right)$$

$$\text{Slope:}\quad m^{\backslash} = \frac{2.356T}{(\mu_g c_t)_i(\phi hA)} = \frac{2.356T}{(\mu_g c_t)_i(\text{pore volume})}$$

For pressure-squared approach:

$$\frac{p_i^2 - p_{wf}^2}{q} = \frac{\Delta(p^2)}{q} = \frac{711\overline{\mu}\overline{Z}T}{kh}\left(\ln\frac{4A}{1.781 C_A r_{wa}^2}\right) + \left[\frac{2.356\,\overline{\mu}\overline{Z}T}{\phi(\mu_g c_g)_i Ah}\right]t$$

and in a linear form as:

$$\frac{\Delta(p^2)}{q} = b_{pss} + m^{\backslash} t$$

This relationship indicates that a plot of $\Delta(p^2)/q$ vs. t on a Cartesian scale will form a straight line with:

$$\text{Intercept:}\quad b_{pss} = \frac{711\overline{\mu}\overline{Z}T}{kh}\left(\ln\frac{4A}{1.781 C_A r_{wa}^2}\right)$$

$$\text{Slope:}\quad m^{\backslash} = \frac{2.356\overline{\mu}\overline{Z}T}{(\mu_g c_t)_i(\phi hA)} = \frac{2.356\overline{\mu}\overline{Z}T}{(\mu_g c_t)_i(\text{pore volume})}$$

where:

q = flow rate, Mscf/day
A = drainage area, ft^2
T = temperature, °R
t = flow time, hours

Meunier et al. (1987) suggested a methodology for expressing the time t and the corresponding pressure p that allows the use of liquid flow equations without special modifications for gas flow. Meunier and his co-authors introduced the following normalized pseudopressure p_{pn} and normalized pseudotime t_{pn}

$$p_{pn} = p_i + \left[\left(\frac{\mu_i Z_i}{p_i}\right)\int_0^p \frac{p}{\mu Z}\,dp\right]$$

$$t_{pn} = \mu_i c_{ti}\left[\int_0^t \frac{1}{\mu c_t}\,dp\right]$$

The subscript "i" on μ, Z, and c_t refers to the evaluation of these parameters at the initial reservoir pressure p_i. By using the Meunier et al. definition of the normalized pseudopressure and normalized pseudotime there is no need to modify any of the liquid analysis equations. However, care should be exercised when replacing the liquid flow rate with the gas flow rate. It should be noted that in all transient flow equations when applied to the oil phase, the flow rate is expressed as the product of $Q_o B_o$ in bbl/day; that is, in reservoir barrels/day. Therefore, when applying these equations to the gas phase, the product of the gas flow rate and gas formation volume factor $Q_g B_g$ should be given in bbl/day. For example, if the gas flow rate is expressed in scf/day, the gas formation volume factor must be expressed in bbl/scf. The recorded pressure and time are then simply replaced by the normalized pressure and normalized time to be used in all the traditional graphical techniques, including pressure buildup.

1.3.2 Pressure buildup test

The use of pressure buildup data has provided the reservoir engineer with one more useful tool in the determination of reservoir behavior. Pressure buildup analysis describes the buildup in wellbore pressure with time after a well has been shut in. One of the principal objectives of this analysis is to determine the static reservoir pressure without waiting weeks or months for the pressure in the entire reservoir to stabilize. Because the buildup in wellbore pressure will generally follow some definite trend, it has been possible to extend the pressure buildup analysis to determine:

- the effective reservoir permeability;
- the extent of permeability damage around the wellbore;
- the presence of faults and to some degree the distance to the faults;
- any interference between producing wells;
- the limits of the reservoir where there is not a strong water drive or where the aquifer is no larger than the hydrocarbon reservoir.

Certainly all of this information will probably not be available from any given analysis, and the degree of usefulness of any of this information will depend on the experience in the area

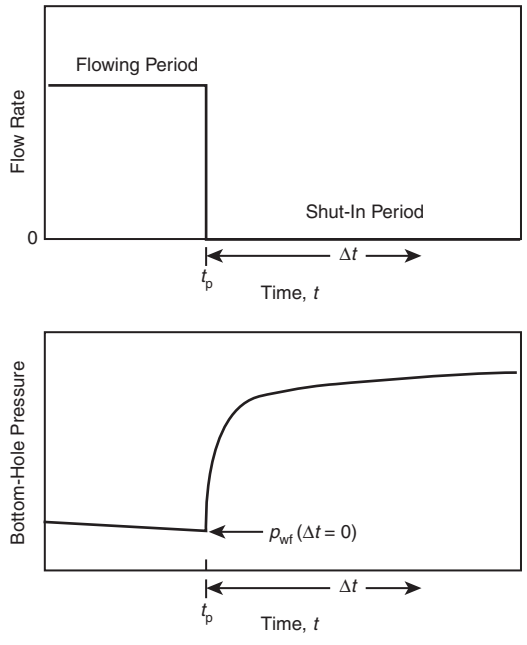

Figure 1.36 *Idealized pressure buildup test.*

and the amount of other information available for correlation purposes.

The general formulas used in analyzing pressure buildup data come from a solution of the diffusivity equation. In pressure buildup and drawdown analyses, the following assumptions, as regards the reservoir, fluid, and flow behavior, are usually made:

- Reservoir: homogeneous; isotropic; horizontal of uniform thickness.
- Fluid: single phase; slightly compressible; constant μ_o and B_o.
- Flow: laminar flow; no gravity effects.

Pressure buildup testing requires shutting in a producing well and recording the resulting increase in the wellbore pressure as a function of shut-in time. The most common and simplest analysis techniques require that the well produce at a constant rate for a flowing time of t_p, either from startup or long enough to establish a stabilized pressure distribution, before shut in. Traditionally, the shut-in time is denoted by the symbol Δt. Figure 1.36 schematically shows the stabilized constant flow rate before shut-in and the ideal behavior of the pressure increase during the buildup period. The pressure is measured immediately before shut-in and is recorded as a function of time during the shut-in period. The resulting pressure buildup curve is then analyzed to determine reservoir properties and the wellbore condition.

Stabilizing the well at a constant rate before testing is an important part of a pressure buildup test. If stabilization is overlooked or is impossible, standard data analysis techniques may provide erroneous information about the formation.

Two widely used methods are discussed below; these are:

(1) the Horner plot;
(2) the Miller–Dyes–Hutchinson method.

1.3.3 Horner plot

A pressure buildup test is described mathematically by using the principle of superposition. Before the shut-in, the well is allowed to flow at a constant flow rate of Q_o STB/day for t_p days. At the end of the flowing period, the well is shut in with a corresponding change in the flow rate from the "old" rate of Q_o to the "new" flow rate of $Q^{new} = 0$, i.e., $Q^{new} - Q^{old} = -Q_o$.

Calculation of the total pressure change which occurs at the sand face during the shut-in time is basically the sum of the pressure changes that are caused by:

- flowing the well at a stabilized flow rate of Q^{old}, i.e., the flow rate before shut-in Q_o, and is in effect over the entire time of $t_p + \Delta t$;
- the net change in the flow rate from Q_o to 0 and is in effect over Δt.

The composite effect is obtained by adding the individual constant-rate solutions at the specified rate–time sequence, as:

$$p_i - p_{ws} = (\Delta p)_{\text{total}} = (\Delta p)_{\text{due to}(Q_o - 0)} + (\Delta p)_{\text{due to}(0 - Q_o)}$$

where:

p_i = initial reservoir pressure, psi
p_{ws} = wellbore pressure during shut in, psi

The above expression indicates that there are two contributions to the total pressure change at the wellbore resulting from the two individual flow rates.

The first contribution results from increasing the rate from 0 to Q_o and is in effect over the entire time period $t_p + \Delta t$, thus:

$$(\Delta p)_{Q_o - 0} = \left[\frac{162.6(Q_o - 0)B_o\mu_o}{kh}\right] \times \left[\log\left(\frac{k(t_p + \Delta t)}{\phi\mu_o c_t r_w^2}\right) - 3.23 + 0.87s\right]$$

The second contribution results from decreasing the rate from Q_o to 0 at t_p, i.e., shut-in time, thus:

$$(\Delta p)_{0 - Q_o} = \left[\frac{162.6\,(0 - Q_o)\,B_o\mu_o}{kh}\right] \times \left[\log\left(\frac{k\Delta t}{\phi\mu_o c_t r_w^2}\right) - 3.23 + 0.87s\right]$$

The pressure behavior in the well during the shut-in period is then given by:

$$p_i - p_{ws} = \frac{162.6Q_o\mu_o B_o}{kh}\left[\log\frac{k(t_p + \Delta t)}{\phi\mu_o c_t r_w^2} - 3.23\right] - \frac{162.6(-Q_o)\mu_o B_o}{kh}\left[\log\frac{k\Delta t}{\phi\mu_o c_t r_w^2} - 3.23\right]$$

Expanding this equation and canceling terms gives:

$$p_{ws} = p_i - \frac{162.6Q_o\mu_o B_o}{kh}\left[\log\left(\frac{t_p + \Delta t}{\Delta t}\right)\right] \qquad [1.3.6]$$

where:

p_i = initial reservoir pressure, psi
p_{ws} = sand face pressure during pressure buildup, psi
t_p = flowing time before shut-in, hours
Q_o = stabilized well flow rate before shut-in, STB/day
Δt = shut-in time, hours

The pressure buildup equation, i.e., Equation 1.3.6 was introduced by Horner (1951) and is commonly referred to as the Horner equation.

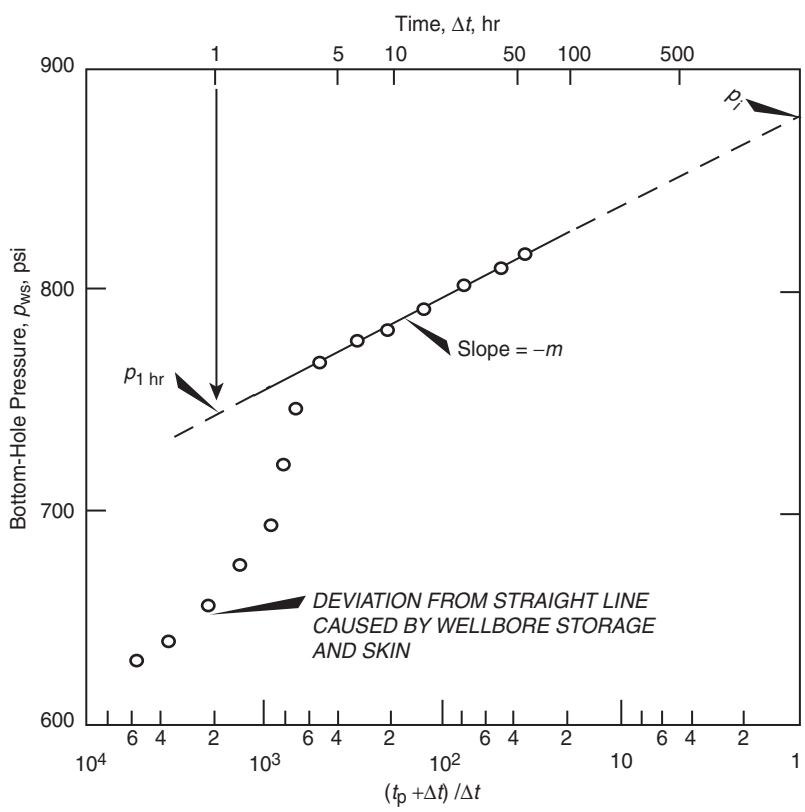

Figure 1.37 *Horner plot (After Earlougher, R.* Advances in Well Test Analysis*) (Permission to publish by the SPE, copyright SPE, 1977).*

Equation 1.3.6 is basically an equation of a straight line that can be expressed as:

$$p_{ws} = p_i - m\left[\log\left(\frac{t_p + \Delta t}{\Delta t}\right)\right] \qquad [1.3.7]$$

This expression suggests that a plot of p_{ws} vs. $(t_p + \Delta t)/\Delta t$ on a semilog scale would produce a straight-line relationship with intercept p_i and slope m, where:

$$m = \frac{162.6 Q_o B_o \mu_o}{kh} \qquad [1.3.8]$$

or:

$$k = \frac{162.6 Q_o B_o \mu_o}{mh}$$

and where:

m = slope of straight line, psi/cycle
k = permeability, md

This plot, commonly referred to as the Horner plot, is illustrated in Figure 1.37. Note that on the Horner plot, the scale of time ratio $(t_p + \Delta t)/\Delta t$ increases from right to left. It is observed from Equation 1.3.6 that $p_{ws} = p_i$ when the time ratio is unity. Graphically this means that the initial reservoir pressure, p_i, can be obtained by extrapolating the Horner plot straight line to $(t_p + \Delta t)/\Delta t = 1$.

The time corresponding to the point of shut-in, t_p can be estimated from the following equation:

$$t_p = \frac{24 N_p}{Q_o}$$

where:

N_p = well cumulative oil produced before shut in, STB
Q_o = stabilized well flow rate before shut in, STB/day
t_p = total production time, hours

Earlougher (1977) pointed out that a result of using the superposition principle is that the skin factor, s, does not appear in the general pressure buildup equation, Equation 1.3.6. That means the Horner-plot slope is not affected by the skin factor; however, the skin factor still does affect the shape of the pressure buildup data. In fact, an early-time deviation from the straight line can be caused by the skin factor as well as by wellbore storage, as illustrated in Figure 1.36. The deviation can be significant for the large negative skins that occur in hydraulically fractured wells. The skin factor does affect flowing pressure before shut-in and its value may be estimated from the buildup test data plus the flowing pressure immediately before the buildup test, as given by:

$$s = 1.151\left[\frac{p_{1\ hr} - p_{wf\ at\ \Delta t=0}}{|m|} - \log\left(\frac{k}{\phi \mu c_t r_w^2}\right) + 3.23\right] \qquad [1.3.9]$$

with an additional pressure drop across the altered zone of:

$$\Delta p_{skin} = 0.87\,|m|\,s$$

where:

$p_{wf\ at\ \Delta t=0}$ = bottom-hole flowing pressure *immediately before shut in*, psi

s = skin factor
$|m|$ = absolute value of the slope in the Horner plot, psi/cycle
r_w = wellbore radius, ft

The value of $p_{1\,hr}$ must be taken from the Horner straight line. Frequently, the pressure data does not fall on the straight line at 1 hour because of wellbore storage effects or large negative skin factors. In that case, the semilog line must be extrapolated to 1 hour and the corresponding pressure is read.

It should be noted that for a *multiphase flow*, Equations 1.3.6 and 1.3.9 become:

$$p_{ws} = p_i - \frac{162.6 q_t}{\lambda_t h}\left[\log\left(\frac{t_p + \Delta t}{\Delta t}\right)\right]$$

$$s = 1.151\left[\frac{p_{1\,hr} - p_{wf\ at \Delta t=0}}{|m|} - \log\left(\frac{\lambda_t}{\phi c_t r_w^2}\right) + 3.23\right]$$

with:

$$\lambda_t = \frac{k_o}{\mu_o} + \frac{k_w}{\mu_w} + \frac{k_g}{\mu_g}$$

$$q_t = Q_o B_o + Q_w B_w + (Q_g - Q_o R_s) B_g$$

or equivalently in terms of GOR as:

$$q_t = Q_o B_o + Q_w B_w + (\mathrm{GOR} - R_s) Q_o B_g$$

where:

q_t = total fluid voidage rate, bbl/day
Q_o = oil flow rate, STB/day
Q_w = water flow rate, STB/day
Q_g = gas flow rate, scf/day
R_s = gas solubility, scf/STB
B_g = gas formation volume factor, bbl/scf
λ_t = total mobility, md/cp
k_o = effective permeability to oil, md
k_w = effective permeability to water, md
k_g = effective permeability to gas, md

The regular Horner plot would produce a semilog straight line with a slope m that can be used to determine the total mobility λ_t from:

$$\lambda_t = \frac{162.6 q_t}{mh}$$

Perrine (1956) showed that the effective permeability of each phase, i.e., k_o, k_w, and k_g, can be determined as:

$$k_o = \frac{162.6 Q_o B_o \mu_o}{mh}$$

$$k_w = \frac{162.6 Q_w B_w \mu_w}{mh}$$

$$k_g = \frac{162.6 (Q_g - Q_o R_s) B_g \mu_g}{mh}$$

For gas systems, a plot of $m(p_{ws})$ or p_{ws}^2 vs. $(t_p + \Delta t)/\Delta t$ on a semilog scale would produce a straight line relationship with a slope of m and apparent skin factor s as defined by:
For pseudopressure approach:

$$m = \frac{1637 Q_g T}{kh}$$

$$s = 1.151\left[\frac{m(p_{1\,hr}) - m(p_{wf\ at\ \Delta t=0})}{|m|} - \log\left(\frac{k}{\phi \mu_i c_{ti} r_w^2}\right) + 3.23\right]$$

For pressure-squared approach:

$$m = \frac{1637 Q_g \overline{Z}\,\overline{\mu}_g}{kh}$$

$$s = 1.151\left[\frac{p_{1\,hr}^2 - p_{wf\ at\ \Delta t=0}^2}{|m|} - \log\left(\frac{k}{\phi \mu_i c_{ti} r_w^2}\right) + 3.23\right]$$

where the gas flow rate Q_g is expressed in Mscf/day.

It should be pointed out that when a well is shut in for a pressure buildup test, the well is usually closed at the surface rather than the sand face. Even though the well is shut in, the reservoir fluid continues to flow and accumulates in the wellbore until the well fills sufficiently to transmit the effect of shut-in to the formation. This "afterflow" behavior is caused by the wellbore storage and it has a significant influence on pressure buildup data. During the period of wellbore storage effects, the pressure data points fall below the semilog straight line. The duration of these effects may be estimated by making the log–log data plot described previously of $\log(p_{ws} - p_{wf})$ vs. $\log(\Delta t)$ with p_{wf} as the value recorded immediately before shut-in. When wellbore storage dominates, that plot will have a unit-slope straight line; as the semilog straight line is approached, the log–log plot bends over to a gently curving line with a low slope.

The wellbore storage coefficient C is, by selecting *a point on the log–log unit-slope straight line* and reading the coordinate of the point in terms of Δt and Δp:

$$C = \frac{q\Delta t}{24\Delta p} = \frac{QB\Delta t}{24\Delta p}$$

where

Δt = shut-in time, hours
Δp = pressure difference $(p_{ws} - p_{wf})$, psi
q = flow rate, bbl/day
Q = flow rate, STB/day
B = formation volume factor, bbl/STB

with a dimensionless wellbore storage coefficient as given by Equation 1.3.4 as:

$$C_D = \frac{0.8936 C}{\phi h c_t r_w^2}$$

In all the pressure buildup test analyses, the log–log data plot should be made before the straight line is chosen on the semilog data plot. This log–log plot is essential to avoid drawing a semilog straight line through the wellbore storage-dominated data. The beginning of the semilog line can be estimated by observing when the data points on the log–log plot reach the slowly curving low-slope line and adding 1 to $1\frac{1}{2}$ cycles in time after the end of the unit-slope straight line. Alternatively, the time to the beginning of the semilog straight line can be estimated from:

$$\Delta t > \frac{170000\, C e^{0.14s}}{(kh/\mu)}$$

where:

c = calculated wellbore storage coefficient, bbl/psi
k = permeability, md
s = skin factor
h = thickness, ft

Table 1.5 *Earlougher's pressure buildup data (Permission to publish by the SPE, copyright SPE, 1977.)*

Δt (hr)	$t_p + \Delta t$ (hr)	$t_p + \Delta t \Delta t$	p_{ws} (psig)
0.0	–	–	2761
0.10	310.30	3101	3057
0.21	310.21	1477	3153
0.31	310.31	1001	3234
0.52	310.52	597	3249
0.63	310.63	493	3256
0.73	310.73	426	3260
0.84	310.84	370	3263
0.94	310.94	331	3266
1.05	311.05	296	3267
1.15	311.15	271	3268
1.36	311.36	229	3271
1.68	311.68	186	3274
1.99	311.99	157	3276
2.51	312.51	125	3280
3.04	313.04	103	3283
3.46	313.46	90.6	3286
4.08	314.08	77.0	3289
5.03	315.03	62.6	3293
5.97	315.97	52.9	3297
6.07	316.07	52.1	3297
7.01	317.01	45.2	3300
8.06	318.06	39.5	3303
9.00	319.00	35.4	3305
10.05	320.05	31.8	3306
13.09	323.09	24.7	3310
16.02	326.02	20.4	3313
20.00	330.00	16.5	3317
26.07	336.07	12.9	3320
31.03	341.03	11.0	3322
34.98	344.98	9.9	3323
37.54	347.54	9.3	3323

Example 1.27[a] Table 1.5 shows the pressure buildup data from an oil well with an estimated drainage radius of 2640 ft. Before shut-in, the well had produced at a stabilized rate of 4900 STB/day for 310 hours. Known reservoir data is:

depth $= 10\,476$ ft, $r_w = 0.354$ ft, $c_t = 22.6 \times 10^{-6}$ psi^{-1}

$Q_o = 4900$ STB/D, $h = 482$ ft, $p_{wf}(\Delta t = 0) = 2761$ psig

$\mu_o = 0.20$ cp, $B_o = 1.55$ bbl/STB, $\phi = 0.09$

$t_p = 310$ hours, $r_e = 2640$ ft

Calculate:

- the average permeability k;
- the skin factor;
- the additional pressure drop due to skin.

Solution

Step 1. Plot p_{ws} vs. $(t_p + \Delta t)/\Delta t$ on a semilog scale as shown in Figure 1.38).

Step 2. Identify the correct straight-line portion of the curve and determine the slope m:

$$m = 40 \text{ psi/cycle}$$

[a]This example problem and the solution procedure are given in Earlougher, R. *Advance Well Test Analysis*, Monograph Series, SPE, Dallas (1977).

Step 3. Calculate the average permeability by using Equation 1.3.8:

$$k = \frac{162.6 Q_o B_o \mu_o}{mh}$$

$$= \frac{(162.6)(4900)(1.55)(0.22)}{(40)(482)} = 12.8 \text{ md}$$

Step 4. Determine p_{wf} after 1 hour from the straight-line portion of the curve:

$$p_{1\,hr} = 3266 \text{ psi}$$

Step 5. Calculate the skin factor by applying Equation 1.3.9

$$s = 1.151\left[\frac{p_{1\,hr} - p_{wf\Delta t=0}}{m} - \log\left(\frac{k}{\phi\mu c_t r_w^2}\right) + 3.23\right]$$

$$= 1.151\left[\frac{3266 - 2761}{40} - \log\left(\frac{(12.8)}{(0.09)(0.20)(22.6 \times 10^{-6})(0.354)^2}\right) + 3.23\right]$$

$$= 8.6$$

Step 6. Calculate the additional pressure drop by using:

$$\Delta p_{skin} = 0.87|m|s$$

$$= 0.87(40)(8.6) = 299.3 \text{ psi}$$

It should be pointed out that Equation 1.3.6 assumes the reservoir to be infinite in size, i.e., $r_e = \infty$, which implies that at some point in the reservoir the pressure would be always equal to the initial reservoir pressure p_i and the Horner straight-line plot will always extrapolate to p_i. However, reservoirs are finite and soon after production begins, fluid removal will cause a pressure decline everywhere in the reservoir system. Under these conditions, the straight line will not extrapolate to the initial reservoir pressure p_i but, instead, the pressure obtained will be a false pressure as denoted by p^*. The false pressure, as illustrated by Matthews and Russell (1967) in Figure 1.39, has no physical meaning but it is usually used to determine the average reservoir pressure $\bar{p}$. It is clear that p^* will *only equal* the initial (original) reservoir pressure p_i when a new well in a newly discovered field is tested. Using the concept of the false pressure p^*, Horner expressions as given by Equations 1.3.6 and 1.3.7 should be expressed in terms of p^* instead of p_i as:

$$p_{ws} = p^* - \frac{162.6 Q_o \mu_o B_o}{kh}\left[\log\left(\frac{t_p + \Delta t}{\Delta t}\right)\right]$$

and:

$$p_{ws} = p^* - m\left[\log\left(\frac{t_p + \Delta t}{\Delta t}\right)\right] \quad [1.3.10]$$

Bossie-Codreanu (1989) suggested that the well drainage area can be determined from the Horner pressure buildup plot or the MDH plot, discussed next, by selecting the coordinates of any three points located on the semilog straight-line portion of the plot to determine the slope of the pseudosteady-state line m_{pss}. The coordinates of these three points are designated as:

- shut-in time Δt_1 and with a corresponding shut-in pressure p_{ws1};
- shut-in time Δt_2 and with a corresponding shut-in pressure p_{ws2};
- shut-in time Δt_3 and with a corresponding shut-in pressure p_{ws3}.

The selected shut-in times satisfy $\Delta t_1 < \Delta t_2 < \Delta t_3$. The slope of the pseudosteady-state straight-line m_{pss} is then

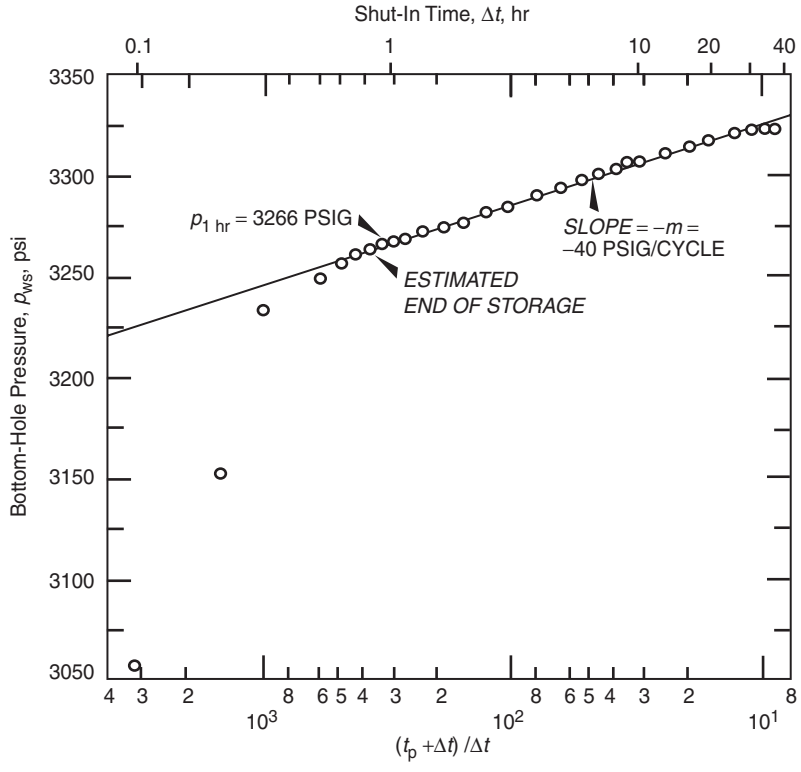

Figure 1.38 *Earlougher's semilog data plot for the buildup test (Permission to publish by the SPE, copyright SPE, 1977).*

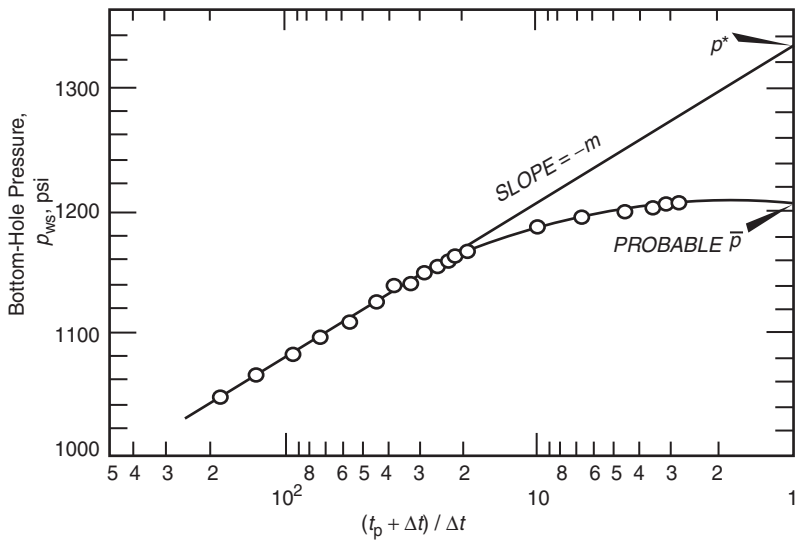

Figure 1.39 *Typical pressure buildup curve for a well in a finite (After Earlougher, R.* Advances in Well Test Analysis*) (Permission to publish by the SPE, copyright SPE, 1977).*

approximated by:

$$m_{\text{pss}} = \frac{(p_{\text{ws2}} - p_{\text{ws1}}) \log(\Delta t_3/\Delta t_1) - (p_{\text{ws3}} - p_{\text{ws1}}) \log[\Delta t_2/\Delta t_1]}{(\Delta t_3 - \Delta t_1) \log(\Delta t_2 \Delta t_1) - (\Delta t_2 - \Delta t_1) \log(\Delta t_3/\Delta t_1)} \quad [1.3.11]$$

The well drainage area can be calculated from Equation 1.2.116:

$$m^{\backslash} = m_{\text{pss}} = \frac{0.23396 Q_o B_o}{c_t A h \phi}$$

Solving for the drainage area gives:

$$A = \frac{0.23396 Q_o B_o}{c_t m_{\text{pss}} h \phi}$$

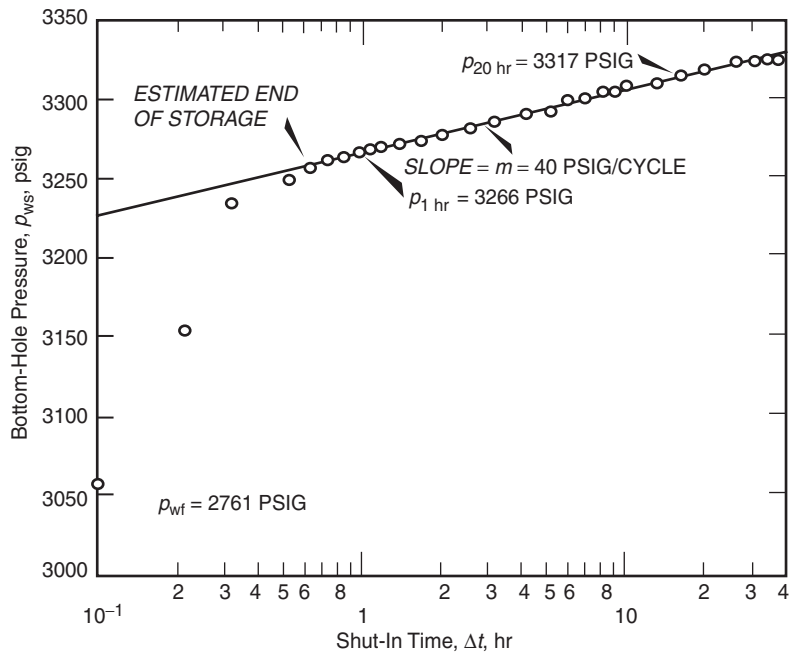

Figure 1.40 *Miller–Dyes–Hutchinson plot for the buildup test (After Earlougher, R.* Advances in Well Test Analysis*) (Permission to publish by the SPE, copyright SPE, 1977).*

where:

m_{pss} or $m^{\backslash}$ = slope of *straight line* during the pseudosteady-state flow, psi/hr
Q_o = flow rate, bbl/day
A = well drainage area, ft^2

1.3.4 Miller–Dyes–Hutchinson method

The Horner plot may be simplified if the well has been producing long enough to reach a pseudosteady state. Assuming that the production time t_p is much greater than the total shut-in time Δt, i.e., $t_p \gg \Delta t$, the term $t_p + \Delta t \simeq t_p$ and:

$$\log\left(\frac{t_p + \Delta t}{\Delta t}\right) \cong \log\left(\frac{t_p}{\Delta t}\right) = \log(t_p) - \log(\Delta t)$$

Applying the above mathematical assumption to Equation 1.3.10, gives:

$$p_{ws} = p^* - m[\log(t_p) - \log(\Delta t)]$$

or:

$$p_{ws} = [p^* - m\log(t_p)] + m\log(\Delta t)$$

This expression indicates that a plot of p_{ws} vs. $\log(\Delta t)$ would produce a semilog straight line with a positive slope of $+m$ that is identical to that obtained from the Horner plot. The slope is defined mathematically by Equation 1.3.8 as:

$$m = \frac{162.6 Q_o B_o \mu_o}{kh}$$

The semilog straight-line slope m has the same value as of the Horner plot. This plot is commonly called the Miller–Dyes–Hutchinson (MDH) plot. The false pressure p^* may be estimated from the MDH plot by using:

$$p^* = p_{1\ hr} + m\log(t_p + 1) \qquad [1.3.12]$$

where $p_{1\ hr}$ is read from the semilog straight-line plot at $\Delta t =$ 1 hour. The MDH plot of the pressure buildup data given in Table 1.5 in terms of p_{ws} vs. $\log(\Delta t)$ is shown in Figure 1.40. Figure 1.40 shows a positive slope of $m = 40$ psi/cycle that is identical to the value obtained in Example 1.26 with a $p_{1\ hr} = 3266$ psig.

As in the Horner plot, the time that marks the beginning of the MDH semilog straight line may be estimated by making the log–log plot of $(p_{ws} - p_{wf})$ *vs.* Δt and observing when the data points deviate from the 45° angle (unit slope). The exact time is determined by moving 1 to $1\frac{1}{5}$ cycles in time after the end of the unit-slope straight line.

The observed pressure behavior of the test well following the end of the transient flow will depend on:

- shape and geometry of the test well drainage area;
- the position of the well relative to the drainage boundaries;
- length of the producing time t_p before shut-in.

If the well is located in a reservoir with no other wells, the shut-in pressure would eventually become constant (as shown in Figure 1.38) and equal to the *volumetric average reservoir pressure* $\bar{p}_r$. This pressure is required in many reservoir engineering calculations such as:

- material balance studies;
- water influx;
- pressure maintenance projects;
- secondary recovery;
- degree of reservoir connectivity.

Finally, in making future predictions of production as a function of $\bar{p}_r$, pressure measurements throughout the reservoir's life are almost mandatory if one is to compare such a prediction to actual performance and make the necessary adjustments to the predictions. One way to obtain this pressure is to shut in all wells producing from the reservoir for a period of time that is sufficient for pressures to equalize throughout the system to give $\bar{p}_r$. Obviously, such a procedure is not practical.

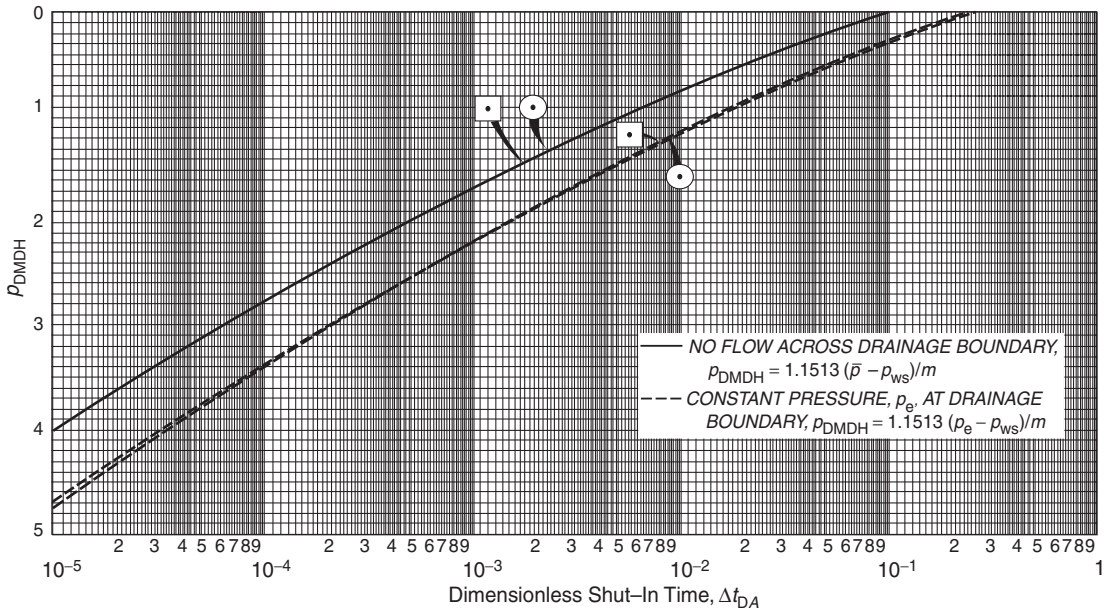

Figure 1.41 *Miller–Dyes–Hutchinson dimensionless pressure for circular and square drainage areas (After Earlougher, R.* Advances in Well Test Analysis*) (Permission to publish by the SPE, copyright SPE, 1977).*

To use the MDH method to estimate average drainage region pressure $\bar{p}_r$ for a circular or square system producing at *pseudosteady state before shut-in*:

(1) Choose any convenient time on the semilog straight line Δt and read the corresponding pressure p_{ws}.
(2) Calculate the dimensionless shut-in time based on the drainage area A from:

$$\Delta t_{DA} = \frac{0.0002637k\Delta t}{\phi\mu c_t a}$$

(3) Enter Figure 1.41 with the dimensionless time $\Delta t_D A$ and determine an MDH dimensionless pressure p_{DMDH} from the upper curve of Figure 1.41.
(4) Estimate the average reservoir pressure in the closed drainage region from:

$$\bar{p}_r = p_{ws} + \frac{mp_{DMDH}}{1.1513}$$

where m is the semilog straight line of the MDH plot.

There are several other methods for determining $\bar{p}_r$ from a buildup test. Three of these methods are briefly presented below:

(1) the Matthews–Brons–Hazebroek (MBH) method;
(2) the Ramey-Cobb method;
(3) the Dietz method.

1.3.5 MBH method

As noted previously, the buildup test exhibits a semilog straight line which begins to bend down and become flat at the later shut-in times because of the effect of the boundaries. Matthews et al. (1954) proposed a methodology for estimating average pressure from buildup tests in bounded drainage regions. The MBH method is based on theoretical correlations between the extrapolated semilog straight line to the false pressure p^* and current average drainage area pressure $\bar{p}$. The authors point out that the average pressure in the drainage area of each well can be related to p^* if the geometry, shape, and location of the well relative to the drainage boundaries are known. They developed a set of correction charts, as shown in Figures 1.42 through 1.45, for various drainage geometries.

The y axis of these figures represents the MBH dimensionless pressure p_{DMBH} that is defined by:

$$p_{DMBH} = \frac{2.303(p^* - \bar{p})}{|m|}$$

or:

$$\bar{p} = p^* - \left(\frac{|m|}{2.303}\right) p_{DMBH} \qquad [1.3.13]$$

where m is the *absolute* value of the slope obtained from the Horner semilog straight-line plot. The MBH dimensionless pressure is determined at the dimensionless producing time t_{pDA} that corresponds to the flowing time t_p. That is:

$$t_{pDA} = \left[\frac{0.0002637k}{\phi\mu c_t A}\right] t_p \qquad [1.3.14]$$

where:

t_p = flowing time before shut-in, hours
A = drainage area, ft^2
k = permeability, md
c_t = total compressibility, psi^{-1}

The following steps summarize the procedure for applying the MBH method:

Step 1. Make a Horner plot.
Step 2. Extrapolate the semilog straight line to the value of p^* at $(t_p + \Delta t)/\Delta t = 1.0$.
Step 3. Evaluate the slope of the semilog straight line m.
Step 4. Calculate the MBH dimensionless producing time t_{pDA} from Equation 1.3.14:

$$t_{pDA} = \left[\frac{0.0002637k}{\phi\mu c_t A}\right] t_p$$

Step 5. Find the closest approximation to the shape of the well drainage area in Figures 1.41 through 1.44 and identify the correction curve.

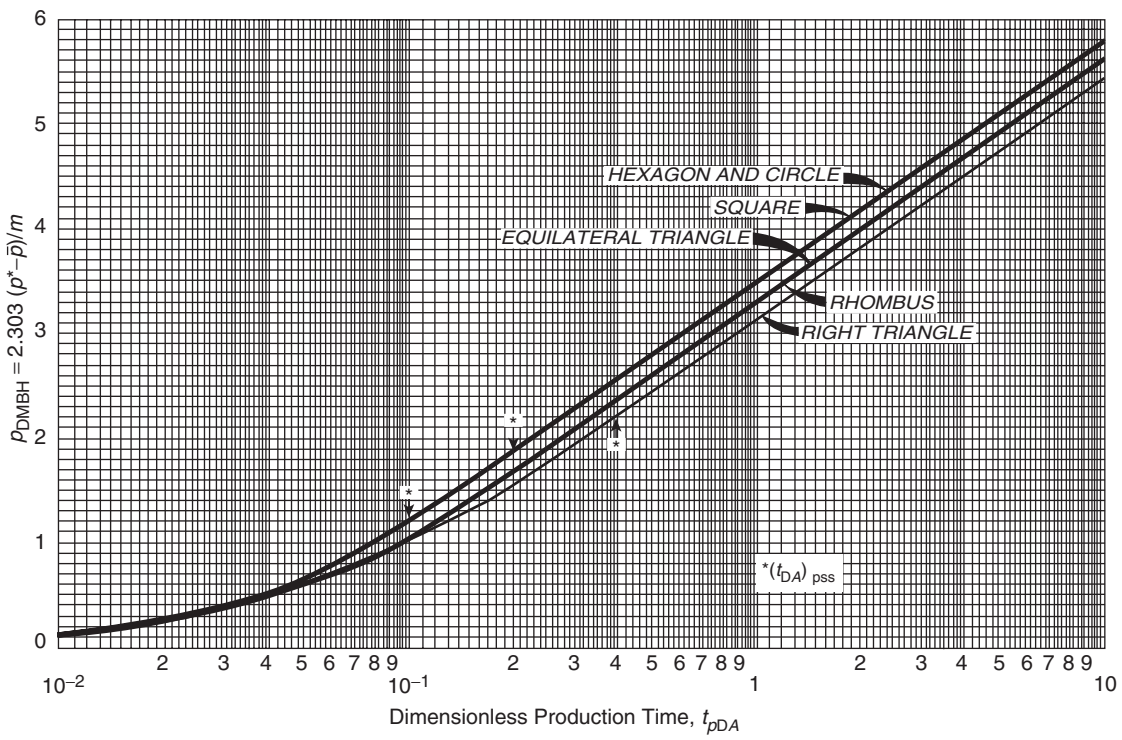

Figure 1.42 *Matthews–Brons–Hazebroek dimensionless pressure for a well in the center of equilateral drainage areas (After Earlougher, R.* Advances in Well Test Analysis*) (Permission to publish by the SPE, copyright SPE, 1977).*

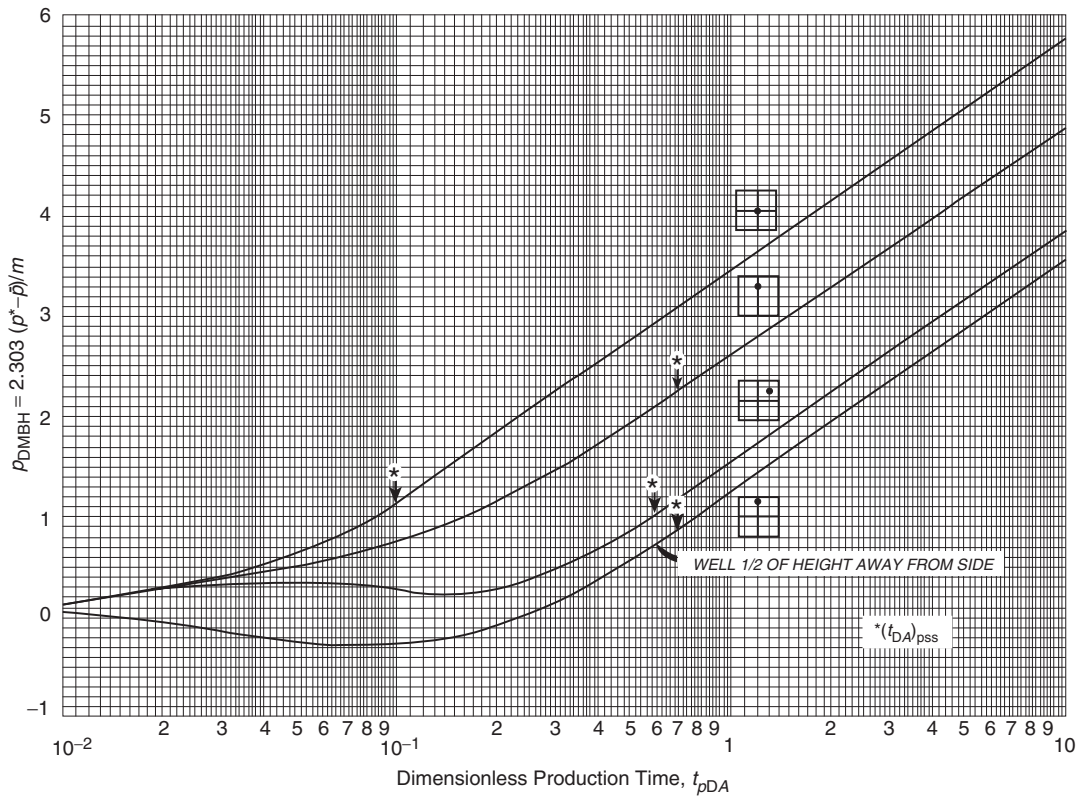

Figure 1.43 *Matthews–Brons–Hazebroek dimensionless pressure for different well locations in a square drainage area. (After Earlougher, R.* Advances in Well Test Analysis*) (Permission to publish by the SPE, copyright SPE, 1977).*

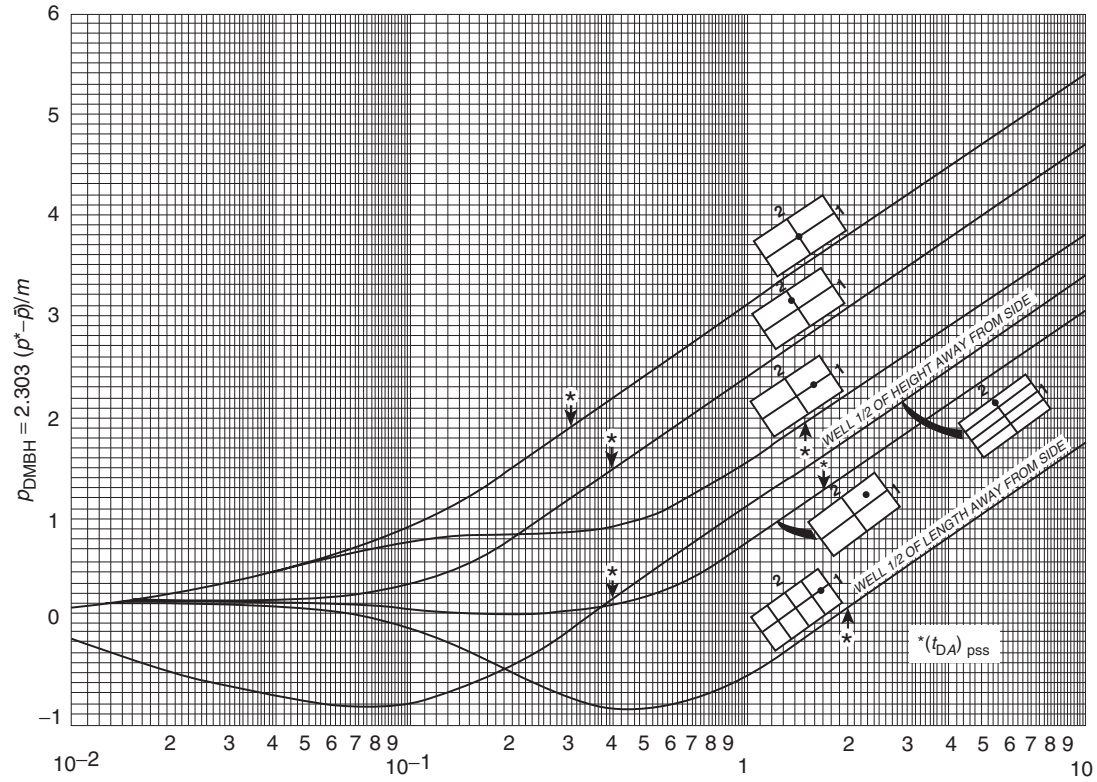

Figure 1.44 *Matthews–Brons–Hazebroek dimensionless pressure for different well locations in a 2:1 rectangular drainage area (After Earlougher, R.* Advances in Well Test Analysis*) (Permission to publish by the SPE, copyright SPE, 1977).*

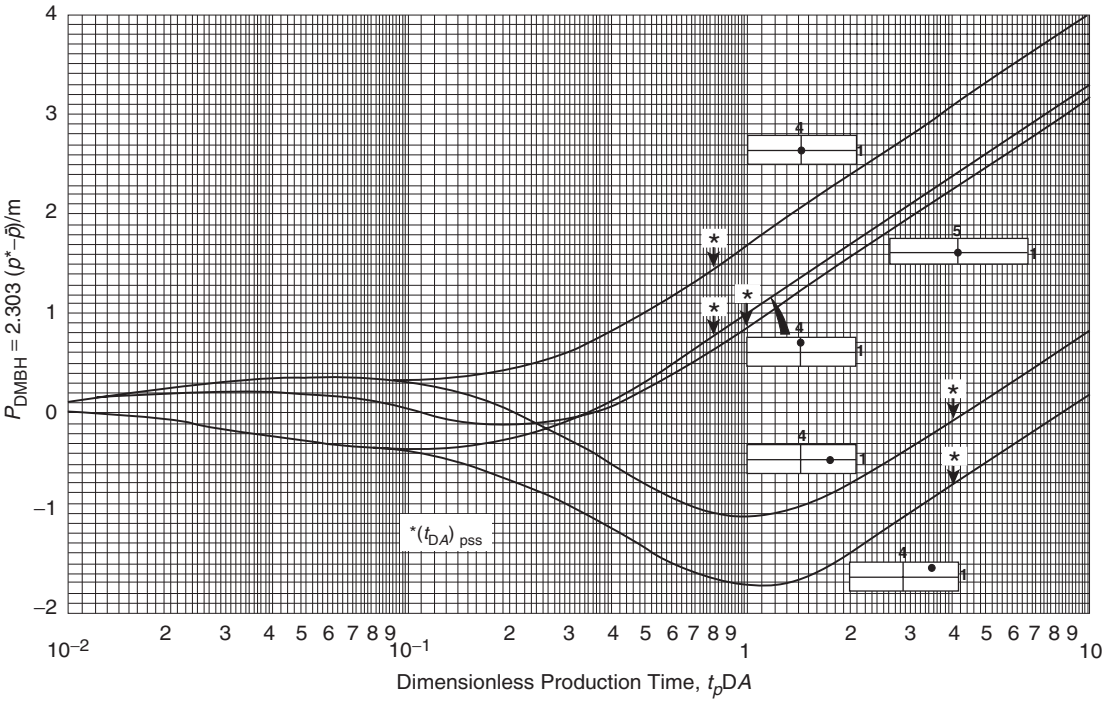

Figure 1.45 *Matthews–Brons–Hazebroek dimensionless pressure for different well locations in 4:1 and 5:1 rectangular drainage areas (After Earlougher, R.* Advances in Well Test Analysis*) (Permission to publish by the SPE, copyright SPE, 1977).*

Step 6. Read the value of p_{DMBH} from the correction curve at t_{PDA}

Step 7. Calculate the value of $\bar{p}$ from Equation 1.3.13:

$$\bar{p} = p^* - \left(\frac{|m|}{2.303}\right) p_{DMBH}$$

As in the normal Horner analysis technique, the producing time t_p is given by:

$$t_p = \frac{24N_p}{Q_o}$$

where N_p is the cumulative volume produced since the *last pressure buildup test* and Q_o is the constant flow rate just before shut-in. Pinson (1972) and Kazemi (1974) indicate that t_p should be compared with the time required to reach the pseudosteady state, t_{pss}:

$$t_{pss} = \left[\frac{\phi\mu c_t A}{0.0002367k}\right](t_{DA})_{pss} \qquad [1.3.15]$$

For a symmetric closed or circular drainage area, $(t_{DA})_{pss} = 0.1$ as given in Table 1.4 and listed in the fifth column.

If $t_p \gg t_{pss}$, then t_{pss} should ideally replace t_p in both the Horner plot and for use with the MBH dimensionless pressure curves.

The above methodology gives the value of $\bar{p}$ in the drainage area of *one well*, e.g., well *i*. If a number of wells are producing from the reservoir, each well can be analyzed separately to give $\bar{p}$ for its own drainage area. The reservoir average pressure $\bar{p}_r$ can be estimated from these *individual well average drainage pressures* by using one of the relationships given by Equations 1.2.118 and 1.2.119. That is:

$$\bar{p}_r = \frac{\sum_i (\bar{p}q)_i/(\partial\bar{p}/\partial t)_i}{\sum_i q_i/(\partial\bar{p}/\partial t)_i}$$

or:

$$\bar{p}_r = \frac{\sum_i [\bar{p}\Delta(F)/\Delta\bar{p}]_i}{\sum_i [\Delta(F)/\Delta\bar{p}]_i}$$

with:

$$F_t = \int_0^t [Q_o B_o + Q_w B_w + (Q_g - Q_o R_s - Q_w R_{sw}) B_g]\, dt$$

$$F_{t+\Delta t} = \int_0^{t+\Delta t} [Q_o B_o + Q_w B_w + (Q_g - Q_o R_s - Q_w R_{sw}) B_g]\, dt$$

and:

$$\Delta(F) = F_{t+\Delta t} - F_t$$

Similarly, it should be noted that the MBH method and the Figures 1.41 through 1.44 can be applied for compressible gases by defining p_{DMBH} as:

For the pseudopressure approach

$$p_{DMBH} = \frac{2.303[m(p^*) - m(\bar{p})]}{|m|} \qquad [1.3.16]$$

For the pressure-squared approach

$$p_{DMBH} = \frac{2.303[(p^*)^2 - (\bar{p})^2]}{|m|} \qquad [1.3.17]$$

Example 1.28 Using the information given in Example 1.27 and pressure buildup data listed in Table 1.5, calculate the average pressure in the well drainage area and the drainage area by applying Equation 1.3.11. The data is listed below for convenience:

$r_e = 2640$ ft, $r_w = 0.354$ ft, $c_t = 22.6 \times 10^{-6}$ psi^{-1}

$Q_o = 4,900$ STB/D, $h = 482$ ft,

$p_{wf \text{ at } \Delta t=0} = 2761$ psig

$\mu_o = 0.20$ cp, $B_o = 1.55$ bbl/STB, $\phi = 0.09$

$t_p = 310$ hours, depth $= 10\,476$ ft,

reported average pressure $= 3323$ psi

Solution

Step 1. Calculate the drainage area of the well:

$$A = \pi r_e^2 = \pi(2640)^2$$

Step 2. Compare the production time t_p, i.e., 310 hours, with the time required to reach the pseudosteady state t_{pss} by applying Equation 1.3.15. Estimate t_{pss} using $(t_{DA})_{pss} = 0.1$ to give:

$$t_{pss} = \left[\frac{\phi\mu c_t A}{0.0002367k}\right](t_{DA})_{pss}$$

$$= \left[\frac{(0.09)(0.2)(22.6\times10^{-6})(\pi)(2640)^2}{(0.0002637)(12.8)}\right]0.1$$

$$= 264 \text{ hours}$$

Thus, we could replace t_p by 264 hours in our analysis because $t_p > t_{pss}$. However, since t_p is only about $1.2t_{pss}$, we use the actual production time of 310 hours in the calculation.

Step 3. Figure 1.38 does not show p^* since the semilog straight line is not extended to $(t_p + \Delta t)/\Delta t = 1.0$. However, p^* can be calculated from p_{ws} at $(t_p + \Delta t)/\Delta t = 10.0$ by extrapolating one cycle. That is:

$$p^* = 3325 + (1 \text{ cycle})(40 \text{ psi/cycle}) = 3365 \text{ psig}$$

Step 4. Calculate t_{pDA} by applying Equation 1.3.14 to give:

$$t_{pDA} = \left[\frac{0.0002637k}{\phi\mu c_t A}\right]t_p$$

$$= \left[\frac{0.0002637(12.8)}{(0.09)(0.2)(22.6\times10^{-6})(\pi)(2640)^2}\right]310$$

$$= 0.117$$

Step 5. From the curve of the circle in Figure 1.42, obtain the value of p_{DMBH} at $t_{pDA} = 0.117$, to give:

$$p_{DMBH} = 1.34$$

Step 6. Calculate the average pressure from Equation 1.3.13:

$$\bar{p} = p^* - \left(\frac{|m|}{2.303}\right)p_{DMBH}$$

$$= 3365 - \left(\frac{40}{2.303}\right)(1.34) = 3342 \text{ psig}$$

This is 19 psi higher than the maximum pressure recorded of 3323 psig.

Step 7. Select the coordinates of any three points located on the semilog straight line portion of the Horner plot, to give:

- $(\Delta t_1, p_{ws1}) = (2.52, 3280)$
- $(\Delta t_2, p_{ws2}) = (9.00, 3305)$
- $(\Delta t_3, p_{ws3}) = (20.0, 3317)$

Step 8. Calculate m_{pss} by applying Equation 1.3.11:

$$m_{pss} = \frac{(p_{ws2} - p_{ws1})\log(\Delta t_3/\Delta t_1) - (p_{ws3} - p_{ws1})\log(\Delta t_2/\Delta t_1)}{(\Delta t_3 - \Delta t_1)\log(\Delta t_2/\Delta t_1) - (\Delta t_2 - \Delta t_1)\log(\Delta t_3/\Delta t_1)}$$

$$= \frac{(3305-3280)\log(20/2.51) - (3317-3280)\log(9/2.51)}{(20-2.51)\log(9/2.51) - (9-2.51)\log(20/2.51)}$$

$$= 0.52339 \text{ psi/hr}$$

Step 9. The well drainage area can then be calculated from Equation 1.2.116:

$$A = \frac{0.23396 Q_o B_o}{c_t m_{pss} h \phi}$$

$$= \frac{0.23396(4900)(1.55)}{(22.6 \times 10^{-6})(0.52339)(482)(0.09)}$$

$$= 3\,462\,938 \text{ ft}^2$$

$$= \frac{3\,363\,938}{43\,560} = 80 \text{ acres}$$

The corresponding drainage radius is 1050 ft which differs considerably from the given radius of 2640 ft. Using the calculated drainage radius of 1050 ft and repeating the MBH calculations gives:

$$t_{pss} = \left[\frac{(0.09)(0.2)(22.6 \times 10^{-6})(\pi)(1050)^2}{(0.0002637)(12.8)}\right] 0.1$$

$$= 41.7 \text{ hours}$$

$$t_{pDA} = \left[\frac{0.0002637(12.8)}{(0.09)(0.2)(22.6 \times 10^{-6})(\pi)(1050)^2}\right] 310 = 0.743$$

$$p_{DMBH} = 3.15$$

$$\bar{p} = 3365 - \left(\frac{40}{2.303}\right)(3.15) = 3311 \text{ psig}$$

The value is 12 psi higher than the reported value of average reservoir pressure.

1.3.6 Ramey–Cobb method

Ramey and Cobb (1971) proposed that the average pressure in the well drainage area can be read directly from the Horner semilog straight line if the following data is available:

- shape of the well drainage area;
- location of the well within the drainage area;
- size of the drainage area.

The proposed methodology is based on calculating the dimensionless producing time t_{pDA} as defined by Equation 1.3.14:

$$t_{pDA} = \left[\frac{0.0002637k}{\phi\mu c_t A}\right] t_p$$

where:

t_p = producing time since the last shut-in, hours
A = drainage area, ft^2

Knowing the shape of the drainage area and well location, determine the dimensionless time to reach pseudosteady state $(t_{DA})_{pss}$, as given in Table 1.4 in the fifth column. Compare t_{pDA} with $(t_{DA})_{pss}$:

- If $t_{pDA} < (t_{DA})_{pss}$, then read the average pressure $\bar{p}$ from the Horner semilog straight line at:

$$\left(\frac{t_p + \Delta t}{\Delta t}\right) = \exp(4\pi t_{pDA}) \quad [1.3.18]$$

or use the following expression to estimate $\bar{p}$:

$$\bar{p} = p^* - m \log\left[\exp(4\pi t_{pDA})\right] \quad [1.3.19]$$

- If $t_{pDA} > (t_{DA})_{pss}$, then read the average pressure $\bar{p}$ from the Horner semilog straight-line plot at:

$$\left(\frac{t_p + \Delta t}{\Delta t}\right) = C_A t_{pDA} \quad [1.3.20]$$

where C_A is the shape factor as determined from Table 1.4.s Equivalently, the average pressure can be estimated from:

$$\bar{p} = p^* - m \log(C_A t_{pDA}) \quad [1.3.21]$$

where:

m = absolute value of the semilog straight-line slope, psi/cycle
p^* = false pressure, psia
C_A= shape factor, from Table 1.4

Example 1.29 Using the data given in Example 1.27, recalculate the average pressure using the Ramey and Cobb method.

Solution

Step 1. Calculate t_{pDA} by applying Equation (1.3.14):

$$t_{pDA} = \left[\frac{0.0002637k}{\phi\mu c_t A}\right] t_p$$

$$= \left[\frac{0.0002637(12.8)}{(0.09)(0.2)(22.6 \times 10^{-6})(\pi)(2640)^2}\right] (310)$$

$$= 0.1175$$

Step 2. Determine C_A and $(t_{DA})_{pss}$ from Table 1.4 for a well located in the centre of a circle, to give:

$$C_A = 31.62$$
$$(t_{DA})_{pss} = 0.1$$

Step 3. Since $t_{pDA} > (t_{DA})_{pss}$, calculate $\bar{p}$ from Equation 1.3.21:

$$\bar{p} = p^* - m \log(C_A t_{pDA})$$

$$= 3365 - 40 \log[31.62(0.1175)] = 3342 \text{ psi}$$

This value is identical to that obtained from the MBH method.

1.3.7 Dietz method

Dietz (1965) indicated that if the test well has been producing long enough to reach the pseudosteady state before shut-in, the average pressure can be read directly from the MDH semilog straight-line plot, i.e., p_{ws} vs. $\log(\Delta t)$, at the following shut-in time:

$$(\Delta t)_{\bar{p}} = \frac{\phi\mu c_t A}{0.0002637 C_A k} \quad [1.3.22]$$

where:

Δt = shut-in time, hours
A = drainage area, ft^2
C_A = shape factor
k = permeability, md
c_t = total compressibility, psi^{-1}

Example 1.30 Using the Dietz method and the buildup data given in Example 1.27, calculate the average pressure:

Solution

Step 1. Using the buildup data given in Table 1.5, construct the MDH plot of p_{ws} vs. $\log(\Delta t)$ as shown in Figure 1.40. From the plot, read the following values:

$$m = 40 \text{ psi/cycle}$$
$$p_{1\,hr} = 3266 \text{ psig}$$

Step 2. Calculate false pressure p^* from Equation 1.3.12 to give:

$$p^* = p_{1\,\text{hr}} + m\log(t_\text{p} + 1)$$

$$= 3266 + 40\log(310 + 1) = 3365.7 \text{ psi}$$

Step 3. Calculate the shut-in time $(\Delta t)_{\bar{p}}$ from Equation 1.3.20:

$$(\Delta t)_{\bar{p}} = \frac{(0.09)(0.2)(22.6 \times 10^{-6})(\pi)(2640)^2}{(0.0002637)(12.8)(31.62)}$$

$$= 83.5 \text{ hours}$$

Step 4. Since the MDH plot does not extend to 83.5 hours, the average pressure can be calculated from the semilog straight-line equation as given by:

$$p = p_{1\,\text{hr}} + m\log(\Delta t - 1) \qquad [1.3.23]$$

or:

$$\bar{p} = 3266 + 40\log(83.5 - 1) = 3343 \text{ psi}$$

As indicated earlier, the skin factor s is used to calculate the additional pressure drop in the altered permeability area around the wellbore and to characterize the well through the calculation of the flow coefficient E. That is:

$$\Delta p_\text{skin} = 0.87\,|m|\,s$$

and:

$$E = \frac{J_\text{actual}}{J_\text{ideal}} = \frac{\bar{p} - p_\text{wf} - \Delta p_\text{skin}}{\bar{p} - p_\text{wf}}$$

where $\bar{p}$ is the average pressure in the well drainage area. Lee (1982) suggested that for rapid analysis of the pressure buildup, the flow efficiency can be approximated by using the extrapolated straight-line pressure p^*, to give:

$$E = \frac{J_\text{actual}}{J_\text{ideal}} \approx \frac{p^* - p_\text{wf} - \Delta p_\text{skin}}{\bar{p} - p_\text{wf}}$$

Earlougher (1977) pointed out that there are a surprising number of situations where a single pressure point or "spot pressure" is the only pressure information available about a well. The average drainage region pressure $\bar{p}$ can be estimated from the spot pressure reading at shut-in time Δt using:

$$\bar{p} = p_{\text{ws at }\Delta t} + \frac{162.6 Q_\text{o}\mu_\text{o}B_\text{o}}{kh}\left[\log\left(\frac{\phi\mu c_\text{t}A}{0.0002637 k C_A \Delta t}\right)\right]$$

For a closed square drainage region $C_\text{A} = 30.8828$ and:

$$\bar{p} = p_{\text{ws at }\Delta t} + \frac{162.6 Q_\text{o}\mu_\text{o}B_\text{o}}{kh}\left[\log\left(\frac{122.8\phi\mu c_\text{t}A}{k\Delta t}\right)\right]$$

where $p_{\text{ws at }\Delta t}$ is the spot pressure reading at shut-in time Δt and:

Δt = shut-in time, hours
A = drainage area, ft^2
C_A = shape factor
k = permeability, md
c_t = total compressibility, psi^{-1}

It is appropriate at this time to briefly introduce the concept of type curves and discuss their applications in well testing analysis.

1.4 Type Curves

The type curve analysis approach was introduced in the petroleum industry by Agarwal et al. (1970) as a valuable tool when used in conjunction with conventional semilog plots. A type curve is a graphical representation of the theoretical solutions to flow equations. The type curve analysis consists of finding the theoretical type curve that "matches" the actual response from a test well and the reservoir when subjected to changes in production rates or pressures. The match can be found graphically by physically superposing a graph of actual test data with a similar graph of type curve(s) and searching for the type curve that provides the best match. Since type curves are plots of theoretical solutions to transient and pseudosteady-state flow equations, they are usually presented in terms of dimensionless variables (e.g., p_D, t_D, r_D, and C_D) rather than real variables (e.g., Δp, t, r, and C). The reservoir and well parameters, such as permeability and skin, can then be calculated from the dimensionless parameters defining that type curve.

Any variable can be made "dimensionless" by multiplying it by a group of constants with opposite dimensions, but the choice of this group will depend on the type of problem to be solved. For example, to create the dimensionless pressure drop p_D, the actual pressure drop Δp in psi is multiplied by the group A with units of psi^{-1}, or:

$$p_\text{D} = A\Delta p$$

Finding the group A that makes a variable dimensionless is derived from equations that describe reservoir fluid flow. To introduce this concept, recall Darcy's equation that describes radial, incompressible, steady-state flow as expressed by:

$$Q = \left[\frac{kh}{141.2B\mu[\ln(r_\text{e}/r_\text{wa}) - 0.5]}\right]\Delta p \qquad [1.4.1]$$

where r_wa is the apparent (effective) wellbore radius and defined by Equation 1.2.140 in terms of the skin factor s as:

$$r_\text{wa} = r_\text{w}\text{e}^{-s}$$

Group A can be defined by rearranging Darcy's equation as:

$$\ln\left(\frac{r_\text{e}}{r_\text{wa}}\right) - \frac{1}{2} = \left[\frac{kh}{141.2QB\mu}\right]\Delta p$$

Because the left-hand slide of this equation is dimensionless, the right-hand side must be accordingly dimensionless. This suggests that the term $kh/141.2QB\mu$ is essentially group A with units of psi^{-1} that defines the dimensionless variable p_D, or:

$$p_\text{D} = \left[\frac{kh}{141.2QB\mu}\right]\Delta p \qquad [1.4.2]$$

Taking the logarithm of both sides of this equation gives:

$$\log(p_\text{D}) = \log(\Delta p) + \log\left(\frac{kh}{141.2QB\mu}\right) \qquad [1.4.3]$$

where:

Q = flow rate, STB/day
B = formation, volume factor, bbl/STB
μ = viscosity, cp

For a constant flow rate, Equation 1.4.3 indicates that the logarithm of dimensionless pressure drop, $\log(p_\text{D})$, will differ from the logarithm of the *actual* pressure drop, $\log(\Delta p)$, by a constant amount of:

$$\log\left(\frac{kh}{141.2QB\mu}\right)$$

Similarly, the dimensionless time t_D is given by Equation 1.2.75 as:

$$t_\text{D} = \left[\frac{0.0002637k}{\phi\mu c_\text{t} r_\text{w}^2}\right]t$$

Taking the logarithm of both sides of this equation gives:

$$\log(t_\text{D}) = \log(t) + \log\left[\frac{0.0002637k}{\phi\mu c_\text{t} r_\text{w}^2}\right] \qquad [1.4.4]$$

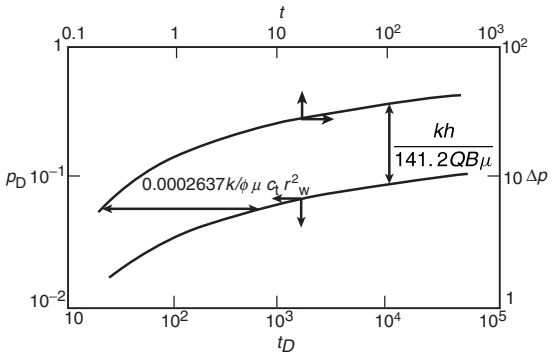

Figure 1.46 *Concept of type curves.*

where:

t = time, hours
c_t = total compressibility coefficient, psi^{-1}
ϕ = porosity

Hence, a graph of $\log(\Delta p)$ vs. $\log(t)$ will have an *identical shape* (i.e., parallel) to a graph of $\log(p_D)$ vs. $\log(t_D)$, although the curve will be shifted by $\log[kh/(141.2QB\mu)]$ vertically in pressure and $\log[0.0002637k/(\phi\mu c_t r_w^2)]$ horizontally in time. This concept is illustrated in Figure 1.46.

Not only do these two curves have the same shape, but if they are *moved relative to each other until they coincide or "match"*, the vertical and horizontal displacements required to achieve the match are related to these constants in Equations 1.4.3 and 1.4.4. Once these constants are determined from the vertical and horizontal displacements, it is possible to estimate reservoir properties such as permeability and porosity. This process of matching two curves through the vertical and horizontal displacements and determining the reservoir or well properties is called type curve matching.

As shown by Equation 1.2.83, the solution to the diffusivity equation can be expressed in terms of the dimensionless pressure drop as:

$$p_D = -\frac{1}{2}\text{Ei}\left(-\frac{r_D^2}{4t_D}\right)$$

Equation 1.2.84 indicates that when $t_D/r_D^2 > 25$, p_D can be approximated by:

$$p_D = \frac{1}{2}\left[\ln\left(t_D/r_D^2\right) + 0.080907\right]$$

Notice that:

$$\frac{t_D}{r_D^2} = \left(\frac{0.0002637k}{\phi\mu c_t r^2}\right)t$$

Taking the logarithm of both sides of this equation, gives:

$$\log\left(\frac{t_D}{r_D^2}\right) = \log\left(\frac{0.0002637k}{\phi\mu c_t r^2}\right) + \log(t) \qquad [1.4.5]$$

Equations 1.4.3 and 1.4.5 indicate that a graph of $\log(\Delta p)$ vs. $\log(t)$ will have an *identical shape* (i.e., parallel) to a graph of $\log(p_D)$ vs. $\log(t_D/r_D^2)$, although the curve will be shifted by $\log(kh141.2/QB\mu)$ vertically in pressure and $\log(0.0002637k/\phi\mu c_t r^2)$ horizontally in time. When these two curves are moved relative to each other until they coincide or "match," the vertical and horizontal movements, in mathematical terms, are given by:

$$\left(\frac{p_D}{\Delta p}\right)_{MP} = \frac{kh}{141.2QB\mu} \qquad [1.4.6]$$

and:

$$\left(\frac{t_D/r_D^2}{t}\right)_{MP} = \frac{0.0002637k}{\phi\mu c_t r^2} \qquad [1.4.7]$$

The subscript "MP" denotes a match point.

A more practical solution then to the diffusivity equation is a plot of the dimensionless p_D vs. t_D/r_D^2 as shown in Figure 1.47 that can be used to determine the pressure at any time and radius from the producing well. Figure 1.47 is basically a type curve that is mostly used in interference tests when analyzing pressure response data in a shut-in observation well at a distance r from an active producer or injector well.

In general, the type curve approach employs the flowing procedure that will be illustrated by the use of Figure 1.47:

Step 1. Select the proper type curve, e.g., Figure 1.47.
Step 2. Place tracing paper over Figure 1.47 and construct a log–log scale having the same dimensions as those of the type curve. This can be achieved by tracing the major and minor grid lines from the type curve to the tracing paper.
Step 3. Plot the well test data in terms of Δp vs. t on the tracing paper.
Step 4. Overlay the tracing paper on the type curve and slide the actual data plot, keeping the x and y axes of both graphs parallel, until the actual data point curve coincides or matches the type curve.
Step 5. Select any arbitrary point match point MP, such as an intersection of major grid lines, and record $(\Delta p)_{MP}$ and $(t)_{MP}$ from the actual data plot and the corresponding values of $(p_D)_{MP}$ and $(t_D/r_D^2)_{MP}$ from the type curve.
Step 6. Using the match point, calculate the properties of the reservoir.

The following example illustrates the convenience of using the type curve approach in an interference test for 48 hours followed by a falloff period of 100 hours.

Example 1.31[a] During an interference test, water was injected at a 170 bbl/day for 48 hours. The pressure response in an observation well 119 ft away from the injector is given below:

t (hrs)	p (psig)	$\Delta p_{ws} = p_i - p$ (psi)
0	$p_i = 0$	0
4.3	22	−22
21.6	82	−82
28.2	95	−95
45.0	119	−119
48.0		injection ends
51.0	109	−109
69.0	55	−55
73.0	47	−47
93.0	32	−32
142.0	16	−16
148.0	15	−15

Other given data includes:

$$p_i = 0 \text{ psi}, \quad B_w = 1.00 \text{ bbl/STB}$$

[a]This example problem and the solution procedure are given in Earlougher, R. *Advanced Well Test Analysis*, Monograph Series, SPE, Dallas (1977).

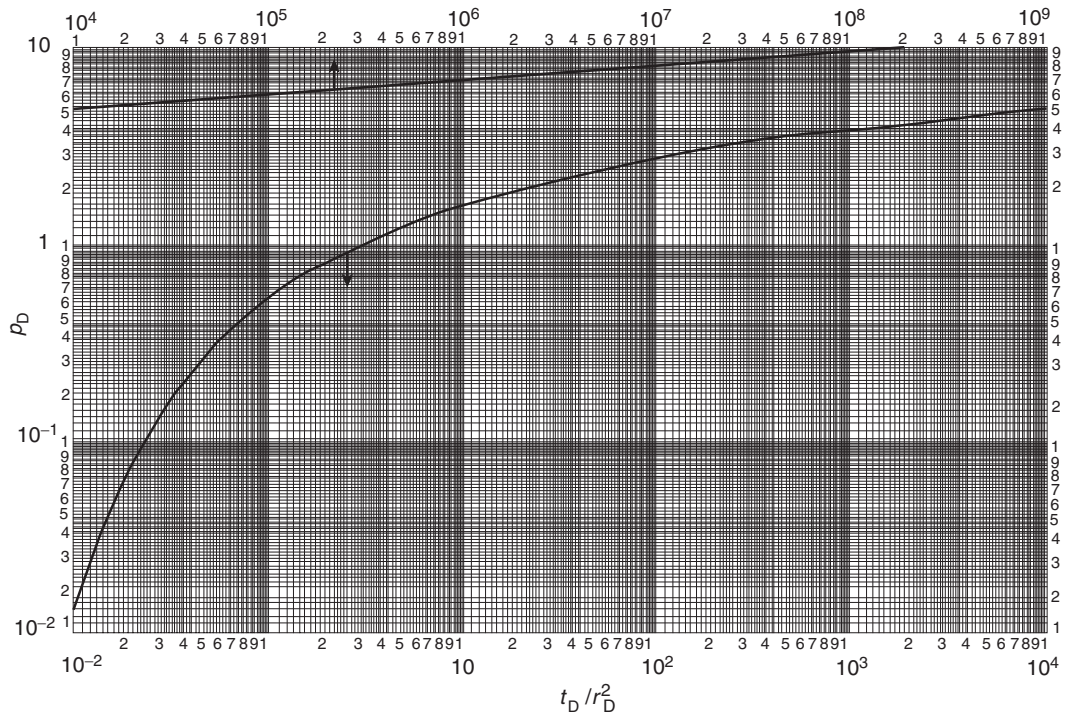

Figure 1.47 *Dimensionless pressure for a single well in an infinite system, no wellbore storage, no skin. Exponential–integral solution (After Earlougher, R.* Advances in Well Test Analysis*) (Permission to publish by the SPE, copyright SPE, 1977).*

$$c_t = 9.0 \times 10^{-6}\ \text{psi}^{-1}, \quad h = 45\ \text{ft}$$
$$\mu_w = 1.3\ \text{cp}, \quad q = -170\ \text{bbl/day}$$

Calculate the reservoir permeability and porosity.

Solution

Step 1. Figure 1.48 show a plot of the well test data during the injection period, i.e., 48 hours, in terms of Δp vs. t on tracing paper with the same scale dimensions as in Figure 1.47. Using the overlay technique with the vertical and horizontal movements, find the segment of the type curve that matches the actual data.

Step 2. Select any point on the graph that will be defined as a match point MP, as shown in Figure 1.48. Record $(\Delta p)_{MP}$ and $(t)_{MP}$ from the actual data plot and the corresponding values of $(p_D)_{MP}$ and $(t_D/r_D^2)_{MP}$ from the type curve, to give:
Type curve match values:

$$(p_D)_{MP} = 0.96, \quad (t_D/r_D^2)_{MP} = 0.94$$

Actual data match values:

$$(\Delta p)_{MP} = -100\ \text{psig}, \quad (t)_{MP} = 10\ \text{hours}$$

Step 3. Using Equations 1.4.6 and 1.4.7, solve for the permeability and porosity:

$$k = \frac{141.2QB\mu}{h}\left(\frac{p_D}{\Delta p}\right)_{MP}$$
$$= \frac{141.2(-170)(1.0)(1.0)}{45}\left(\frac{0.96}{-100}\right)_{MP} = 5.1\ \text{md}$$

and:

$$\phi = \frac{0.0002637k}{\mu c_t r^2[(t_D/r_D^2)/t]_{MP}}$$
$$= \frac{0.0002637(5.1)}{(1.0)(9.0\times10^{-6})(119)^2[0.94/10]_{MP}} = 0.11$$

Equation 1.2.83 shows that the dimensionless pressure is related to the dimensionless radius and time by:

$$p_D = -\frac{1}{2}\text{Ei}\left(-\frac{r_D^2}{4t_D}\right)$$

At the wellbore radius where $r = r_w$, i.e., r_D=1, and $p(r,t) = p_{wf}$, the above expression is reduced to:

$$p_D = -\frac{1}{2}\text{Ei}\left(\frac{-1}{4t_D}\right)$$

The log approximation as given by Equation 1.2.80 can be applied to the above solution to give:

$$p_D = \frac{1}{2}[\ln(t_D) + 0.80901]$$

and, to account for the skin s, by:

$$p_D = \frac{1}{2}[\ln(t_D) + 0.80901] + s$$

or:

$$p_D = \frac{1}{2}[\ln(t_D) + 0.80901 + 2s]$$

Notice that the above expressions assume zero wellbore storage, i.e., dimensionless wellbore storage $C_D = 0$. Several authors have conducted detailed studies on the effects and duration of wellbore storage on pressure drawdown and buildup data. Results of these studies were presented in the type curve format in terms of the dimensionless pressure as

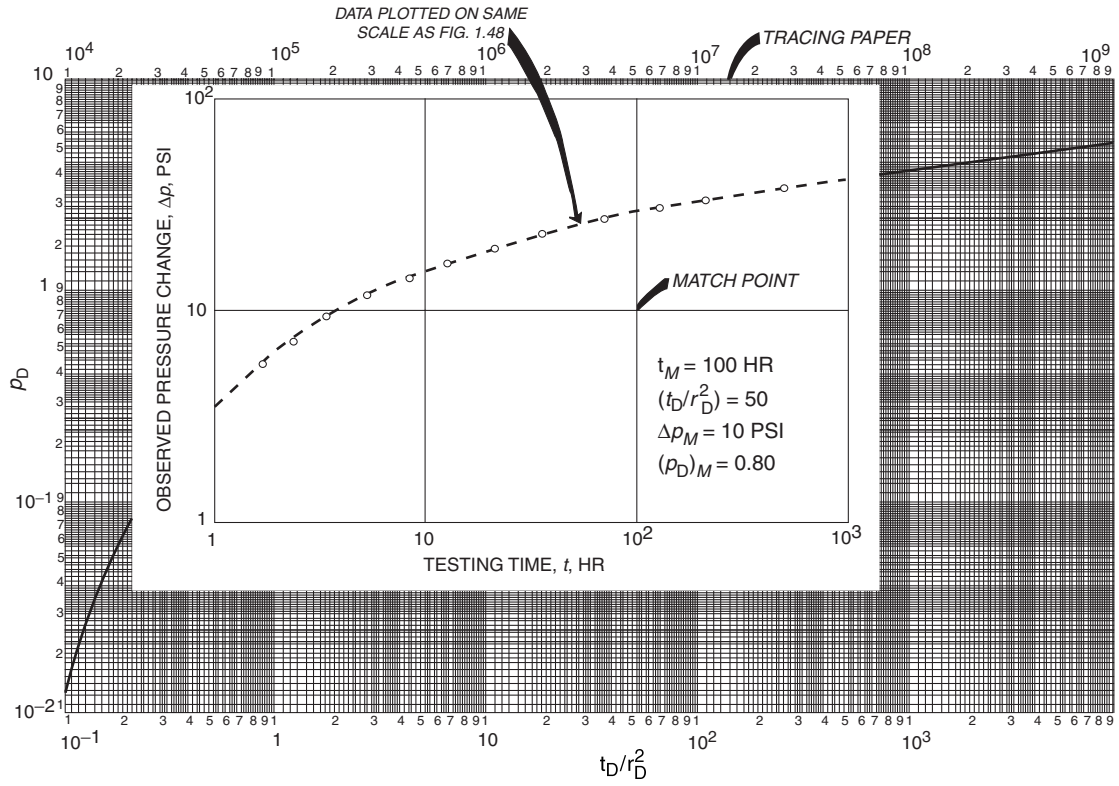

Figure 1.48 *Illustration of type curve matching for an interference test using the type curve (After Earlougher, R.* Advances in Well Test Analysis*) (Permission to publish by the SPE, copyright SPE, 1977).*

a function of dimensionless time, radius, and wellbore storage, i.e., $p_D = f(t_D, r_D, C_D)$. The following two methods that utilize the concept of the type curve approach are briefly introduced below:

(1) the Gringarten type curve;
(2) the pressure derivative method

1.4.1 Gringarten type curve

During the *early-time period* where the flow is dominated by the wellbore storage, the wellbore pressure is described by Equation 1.3.5 as:

$$p_D = \frac{t_D}{C_D}$$

or:

$$\log(p_D) = \log(t_D) - \log(C_D)$$

This relationship gives the characteristic signature of wellbore storage effects on well testing data which indicates that a plot of p_D vs. t_D on a log–log scale will yield a straight line of a *unit slope.* At the end of the storage effect, which signifies the beginning of the infinite-acting period, the resulting pressure behavior produces the usual straight line on a semilog plot as described by:

$$p_D = \frac{1}{2}[\ln(t_D) + 0.80901 + 2s]$$

It is convenient when using the type curve approach in well testing to include the dimensionless wellbore storage coefficient in the above relationship. Adding and subtracting $\ln(C_D)$ inside the brackets of the above equation gives:

$$p_D = \frac{1}{2}[\ln(t_D) - \ln(C_D) + 0.80901 + \ln(C_D) + 2s]$$

or, equivalently:

$$p_D = \frac{1}{2}\left[\ln\left(\frac{t_D}{C_D}\right) + 0.80907 + \ln(C_D e^{2s})\right] \qquad [1.4.8]$$

where:

p_D = dimensionless pressure
C_D = dimensionless wellbore storage coefficient
t_D = dimensionless time
s = skin factor

Equation 1.4.8 describes the pressure behavior of a well with a wellbore storage and a skin in a homogeneous reservoir during the transient (infinite-acting) flow period. Gringarten et al. (1979) expressed the above equation in the graphical type curve format shown in Figure 1.49. In this figure, the dimensionless pressure p_D is plotted on a log–log scale versus dimensionless time group t_D/C_D. The resulting curves, characterized by the dimensionless group $C_D e^{2s}$, represent different well conditions ranging from damaged wells to stimulated wells.

Figure 1.49 shows that all the curves merge, in early time, into a unit-slope straight line corresponding to pure wellbore storage flow. At a later time with the end of the wellbore storage-dominated period, curves correspond to infinite-acting radial flow. The end of wellbore storage and the start of infinite-acting radial flow are marked on the type curves of Figure 1.49. There are three dimensionless

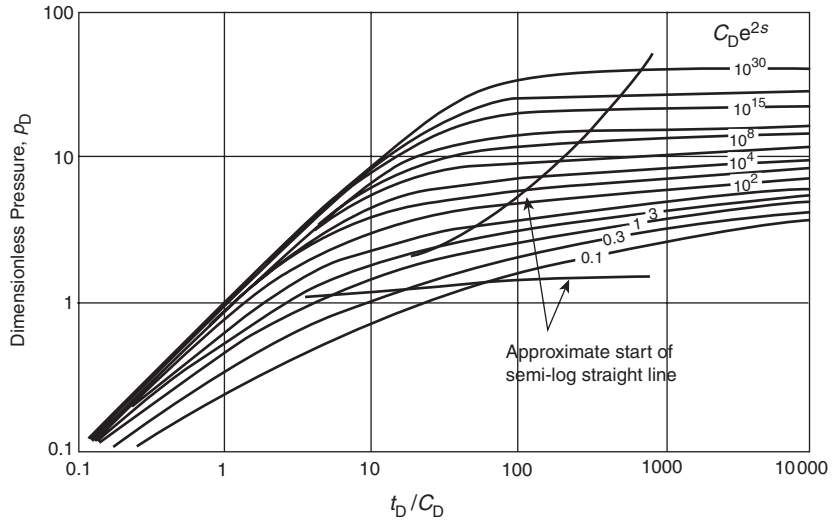

Figure 1.49 *Type curves for a well with wellbore storage and skin in a reservoir with homogeneous behavior (Copyright ©1983 World Oil, Bourdet et al., May 1983).*

groups that Gringarten et al. used when developing the type curve:

(1) dimensionless pressure p_D;
(2) dimensionless ratio t_D/C_D;
(3) dimensionless characterization group C_De^{2s}.

The above three dimensionless parameters are defined mathematically for both the drawdown and buildup tests as follows.

For drawdown

Dimensionless pressure p_D

$$p_D = \frac{kh(p_i - p_{wf})}{141.2QB\mu} = \frac{kh\Delta p}{141.2QB\mu} \qquad [1.4.9]$$

where:

k = permeability, md
p_{wf} = bottom-hole flowing pressure, psi
Q = flow rate, bbl/day
B = formation volume factor, bbl/STB

Taking logarithms of both sides of the above equation gives:

$$\log(p_D) = \log(p_i - p_{wf}) + \log\left(\frac{kh}{141.2QB\mu}\right)$$

$$\log(p_D) = \log(\Delta p) + \log\left(\frac{kh}{141.2QB\mu}\right) \qquad [1.4.10]$$

Dimensionless ratio t_D/C_D

$$\frac{t_D}{C_D} = \left(\frac{0.0002637kt}{\phi\mu c_t r_w^2}\right)\left(\frac{\phi hc_t r_w^2}{0.8396C}\right)$$

Simplifying gives:

$$\frac{t_D}{C_D} = \left(\frac{0.0002951kh}{\mu C}\right)t \qquad [1.4.11]$$

where:

t = flowing time, hours
C = wellbore storage coefficient, bbl/psi

Taking logarithms gives:

$$\log\left(\frac{t_D}{C_D}\right) = \log(t) + \log\left[\frac{0.0002951kh}{\mu C}\right] \qquad [1.4.12]$$

Equations 1.4.10 and 1.4.12 indicate that a plot of the actual drawdown data of $\log(\Delta p)$ vs. $\log(t)$ will produce a parallel curve that has an identical shape to a plot of $\log(p_D)$ vs. $\log(t_D/C_D)$. When displacing the actual plot, vertically and horizontally, to find a dimensionless curve that coincides or closely fits the actual data, these displacements are given by the constants of Equations 1.4.9 and 1.4.11 as:

$$\left(\frac{p_D}{\Delta p}\right)_{MP} = \frac{kh}{141.2QB\mu} \qquad [1.4.13]$$

and:

$$\left(\frac{t_D/C_D}{t}\right)_{MP} = \frac{0.0002951kh}{\mu C} \qquad [1.4.14]$$

where MP denotes a match point.

Equations 1.4.13 and 1.4.14 can be solved for the permeability k (or the flow capacity kh) and the wellbore storage coefficient C respectively:

$$k = \frac{141.2QB\mu}{h}\left(\frac{p_D}{\Delta p}\right)_{MP}$$

and:

$$C = \frac{0.0002951kh}{\mu\left(\frac{t_D/C_D}{t}\right)_{MP}}$$

Dimensionless characterization group C_De^{2s} The mathematical definition of the dimensionless characterization group C_De^{2s} as given below is valid for both the drawdown and buildup tests:

$$C_De^{2s} = \left[\frac{5.615C}{2\pi\phi\mu c_t r_w^2}\right]e^{2s} \qquad [1.4.15]$$

where:

ϕ = porosity
c_t = total isothermal compressibility, psi^{-1}
r_w = wellbore radius, ft

When the match is achieved, the dimensionless group C_De^{2s} describing the matched curve is recorded.

For buildup

It should be noted that *all type curve solutions* are obtained for the drawdown solution. Therefore, these type curves

cannot be used for buildup tests without restriction or modification. The only restriction is that the flow period, i.e., t_p, before shut-in must be somewhat large. However, Agarwal (1980) empirically found that by plotting the buildup data $p_{ws} - p_{wf \text{ at } \Delta t=0}$ versus "equivalent time" Δt_e instead of the shut-in time Δt, on a log–log scale, the type curve analysis can be made without the requirement of a long drawdown flowing period before shut-in. Agarwal introduced the equivalent time Δt_e as defined by:

$$\Delta t_e = \frac{\Delta t}{1 + (\Delta t / t_p)} = [\Delta t / t_p + \Delta t]\, t_p \qquad [1.4.16]$$

where:

Δt = shut-in time, hours
t_p = total flowing time since the last shut-in, hours
Δt_e = Agarwal equivalent time, hours

Agarwal's equivalent time Δt_e is simply designed to account for the effects of producing time t_p on the pressure buildup test. The concept of Δt_e is that the pressure change $\Delta p = p_{ws} - p_{wf}$ at time Δt during a buildup test is the same as the pressure change $\Delta p = p_i - p_{wf}$ at Δt_e during a drawdown test. Thus, a graph of buildup test in terms of $p_{ws} - p_{wf}$ vs. Δt_e will overlay a graph of pressure change versus flowing time for a drawdown test. Therefore, when applying the type curve approach in analyzing pressure buildup data, the actual shut-in time Δt is replaced by the equivalent time Δt_e.

In addition to the characterization group $C_D e^{2s}$ as defined by Equation 1.4.15, the following two dimensionless parameters are used when applying the Gringarten type curve in analyzing pressure buildup test data.

Dimensionless pressure p_D

$$p_D = \frac{kh(p_{ws} - p_{wf})}{141.2QB\mu} = \frac{kh\Delta p}{141.2QB\mu} \qquad [1.4.17]$$

where:

p_{ws} = shut-in pressure, psi
p_{wf} = flow pressure just before shut-in, i.e., at $\Delta t = 0$, psi

Taking the logarithms of both sides of the above equation gives:

$$\log(p_D) = \log(\Delta p) + \log\left(\frac{kh}{141.2QB\mu}\right) \qquad [1.4.18]$$

Dimensionless ratio t_D/C_D

$$\frac{t_D}{C_D} = \left[\frac{0.0002951kh}{\mu C}\right] \Delta t_e \qquad [1.4.19]$$

Taking the logarithm of each side of Equation 1.4.9 gives:

$$\log\left(\frac{t_D}{C_D}\right) = \log(\Delta t_e) + \log\left(\frac{0.0002951kh}{\mu C}\right) \qquad [1.4.20]$$

Similarly, a plot of actual pressure buildup data of $\log(\Delta p)$ vs. $\log(\Delta t_e)$ would have a shape identical to that of $\log(p_D)$ vs. $\log(t_D/C_D)$. When the actual plot is matched to one of the curves of Figure 1.49, then:

$$\left(\frac{p_D}{\Delta p}\right)_{MP} = \frac{kh}{141.2QB\mu}$$

which can be solved for the flow capacity kh or the permeability k. That is:

$$k = \left[\frac{141.2QB\mu}{h}\right]\left(\frac{p_D}{\Delta p}\right)_{MP} \qquad [1.4.21]$$

and:

$$\left(\frac{t_D/C_D}{\Delta t_e}\right)_{MP} = \frac{0.0002951kh}{\mu C} \qquad [1.4.22]$$

Solving for C gives:

$$C = \left[\frac{0.0002951kh}{\mu}\right]\frac{(\Delta t_e)_{MP}}{(t_D/C_D)_{MP}} \qquad [1.4.23]$$

The recommended procedure for using the Gringarten type curve is given by the following steps:

Step 1. Using the test data, perform *conventional* test analysis and determine:
- wellbore storage coefficient C and C_D;
- permeability k;
- false pressure p^*;
- average pressure $\bar{p}$;
- skin factor s;
- shape factor C_A;
- drainage area A.

Step 2. Plot $p_i - p_{wf}$ versus flowing time t for a drawdown test or $(p_{ws} - p_{wp})$ versus equivalent time Δt_e for a buildup test on log – log paper (tracing paper) with the same size log cycles as the Gringarten type curve.

Step 3. Check the early-time points on the actual data plot for the unit-slope (45° angle) straight line to verify the presence of the wellbore storage effect. If a unit-slope straight line presents, calculate the wellbore storage coefficient C and the dimensionless C_D from any point on the unit-slope straight line with coordinates of $(\Delta p, t)$ or $(\Delta p, \Delta t_e)$, to give:

For drawdown
$$C = \frac{QBt}{24(p_i - p_{wf})} = \frac{QB}{24}\left(\frac{t}{\Delta p}\right) \qquad [1.4.24]$$

For buildup
$$C = \frac{QB\Delta t_e}{24(p_{ws} - p_{wf})} = \frac{QB}{24}\left(\frac{\Delta t_e}{\Delta p}\right) \qquad [1.4.25]$$

Estimate the dimensionless wellbore storage coefficient from:

$$C_D = \left[\frac{0.8936}{\phi h c_t r_w^2}\right] C \qquad [1.4.26]$$

Step 4. Overlay the graph of the test data on the type curves and find the type curve that nearly fits most of the actual plotted data. Record the type curve dimensionless group $(C_D e^{2s})_{MP}$.

Step 5. Select a match point MP and record the corresponding values of $(p_D, \Delta p)_{MP}$ from the y axis and $(t_D/C_D, t)_{MP}$ or $(t_D/C_D, \Delta t_e)_{MP}$ from the x axis.

Step 6. From the match, calculate:

$$k = \left[\frac{141.2QB\mu}{h}\right]\left(\frac{p_D}{\Delta p}\right)_{MP}$$

and:

$$C = \left[\frac{0.0002951kh}{\mu}\right]\left(\frac{t}{(t_D/C_D)}\right)_{MP} \quad \text{for drawdown}$$

or:

$$C = \left[\frac{0.0002951kh}{\mu}\right]\left(\frac{\Delta t_e}{(t_D/C_D)}\right)_{MP} \quad \text{for buildup}$$

and:

$$C_D = \left[\frac{0.8936}{\phi h c_t r_w^2}\right] C$$

$$s = \frac{1}{2}\ln\left[\frac{(C_D e^{2s})_{MP}}{C_D}\right] \qquad [1.4.27]$$

Sabet (1991) used the buildup data presented by Bourdet et al. (1983) to illustrate the use of Gringarten type curves. The data is used in the following example:

Example 1.32 Table 1.6 summarizes the pressure buildup data for an oil well that has been producing at a constant flow rate of 174 STB/day before shut-in. Additional pertinent data is given below:

$$\phi = 25\%, \quad c_t = 4.2 \times 10^{-6}\ \text{psi}^{-1}$$
$$Q = 174\ \text{STB/day}, \quad t_p = 15\ \text{hours}$$
$$B = 1.06\ \text{bbl/STB}, \quad r_w = 0.29\ \text{ft}$$
$$\mu = 2.5\ \text{cp}, \quad h = 107\ \text{ft}$$

Perform the conventional the pressure buildup analysis by using the Horner plot approach and compare the results with those obtained by using the Gringarten type curve approach.

Table 1.6 *Pressure buildup test with afterflow (After Sabet, M. A. "Well Test Analysis" 1991, Gulf Publishing Company)*

Δt(hr)	p_{ws} (psi)	Δp (psi)	$\frac{t_p + \Delta t}{\Delta t}$	Δt_e
0.00000	3086.33	0.00	–	0.00000
0.00417	3090.57	4.24	3600.71	0.00417
0.00833	3093.81	7.48	1801.07	0.00833
0.01250	3096.55	10.22	1201.00	0.01249
0.01667	3100.03	13.70	900.82	0.01666
0.02083	3103.27	16.94	721.12	0.02080
0.02500	3106.77	20.44	601.00	0.02496
0.02917	3110.01	23.68	515.23	0.02911
0.03333	3113.25	26.92	451.05	0.03326
0.03750	3116.49	30.16	401.00	0.03741
0.04583	3119.48	33.15	328.30	0.04569
0.05000	3122.48	36.15	301.00	0.04983
0.05830	3128.96	42.63	258.29	0.05807
0.06667	3135.92	49.59	225.99	0.06637
0.07500	3141.17	54.84	201.00	0.07463
0.08333	3147.64	61.31	181.01	0.08287
0.09583	3161.95	75.62	157.53	0.09522
0.10833	3170.68	84.35	139.47	0.10755
0.12083	3178.39	92.06	125.14	0.11986
0.13333	3187.12	100.79	113.50	0.13216
0.14583	3194.24	107.91	103.86	0.14443
0.16250	3205.96	119.63	93.31	0.16076
0.17917	3216.68	130.35	84.72	0.17706
0.19583	3227.89	141.56	77.60	0.19331
0.21250	3238.37	152.04	71.59	0.20953
0.22917	3249.07	162.74	66.45	0.22572
0.25000	3261.79	175.46	61.00	0.24590
0.29167	3287.21	200.88	52.43	0.28611
0.33333	3310.15	223.82	46.00	0.32608
0.37500	3334.34	248.01	41.00	0.36585
0.41667	3356.27	269.94	37.00	0.40541
0.45833	3374.98	288.65	33.73	0.44474
0.50000	3394.44	308.11	31.00	0.48387
0.54167	3413.90	327.57	28.69	0.52279
0.58333	3433.83	347.50	26.71	0.56149
0.62500	3448.05	361.72	25.00	0.60000
0.66667	3466.26	379.93	23.50	0.63830
0.70833	3481.97	395.64	22.18	0.67639
0.75000	3493.69	407.36	21.00	0.71429
0.81250	3518.63	432.30	19.46	0.77075
0.87500	3537.34	451.01	18.14	0.82677
0.93750	3553.55	467.22	17.00	0.88235
1.00000	3571.75	485.42	16.00	0.93750
1.06250	3586.23	499.90	15.12	0.99222
1.12500	3602.95	516.62	14.33	1.04651
1.18750	3617.41	531.08	13.63	1.10039
1.25000	3631.15	544.82	13.00	1.15385
1.31250	3640.86	554.53	12.43	1.20690
1.37500	3652.85	566.52	11.91	1.25954
1.43750	3664.32	577.99	11.43	1.31179
1.50000	3673.81	587.48	11.00	1.36364
1.62500	3692.27	605.94	10.23	1.46617
1.75000	3705.52	619.19	9.57	1.56716
1.87500	3719.26	632.93	9.00	1.66667
2.00000	3732.23	645.90	8.50	1.76471
2.25000	3749.71	663.38	7.67	1.95652
2.37500	3757.19	670.86	7.32	2.05036
2.50000	3763.44	677.11	7.00	2.14286
2.75000	3774.65	688.32	6.45	2.32394
3.00000	3785.11	698.78	6.00	2.50000
3.25000	3794.06	707.73	5.62	2.67123
3.50000	3799.80	713.47	5.29	2.83784
3.75000	3809.50	723.17	5.00	3.00000
4.00000	3815.97	729.64	4.75	3.15789
4.25000	3820.20	733.87	4.53	3.31169
4.50000	3821.95	735.62	4.33	3.46154
4.75000	3823.70	737.37	4.16	3.60759
5.00000	3826.45	740.12	4.00	3.75000
5.25000	3829.69	743.36	3.86	3.88889
5.50000	3832.64	746.31	3.73	4.02439
5.75000	3834.70	748.37	3.61	4.15663
6.00000	3837.19	750.86	3.50	4.28571
6.25000	3838.94	752.61	3.40	4.41176
6.75000	3838.02	751.69	3.22	4.65517
7.25000	3840.78	754.45	3.07	4.88764
7.75000	3843.01	756.68	2.94	5.10989
8.25000	3844.52	758.19	2.82	5.32258
8.75000	3846.27	759.94	2.71	5.52632
9.25000	3847.51	761.18	2.62	5.72165
9.75000	3848.52	762.19	2.54	5.90909
10.25000	3850.01	763.68	2.46	6.08911
10.75000	3850.75	764.42	2.40	6.26214
11.25000	3851.76	765.43	2.33	6.42857
11.75000	3852.50	766.17	2.28	6.58879
12.25000	3853.51	767.18	2.22	6.74312
12.75000	3854.25	767.92	2.18	6.89189
13.25000	3855.07	768.74	2.13	7.03540
13.75000	3855.50	769.17	2.09	7.17391
14.50000	3856.50	770.17	2.03	7.37288
15.25000	3857.25	770.92	1.98	7.56198
16.00000	3857.99	771.66	1.94	7.74194
16.75000	3858.74	772.41	1.90	7.91339
17.50000	3859.48	773.15	1.86	8.07692
18.25000	3859.99	773.66	1.82	8.23308
19.00000	3860.73	774.40	1.79	8.38235
19.75000	3860.99	774.66	1.76	8.52518
20.50000	3861.49	775.16	1.73	8.66197
21.25000	3862.24	775.91	1.71	8.79310
22.25000	3862.74	776.41	1.67	8.95973
23.25000	3863.22	776.89	1.65	9.11765
24.25000	3863.48	777.15	1.62	9.26752
25.25000	3863.99	777.66	1.59	9.40994
26.25000	3864.49	778.16	1.57	9.54545
27.25000	3864.73	778.40	1.55	9.67456
28.50000	3865.23	778.90	1.53	9.82759
30.00000	3865.74	779.41	1.50	10.00000

Adapted from Bourdet et al. (1983).

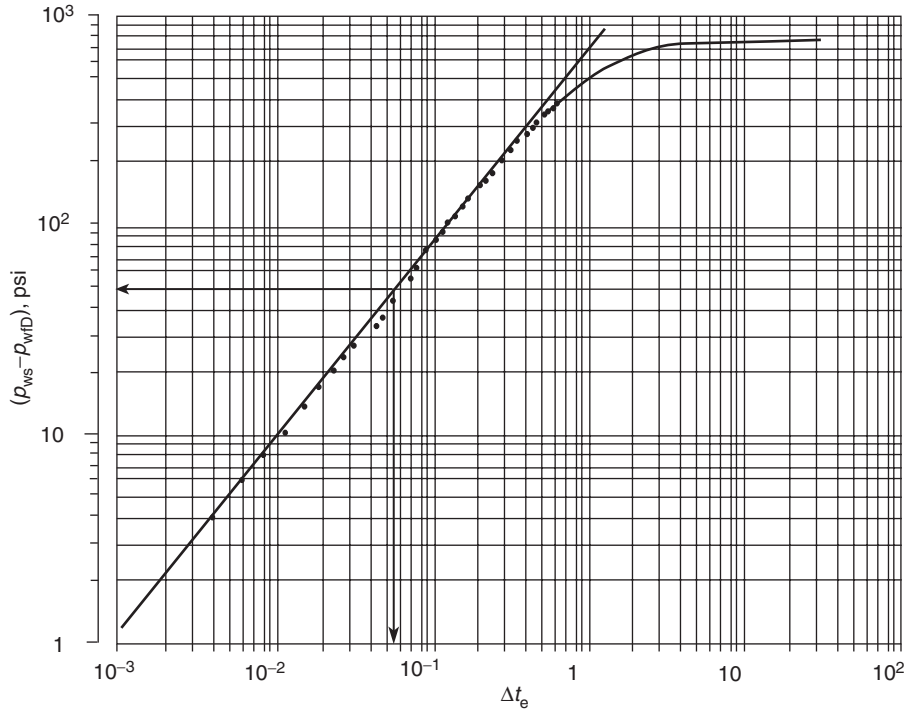

Figure 1.50 *Log–log plot. Data from Table 1.6 (After Sabet, M. A.* Well Test Analysis*, 1991, Gulf Publishing Company).*

Solution

Step 1. Plot Δp vs. Δt_e on a log – log scale, as shown in Figure 1.50. The plot shows that the early data form a straight line with a 45° angle, which indicates the wellbore storage effect. Determine the coordinates of a point on the straight line, e.g., $\Delta p = 50$ and $\Delta t_e = 0.06$, and calculate C and C_D:

$$C = \frac{QB\Delta t_e}{24\Delta p} = \frac{(174)(1.06)(0.06)}{(24)(50)} = 0.0092 \text{ bbl/psi}$$

$$C_D = \frac{0.8936C}{\phi h c_t r_w^2} = \frac{0.8936(0.0092)}{(0.25)(107)(4.2\times10^{-6})(0.29)^2} = 872$$

Step 2. Make a Horner plot of p_{ws} vs. $(t_p+\Delta t)/\Delta t$ on semilog paper, as shown in Figure 1.51, and perform the conventional well test analysis, to give:

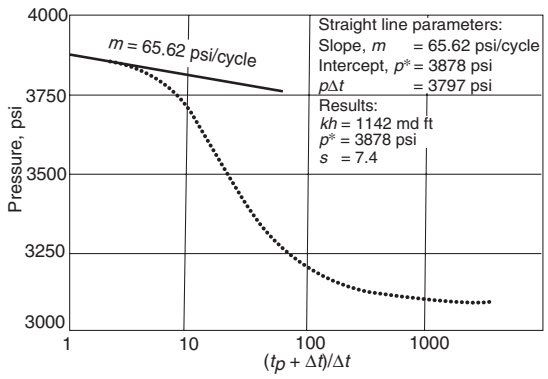

Figure 1.51 *The Horner plot: data from Table 1.6 (Copyright ©1983 World Oil, Bourdet et al., May 1983).*

$$m = 65.62 \text{ psi/cycle}$$

$$k = \frac{162.6QB\mu}{mh}\frac{(162.6)(174)(2.5)}{(65.62)(107)} = 10.1 \text{ md}$$

$$p_{1\,hr} = 3797 \text{ psi}$$

$$s = 1.151\left[\frac{p_{1\,hr}-p_{wf}}{(m)} - \log\left(\frac{k}{\phi\mu c_t r_w^2}\right) + 3.23\right]$$

$$= 1.151\left[\frac{3797-3086.33}{65.62} - \log\left(\frac{10.1}{(0.25)(2.5)(4.2\times10^{-6})(0.29)^2}\right) + 3.23\right]$$

$$= 7.37$$

$$\Delta p_{skin} = (0.87)(65.62)(7.37) = 421 \text{ psi}$$

$$p^* = 3878 \text{ psi}$$

Step 3. Plot Δp vs. Δt_e, on log–log graph paper with the same size log cycles as the Gringarten type curve. Overlay the actual test data plot on the type curve and find the type curve that matches the test data. As shown in Figure 1.52, the data matched the curve with the dimensionless group of $C_D e^{2s} = 10^{10}$ and a match point of:

$$(p_D)_{MP} = 1.79$$

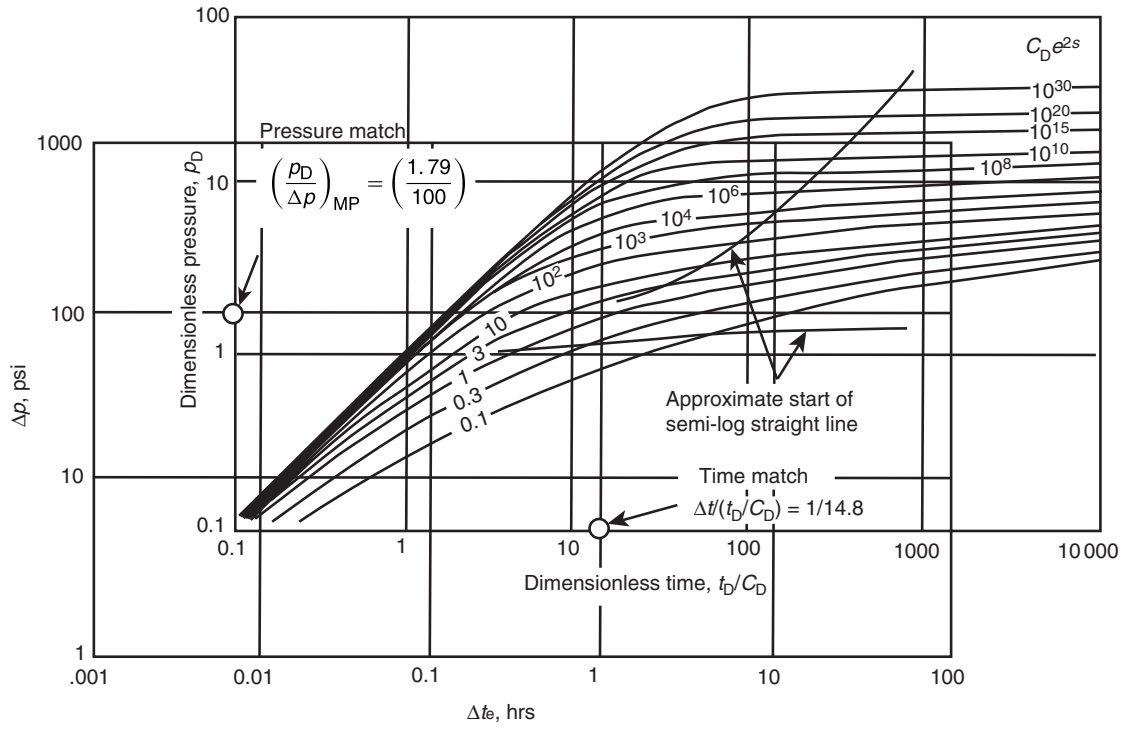

Figure 1.52 *Buildup data plotted on log–log graph paper and matched to type curve by Gringarten et al. (Copyright © 1983 World Oil, Bourdet et al., May 1983).*

$$(\Delta p)_{MP} = 100$$

$$(t_D/C_D) = 14.8$$

$$(\Delta t_e) = 1.0$$

Step 4. From the match, calculate the following properties:

$$k = \left[\frac{141.2QB\mu}{h}\right]\left(\frac{p_D}{\Delta p}\right)_{MP}$$

$$= \frac{141.2(174)(1.06)(2.5)}{(107)}\left(\frac{1.79}{100}\right) = 10.9 \text{ md}$$

$$C = \left[\frac{0.0002951kh}{\mu}\right]\left[\frac{\Delta t_e}{(t_D/C_D)}\right]_{MP}$$

$$= \left[\frac{0.0002951(10.9)(107)}{2.5}\right]\left[\frac{1.0}{14.8}\right] = 0.0093$$

$$C_D = \left[\frac{0.8936}{\phi h c_t r_w^2}\right]C$$

$$= \left[\frac{0.8936}{(0.25)(107)(4.2\times10^{-6})(0.29)^2}\right](0.0093)$$

$$= 879$$

$$s = \frac{1}{2}\ln\left[\frac{(C_D e^{2s})_{MP}}{C_D}\right] = \frac{1}{2}\ln\left[\frac{10^{10}}{879}\right] = 8.12$$

Results of the example show a good agreement between the conventional well testing analysis and that of the Gringarten type curve approach.

Similarly, the Gringarten type curve can also be used for gas systems by redefining the dimensionless pressure drop and time as:

For the gas pseudopressure approach $p_D = \dfrac{kh\Delta[m(p)]}{1422Q_gT}$

For the pressure-squared approach $p_D = \dfrac{kh\Delta[p^2]}{1422Q_g\mu_i Z_i T}$

with the dimensionless time as:

$$t_D = \left[\frac{0.0002637k}{\phi\mu c_t r_w^2}\right]t$$

where:

Q_g = gas flow rate, Mscf/day
T = temperature, ° R
$\Delta[m(p)] = m(p_{ws}) - m(p_{wf \text{ at } \Delta t=0})$ for the buildup test
$= m(p_i) - m(p_{wf})$ for the drawdown test
$\Delta[p^2] = (p_{ws})^2 - (p_{wf \text{ at } \Delta t=0})^2$ for the buildup test
$= (p_i)^2 - (p_{wf})^2$ for the drawdown test

and for buildup, the shut-in time Δt replaces flowing time t in the above equation.

1.5 Pressure Derivative Method

The type curve approach for the analysis of well testing data was developed to allow for the identification of flow regimes during the wellbore storage-dominated period and the infinite-acting radial flow. As illustrated through Example 1.31, it can be used to estimate the reservoir properties and wellbore condition. However, because of the similarity of curves shapes, it is difficult to obtain a unique solution. As shown in Figure 1.49, all type curves have very similar

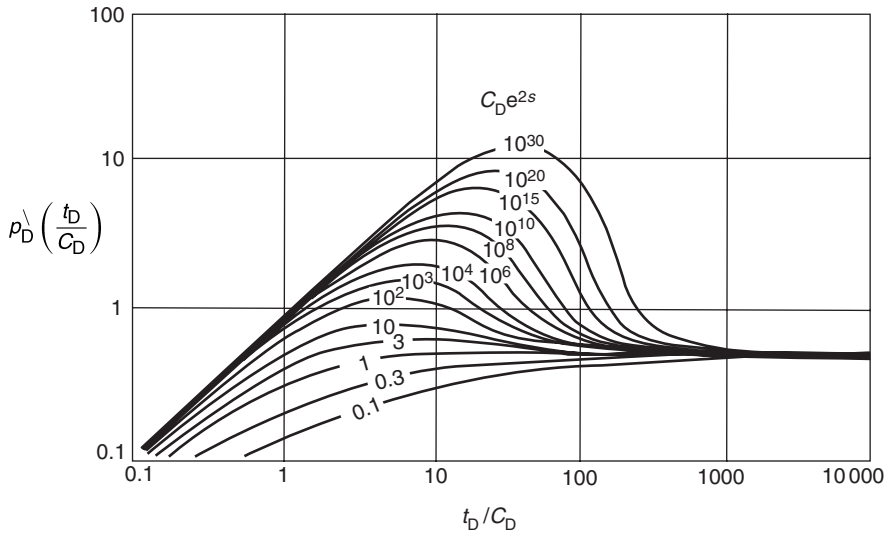

Figure 1.53 *Pressure derivative type curve in terms of $P_D^{\backslash}(t_D/C_D)$ (Copyright ©1983 World Oil, Bourdet et al., May 1983).*

shapes for high values of C_De^{2s} which lead to the problem of finding a unique match by a simple comparison of shapes and determining the correct values of k, s, and C.

Tiab and Kumar (1980) and Bourdet et al. (1983) addressed the problem of identifying the correct flow regime and selecting the proper interpretation model. Bourdet and his co-authors proposed that flow regimes can have clear characteristic shapes if the "pressure derivative" rather than pressure is plotted versus time on the log–log coordinates. Since the introduction of the pressure derivative type curve, well testing analysis has been greatly enhanced by its use. The use of this pressure derivative type curve offers the following advantages:

- Heterogeneities hardly visible on the conventional plot of well testing data are amplified on the derivative plot.
- Flow regimes have clear characteristic shapes on the derivative plot.
- The derivative plot is able to display in a single graph many separate characteristics that would otherwise require different plots.
- The derivative approach improves the definition of the analysis plots and therefore the quality of the interpretation.

Bourdet et al. (1983) defined the pressure derivative as the derivative of p_D with respect to t_D/C_D as:

$$P_D^{\backslash} = \frac{d(P_D)}{d(t_D/C_D)} \qquad [1.5.1]$$

It has been shown that during the wellbore storage-dominated period the pressure behavior is described by:

$$P_D = \frac{t_D}{C_D}$$

Taking the derivative of p_D with respect to t_D/C_D gives:

$$\frac{d(P_D)}{d(t_D/C_D)} = P_D^{\backslash} = 1.0$$

Since $p_D^{\backslash} = 1$, this implies that multiplying $p_D^{\backslash}$ by t_D/C_D gives t_D/C_D, or:

$$p_D^{\backslash}\left(\frac{t_D}{C_D}\right) = \frac{t_D}{C_D} \qquad [1.5.2]$$

Equation 1.5.2 indicates that a plot of $p_D^{\backslash}(t_D/C_D)$ vs. t_D/C_D in log–log coordinates will produce a unit-slope straight line during the wellbore storage-dominated flow period.

Similarly, during the radial infinite-acting flow period, the pressure behavior is given by Equation 1.5.1 as:

$$p_D = \frac{1}{2}\left[\ln\left(\frac{t_D}{C_D}\right) + 0.80907 + \ln(C_De^{2s})\right]$$

Differentiating with respect to t_D/C_D, gives:

$$\frac{d(p_D)}{d(t_D/C_D)} = p_D^{\backslash} = \frac{1}{2}\left[\frac{1}{(t_D/C_D)}\right]$$

Simplifying gives:

$$p_D^{\backslash}\left(\frac{t_D}{C_D}\right) = \frac{1}{2} \qquad [1.5.3]$$

This indicates that a plot of $p_D^{\backslash}(t_D/C_D)$ vs. t_D/C_D on a log–log scale will produce a *horizontal line* at $p_D^{\backslash}(t_D/C_D) = \frac{1}{2}$ during the transient flow (radial infinite-acting) period. As shown by Equations 1.5.2 and 1.5.3 the derivative plot of $p_D^{\backslash}(t_D/C_D)$ vs. t_D/C_D for the entire well test data will produce *two straight lines* that are characterized by:

- a unit-slope straight line during the wellbore storage-dominated flow;
- a horizontal line at $p_D^{\backslash}(t_D/C_D) = 0.5$ during the transient flow period.

The fundamental basis for the pressure derivative approach is essentially based on identifying these two straight lines that can be used as reference lines when selecting the proper well test data interpreting model.

Bourdet et al. replotted the Gringarten type curve in terms of $p_D^{\backslash}(t_D/C_D)$ vs. t_D/C_D on a log–log scale as shown in Figure 1.53. It shows that at the early time during the wellbore storage-dominated flow, the curves follow a unit-slope log–log straight line. When infinite-acting radial flow is reached, the curves become horizontal at a value of $p_D^{\backslash}(t_D/C_D) = 0.5$ as indicated by Equation 1.5.3. In addition, notice that the transition from pure wellbore storage to infinite-acting behavior gives a "hump" with a height that characterizes the value of the skin factor s.

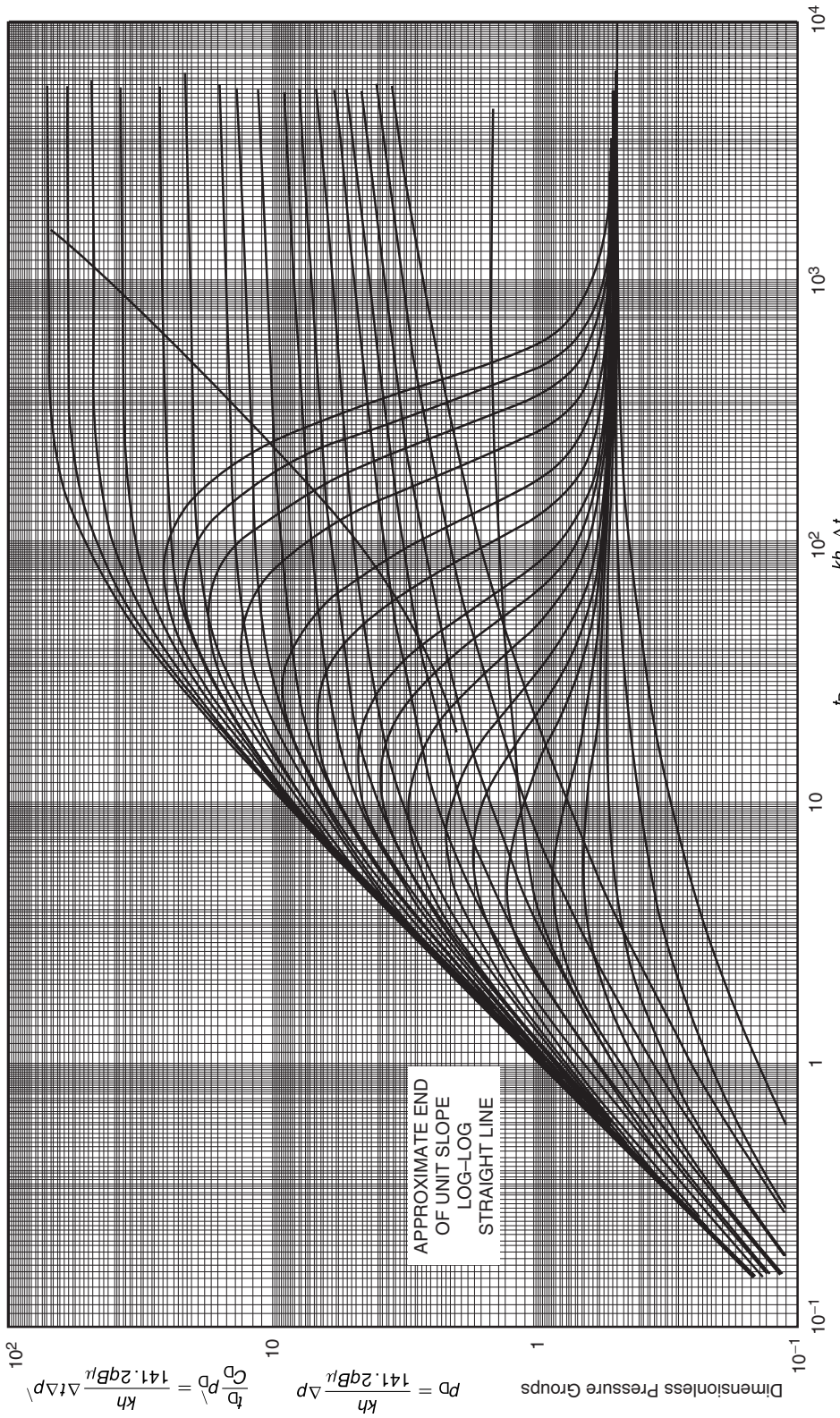

Figure 1.54 *Pressure derivative type curves (Copyright ©1983 World Oil, Bourdet et al., May 1983).*

Figure 1.53 illustrates that the effect of skin is only manifested in the curvature between the straight line due to wellbore storage flow and the *horizontal straight line* due to the infinite-acting radial flow. Bourdet et al. indicated that the data in this curvature portion of the curve is not always well defined. For this reason, the authors found it useful to combine their derivative type curves with that of the Gringarten type curve by superimposing the two type curves, i.e., Figures 1.49 and 1.53, on the same scale. The result of superimposing the two sets of type curves on the same graph is shown in Figure 1.54. The use of the new type curve allows the *simultaneous* matching of pressure-change data and derivative data since both are plotted on the same scale. The derivative pressure data provides, without ambiguity, the pressure match and the time match, while the $C_D e^{2s}$ value is obtained by comparing the label of the match curves for the derivative pressure data and pressure drop data.

The procedure for analyzing well test data using the derivative type curve is summarized by the following steps:

Step 1. Using the actual well test data, calculate the pressure difference Δp and the pressure derivative plotting functions as defined below for drawdown and buildup tests.

For the drawdown tests, for every recorded drawdown pressure point, i.e., flowing time t and a corresponding bottom-hole flowing pressure p_{wf}, calculate:

The pressure difference $\Delta p = p_i - p_{wf}$

The derivative function
$$t\Delta p' = -t\left(\frac{d(\Delta p)}{d(t)}\right) \qquad [1.5.4]$$

For the buildup tests, for every recorded buildup pressure point, i.e., shut-in time Δt and corresponding shut-in pressure p_{ws}, calculate:

The pressure difference $\Delta p = p_{ws} - p_{wf \text{ at } \Delta t = 0}$

The derivative function
$$\Delta t_e \Delta p' = \Delta t\left(\frac{t_p + \Delta t}{\Delta t}\right)\left[\frac{d(\Delta p)}{d(\Delta t)}\right] \qquad [1.5.5]$$

The derivatives included in Equations 1.5.4 and 1.5.5, i.e., $[dp_{wf}/dt]$ and $[d(\Delta p_{ws})/d(\Delta t)]$, can be determined numerically at any data point i by using the central difference formula for *evenly spaced time* or the three-point weighted average approximation as shown graphically in Figure 1.55 and mathematically by the following expressions:
Central differences:
$$\left(\frac{dp}{dx}\right)_i = \frac{p_{i+1} - p_{i-1}}{x_{i+1} - x_{i-1}} \qquad [1.5.6]$$

Three-point weighted average:
$$\left(\frac{dp}{dx}\right)_i = \frac{(\Delta p_1/\Delta x_1)\Delta x_2 + (\Delta p_2/\Delta x_2)\Delta x_1}{\Delta x_1 + \Delta x_2} \qquad [1.5.7]$$

It should be pointed out that selection of the method of numerical differentiation is a problem that must be considered and examined when applying the pressure derivative method. There are many differentiation methods that use only two points, e.g., backward difference, forward difference, and central difference formulas, and very complex algorithms that utilize several pressure points. It is important to try several different methods in order to find one which best smoothes the data.

Step 2. On tracing paper with the same size log cycles as the Bourdet–Gringarten type curve graph, i.e., Figure 1.54, plot:

- (Δp) and $(t\Delta p')$ as a function of the flowing time t when analyzing drawdown test data. Notice that there are two sets of data on the same log–log graph as illustrated in Figure 1.56; the first is the analytical solution and the second is the actual drawdown test data.
- The pressure difference Δp versus the equivalent time Δt_e and the derivative function $(\Delta t_e \Delta p')$ versus the *actual shut-in time* Δt. Again, there are two sets of data on the same graph as shown in Figure 1.56.

Step 3. Check the actual early-time pressure points, i.e., pressure difference versus time on a log–log scale, for the unit-slope line. If it exists, draw a line through the points and calculate the wellbore storage coefficient C by selecting a point on the unit-slope line as identified with coordinates of $(t, \Delta p)$ or $(\Delta t_e, \Delta p)$ and applying Equation 1.4.24 or Equation 1.4.25, as follows:

$$\text{For drawdown} \quad C = \frac{QB}{24}\left(\frac{t}{\Delta p}\right)$$

$$\text{For buildup} \quad C = \frac{QB}{24}\left(\frac{\Delta t_e}{\Delta p}\right)$$

Step 4. Calculate the dimensionless wellbore storage coefficient C_D by applying Equation 1.4.26 and using the value of C as calculated in Step 3. That is:
$$C_D = \left[\frac{0.8936}{\phi h c_t r_w^2}\right] C$$

Step 5. Check the late-time data points on the *actual pressure derivative* plot to see if they form a horizontal line which indicates the occurrence of transient (unsteady-state) flow. If it exists, draw a horizontal line through these derivative plot points.

Step 6. Place the actual two sets of plots, i.e., the pressure difference plot and derivative function plot, on the Gringarten–Bourdet type curve of Figure 1.54, and force a simultaneous match of the two plots to Gringarten–Bourdet type curves. The unit-slope line should overlay the unit slope on the type curve and the late-time horizontal line should overlay the horizontal line on the type cure which corresponds to a value of 0.5. Note that it is convenient to match both pressure and pressure derivative curves, even though it is redundant. With the double match, a high degree of confidence in the results is obtained.

Step 7. From the match of the best fit, select a match point MP and record the corresponding values of the following:

- From the Gringarten type curve, determine $(p_D, \Delta p)_{MP}$ and the corresponding $(t_D/C_D, t)_{MP}$ or $(t_D/C_D, \Delta t_e)_{MP}$.
- Record the value of the type curve dimensionless group $(C_D e^{2s})_{MP}$ from the Bourdet type curves.

Step 8. Calculate the permeability by applying Equation 1.4.21:
$$k = \left[\frac{141.2QB\mu}{h}\right]\left[\frac{p_D}{\Delta p}\right]_{MP}$$

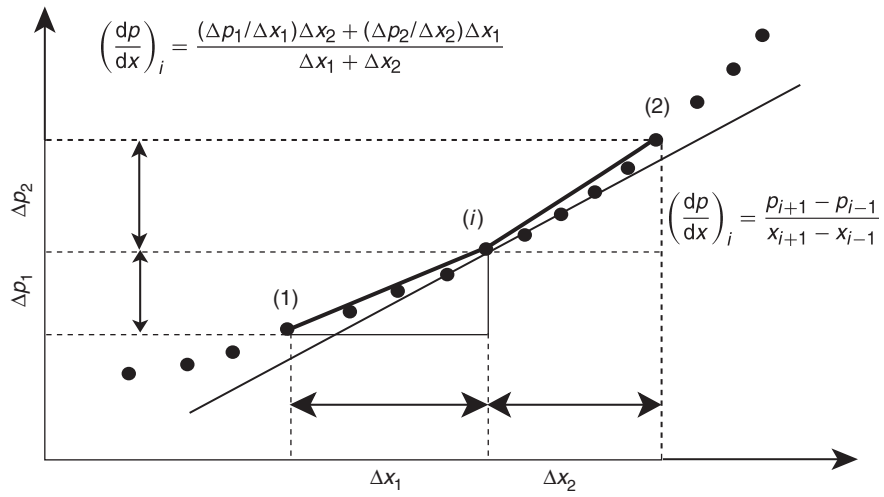

Figure 1.55 *Differentiation algorithm using three points.*

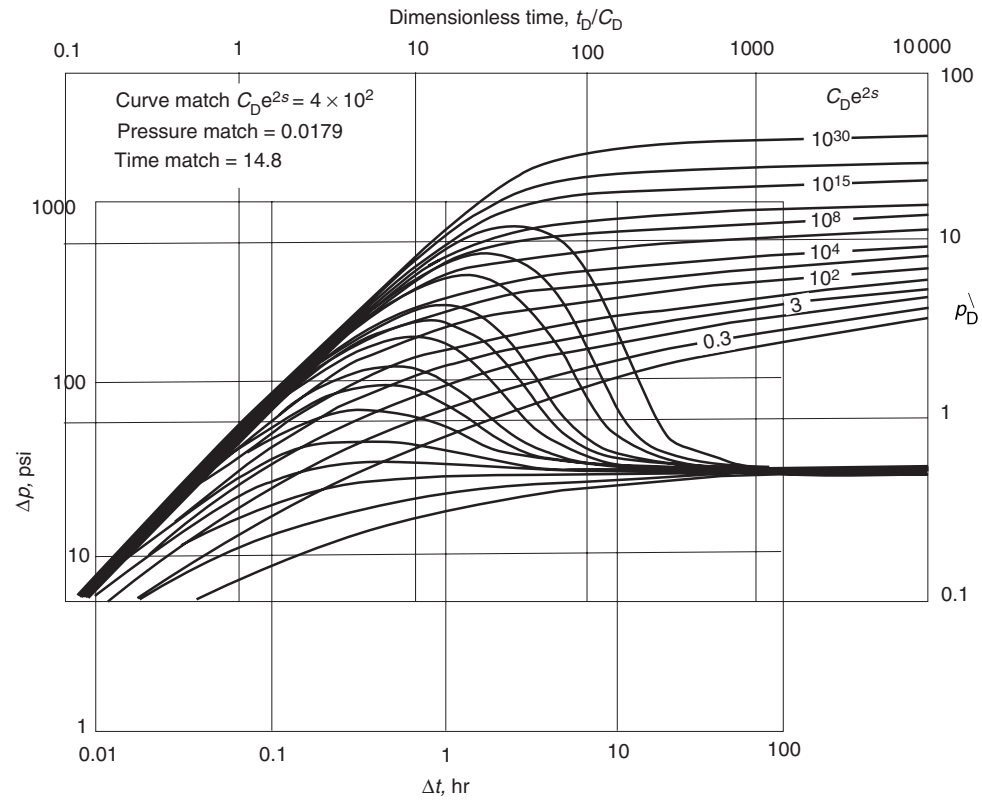

Figure 1.56 *Type curve matching. Data from Table 1.6 (Copyright ©1983 World Oil, Bourdet et al., May 1983).*

Step 9. Recalculate the wellbore storage coefficient C and C_D by applying Equations 1.4.23 and 1.4.26, or:

$$\text{For drawdown} \quad C = \left[\frac{0.0002951kh}{\mu}\right]\frac{(t)_{MP}}{(t_D/C_D)_{MP}}$$

$$\text{For buildup} \quad C = \left[\frac{0.0002951kh}{\mu}\right]\frac{(\Delta t_e)_{MP}}{(t_D/C_D)_{MP}}$$

with:

$$C_D = \left[\frac{0.8936}{\phi h c_t r_w^2}\right]C$$

Compare the calculated values of C and C_D with those calculated in steps 3 and 4.

Step 10. Calculate the skin factor s by applying Equation 1.4.27 and using the value of C_D in step 9 and the value of $(C_D e^{2s})_{MP}$ in step 7, to give:

$$s = \frac{1}{2} \ln \left[\frac{(C_D e^{2s})_{MP}}{C_D} \right]$$

Example 1.33 Using the same data of Example 1.31, analyze the given well test data using the pressure derivative approach.

Solution

Step 1. Calculate the derivative function for every recorded data point by applying Equation 1.5.5 or the approximation method of Equation 1.5.6 as tabulated Table 1.7 and shown graphically in Figure 1.57.

Table 1.7 *Pressure derivative method. Data of Table 6.6 After Sabet, M.A. "Well Test Analysis" 1991, Gulf Publishing Company*

Δt (hr)	Δp (psi)	*Slope* (psi/hr)	$\Delta p'$ (psi/hr)	$\Delta t \Delta t' (t_p + \Delta t) t_p$
0.00000	0.00	1017.52	–	–
0.00417	4.24	777.72	897.62	3.74
0.00833	7.48	657.55	717.64	5.98
0.01250	10.22	834.53	746.04	9.33
0.01667	13.70	778.85	806.69	13.46
0.02083	16.94	839.33	809.09	16.88
0.02500	20.44	776.98	808.15	20.24
0.02917	23.68	778.85	777.91	22.74
0.03333	26.92	776.98	777.91	25.99
0.03750	30.16	358.94	567.96	21.35
0.04583	33.15	719.42	539.18	24.79
0.05000	36.15	780.72	750.07	37.63
0.05830	42.63	831.54	806.13	47.18
0.06667	49.59	630.25	730.90	48.95
0.07500	54.84	776.71	703.48	53.02
0.08333	61.31	1144.80	960.76	80.50
0.09583	75.62	698.40	921.60	88.88
0.10833	84.35	616.80	657.60	71.75
0.12083	92.06	698.40	657.60	80.10
0.13333	100.79	569.60	634.00	85.28
0.14583	107.91	703.06	636.33	93.70
0.16250	119.63	643.07	673.07	110.56
0.17917	130.35	672.87	657.97	119.30
0.19583	141.56	628.67	650.77	129.10
0.21250	152.04	641.87	635.27	136.91
0.22917	162.74	610.66	626.26	145.71
0.25000	175.46	610.03	610.34	155.13
0.29167	200.88	550.65	580.34	172.56
0.33333	223.82	580.51	565.58	192.71
0.37500	248.01	526.28	553.40	212.71
0.41667	269.94	449.11	487.69	208.85
0.45833	288.65	467.00	458.08	216.36
0.50000	308.11	467.00	467.00	241.28
0.54167	327.57	478.40	472.70	265.29
0.58333	347.50	341.25	409.82	248.36
0.62500	361.72	437.01	389.13	253.34
0.66667	379.93	377.10	407.05	283.43
0.70833	395.64	281.26	329.18	244.18
0.75000	407.36	399.04	340.15	267.87
0.81250	432.30	299.36	349.20	299.09
0.87500	451.01	259.36	279.36	258.70
0.93750	467.22	291.20	275.28	274.20
1.00000	485.42	231.68	261.44	278.87
1.06250	499.90	267.52	249.60	283.98
1.12500	516.62	231.36	249.44	301.67
1.18750	531.08	219.84	225.60	289.11
1.25000	544.82	155.36	187.60	254.04
1.31250	554.53	191.84	173.60	247.79
1.37500	566.52	183.52	187.68	281.72
1.43750	577.99	151.84	167.68	264.14
1.50000	587.48	147.68	149.76	247.10
1.62500	605.94	106.00	126.84	228.44
1.75000	619.19	109.92	107.96	210.97
1.87500	632.93	103.76	106.84	225.37
2.00000	645.90	69.92	86.84	196.84
2.25000	663.38	59.84	64.88	167.88
2.37500	670.66	50.00	54.92	151.09
2.50000	677.11	44.84	47.42	138.31
2.75000	688.32	41.84	43.34	141.04
3.00000	698.78	35.80	38.82	139.75
3.25000	707.73	22.96	29.38	118.17
3.50000	713.47	38.80	30.88	133.30
3.75000	723.17	25.88	32.34	151.59
4.00000	729.64	16.92	21.40	108.43
4.25000	733.87	7.00	11.96	65.23
4.50000	735.62	7.00	7.00	40.95
4.75000	737.37	11.00	9.00	56.29
5.00000	740.12	12.96	11.98	79.87
5.25000	743.36	11.80	12.38	87.74
5.50000	746.31	8.24	10.02	75.32
5.75000	748.37	9.96	9.10	72.38
6.00000	750.86	7.00	8.48	71.23
6.25000	752.51	−1.84	2.58	22.84
6.75000	751.69	5.52	1.84	18.01
7.25000	754.45	4.46	4.99	53.66
7.75000	756.68	3.02	3.74	43.96
8.25000	758.19	3.50	3.26	41.69
8.75000	759.94	2.48	2.99	41.42
9.25000	761.18	2.02	2.25	33.65
9.75000	762.19	2.98	2.50	40.22
10.25000	763.68	1.48	2.23	38.48
10.75000	764.42	2.02	1.75	32.29
11.25000	765.43	1.48	1.75	34.45
11.75000	766.17	2.02	1.75	36.67
12.25000	767.18	1.48	1.75	38.94
12.75000	767.92	1.64	1.56	36.80
13.25000	768.74	0.86	1.25	31.19
13.75000	769.17	1.33	1.10	28.90
14.50000	770.17	1.00	1.17	33.27
15.25000	770.92	0.99	0.99	30.55
16.00000	771.66	1.00	0.99	32.85
16.75000	772.41	0.99	0.99	35.22
17.50000	773.15	0.68	0.83	31.60
18.25000	773.66	0.99	0.83	33.71
19.00000	774.40	0.35	0.67	28.71
19.75000	774.66	0.67	0.51	23.18
20.50000	775.16	1.00	0.83	40.43
21.25000	775.91	0.50	0.75	38.52
22.25000	776.41	0.48	0.49	27.07
23.25000	776.89	0.26	0.37	21.94
24.25000	777.15	0.51	0.38	24.43
25.25000	777.66	0.50	0.50	34.22
26.25000	778.16	0.24	0.37	26.71
27.25000	778.40	0.40[a]	0.32[b]	24.56[c]
28.50000	778.90	0.34	0.37	30.58
30.00000	779.41	25.98	13.16	1184.41

[a] $(778.9 - 778.4)/(28.5 - 27.25) = 0.40$.
[b] $(0.40 + 0.24)/2 = 0.32$.
[c] $27.25 - 0.32 - (15 + 27.25)/15 = 24.56$.

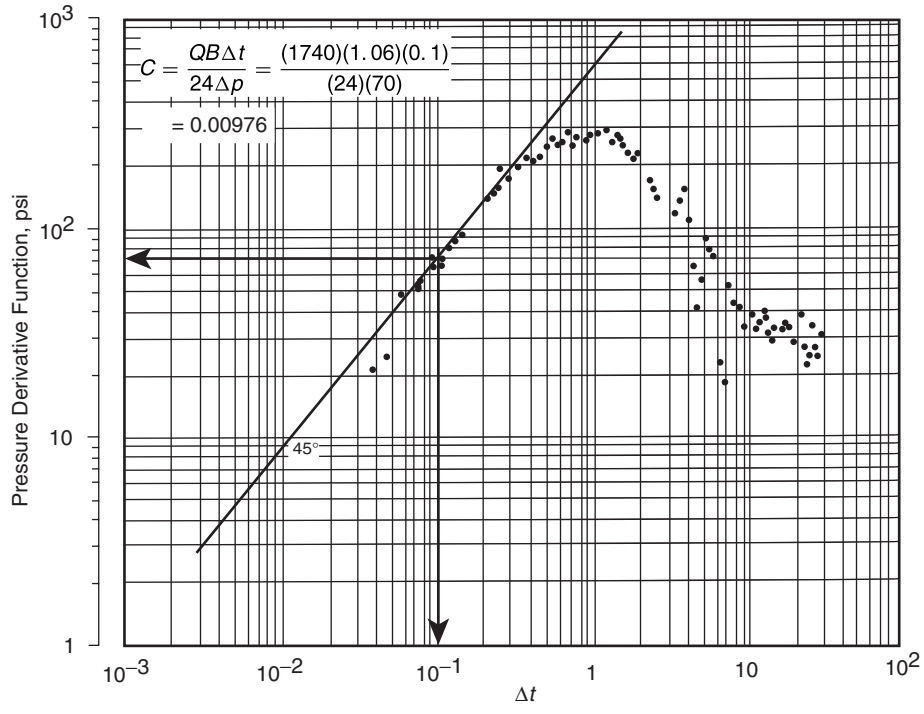

Figure 1.57 *Log–log plot. Data from Table 1.7.*

Step 2. Draw a straight line with a 45° angle that fits the early-time test points, as shown in Figure 1.57, and select the coordinates of a point on the straight line, to give (0.1, 70). Calculate C and C_D:

$$C = \frac{QB\Delta t}{24\Delta p} = \frac{1740(1.06)(0.1)}{(24)(70)} = 0.00976$$

$$C_D = \left[\frac{0.8936}{\phi h c_t r_w^2}\right] = \frac{0.8936(0.00976)}{(0.25)(107)(4.2\times10^{-6})(0.29)^2}$$

$$= 923$$

Step 3. Overlay the pressure difference data and pressure derivative data over the Gringarten–Bourdet type curve to match the type curve, as shown in Figure 1.57, with the following match points:

$$(C_D e^{2s})_{MP} = 4\times10^9$$

$$(p_D/\Delta p)_{MP} = 0.0179$$

$$\left[(t_D/C_D)/\Delta t\right]_{MP} = 14.8$$

Step 4. Calculate the permeability k:

$$k = \left[\frac{141.2QB\mu}{h}\right]\left(\frac{p_D}{\Delta p}\right)_{MP}$$

$$= \left[\frac{141.2(174)(1.06)(2.5)}{107}\right](0.0179)$$

$$= 10.9 \text{ md}$$

Step 5. Calculate C and C_D:

$$C = \left[\frac{0.0002951kh}{\mu}\right]\frac{(\Delta t_e)_{MP}}{(t_D/C_D)_{MP}}$$

$$= \left[\frac{0.0002951(10.9)(107)}{2.5}\right]\left(\frac{1}{14.8}\right)$$

$$= 0.0093 \text{ bbl/psi}$$

$$C_D = \frac{0.8936C}{\phi h c_t r_w^2} = \frac{0.8936(0.0093)}{(0.25)(107)(4.2\times10^{-6})(0.29)^2}$$

$$= 879$$

Step 6. Calculate the skin factor s:

$$s = \frac{1}{2}\ln\left[\frac{(C_D e^{2s})_{MP}}{C_D}\right] = \frac{1}{2}\ln\left[\frac{4\times10^9}{879}\right] = 7.7$$

Notice that the derivative function, as plotted in Figure 1.57, shows an appreciable amount of scatter points and the horizontal line which signifies the radial infinite-acting state is not clear. A practical limitation associated with the use of the pressure derivative approach is the ability to measure pressure transient data with sufficient frequency and accuracy so that it can be differentiated. Generally, the derivative function will show severe oscillations unless the data is smoothed before taking the derivative.

Smoothing of any time series, such as pressure–time data, is not an easy task, and unless it is done with care and know-how, a portion of the data which is representative of the reservoir (signal) could be lost. Signal filtering, smoothing, and interpolation is a very advanced subject of science and engineering, and unless the proper smoothing techniques are applied to the field data, the results could be utterly misleading.

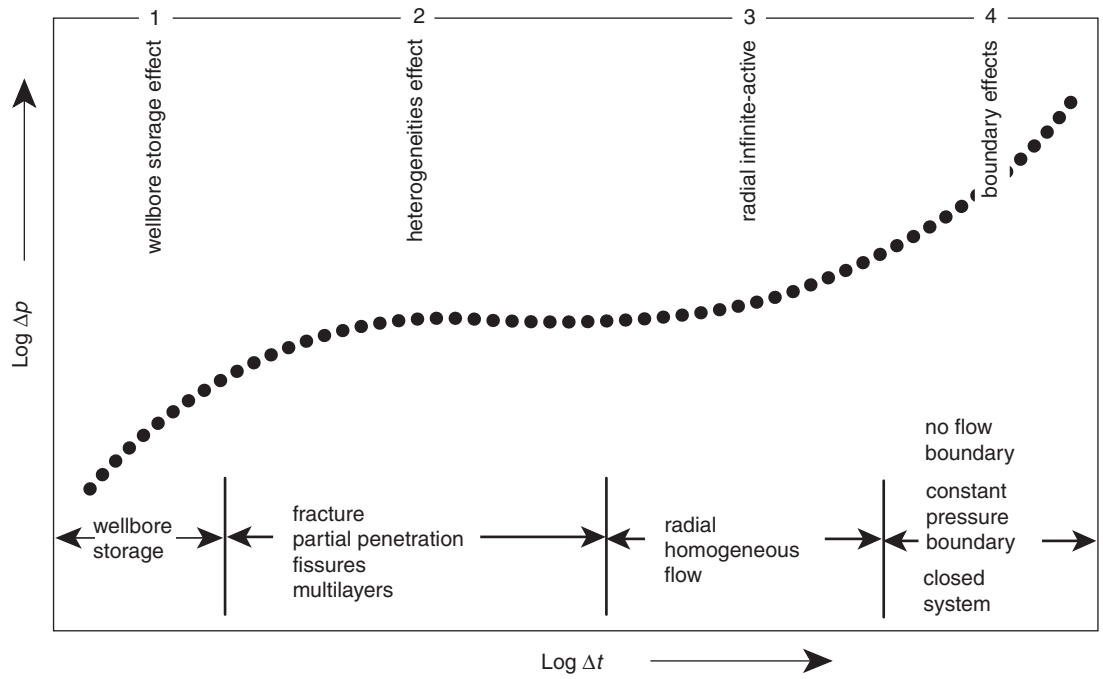

Figure 1.58 *Log–log plot of a typical drawdown.*

In addition to the reservoir heterogeneity, there are many inner and outer reservoir boundary conditions that will cause the transient state plot to deviate from the expected semilog straight-line behavior during the infinite-acting behavior of the test well, such as:

- faults and other impermeable flow barriers;
- partial penetration;
- phase separation and packer failures;
- interference;
- stratified layers;
- naturally and hydraulically fractured reservoirs;
- boundary;
- lateral increase in mobility.

The theory which describes the unsteady-state flow data is based on the ideal radial flow of fluids in a homogeneous reservoir system of uniform thickness, porosity, and permeability. Any deviation from this ideal concept can cause the predicted pressure to behave differently from the actual measured pressure. In addition, a well test response may have different behavior at different times during the test. In general, the following four different time periods can be identified on a log–log plot of Δp vs. Δt as shown in Figure 1.58:

(1) The *wellbore storage effect* is always the first flow regime to appear.
(2) Evidence of the well and reservoir *heterogeneities effect* will then appear in the pressure behavior response. This behavior may be a result of multilayered formation, skin, hydraulic fractures, or fissured formation.
(3) The pressure response exhibits the *radial infinite-active* behavior and represents an equivalent homogeneous system.
(4) The last period represents the *boundary effects* that may occur at late time.

Thus, many types of flow regimes can appear before and after the actual semilog straight line develops, and they follow a very strict chronology in the pressure response. Only global diagnosis, with identification of all successive regimes present, will indicate exactly when conventional analysis, e.g., the semilog plot technique, is justified. Recognition of the above four different sequences of responses is perhaps the most important element in well test analysis. The difficulty arises from the fact that some of these responses could be missing, overlapping, or undetectable through the traditional graphical semilog straight-line approach. Selection of the correct *reservoir interpretation model* is a prerequisite and an important step before analyzing well test data and interpreting the test results. With proper well test design and sufficient test length for the response to be detected, most pressure transient data can provide an unambiguous indicator of the type and the associated characteristics of the reservoir. However, many well tests cannot or are not run for sufficient test duration to eliminate ambiguity in selecting the proper model to analyze test data. With a sufficient length of well testing time, the reservoir response during well testing is then used to identify a well test interpretation model from which well and reservoir parameters, such as permeability and skin, can be determined. This *model identification* requirement holds for both traditional graphical analyses as well as for computer-aided techniques.

It should be pointed out that both the semilog and log–log plots of pressure versus time data are often insensitive to pressure changes and cannot be solely used as diagnostic plots to find the interpretation model that best represents the dynamic behavior of the well and reservoir during the test. The pressure derivative type curve, however, is the most definitive of the type curves for identifying the proper interpretation model. The pressure derivative approach has been applied with tremendous success as a diagnostic tool for the following reasons:

- It magnifies small pressure changes.
- Flow regimes have *clear characteristic shapes* on the pressure derivative plot.

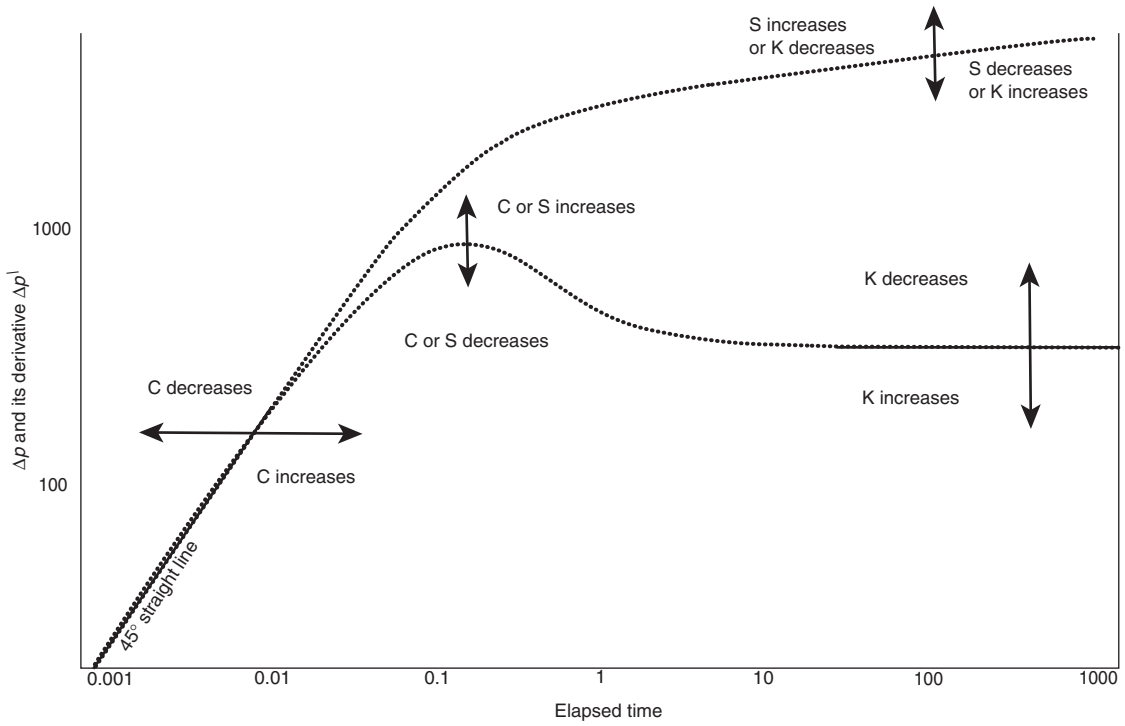

Figure 1.59 *Δ p and its derivative vs. elapsed time.*

- It clearly differentiates between responses of various reservoir models; such as:
  - dual-porosity behavior;
  - naturally and hydraulically fractured reservoirs;
  - closed boundary systems;
  - constant pressure boundaries;
  - faults and impermeable boundaries;
  - infinite acting systems
- It identifies various reservoir behavior and conditions that are not apparent in the traditional well analysis approach.
- It defines a clear recognizable pattern of various flow periods.
- It improves the overall accuracy of test interpretation.
- It provides an accurate estimation of relevant reservoir parameters.

Al-Ghamdi and Issaka (2001) pointed out that there are three major difficulties during the process of identifying the proper interpretation model:

(1) The limited number of available interpretation models that is restricted to prespecified setting and idealized conditions.
(2) The limitation of the majority of existing heterogeneous reservoir models to one type of heterogeneities and its ability to accommodate multiple heterogeneities within the same model.
(3) The non-uniqueness problem where identical responses are generated by completely different reservoir models of totally different geological configuration.

Lee (1982) suggested that the best approach of identifying the correct interpretation model incorporates the following three plotting techniques:

(1) The traditional log–log type curve plot of pressure difference Δp versus time.
(2) The derivative type curve.
(3) The "specialized graph" such as the Horner plot for a homogeneous system among other plots.

Based on knowledge of the shape of different flow regimes, the double plot of pressure and its derivative is used to diagnose the system and choose a well/reservoir model to match the well test data. The specialized plots can then be used to confirm the results of the pressure-derivative type curve match. Therefore, after reviewing and checking the quality of the test raw data, the analysis of well tests can be divided into the following two steps:

(1) The reservoir model identification and various flow regimes encountered during the tests are determined.
(2) The values of various reservoir and well parameters are calculated.

1.5.1 Model identification

The validity of the well test interpretation is totally dependent on two important factors, the accuracy of the measured field data and the applicability of the selected interpretation model. Identifying the correct model for analyzing the well test data can be recognized by plotting the data in several formats to eliminate the ambiguity in model selection. Gringarten (1984) pointed out that the interoperation model consists of three main components that are independent of each other and dominate at different times during the test and they follow the chronology of the pressure response. These are:

(I) *Inner boundaries*. Identification of the inner boundaries is performed on the early-time test data. There are only five possible inner boundaries and flow conditions in and around the wellbore:
  (1) wellbore storage;
  (2) skin;
  (3) phase separation;

(4) partial penetration;
(5) fracture.

(II) *Reservoir behavior*. Identification of the reservoir is performed on the middle-time data during the infinite acting behavior and includes two main types:
(1) homogeneous;
(2) heterogeneous.

(III) *Outer boundaries*. Identification of the outer boundaries is performed on the late-time data. There are two outer boundaries:
(1) no-flow boundary;
(2) constant-pressure boundary.

Each of the above three components exhibits a distinctly different characteristic that can be identified separately, and described by different mathematical forms.

1.5.2 Analysis of early-time test data

Early-time data is meaningful and can be used to obtain unparalleled information on the reservoir around the wellbore. During this early-time period, wellbore storage, fractures, and other inner boundary flow regimes are the dominant flowing conditions and exhibit a distinct different behavior. These inner boundary conditions and their associated flow regimes are briefly discussed below.

Wellbore storage and skin

The most effective procedure for analyzing and understanding the entire recorded transient well test data is by employing the log–log plot of the pressure difference Δp and its derivative $\Delta p'$ versus elapsed time. Identification of the inner boundaries is performed on early-time test data and starts with the wellbore storage. During this time when the wellbore storage dominates, Δp and its derivative $\Delta p'$ are proportional to the elapsed time and produce a 45° straight line on the log–log plot, as shown in Figure 1.59. On the derivative plot, the transition from the wellbore storage to the infinite-acting radial flow gives a "hump" with a maximum that indicates wellbore damage (positive skin). Conversely, the absence of a maximum indicates a non-damaged or stimulated well.

Phase separation in tubing

Stegemeier and Matthews (1958), in a study of anomalous pressure buildup behavior, graphically illustrated and discussed the effects of several reservoir conditions on the Horner straight-line plot, as shown in Figure 1.60. The problem occurs when gas and oil are segregated in the tubing and annulus during shut-in, which can cause the wellbore pressure to increase. This increase in the pressure could exceed the reservoir pressure and force the liquid to flow back into the formation with a resulting decrease in the wellbore pressure. Stegemeier and Matthews investigated this "humping" effect, as shown in Figure 1.60, which means that bottom-hole pressure builds up to a maximum and then decreases. They attributed this behavior to the rise of bubbles of gas and the redistribution of fluids within the wellbore. Wells which show the humping behavior have the following characteristics:

- They are completed in moderately permeable formations with a considerable skin effect or restriction to flow near the wellbore.
- The annulus is packed off.

The phenomenon does not occur in tighter formations because the production rate is small and thus there is ample space for the segregated gas to move into and expand. Similarly, if there is no restriction to flow near the wellbore, fluid can flow easily back into the formation to equalize the pressure and prevent humping. If the annulus is not packed off, bubble rise in the tubing will simply unload liquid into the casing–tubing annulus rather than displace the fluid back into the formation.

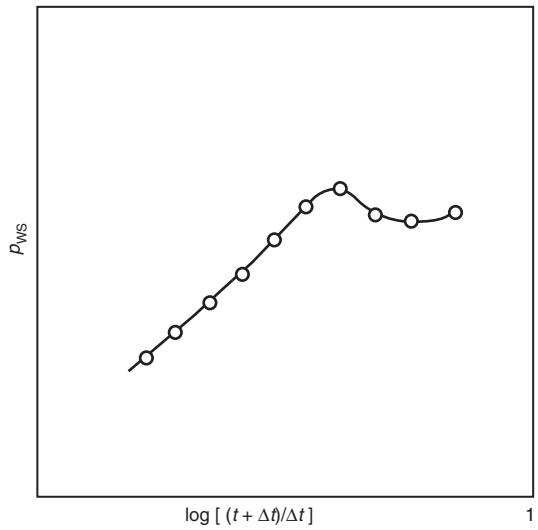

Figure 1.60 *Phase separation in tubing (After Stegemeier and Matthews, 1958).*

Stegemeier and Matthews also showed how *leakage through the wellbore* between dually completed zones at different pressure can cause an anomalous hump in measured pressures. When this leakage this occurs, the pressure differential between zones becomes small, allowing fluid to flow, and causes a hump in the pressure observed in the other zone.

Effect of partial penetration

Depending on the type of wellbore completion configuration, it is possible to have spherical or hemispherical flow near the wellbore. If the well penetrates the reservoir for a short distance below the cap rock, the flow will be hemispherical. When the well is cased through a thick pay zone and only a small part of the casing is perforated, the flow in the immediate vicinity of the wellbore will be spherical. Away from the wellbore, the flow is essentially radial. However, for a short duration of transient test, the flow will remain spherical during the test.

In the case of a pressure buildup test of a partially depleted well, Culham (1974) described the flow by the following expression:

$$p_i - p_{ws} = \frac{2453QB\mu}{k^{2/3}}\left[\frac{1}{\sqrt{\Delta t}} - \frac{1}{\sqrt{t_p + \Delta t}}\right]$$

This relationship suggests that a plot of $(p_i - p_{ws})$ vs. $[1/\sqrt{\Delta t} - 1/\sqrt{t_p + \Delta t}]$ on a Cartesian scale would be a straight line that passes through the origin with a slope of m as given by:

For spherical flow $$m = \frac{2453QB\mu}{k^{2/3}}$$

For hemispherical flow $$m = \frac{1226QB\mu}{k^{2/3}}$$

with the *total* skin factor s defined by:

$$s = 34.7 r_{ew}\sqrt{\frac{\phi\mu c_t}{k}}\left[\frac{(p_{ws})_{\Delta t} - p_{wf \text{ at } \Delta t=0}}{m} + \frac{1}{\sqrt{\Delta t}}\right] - 1$$

The dimensionless parameter r_{ew} is given by:

For spherical flow $$r_{ew} = \frac{h_p}{2\ln(h_p/r_w)}$$

For hemispherical flow $$r_{ew} = \frac{h_p}{\ln(2h_p/r_w)}$$

where:

$(p_{ws})_{\Delta t}$ = the shut-in pressure at any shut-in time Δt, hours
h_p = perforated length, ft
r_w = wellbore radius, ft

An important factor in determining the partial penetration skin factor is the ratio of the horizontal permeability k_h to the vertical permeability k_v, i.e., k_h/k_v. If the vertical permeability is small, the well will tend to behave as if the formation thickness h is equal to the completion thickness h_P. When the vertical permeability is high, the effect of the partial penetration is to introduce an extra pressure drop near the wellbore. This extra pressure drop will cause a large positive skin factor or smaller apparent wellbore radius when analyzing well test data. Similarly, opening only a few holes in the casing can also cause additional skin damage. Saidikowski (1979) indicated that the total skin factor s as calculated from a pressure transient test is related to the true skin factor caused by formation damage s_d and skin factor due to partial penetration s_P by the following relationship:

$$s = \left(\frac{h}{h_P}\right) s_d + s_P$$

Saidikowski estimated the skin factor due to partial penetration from the following expression:

$$s_P = \left(\frac{h}{h_P} - 1\right)\left[\ln\left(\frac{h}{r_w}\sqrt{\frac{k_h}{k_v}}\right) - 2\right]$$

where:

r_w = wellbore radius, ft
h_p = perforated interval, ft
h = total thickness, ft
k_h = horizontal permeability, md
k_v = vertical permeability, md

1.5.3 Analysis of middle-time test data

Identification of the basic reservoir characteristics is performed during the reservoir infinite-acting period and by using the middle-time test data. Infinite-acting flow occurs after the inner boundary effects have disappeared (e.g., wellbore storage, skin, etc.) and before the outer boundary effects have been felt. Gringarten et al. (1979) suggested that all reservoir behaviors can be classified as homogeneous or heterogeneous systems. The homogeneous system is described by only one porous medium that can be characterized by average rock properties through the conventional well testing approach. Heterogeneous systems are subclassified into the following two categories:

(1) double porosity reservoirs;
(2) multilayered or double-permeability reservoirs.

A brief discussion of the above two categories is given below.

Naturally fractured (double-porosity) reservoirs

Naturally fractured reservoirs are typically characterized by a double-porosity behavior; a primary porosity that represents the matrix ϕ_m and a secondary porosity ϕ_f that represents the fissure system. Basically, "fractures" are created hydraulically for well stimulation while "fissures" are considered natural fractures. The double- or dual-porosity model assumes two porous regions of distinctly different porosities and permeabilities within the formation. Only one, the "fissure system," has a permeability k_f high enough to produce to the well. The matrix system does not produce directly to the well but acts as a source of fluid to the fissure system. A very important characteristic of the double-porosity system is the nature of the fluid exchange between the two distinct porous systems. Gringarten (1984) presented a comprehensive treatment and an excellent review of the behavior of fissured reservoirs and the appropriate methodologies of analyzing well test data.

Warren and Root (1963) presented extensive theoretical work on the behavior of naturally fractured reservoirs. They assumed that the formation fluid flows from the matrix system into the fractures under pseudosteady-state conditions with the fractures acting like conduits to the wellbore. Kazemi (1969) proposed a similar model with the main assumption that the interporosity flow occurs under transient flow. Warren and Root indicated that two characteristic parameters, in addition to permeability and skin, control the behavior of double-porosity systems. These are:

(1) The dimensionless parameter ω that defines the storativity of the fractures as a ratio to that of the total reservoir. Mathematically, it is given by:

$$\omega = \frac{(\phi h c_t)_f}{(\phi h c_t)_{f+m}} = \frac{(\phi h c_t)_f}{(\phi h c_t)_f + (\phi h c_t)_m} \quad [1.5.8]$$

where:

ω = storativity ratio
h = thickness
c_t = total compressibility, psi^{-1}
ϕ = porosity

The subscripts f and m refer to the fissure and matrix respectively. A typical range of ω is 0.1 to 0.001.

(2) The second parameter λ is the interporosity flow coefficient which describes the ability of the fluid to flow from the matrix into the fissures and is defined by the following relationship:

$$\lambda = \alpha\left(\frac{k_m}{k_f}\right) r_w^2 \quad [1.5.9]$$

where:

λ = interporosity flow coefficient
k = permeability
r_w = wellbore radius

The factor α is the block-shape parameter that depends on the geometry and the characteristic shape of the matrix–fissures system and has the dimension of a reciprocal of the area defined by the following expression:

$$\alpha = \frac{A}{Vx}$$

where:

A = surface area of the matrix block, ft^2
V = volume of the matrix block
x = characteristic length of the matrix block, ft

Most of the proposed models assume that the matrix–fissures system can be represented by one the following four geometries:

(a) *Cubic* matrix blocks separated by fractures with λ as given by:

$$\lambda = \frac{60}{l_m^2}\left(\frac{k_m}{k_f}\right) r_w^2$$

where l_m is the length of a block side.

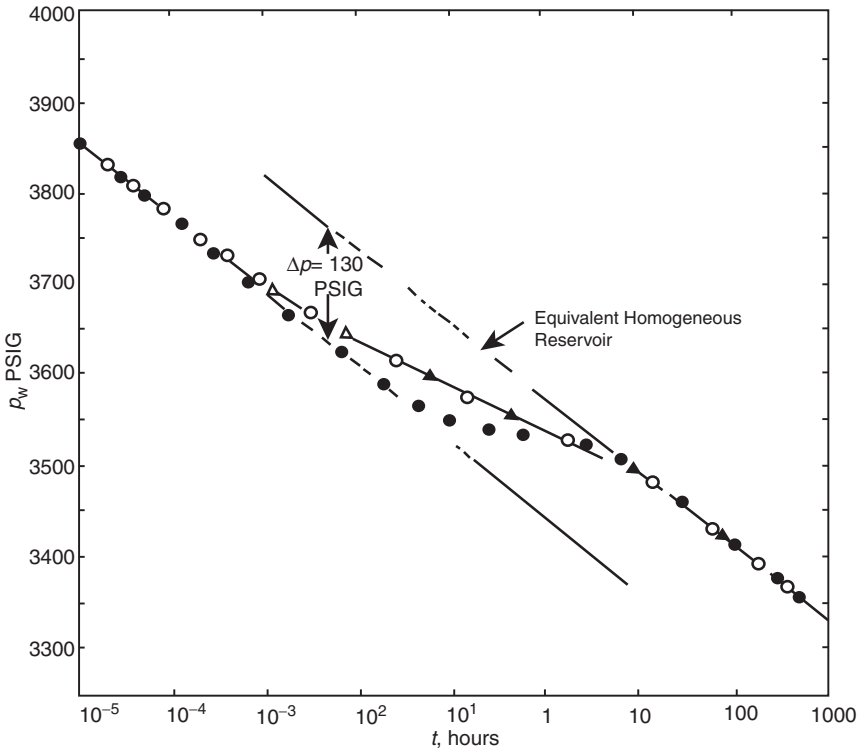

Figure 1.61 *Pressure drawdown according to the model by Warren and Root (Copyright ©1969 SPE, Kazemi, SPEJ, Dec. 1969).*

(b) *Spherical* matrix blocks separated by fractures with λ as given by:

$$\lambda = \frac{15}{r_m^2}\left(\frac{k_m}{k_f}\right) r_w^2$$

where r_m is the radius of the sphere.

(c) *Horizontal strata* (rectangular slab) matrix blocks separated by fractures with λ as given by:

$$\lambda = \frac{12}{h_f^2}\left(\frac{k_m}{k_f}\right) r_w^2$$

where h_f is the thickness of an individual fracture or high-permeability layer.

(d) *Vertical cylinder* matrix blocks separated by fractures with λ as given by:

$$\lambda = \frac{8}{r_m^2}\left(\frac{k_m}{k_f}\right) r_w^2$$

where r_m is the radius of the each cylinder

In general, the value of the interporosity flow parameter ranges between 10^{-3} and 10^{-9}. Cinco and Samaniego (1981) identified the following extreme interporosity flow conditions:

- Restricted interporosity flow which corresponds to a high skin between the least permeable media (matrix) and the highest permeable media (fissures) and is mathematically equivalent to the pseudosteady-state solution, i.e., the Warren and Root model.
- Unrestricted interporosity flow that corresponds to zero skin between the most and highest permeable media and is described be the unsteady-state (transient) solution.

Warren and Root proposed the first identification method of the double-porosity system, as shown by the drawdown semilog plot of Figure 1.61. The curve is characterized by *two parallel straight lines* due to the two separate porosities in the reservoir. Because the secondary porosity (fissures) has the greater transmissivity and is connected to the wellbore, it responds first as described by the first semilog straight line. The primary porosity (matrix), having a much lower transmissivity, responds much later. The combined effect of the two porosities gives rise to the second semilog straight line. The two straight lines are separated by a transition period during which the pressure tends to stabilize.

The first straight line reflects the transient radial flow through the fractures and, thus, *its slope is used to determine the system permeability–thickness product*. However, because the fracture storage is small, the fluid in the fractures is quickly depleted with a combined rapid pressure decline in the fractures. This pressure drop in the fracture allows more fluid to flow from the matrix into the fractures, which causes a slowdown in the pressure decline rate (as shown in Figure 1.61 by the transition period). As the matrix pressure approaches the pressure of the fractures, the pressure is stabilized in the two systems and yields the *second semilog straight line*. It should be pointed out that the first semilog straight line may be shadowed by wellbore storage effects and might not be recognized. Therefore, in practice, only parameters characterizing the homogeneous behavior of the *total* system $k_f h$ can be obtained.

Figure 1.62 shows the pressure buildup data for a naturally fractured reservoir. As for the drawdown, wellbore storage effects may obscure the first semilog straight line. If both semilog straight lines develop, analysis of the total permeability–thickness product is estimated from the slope m of either straight line and the use of Equation 1.3.8, or:

$$(k_f h) = \frac{162.6QB\mu}{m}$$

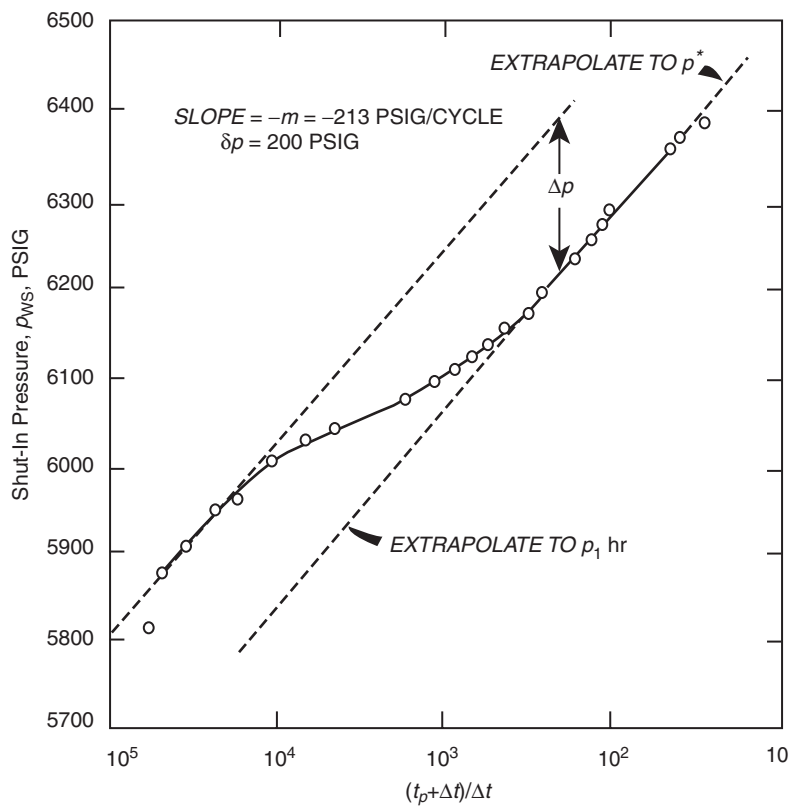

Figure 1.62 *Buildup curve from a fractured reservoir (After Warren and Root, 1963).*

The skin factor s and the false pressure p^* are calculated as described by using the *second straight line*. Warren and Root indicated that the storativity ratio ω can be determined from the vertical displacement between the two straight lines, identified as Δp in Figures 1.61 and 1.62, by the following expression:

$$\omega = 10^{(-\Delta p/m)} \qquad [1.5.10]$$

Bourdet and Gringarten (1980) indicated that by drawing a horizontal line through the *middle* of the transition curve to intersect with both semilog straight lines, as shown in Figures 1.61 and 1.62, the interporosity flow coefficient λ can be determined by reading the corresponding time at the *intersection* of either of the two straight lines, e.g. t_1 or t_2, and applying the following relationships:

In drawdown tests:

$$\lambda = \left[\frac{\omega}{1-\omega}\right]\left[\frac{(\phi h c_t)_m \mu r_w^2}{1.781 k_f t_1}\right] = \left[\frac{1}{1-\omega}\right]\left[\frac{(\phi h c_t)_m \mu r_w^2}{1.781 k_f t_2}\right] \qquad [1.5.11]$$

In buildup tests:

$$\lambda = \left[\frac{\omega}{1-\omega}\right]\left[\frac{(\phi h c_t)_m \mu r_w^2}{1.781 k_f t_p}\right]\left(\frac{t_p+\Delta t}{\Delta t}\right)_1$$

or:

$$\lambda = \left[\frac{1}{1-\omega}\right]\left[\frac{(\phi h c_t)_m \mu r_w^2}{1.781 k_f t_p}\right]\left(\frac{t_p+\Delta t}{\Delta t}\right)_2 \qquad [1.5.12]$$

where:

k_f = permeability of the fracture, md
t_p = producing time before shut-in, hours
r_w = wellbore radius, ft
μ = viscosity, cp

The subscripts 1 and 2 (e.g., t_1) refer to the first and second line time intersection with the horizontal line drawn through the middle of the transition region pressure response during drawdown or buildup tests.

The above relationships indicate that the value of λ is dependent on the value of ω. Since ω is the ratio of fracture to matrix storage, as defined in terms of the *total* isothermal compressibility coefficients of the matrix and fissures by Equation 1.5.8, thus:

$$\omega = \frac{1}{1+\left[\dfrac{(\phi h)_m}{(\phi h)_f}\dfrac{(c_t)_m}{(c_t)_f}\right]}$$

it suggests that ω is also dependent on the *PVT* properties of the fluid. It is quite possible for the oil contained in the fracture to be below the bubble point while the oil contained in the matrix is above the bubble point. Thus, ω is pressure dependent and, therefore, λ is greater than 10, so the level of heterogeneity is insufficient for dual porosity effects to be of importance and the reservoir can be treated with a single porosity.

Example 1.34 The pressure buildup data as presented by Najurieta (1980) and Sabet (1991) for a double-porosity system is tabulated below:

Δt (hr)	p_{ws} (psi)	$\frac{t_p+\Delta t}{\Delta t}$
0.003	6617	31 000 000
0.017	6632	516 668

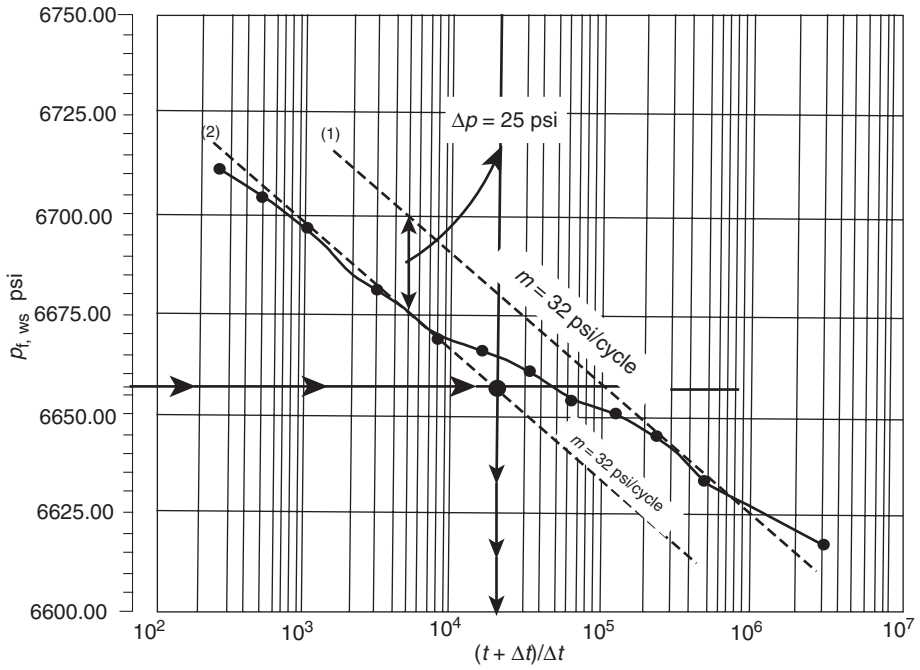

Figure 1.63 *Semilog plot of the buildup test data (After Sabet, M. A.* Well Test Analysis *1991, Gulf Publishing Company).*

Δt (hr)	p_{ws} (psi)	$\frac{t_p+\Delta t}{\Delta t}$
0.033	6644	358 334
0.067	6650	129 168
0.133	6654	64 544
0.267	6661	32 293
0.533	6666	16 147
1.067	6669	8 074
2.133	6678	4 038
4.267	6685	2 019
8.533	6697	1 010
17.067	6704	506
34.133	6712	253

The following additional reservoir and fluid properties are available:

$p_i = 6789.5$ psi, $p_{wf \text{ at } \Delta t=0} = 6352$ psi,

$Q_o = 2554$ STB/day, $B_o = 2.3$ bbl/STB,

$\mu_o = 1$ cp, $t_p = 8611$ hours

$r_w = 0.375$ ft, $c_t = 8.17 \times 10^{-6}$ psi^{-1}, $\phi_m = 0.21$

$k_m = 0.1$ md, $h_m = 17$ ft

Estimate ω and λ.

Solution

Step 1. Plot p_{ws} vs. $(t_p + \Delta t)/\Delta t$ on a semilog scale as shown in Figure 1.63.

Step 2. Figure 1.63 shows two parallel semilog straight lines with a slope of $m = 32$ psi/cycle.

Step 3. Calculate $(k_f h)$ from the slope m:

$$(k_f h) = \frac{162.6 Q_o B_o \mu_o}{m} = \frac{162.6(2556)(2.3)(1.0)}{32}$$
$$= 29\,848.3 \text{ md ft}$$

and:

$$k_f = \frac{29848.3}{17} = 1756 \text{ md}$$

Step 4. Determine the vertical distance Δp between the two straight lines:

$$\Delta p = 25 \text{ psi}$$

Step 5. Calculate the storativity ratio ω from Equation 1.5.10:

$$\omega = 10^{-(\Delta p/m)} = 10^{-(25/32)} = 0.165$$

Step 6. Draw a horizontal line through the middle of the transition region to intersect with the two semilog straight lines. Read the corresponding time at the second intersection, to give:

$$\left(\frac{t_p + \Delta t}{\Delta t}\right)_2 = 20000$$

Step 7. Calculate λ from Equation 1.5.12:

$$\lambda = \left[\frac{1}{1-\omega}\right]\left[\frac{(\phi h c_t)_m \mu r_w^2}{1.781 k_f t_p}\right]\left(\frac{t_p + \Delta t}{\Delta t}\right)_2$$
$$= \left[\frac{1}{1-0.165}\right]$$
$$\times \left[\frac{(0.21)(17)(8.17 \times 10^{-6})(1)(0.375)^2}{1.781(1756)(8611)}\right](20000)$$
$$= 3.64 \times 10^{-9}$$

It should be noted that pressure behavior in a naturally fractured reservoir is similar to that obtained in a *layered reservoir with no crossflow*. In fact, in any reservoir system with two predominant rock types, the pressure buildup behavior is similar to that of Figure 1.62.

Gringarten (1987) pointed out that the two straight lines on the semilog plot may or may not be present depending

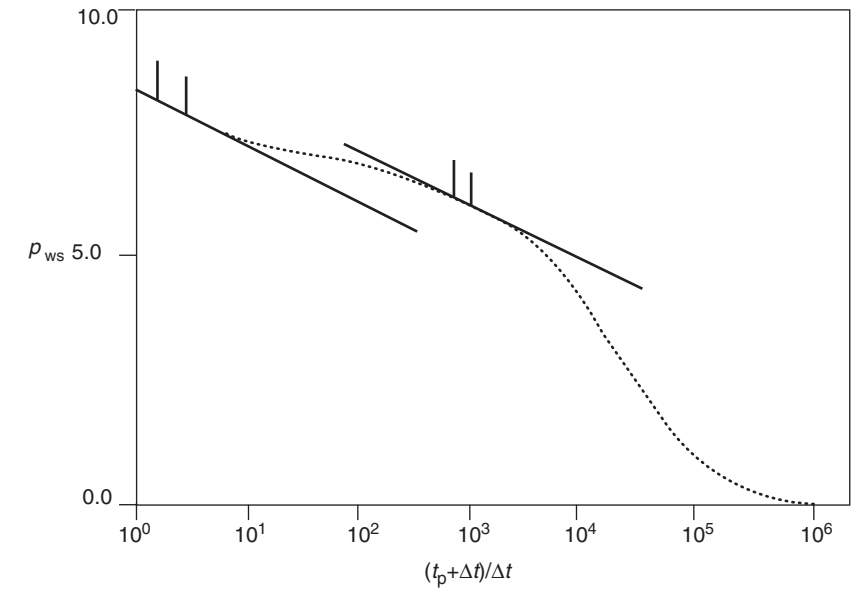

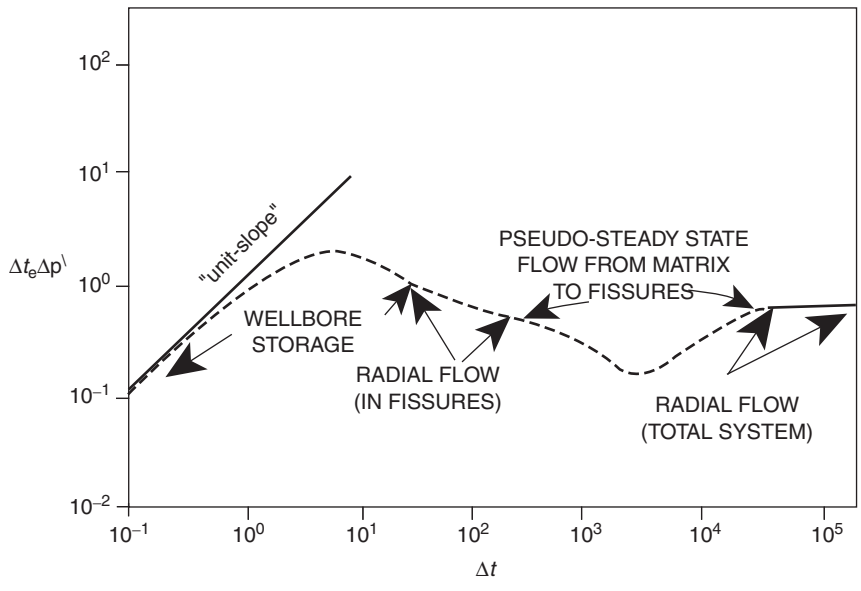

Figure 1.64 *Dual-porosity behavior shows as two parallel semilog straight lines on a semilog plot, as a minimum on a derivative plot.*

on the condition of the well and duration of the test. He concluded that the semilog plot is not an efficient or sufficient tool for identifying double-porosity behavior. In the log–log plot, as shown in Figure 1.62, the double-porosity behavior yields an S-shaped curve. The *initial portion* of the curve represents the homogeneous behavior resulting from depletion in the most permeable medium, e.g., fissures. A *transition period* follows and corresponds to the interporosity flow. Finally, the *last portion* represents the homogeneous behavior of both media when recharge from the least permeable medium (matrix) is fully established and pressure is equalized. The log–log analysis represents a significant improvement over conventional semilog analysis for identifying double-porosity behavior. However, S-shape behavior is difficult to see in highly damaged wells and well behavior can then be erroneously diagnosed as homogeneous. Furthermore, a similar S-shape behavior may be found in irregularly bounded well drainage systems.

Perhaps the most efficient means for identifying double-porosity systems is the use of the pressure derivative plot. It allows unambiguous identification of the system, provided that the quality of the pressure data is adequate and, more importantly, an accurate methodology is used in calculating pressure derivatives. As discussed previously, the pressure derivative analysis involves a log–log plot of the derivative of the pressure with respect to time versus elapsed time. Figure 1.64 shows the combined log–log plot of pressure and derivative versus time for a dual-porosity system. The derivative plot shows a “minimum” or a “dip” on the pressure derivative curve caused by the interporosity flow during the transition period. The “minimum” is between two horizontal lines; the first represents the radial flow controlled by

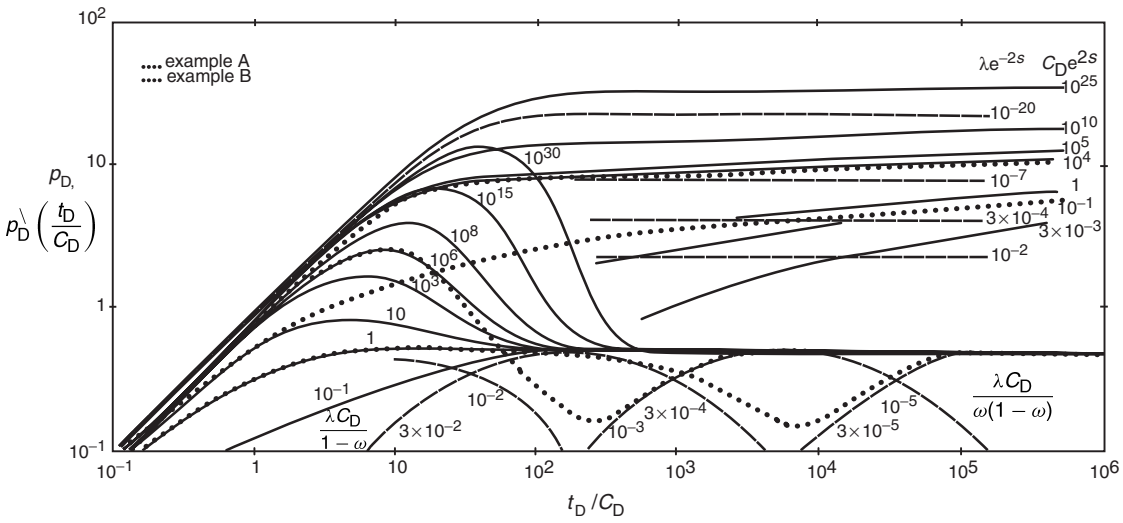

Figure 1.65 *Type curve matching (Copyright ©1984 World Oil, Bourdet et al., April 1984).*

the fissures and the second describes the combined behavior of the double-porosity system. Figure 1.64 shows, at early time, the typical behavior of wellbore storage effects with the deviation from the 45° straight line to a maximum representing a wellbore damage. Gringarten (1987) suggested that the shape of the minimum depends on the double-porosity behavior. For a restricted interporosity flow, the minimum takes a V-shape, whereas unrestricted interporosity yields an open U-shaped minimum.

Based on Warren and Root's double-porosity theory and the work of Mavor and Cinco (1979), Bourdet and Gringarten (1980) developed specialized pressure type curves that can be used for analyzing well test data in dual-porosity systems. They showed that double-porosity behavior is controlled by the following independent variables:

- p_D
- t_D/C_D
- $C_D e^{2s}$
- ω
- λe^{-2s}

with the dimensionless pressure p_D and time t_D as defined below:

$$p_D = \left[\frac{k_f h}{141.2QB\mu}\right]\Delta p$$

$$t_D = \frac{0.0002637k_f t}{[(\phi\mu c_t)_f + (\phi\mu c_t)_m]\mu r_w^2} = \frac{0.0002637k_f t}{(\phi\mu c_t)_{f+m}\mu r_w^2}$$

where:

k = permeability, md
t = time, hours
μ = viscosity, cp
r_w = wellbore radius, ft

and subscripts:

f = fissure
m = matrix
f + m = total system
D = dimensionless

Bourdet et al. (1984) extended the practical applications of these curves and enhanced their use by introducing the pressure derivative type curves to the solution. They developed two sets of pressure derivative type curves as shown in Figures 1.65 and 1.66. The first set, i.e., Figure 1.65, is based on the assumption that the interporosity flow obeys the pseudosteady-state flowing condition and the other set (Figure 1.66) assumes transient interporosity flow. The use of either set involves plotting the pressure difference Δp and the derivative function, as defined by Equation 1.5.4 for drawdown tests or Equation 1.5.5 for buildup tests, versus time with same size log cycles as the type curve. The controlling variables in each of the two type curve sets are given below.

First type curve set: *pseudo steady-state interporosity flow* The actual *pressure response*, i.e., pressure difference Δp, is described by the following three component curves:

(1) At early times, the flow comes from the fissures (most permeable medium) and the actual pressure difference plot, i.e., Δp curve, matches one of the homogeneous curves that is labeled $(C_D e^{2s})$ with a corresponding value of $(C_D e^{2s})_f$ that describes the *fissure flow*. This value is designated as $[(C_D e^{2s})_f]_M$.
(2) As the pressure difference response reaches the transition regime, Δp deviates from the $C_D e^{2s}$ curve and follows one of the transition curves that describes this flow regime by λe^{-2s}, designated as $[\lambda e^{-2s}]_M$.
(3) Finally, the pressure difference response leaves the transition curve and matches a new $C_D e^{2s}$ curve below the first one with a corresponding value of $(C_D e^{2s})_{f+m}$ that describes the *total system* behavior, i.e., matrix and fissures. This value is recorded as $[(C_D e^{2s})_{f+m}]_M$.

On the pressure derivative response, the storativity ratio ω defines the shape of the derivative curve during the transition regime that is described by a "depression" or a "minimum." The duration and depth of the depression are linked by the value of ω; a small ω produces a long and therefore deep transition. The interporosity coefficient λ is the second parameter defining the position of the time axis of the transition regime. A decrease of λ value moves the depression to the right side of the plot.

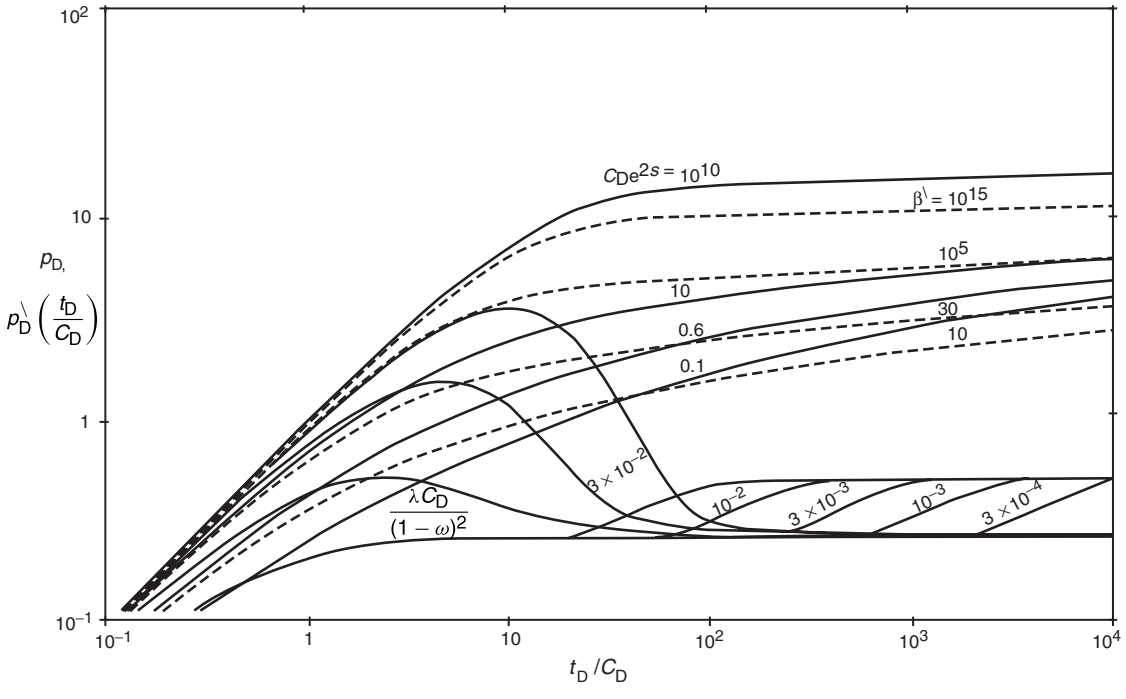

Figure 1.66 *Type curve matching (Copyright ©1984 World Oil, Bourdet et al., April 1984).*

As shown in Figure 1.65, the pressure derivative plots match on four component curves:

(1) The derivative curve follows the fissure flow curve $[(C_De^{2s})_f]_M$.
(2) The derivative curve reaches an early transition period, expressed by a depression and described by an early transition curve $[\lambda(C_D)_{f+m}/\omega(1-\omega)]_M$.
(3) The derivative pressure curve then matches a late transition curve labeled $[\lambda(C_D)_{f+m}/(1-\omega)]_M$.
(4) The total system behavior is reached on the 0.5 line.

Second type curve set: *transient interporosity flow* As developed by Bourdet and Gringarten (1980) and expanded by Bourdet et al. (1984) to include the pressure derivative approach, this type curve is built in the same way as for the pseudosteady-state interporosity flow. As shown in Figure 1.66, the pressure behavior is defined by three component curves, $(C_De^{2s})_f$, $\beta^{\backslash}$, and $(C_De^{2s})_{f+m}$. The authors defined $\beta^{\backslash}$ as the interporosity dimensionless group and given by:

$$\beta^{\backslash} = \delta\left[\frac{(C_De^{2s})_{f+m}}{\lambda^{e-2s}}\right]$$

where the parameter δ is the shape coefficient with assigned values as given below:

$\delta = 1.0508$ for spherical blocks
$\delta = 1.8914$ for slab matrix blocks

As the first fissure flow is short-lived with transient interporosity flow models, the $(C_De^{2s})_f$ curves are not seen in practice and therefore have not been included in the derivative curves. The dual-porosity derivative response starts on the derivative of a $\beta^{\backslash}$ transition curve, then follows a late transition curve labeled $\lambda(C_D)_{f+m}/(1-\omega)^2$ until it reaches the total system regime on the 0.5 line.

Bourdet (1985) points out that the pressure derivative responses during the transition flow regime are very different between the two types of double-porosity model. With the transient interporosity flow solutions, the transition starts from early time and does not drop to a very low level. With pseudosteady-state interporosity flow, the transition starts later and the shape of the depression is much more pronounced. There is *no lower limit* for the depth of the depression when the flow from the matrix to the fissures follows the pseudosteady-state model, whereas for the interporosity transient flow the depth of the *depression does not exceed* 0.25.

In general, the matching procedure and reservoir parameters estimation as applied to the type-curve of Figure 1.66 can be summarized by the following steps:

Step 1. Using the actual well test data, calculate the pressure difference Δp and the pressure derivative plotting functions as defined by Equation 1.5.4 for drawdown or Equation 1.5.5 for buildup tests, i.e.,:
For drawdown tests:

The pressure difference $\Delta p = p_i - p_{wf}$

The derivative function $t\Delta p^{\backslash} = -t\left(\frac{d(\Delta p)}{d(t)}\right)$

For buildup tests:

The pressure difference $\Delta p = p_{ws} - p_{wf \text{ at } \Delta t=0}$

The derivative function $\Delta t_e \Delta p^{\backslash} = \Delta t\left(\frac{t_p + \Delta t}{\Delta t}\right)\left[\frac{d(\Delta p)}{d(\Delta t)}\right]$

Step 2. On tracing paper with the same size log cycles as in Figure 1.66, plot the data of step 1 as a function of flowing time t for drawdown tests or equivalent time Δt_e for buildup tests.

Step 3. Place the actual two sets of plots, i.e., Δp and derivative plots, on Figure 1.65 or Figure 1.66 and force a simultaneous match of the two plots to Gringarten–Bourdet type curves. Read the matched derivative curve $[\lambda(C_D)_{f+m}/(1-\omega)^2]_M$.

Step 4. Choose any point and read its coordinates on both Figures to give:

$$(\Delta p, p_D)_{MP} \quad \text{and} \quad (t \text{ or } \Delta t_e, t_D/C_D)_{MP}$$

Step 5. With the match still maintained, read the values of the curves labeled $(C_D e^{2s})$ which match the initial segment of the curve $[(C_D e^{2s})_f]_M$ and the final segment $[(C_D e^{2s})_{f+m}]_M$ of the data curve.

Step 6. Calculate the well and reservoir parameters from the following relationships:

$$\omega = \frac{[(C_D e^{2s})_{f+m}]_M}{[(C_D e^{2s})_f]_M} \qquad [1.5.13]$$

$$k_f h = 141.2QB\mu \left(\frac{p_D}{\Delta p}\right)_{MP} \text{ md ft} \qquad [1.5.14]$$

$$C = \left[\frac{0.000295 k_f h}{\mu}\right] \frac{(\Delta t)_{MP}}{(C_D/C_D)_{MP}} \qquad [1.5.15]$$

$$(C_D)_{f+m} = \frac{0.8926C}{\phi c_t h r_w^2} \qquad [1.5.16]$$

$$s = 0.5 \ln\left[\frac{[(C_D e^{2s})_{f+m}]_M}{(C_D)_{f+m}}\right] \qquad [1.5.17]$$

$$\lambda = \left[\frac{\lambda(C_D)_{f+m}}{(1-\omega)^2}\right]_M \frac{(1-\omega)^2}{(C_D)_{f+m}} \qquad [1.5.18]$$

The selection of the best solution between the pseudosteady-state and the transient interporosity flow is generally straightforward; with the pseudosteady-state model, the drop of the derivative during transition is a function of the transition duration. Long transition regimes, corresponding to small ω values, produce derivative levels much smaller than the practical 0.25 limit of the transient solution.

The following pressure buildup data as given by Bourdet et al. and reported conveniently by Sabet (1991) is used below as an example to illustrate the use of pressure derivative type curves.

Example 1.35 Table 1.8 shows the pressure buildup and pressure derivative data for a naturally fractured reservoir. The following flow and reservoir data is also given:

$$Q = 960 \text{ STB/day}, \quad B_o = 1.28 \text{ bbl/STB},$$
$$c_t = 1 \times 10^{-5} \text{ psi}^{-1}, \quad \phi = 0.007,$$
$$\mu = 1 \text{ cp}, \quad r_w = 0.29 \text{ ft}, \quad h = 36 \text{ ft}$$

It is reported that the well was opened to flow at a rate of 2952 STB/day for 1.33 hours, shut-in for 0.31 hours, opened again at the same rate for 5.05 hours, closed for 0.39 hours, opened for 31.13 hours at the rate of 960 STB/day, and then shut-in for the pressure buildup test.

Analyze the buildup data and determine the well and reservoir parameters assuming transient interporosity flow.

Solution

Step 1. Calculate the flowing time t_p as follows:

$$\text{Total oil produced} = N_P$$

$$= \frac{2952}{4}[1.33 + 5.05] + \frac{960}{24}31.13 \simeq 2030 \text{ STB}$$

$$t_p = \frac{(24)(2030)}{960} = 50.75 \text{ hours}$$

Table 1.8 *Pressure Buildup Test, Naturally Fractured Reservoir. After Sabet, M. A. "Well Test Analysis" 1991, Gulf Publishing Company*

Δt (hr)	Δp_{ws} (psi)	$\frac{t_p + \Delta t}{\Delta t}$	*Slope* (psi/hr)	$\Delta p \backslash \frac{t_p + \Delta t}{t_p}$ (psi)
0.00000E+00	0.000		3180.10	
3.48888E−03	11.095	14 547.22	1727.63	8.56
9.04446E−03	20.693	5 612.17	847.26	11.65
1.46000E−02	25.400	3 477.03	486.90	9.74
2.01555E−02	28.105	2 518.92	337.14	8.31
2.57111E−02	29.978	1 974.86	257.22	7.64
3.12666E−02	31.407	1 624.14	196.56	7.10
3.68222E−02	32.499	1 379.24	159.66	6.56
4.23777E−02	33.386	1 198.56	127.80	6.10
4.79333E−02	34.096	1 059.76	107.28	5.64
5.90444E−02	35.288	860.52	83.25	5.63
7.01555E−02	36.213	724.39	69.48	5.36
8.12666E−02	36.985	625.49	65.97	5.51
9.23777E−02	37.718	550.38	55.07	5.60
0.10349	38.330	491.39	48.83	5.39
0.12571	39.415	404.71	43.65	5.83
0.14793	40.385	344.07	37.16	5.99
0.17016	41.211	299.25	34.38	6.11
0.19238	41.975	264.80	29.93	6.21
0.21460	42.640	237.49	28.85	6.33
0.23682	43.281	215.30	30.96	7.12
0.25904	43.969	196.92	25.78	7.39
0.28127	44.542	181.43	24.44	7.10
0.30349	45.085	168.22	25.79	7.67
0.32571	45.658	156.81	20.63	7.61
0.38127	46.804	134.11	18.58	7.53
0.43682	47.836	117.18	17.19	7.88
0.49238	48.791	104.07	16.36	8.34
0.54793	49.700	93.62	15.14	8.72
0.60349	50.541	85.09	12.50	8.44
0.66460	51.305	77.36	12.68	8.48
0.71460	51.939	72.02	11.70	8.83
0.77015	52.589	66.90	11.14	8.93
0.82571	53.208	62.46	10.58	9.11
0.88127	53.796	58.59	10.87	9.62
0.93682	54.400	55.17	8.53	9.26
0.99238	54.874	52.14	10.32	9.54
1.04790	55.447	49.43	7.70	9.64
1.10350	55.875	46.99	8.73	9.26
1.21460	56.845	42.78	7.57	10.14
1.32570	57.686	39.28	5.91	9.17
1.43680	58.343	36.32	6.40	9.10
1.54790	59.054	33.79	6.05	9.93
1.65900	59.726	31.59	5.57	9.95
1.77020	60.345	29.67	5.44	10.08
1.88130	60.949	27.98	4.74	9.93
1.99240	61.476	26.47	4.67	9.75
2.10350	61.995	25.13	4.34	9.87
2.21460	62.477	23.92	3.99	9.62
2.43680	63.363	21.83	3.68	9.79
2.69240	64.303	19.85	3.06[a]	9.55[b]
2.91460	64.983	18.41	3.16	9.59
3.13680	65.686	17.18	2.44	9.34
3.35900	66.229	16.11	19.72	39.68

[a] $(64.983 - 64.303)/(2.9146 - 2.69240) = 3.08$.
[b] $[(3.68 + 3.06)/2] \times 19.85 \times 2.69240^2/50.75 = 9.55$.
Adapted from Bourdet et al. (1984).

Step 2. Confirm the double-porosity behavior by constructing the Horner plot as shown in Figure 1.67. The graph shows the two parallel straight lines confirming the dual-porosity system.

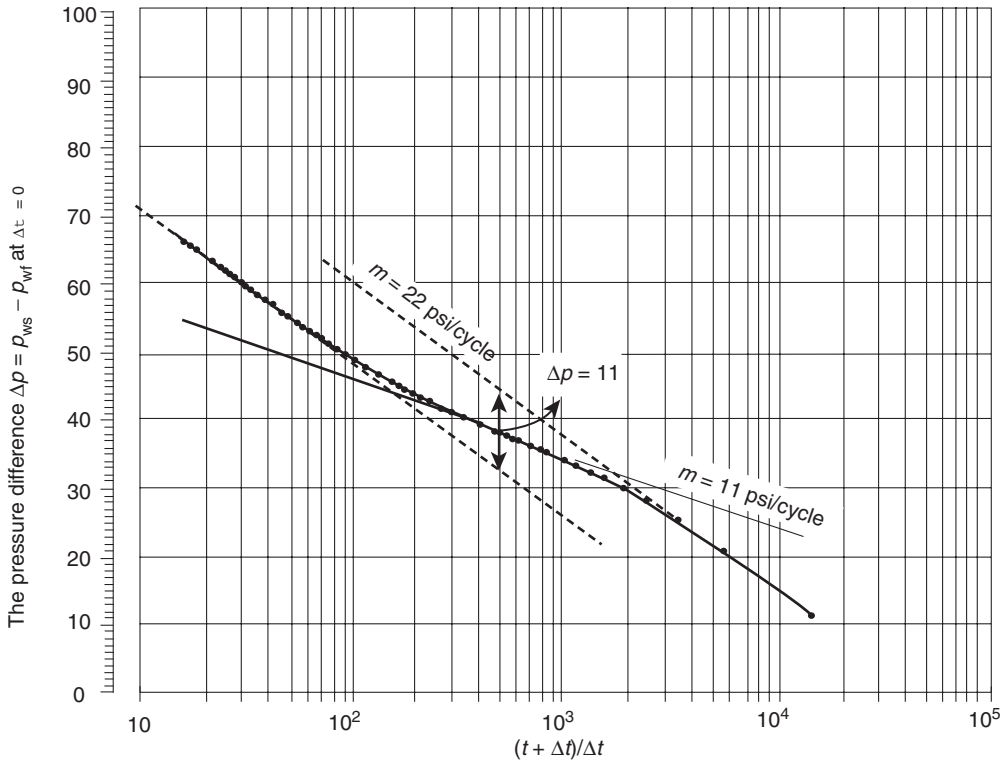

Figure 1.67 *The Horner plot; data from Table 1.8 (After Sabet, M. A.* Well Test Analysis *1991, Gulf Publishing Company).*

Step 3. Using the same grid system of Figure 1.66, plot the *actual pressure derivative* versus shut-in time as shown in Figure 1.68(a) and Δp_{ws} versus time (as shown in Figure 1.68(b)). The 45° line shows that the test was slightly affected by the wellbore storage.

Step 4. Overlay the pressure difference and pressure derivative plots over the transient interporosity type curve, as shown in Figure 1.69, to give the following matching parameters:

$$\left[\frac{p_D}{\Delta p}\right]_{MP} = 0.053$$

$$\left[\frac{t_D/C_D}{\Delta t}\right]_{MP} = 270$$

$$\left[\frac{\lambda(C_D)_{f+m}}{(1-\omega)^2}\right]_M = 0.03$$

$$[(C_D e^{2s})_f]_M = 33.4$$

$$[(C_D e^{2s})_{f+m}]_M = 0.6$$

Step 5. Calculate the well and reservoir parameters by applying Equations 1.5.13 through 1.5.18 to give:

$$\omega = \frac{[(C_D e^{2s})_{f+m}]_M}{[(C_D e^{2s})_f]_M} = \frac{0.6}{33.4} = 0.018$$

Kazemi (1969) pointed out that if the vertical separation between the two parallel slopes Δp is less the 100 psi, the calculation of ω by Equation 1.5.10 will produce a significant error in its values. Figure 1.67 shows that Δp is about 11 psi and Equation 1.5.10 gives an *erroneous value* of:

$$\omega = 10^{-(\Delta p/m)} = 10^{-(11/22)} = 0.316$$

Also:

$$k_f h = 141.2QB\mu \left(\frac{p_D}{\Delta p}\right)_{MP}$$

$$= 141.2(960)(1)(1.28)(0.053) = 9196 \text{ md ft}$$

$$C = \left[\frac{0.000295 k_f h}{\mu}\right] \frac{(\Delta t)_{MP}}{(C_D/C_D)_{MP}}$$

$$= \frac{(0.000295)(9196)}{(1.0)(270)} = 0.01 \text{ bbl/psi}$$

$$(C_D)_{f+m} = \frac{0.8926C}{\phi c_t h r_w^2}$$

$$= \frac{(0.8936)(0.01)}{(0.07)(1 \times 10^{-5})(36)90.29)^2} = 4216$$

$$s = 0.5 \ln\left[\frac{[(C_D e^{2s})_{f+m}]_M}{(C_D)_{f+m}}\right]$$

$$= 0.5 \ln\left[\frac{0.6}{4216}\right] = -4.4$$

$$\lambda = \left[\frac{\lambda(C_D)_{f+m}}{(1-\omega)^2}\right]_M \frac{(1-\omega)^2}{(C_D)_{f+m}}$$

$$= (0.03)\left[\frac{(1-0.018)^2}{4216}\right] = 6.86 \times 10^{-6}$$

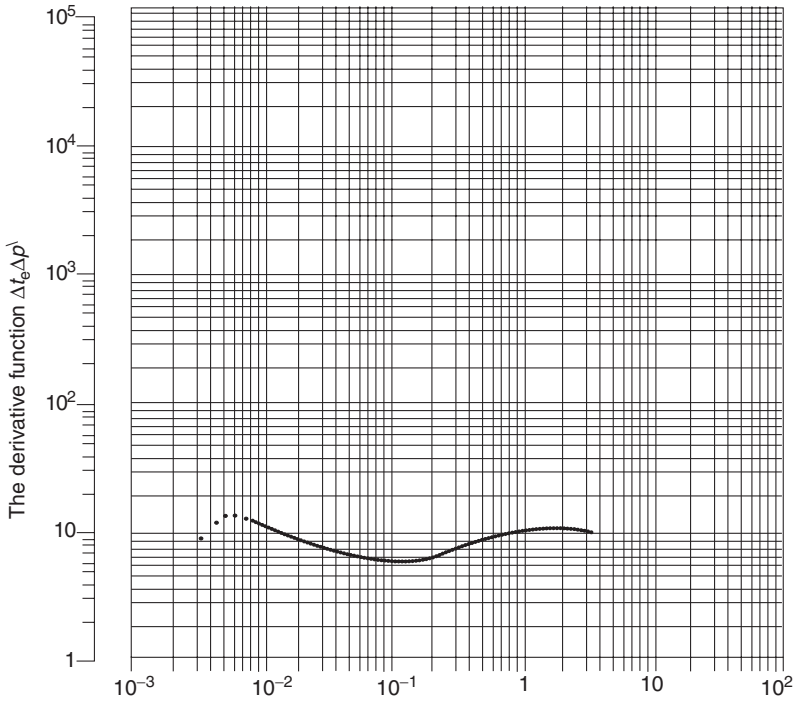

Figure 1.68(a) *Derivative function.*

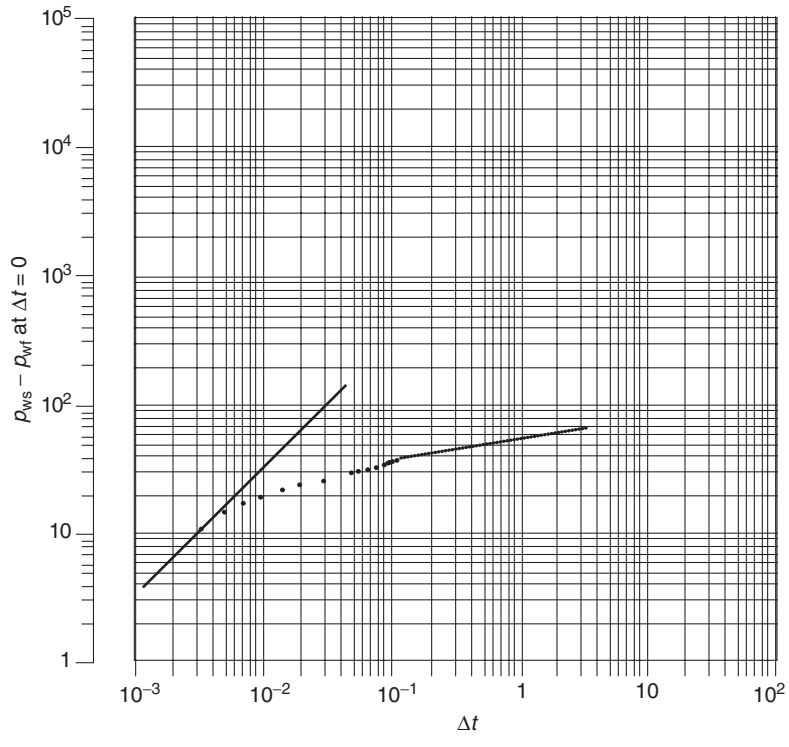

Figure 1.68(b) *Log–log plot of* Δ *p vs.* Δt_e *(After Sabet, M. A.* Well Test Analysis *1991, Gulf Publishing Company).*

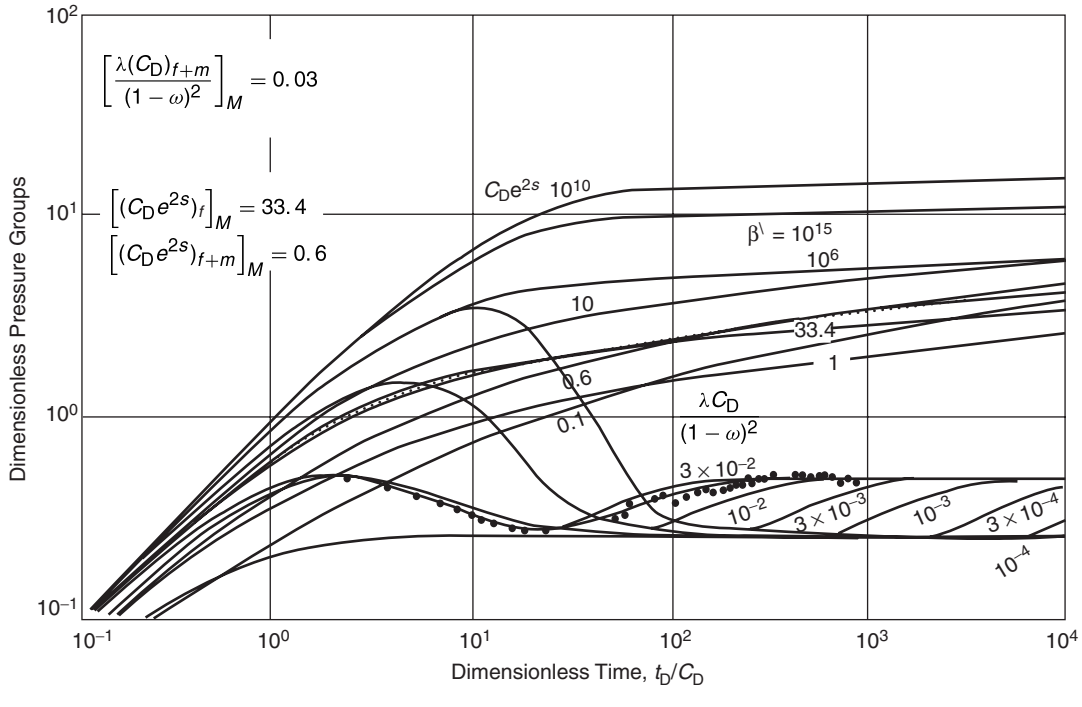

Figure 1.69 *Type curve matching (Copyright ©1984 World Oil, Bourdet et al., April 1984).*

Layered reservoirs

The pressure behavior of a no-crossflow multilayered reservoir with communication only at the wellbore will behave significantly different from a single-layer reservoir. Layered reservoirs can be classified into the following three categories:

(1) *Crossflow layered reservoirs* are those which communicate both in the wellbore and in the reservoir.
(2) *Commingled layered reservoirs* are those which communicate only in the wellbore. A complete permeability barrier exists between the various layers.
(3) *Composite reservoirs* are made up of commingled zones and some of the zones consist of crossflow layers. Each crossflow layer behaves on tests as if it were an homogeneous and isotropic layer; however, the composite reservoir should behave exactly as a commingled reservoir.

Some layered reservoirs behave as double-porosity reservoirs when in fact they are not. When reservoirs are characterized by layers of very low permeabilities interbedded with relatively thin high-permeability layers, they could behave on well tests exactly as if they were naturally fractured systems and could be treated with the interpretation models designed for double-porosity systems. Whether the well produces from a commingled, crossflow, or composite system, the test objectives are to determine skin factor, permeability, and average pressure.

The pressure response of crossflow layered systems during well testing is similar to that of homogeneous systems and can be analyzed with the appropriate conventional semilog and log–log plotting techniques. Results of the well test should be interpreted in terms of the arithmetic total permeability–thickness and porosity–compressibility–thickness products as given by:

$$(kh)_t = \sum_{i=1}^{n \text{ layers}} (kh)_i$$

$$(\phi c_t h)_t = \sum_{i=1}^{n \text{ layers}} (\phi c_t h)_i$$

Kazemi and Seth (1969) proposed that if the total permeability–thickness product $(kh)_t$ is known from a well test, the individual layer permeability k_i may be approximated from the layer flow rate q_i and the total flow rate q_t by applying the following relationship:

$$k_i = \frac{q_i}{q_t}\left[\frac{(kh)_t}{h_i}\right]$$

The pressure buildup behavior of a commingled two-layer system without crossflow is shown schematically in Figure 1.70. The straight line AB that follows the early-time data gives the proper value of the average flow capacity $(kh)_t$ of the reservoir system. The flattening portion BC analogous to a single-layer system attaining statistic pressure indicates that the pressure in the more permeable zone has almost reached its average value. The portion CD represents a repressurization of the more permeable layer by the less depleted, less permeable layer with a final rise DE at the stabilized average pressure. Notice that the buildup is somewhat similar to the buildup in naturally fractured reservoirs.

Sabet (1991) points out that when a commingled system is producing under the pseudosteady-state flow condition, the flow rate from any layer q_i can be approximated from total

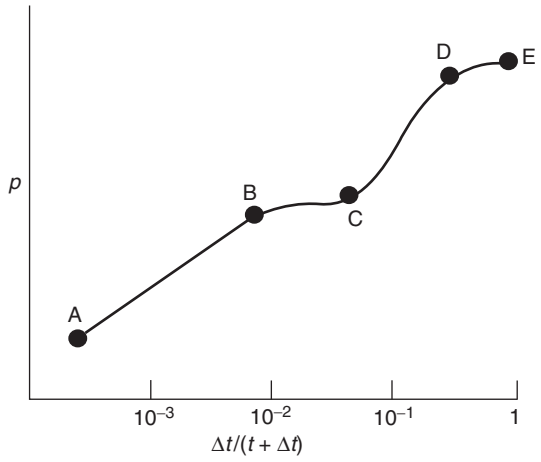

Figure 1.70 *Theoretical pressure buildup curve for two-layer reservoir (Copyright ©1961 SPE, Lefkovits et al., SPEJ, March 1961).*

flow rate and the layer storage capacity $\phi c_t h$ from:

$$q_i = q_t \left[\frac{(\phi c_t h)_i}{\sum_{j=1} (\phi c_t h_i)_j} \right]$$

1.5.4 Hydraulically fractured reservoirs

A fracture is defined as a single crack initiated from the wellbore by hydraulic fracturing. It should be noted that fractures are different from "fissures," which are the formation of natural fractures. Hydraulically induced fractures are usually vertical, but can be horizontal if the formation is less than approximately 3000 ft deep. Vertical fractures are characterized by the following properties:

- fracture half-length x_f, ft;
- dimensionless radius r_{eD}, where $r_{eD} = r_e/x_f$;
- fracture height h_f, which is often assumed equal to the formation thickness, ft;
- fracture permeability k_f, md;
- fracture width w_f, ft;
- fracture conductivity F_C, where $F_C = k_f w_f$.

The analysis of fractured well tests deals with the identification of well and reservoir variables that would have an impact on future well performance. However, fractured wells are substantially more complicated. The well-penetrating fracture has unknown geometric features, i.e., x_f, w_f, and h_f, and unknown conductivity properties.

Gringarten et al. (1974) and Cinco and Samaniego (1981), among others, propose three transient flow models to consider when analyzing transient pressure data from vertically fractured wells. These are:

(1) infinite conductivity vertical fractures;
(2) finite conductivity vertical fractures;
(3) uniform flux fractures.

Descriptions of the above three types of fractures are given below.

Infinite conductivity vertical fractures

These fractures are created by conventional hydraulic fracturing and characterized by a very high conductivity, which for all practical purposes can be considered as infinite. In this case, the fracture acts similar to a large-diameter pipe with *infinite permeability* and, therefore, there is essentially no pressure drop from the tip of the fracture to the wellbore, i.e., no pressure loss in the fracture. This model assumes that the flow into the wellbore is only through the fracture and exhibits three flow periods:

(1) fracture linear flow period;
(2) formation linear flow period;
(3) infinite-acting pseudoradial flow period.

Several specialized plots are used to identify the start and end of each flow period. For example, an early-time log–log plot of Δp vs. Δt will exhibit a straight line of half-unit slope. These flow periods associated with infinite conductivity fractures and the diagnostic specialized plots will be discussed later in this section.

Finite conductivity fractures

These are very long fractures created by massive hydraulic fracture (MHF). These types of fractures need large quantities of propping agent to keep them open and, as a result, the fracture permeability k_f is reduced as compared to that of the infinite conductivity fractures. These finite conductivity vertical fractures are characterized by measurable pressure drops in the fracture and, therefore, exhibit unique pressure responses when testing hydraulically fractured wells. The transient pressure behavior for this system can include the following four sequence flow periods (to be discussed later):

(1) initially "linear flow within the fracture";
(2) followed by "bilinear flow";
(3) then "linear flow in the formation"; and
(4) eventually "infinite acting pseudoradial flow."

Uniform flux fractures

A uniform flux fracture is one in which the reservoir fluid flow rate from the formation into the fracture is uniform along the entire fracture length. This model is similar to the infinite conductivity vertical fracture in several aspects. The difference between these two systems occurs at the boundary of the fracture. The system is characterized by a variable pressure along the fracture and exhibits essentially two flow periods;

(1) linear flow;
(2) infinite-acting pseudoradial flow.

Except for highly propped and conductive fractures, it is thought that the uniform-influx fracture theory better represents reality than the infinite conductivity fracture; however, the difference between the two is rather small.

The fracture has a much greater permeability than the formation it penetrates; hence it influences the pressure response of a well test significantly. The general solution for the pressure behavior in a reservoir is expressed in terms of dimensionless variables. The following dimensionless groups are used when analyzing pressure transient data in a hydraulically fractured well:

$$\text{Diffusivity group} \quad \eta_{fD} = \frac{k_f \phi c_t}{k \phi_f c_{ft}} \qquad [1.5.19]$$

$$\text{Time group} \quad t_{Dx_f} = \left[\frac{0.0002637k}{\phi \mu c_t x_f^2} \right] t = t_D \left(\frac{r_w^2}{x_f^2} \right) \qquad [1.5.20]$$

$$\text{Conductivity group} \quad F_{CD} = \frac{k_f}{k} \frac{w_f}{x_f} = \frac{F_C}{k x_f} \qquad [1.5.21]$$

$$\text{Storage group} \quad C_{Df} = \frac{0.8937C}{\phi c_t h x_f^2} \qquad [1.5.22]$$

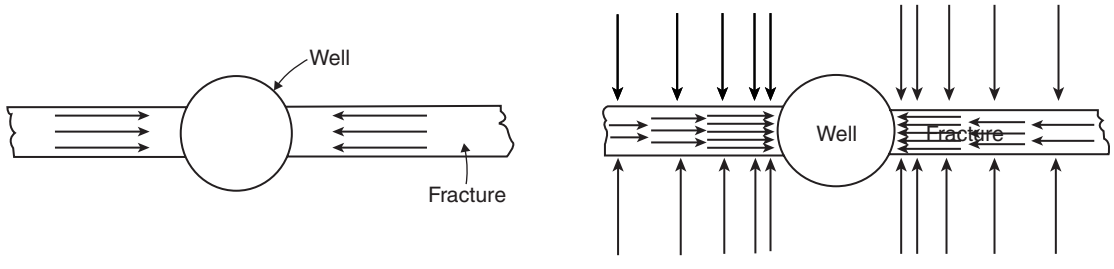

Figure 1.71 *Flow periods for a vertically fractured well (After Cinco and Samaniego, JPT, 1981).*

$$\text{Pressure group} \quad p_D = \frac{kh\Delta p}{141.2QB\mu} \quad \text{for oil} \qquad [1.5.23]$$

$$p_D = \frac{kh\Delta m(p)}{1424QT} \quad \text{for gas} \qquad [1.5.24]$$

$$\text{Fracture group} \quad r_{eD} = \frac{r_e}{x_f}$$

where:

x_f = fracture half-length, ft
w_f = fracture width, ft
k_f = fracture permeability, md
k = pre-frac formation permeability, md
t_{Dx_f} = dimensionless time based on the fracture half-length x_f
t = flowing time in drawdown, Δt or Δt_e in buildup, hours
T = Temperature, °R
F_C = fracture conductivity, md ft
F_{CD} = dimensionless fracture conductivity
η = hydraulic diffusivity
c_{ft} = total compressibility of the fracture, psi^{-1}

Notice that the above equations are written in terms of the pressure drawdown tests. These equations should be modified for buildup tests by replacing the pressure and time with the appropriate values as shown below:

Test	*Pressure*	*Time*
Drawdown	$\Delta p = p_i - p_{wf}$	t
Buildup	$\Delta p = p_{ws} - p_{wf \text{ at } \Delta t=0}$	Δt or Δt_e

In general, a fracture could be classified as an infinite conductivity fracture when the dimensionless fracture conductivity is greater than 300, i.e., $F_{CD} > 300$.

There are four flow regimes, as shown conceptually in Figure 1.71, associated with the three types of vertical fractures. These are:

(1) fracture linear flow;
(2) bilinear flow;
(3) formation linear flow;
(4) infinite-acting pseudoradial flow.

These flow periods can be identified by expressing the pressure transient data in different type of graphs. Some of these graphs are excellent tools for diagnosis and identification of regimes since test data may correspond to different flow periods.

There are specialized graphs of analysis for each flow period that include:

- a graph of Δp vs. $\sqrt{\text{time}}$ for linear flow;
- a graph of Δp vs. $\sqrt[4]{\text{time}}$ for bilinear flow;
- a graph of Δp vs. log(time) for infinite-acting pseudoradial flow.

These types of flow regimes and the diagnostic plots are discussed below.

Fracture linear flow This is the first flow period which occurs in a fractured system. Most of the fluid enters the wellbore during this period of time as a result of expansion within the fracture, i.e., there is negligible fluid coming from the formation. Flow within the fracture and from the fracture to the wellbore during this time period is linear and can be described by the diffusivity equation as expressed in a linear

form and is applied to both the fracture linear flow and formation linear flow periods. The pressure transient test data during the linear flow period can be analyzed with a graph of Δp vs. $\sqrt{\text{time}}$. Unfortunately, the fracture linear flow occurs at very early time to be of practical use in well test analysis. However, if the fracture linear flow exists (for fractures with $F_{CD} > 300$), the formation linear flow relationships as given by Equations 1.5.19 through 1.5.24 can be used in an exact manner to analyze the pressure data during the formation linear flow period.

If fracture linear flow occurs, the duration of the flow period is short, as it often is in finite conductivity fractures with $F_{CD} < 300$, and care must be taken not to misinterpret the early pressure data. It is common in this situation for skin effects or wellbore storage effects to alter pressures to the extent that the linear flow straight line does not occur or is very difficult to recognize. If the early-time slope is used in determining the fracture length, the slope m_{vf} will be erroneously high, the computed fracture length will be unrealistically small, and no quantitative information will be obtained regarding flow capacity in the fracture.

Cinco et al. (1981) observed that the fracture linear flow ends when:

$$t_{Dx_f} \approx \frac{0.01(F_{CD})^2}{(\eta_{fD})^2}$$

Bilinear flow This flow period is called bilinear flow because two types of linear flow occur simultaneously. As originally proposed by Cinco (1981), one flow is a linear incompressible flow within the fracture and the other is a linear compressible flow in the formation. Most of the fluid which enters the wellbore during this flow period comes from the formation. Fracture tip effects do not affect well behavior during bilinear flow and, accordingly, it will not be possible to determine the fracture length from the well bilinear flow period data. However, the actual value of the fracture conductivity F_C can be determined during this flow period. The pressure drop through the fracture is significant for the finite conductivity case and the bilinear flow behavior is observed; however, the *infinite conductivity case does not exhibit bilinear flow behavior* because the pressure drop in the fracture is negligible. Thus, identification of the bilinear flow period is very important for two reasons:

(1) It will not be possible to determine a unique fracture length from the well bilinear flow period data. If this data is used to determine the length of the fracture, it will produce a much smaller fracture length than the actual.
(2) The actual fracture conductivity $k_f w_f$ can be determined from the bilinear flow pressure data.

Cinco and Samaniego suggested that during this flow period, the change in the wellbore pressure can be described by the following expressions.

For fractured oil wells In terms of dimensionless pressure:

$$p_D = \left[\frac{2.451}{\sqrt{F_{CD}}}\right](t_{Dx_f})^{1/4} \quad [1.5.25]$$

Taking the logarithm of both sides of Equation 1.5.25 gives:

$$\log(p_D) = \log\left[\frac{2.451}{\sqrt{F_{CD}}}\right] + \frac{1}{4}\log(t_{Dx_f}) \quad [1.5.26]$$

In terms of pressure:

$$\Delta p = \left[\frac{44.1QB\mu}{h\sqrt{F_C}(\phi\mu c_t k)^{1/4}}\right] t^{1/4} \quad [1.5.27]$$

or equivalently:

$$\Delta p = m_{bf} t^{1/4}$$

Taking the logarithm of both sides of the above expression gives:

$$\log(\Delta p) = \log(m_{bf}) + \frac{1}{4}\log(t) \quad [1.5.28]$$

with the bilinear slope m_{bf} as given by:

$$m_{bf} = \left[\frac{44.1QB\mu}{h\sqrt{F_C}(\phi\mu c_t k)^{1/4}}\right]$$

where F_C is the fracture conductivity as defined by:

$$F_C = k_f w_f \quad [1.5.29]$$

For fractured gas wells In a dimensionless form:

$$m_D = \left[\frac{2.451}{\sqrt{F_{CD}}}\right](t_{Dx_f})^{1/4}$$

or:

$$\log(m_D) = \log\left[\frac{2.451}{\sqrt{F_{CD}}}\right] + \frac{1}{4}\log(t_{Dx_f}) \quad [1.5.30]$$

In terms of $m(p)$:

$$\Delta m(p) = \left[\frac{444.6QT}{h\sqrt{F_C}(\phi\mu c_t k)^{1/4}}\right] t^{1/4} \quad [1.5.31]$$

or equivalently:

$$\Delta m(p) = m_{bf} t^{1/4} \quad [1.5.32]$$

Taking the logarithm of both sides gives:

$$\log[\Delta m(p)] = \log(m_{bf}) + \frac{1}{4}\log(t)$$

Equations 1.5.27 and 1.5.31 indicate that a plot of Δp or $\Delta m(p)$ vs. $(\text{time})^{1/4}$ on a *Cartesian scale* would produce a straight line *passing through the origin* with a slope of "m_{bf} (bilinear flow slope) as given by:

For oil:

$$m_{bf} = \frac{44.1QB\mu}{h\sqrt{F_C}(\phi\mu c_t k)^{1/4}} \quad [1.5.33]$$

The slope can then be used to solve for fracture conductivity F_C:

$$F_C = \left[\frac{44.1QB\mu}{m_{bf}h(\phi\mu c_t k)^{1/4}}\right]^2$$

For gas:

$$m_{bf} = \frac{444.6QT}{h\sqrt{F_C}(\phi\mu c_t k)^{1/4}} \quad [1.5.34]$$

with:

$$F_C = \left[\frac{444.6QT}{m_{bf}h(\phi\mu c_t k)^{1/4}}\right]^2$$

It should be noted that *if the straight-line plot does not pass through the origin*, it indicates an additional pressure drop "Δp_s" caused by flow restriction within the fracture in the vicinity of the wellbore (chocked fracture; where the fracture permeability just away from the wellbore is reduced). Examples of restrictions that cause a loss of resulting production include:

- inadequate perforations;
- turbulent flow which can be reduced by increasing the proppant size or concentration;
- overdisplacement of proppant;
- kill fluid was dumped into the fracture.

Similarly, Equations 1.5.28 and 1.5.32 suggest that a plot of Δp or $\Delta m(p)$ versus (time) on a *log–log scale* would produce a straight line with a slope of $m_{bf} = \frac{1}{4}$ and which can be used as a diagnostic tool for bilinear flow detection.

When the bilinear flow ends, the plot will exhibit curvature which could concave upwards or downwards depending upon the value of the dimensionless fracture conductivity F_{CD}, as shown in Figure 1.72. When the values of F_{CD} is < 1.6, the curve will concave downwards, and will concave upwards if $F_{CD} > 1.6$. The upward trend indicates that the

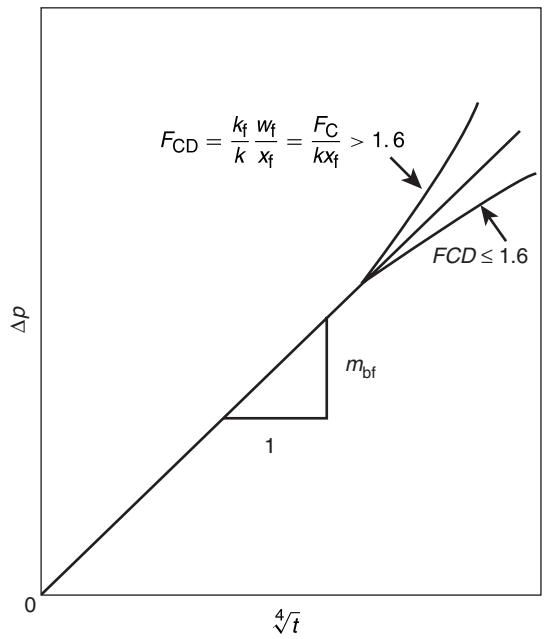

Figure 1.72 *Graph for analysis of pressure data of bilinear flows (After Cinco and Samaniego, 1981).*

fracture tip begins to affect wellbore behavior. If the test is not run sufficiently long for bilinear flow to end when $F_{CD} > 1.6$, it is not possible to determine the length of the fracture. When the dimensionless fracture conductivity $F_{CD} < 1.6$, it indicates that the fluid flow *in the reservoir* has changed from a predominantly one-dimensional linear flow to a two-dimensional flow regime. In this particular case, it is not possible to uniquely determine fracture length even if bilinear flow does end during the test.

Cinco and Samaniego pointed out that the dimensionless fracture conductivity F_{CD} can be estimated from the bilinear flow straight line, i.e., Δp vs. $(\text{time})^{1/4}$, by reading the value of the pressure difference Δp at which the line ends Δp_{ebf} and applying the following approximation:

$$\text{For oil} \quad F_{CD} = \frac{194.9QB\mu}{kh\Delta p_{ebf}} \qquad [1.5.35]$$

$$\text{For gas} \quad F_{CD} = \frac{1965.1QT}{kh\Delta m(p)_{ebf}} \qquad [1.5.36]$$

where:

Q = flow rate, STB/day or Mscf/day
T = temperature, °R

The end of the bilinear flow, "ebf," straight line depends on the fracture conductivity and can be estimated from the following relationships:

$$\text{For } F_{CD} > 3 \qquad t_{Debf} \simeq \frac{0.1}{(F_{CD})^2}$$

$$\text{For } 1.6 \leq F_{CD} \leq 3 \qquad t_{Debf} \simeq 0.0205[F_{CD} - 1.5]^{-1.53}$$

$$\text{For } F_{CD} \leq 1.6 \qquad t_{Debf} \simeq \left[\frac{4.55}{\sqrt{F_{CD}}} - 2.5\right]^{-4}$$

The procedure for analyzing the bilinear flow data is summarized by the following steps:

Step 1. Make a plot of Δp versus time on a log–log scale.
Step 2. Determine if any data fall on a straight line with a $\frac{1}{4}$ slope.
Step 3. If data points do fall on the straight line with a $\frac{1}{4}$ slope, replot the data in terms of Δp vs. $(\text{time})^{1/4}$ on a Cartesian scale and identify the data which forms the bilinear straight line.
Step 4. Determine the slope of the bilinear straight line m_{bf} formed in step 3.
Step 5. Calculate the fracture conductivity $F_C = k_f w_f$ from Equation 1.5.33 or Equation 1.5.34:

$$\text{For oil} \quad F_C = (k_f w_f) = \left[\frac{44.1QB\mu}{m_{bf}h(\phi\mu c_t k)^{1/4}}\right]^2$$

$$\text{For gas} \quad F_C = (k_f w_f) = \left[\frac{444.6QT}{m_{bf}h(\phi\mu c_t k)^{1/4}}\right]^2$$

Step 6. Read the value of the pressure difference at which the line ends, Δp_{ebf} or $\Delta m(p)_{ebf}$.
Step 7. Approximate the dimensionless facture conductivity from:

$$\text{For oil} \quad F_{CD} = \frac{194.9QB\mu}{kh\Delta p_{ebf}}$$

$$\text{For gas} \quad F_{CD} = \frac{1965.1QT}{kh\Delta m(p)_{ebf}}$$

Step 8. Estimate the fracture length from the mathematical definition of F_{CD} as expressed by Equation 1.5.21 and the value of F_C of step 5:

$$x_f = \frac{F_C}{F_{CD}k}$$

Example 1.36 A buildup test was conducted on a fractured well producing from a tight gas reservoir. The following reservoir and well parameters are available:

$Q = 7350$ Mscf/day,	$t_p = 2640$ hours
$h = 118$ ft,	$\phi = 0.10$
$k = 0.025$ md,	$\mu = 0.0252$
$T = 690°$R,	$c_t = 0.129 \times 10^{-3}$ psi^{-1}
$p_{wf \text{ at } \Delta t=0} = 1320$ psia,	$r_w = 0.28$ ft

The graphical presentation of the buildup data is given in terms of the log–log plot of $\Delta m(p)$ vs. $(\Delta t)^{1/4}$, as shown in Figure 1.73.

Calculate the fracture and reservoir parameters by performing conventional well testing analysis.

Solution

Step 1. From the plot of $\Delta m(p)$ vs. $(\Delta t)^{1/4}$, in Figure 1.73, determine:

$$m_{bf} = 1.6 \times 10^8 \text{ psi}^2/\text{cphr}^{1/4}$$

$$t_{sbf} \approx 0.35 \text{ hours (start of bilinear flow)}$$

$$t_{ebf} \approx 2.5 \text{ hours (end of bilinear flow)}$$

$$\Delta m(p)_{ebf} \approx 2.05 \times 10^8 \text{ psi}^2/\text{cp}$$

Step 2. Perform the bilinear flow analysis, as follows:

- Using Equation 1.5.34, calculate fracture conductivity F_C:

$$F_C = \left[\frac{444.6QT}{m_{bf}h(\phi\mu c_t k)^{1/4}}\right]^2$$

$$= \left[\frac{444.6(7350)(690)}{(1.62\times10^8)(118)[(0.1)(0.0252)(0.129\times10^{-3})(0.025)]^{1/4}}\right]^2$$

$$= 154 \text{ md ft}$$

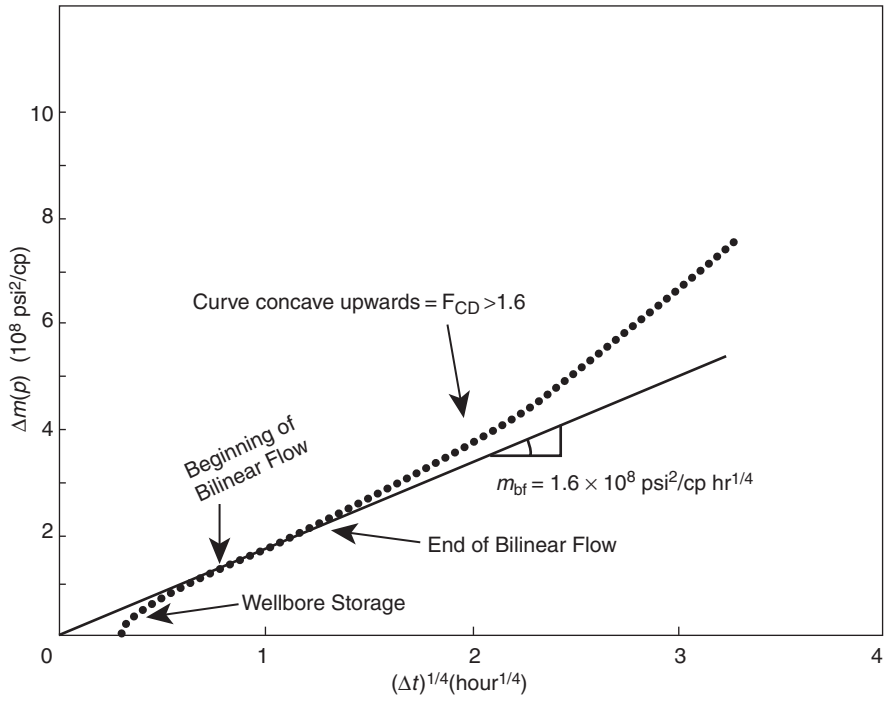

Figure 1.73 *Bilinear flow graph for data of Example 1.36 (After Sabet, M. A.* Well Test Analysis *1991, Gulf Publishing Company).*

- Calculate the dimensionless conductivity F_{CD} by using Equation 1.5.36:

$$F_{CD} = \frac{1965.1QT}{kh\Delta m(p)_{ebf}}$$

$$= \frac{1965.1(7350)(690)}{(0.025)(118)(2.02 \times 10^8)} = 16.7$$

- Estimate the fracture half-length from Equation 1.5.21:

$$x_f = \frac{F_C}{F_{CD}k}$$

$$= \frac{154}{(16.7)(0.025)} = 368 \text{ ft}$$

Formation linear flow At the end of the bilinear flow, there is a transition period after which the fracture tips begin to affect the pressure behavior at the wellbore and a linear flow period might develop. This linear flow period is exhibited by vertical fractures whose dimensionless conductivity is greater that 300, i.e., $F_{CD} > 300$. As in the case of fracture linear flow, the formation linear flow pressure data collected during this period is a function of the fracture length x_f and fracture conductivity F_C. The pressure behavior during this linear flow period can be described by the diffusivity equation as expressed in linear form:

$$\frac{\partial^2 p}{\partial x^2} = \frac{\phi\mu c_t}{0.002637k}\frac{\partial p}{\partial t}$$

The solution to the above linear diffusivity equation can be applied to both fracture linear flow and the formation linear flow, with the solution given in a dimensionless form by:

$$p_D = \left(\pi t_{Dx_f}\right)^{1/2}$$

or in terms of real pressure and time, as:

For oil fractured wells $\Delta p = \left[\frac{4.064QB}{hx_f}\sqrt{\frac{\mu}{k\phi c_t}}\right]t^{1/2}$

or in simplified form as $\Delta p = m_{vf}\sqrt{t}$

For gas fractured wells $\Delta m(p) = \left[\frac{40.925QT}{hx_f}\sqrt{\frac{1}{k\phi\mu c_t}}\right]t^{1/2}$

or equivalently as $\Delta m(p) = m_{vf}\sqrt{t}$

The linear flow period may be recognized by pressure data that exhibits a straight line of a $\frac{1}{2}$ slope on a log–log plot of Δp versus time, as illustrated in Figure 1.74. Another diagnostic presentation of pressure data points is the plot of Δp or $\Delta m(p)$ vs. $\sqrt{\text{time}}$ on a Cartesian scale (as shown in Figure 1.75) which would *produce a straight line* with a slope of m_{vf} related to the fracture length by the following equations:

Oil fractured well $$x_f = \left[\frac{4.064QB}{m_{vf}h}\right]\sqrt{\frac{\mu}{k\phi c_t}} \quad [1.5.37]$$

Gas fractured well $$x_f = \left[\frac{40.925QT}{m_{vf}h}\right]\sqrt{\frac{1}{k\phi\mu c_t}} \quad [1.5.38]$$

where:

Q = flow rate, STB/day or Mscf/day
T = temperature, °R
m_{vf} = slope, psi/$\sqrt{\text{hr}}$ or psi^2/cp$\sqrt{\text{hr}}$
k = permeability, md
c_t = total compressibility, psi^{-1}

The straight-line relationships as illustrated by Figures 1.74 and 1.75 provide distinctive and easily recognizable

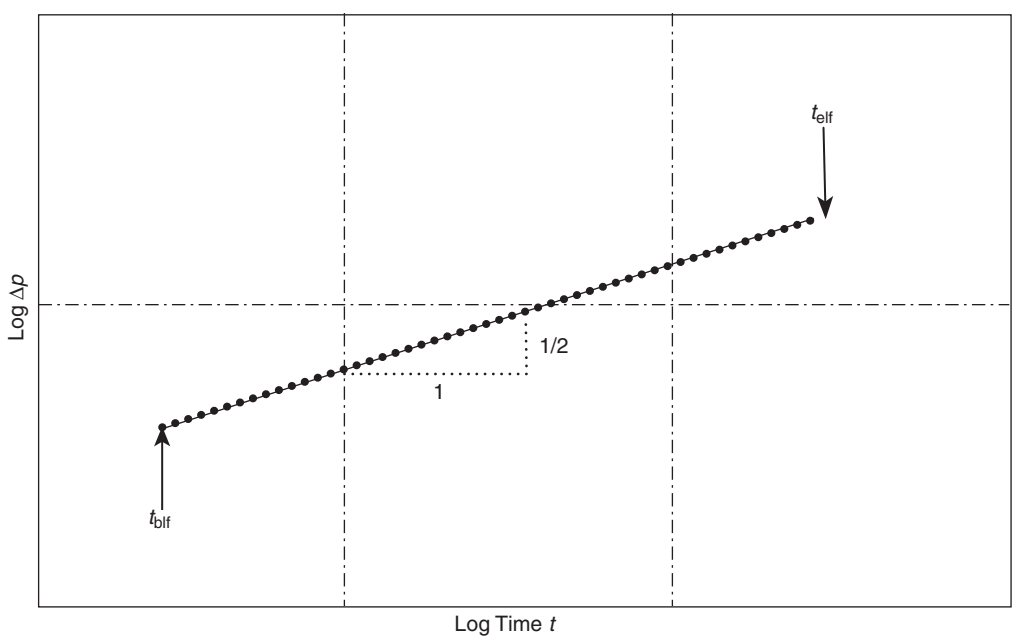

Figure 1.74 *Pressure data for a $\frac{1}{2}$-slope straight line in a log–log graph (After Cinco and Samaniego, 1981).*

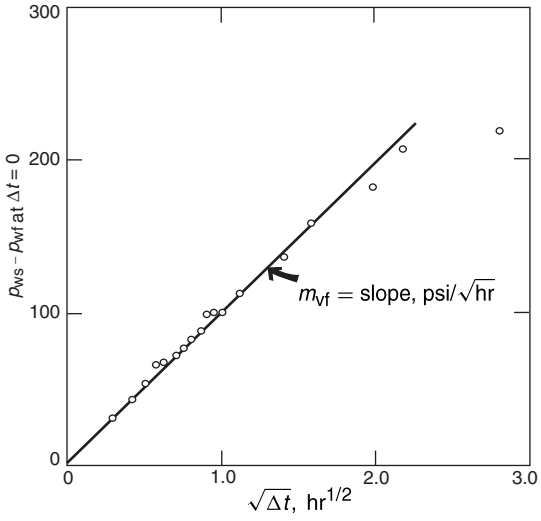

Figure 1.75 *Square-root data plot for buildup test.*

evidence of a fracture. When properly applied, these plots are the best diagnostic tools available for the purpose of detecting a fracture. In practice, the $\frac{1}{2}$ slope is rarely seen except in fractures with high conductivity. Finite conductivity fracture responses generally enter a transition period after the bilinear flow (the $\frac{1}{4}$ slope) and reach the infinite-acting pseudoradial flow regime before ever achieving a $\frac{1}{2}$ slope (linear flow). For a long duration of wellbore storage effect, the bilinear flow pressure behavior may be masked and data analysis becomes difficult with current interpretation methods.

Agarwal et al. (1979) pointed out that the pressure data during the transition period displays a curved portion before straightening to a line of proper slope that represents the fracture linear flow. The duration of the curved portion that represents the transition flow depends on the fracture flow capacity. The lower the fracture flow capacity, the longer the duration of the curved portion. The beginning of formation linear flow, "blf," depends on F_{CD} and can be approximated from the following relationship:

$$t_{Dblf} \approx \frac{100}{(F_{CD})^2}$$

and the end of this linear flow period, "elf," occurs at approximately:

$$t_{Dblf} \approx 0.016$$

Identifying the coordinates of these two points (i.e., beginning and end of the straight line) in terms of time can be used to estimate F_{CD} from:

$$F_{CD} \approx 0.0125\sqrt{\frac{t_{elf}}{t_{blf}}}$$

where t_{elf} and t_{blf} are given in hours.

Infinite-acting pseudoradial flow During this period, the flow behavior is similar to the radial reservoir flow with a negative skin effect caused by the fracture. The traditional semilog and log–log plots of transient pressure data can be used during this period; for example, the drawdown pressure data can be analyzed by using Equations 1.3.1 through 1.3.3. That is:

$$p_{wf} = p_i - \frac{162.6 Q_o B_o \mu}{kh} \times \left[\log(t) + \log\left(\frac{k}{\phi \mu c_t r_w^2}\right) - 3.23 + 0.87s\right]$$

or in a linear form as:

$$p_i - p_{wf} = \Delta p = a + m \log(t)$$

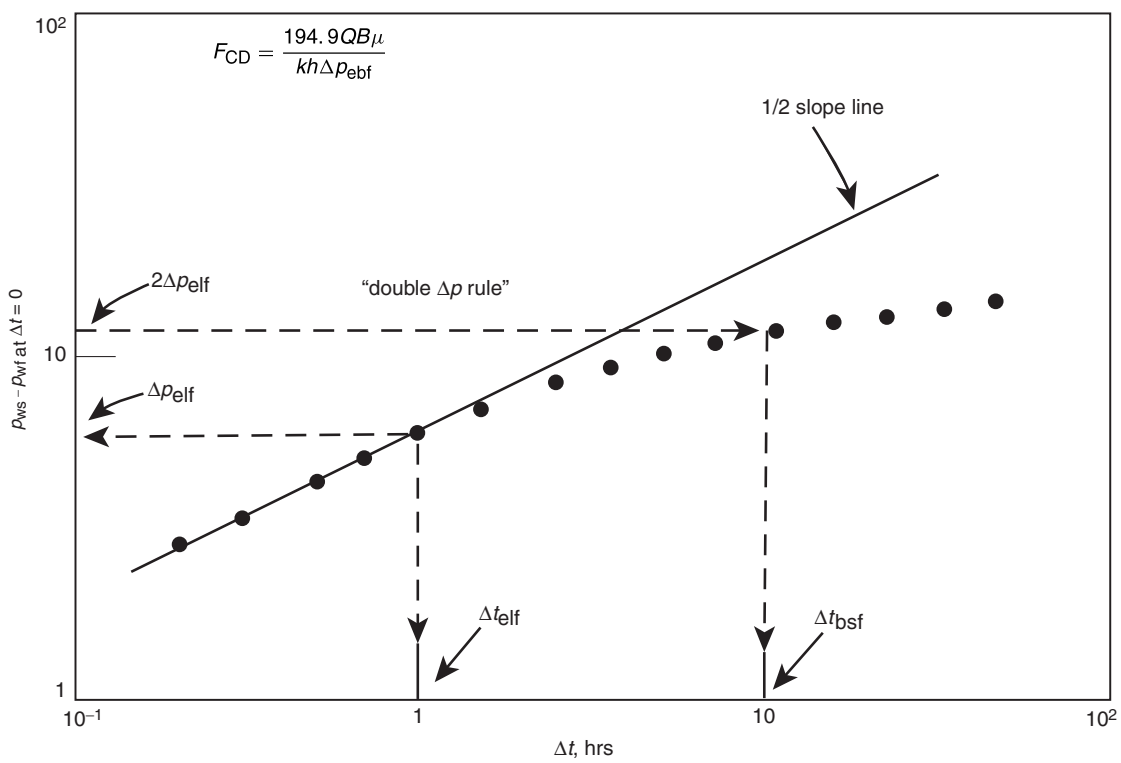

Figure 1.76 *Use of the log–log plot to approximate the beginning of pseudoradial flow.*

with the slope m of:

$$m = \frac{162.6Q_oB_o\mu_o}{kh}$$

Solving for the formation capacity gives:

$$kh = \frac{162.6Q_oB_o\mu_o}{|m|}$$

The skin factor s can be calculated by Equation 1.3.3:

$$s = 1.151\left[\frac{p_i - p_{1\text{ hr}}}{|m|} - \log\left(\frac{k}{\phi\mu c_t r_w^2}\right) + 3.23\right]$$

If the semilog plot is made in terms of Δp vs. t, notice that the slope m is the same when making the semilog plot in terms of p_{wf} vs. t. Then:

$$s = 1.151\left[\frac{\Delta p_{1\text{ hr}}}{|m|} - \log\left(\frac{k}{\phi\mu c_t r_w^2}\right) + 3.23\right]$$

$\Delta p_{1\text{ hr}}$ can then be calculated from the mathematical definition of the slope m, i.e., rise/run, by using two points on the semilog straight line (conveniently, one point could be Δp at $\log(10)$) to give:

$$m = \frac{\Delta p_{\text{ at }\log(10)} - \Delta p_{1\text{ hr}}}{\log(10) - \log(1)}$$

Solving this expression for $\Delta p_{1\text{ hr}}$ gives:

$$\Delta p_{1\text{ hr}} = \Delta p_{\text{ at }\log(10)} - m \qquad [1.5.39]$$

Again, $\Delta p_{\text{ at }\log(10)}$ must be read at the corresponding point on the straight line at $\log(10)$.

Wattenbarger and Ramey (1968) have shown that an approximate relationship exists between the pressure change Δp at the end of the linear flow, i.e., Δp_{elf}, and the beginning of the infinite acting pseudoradial flow, Δp_{bsf}, as given by:

$$\Delta p_{bsf} \geq 2\Delta p_{elf} \qquad [1.5.40]$$

The above rule is commonly referred to as the "double-Δp rule" and can be obtained from the log–log plot when the $\frac{1}{2}$ slope ends and by reading the value of Δp, i.e., Δp_{elf}, at this point. For fractured wells, doubling the value of Δp_{elf} will mark the beginning of the infinite-acting pseudoradial flow period. Equivalently, a time rule as referred to as the "$10\Delta t$ rule" can be applied to mark the beginning of pseudoradial flow by:

For drawdown $\quad t_{bsf} \geq 10t_{elf}$ [1.5.41]

For buildup $\quad \Delta t_{bsf} \geq 10\Delta t_{elf}$ [1.5.42]

which indicates that correct infinite-acting pseudoradial flow occurs one log cycle beyond the end of the linear flow. The concept of the above two rules is illustrated graphically in Figure 1.76.

Another approximation that can be used to mark the start of the infinite-acting radial flow period for a finite conductivity fracture is given by:

$$t_{Dbs} \approx 5\exp[-0.5(F_{CD})^{-0.6}] \quad \text{for} \quad F_{CD} > 0.1$$

Sabet (1991) used the following drawdown test data, as originally given by Gringarten et al. (1975), to illustrate the process of analyzing a hydraulically fractured well test data.

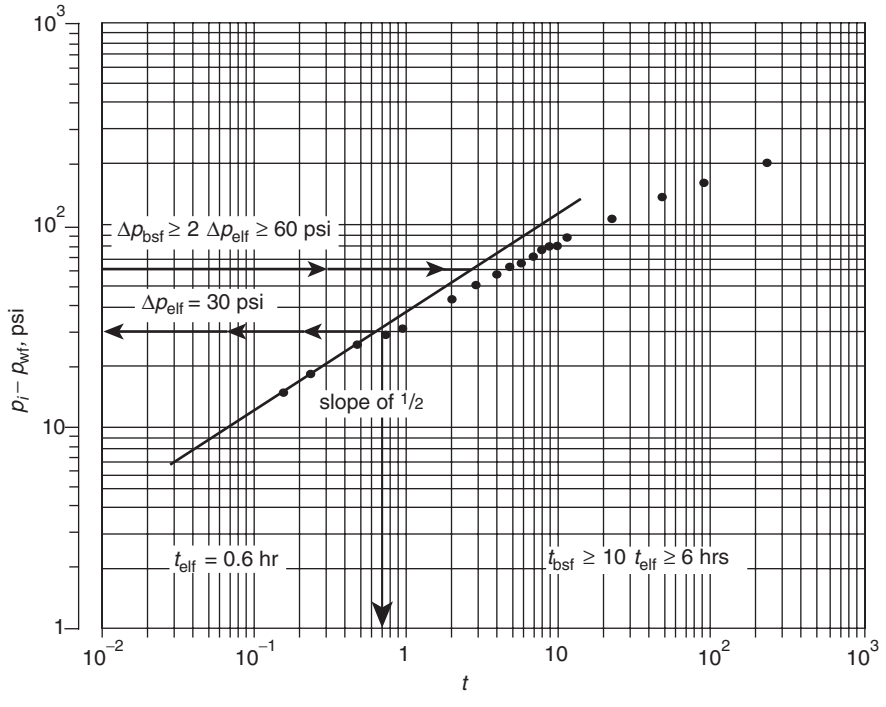

Figure 1.77 *Log–log plot, drawdown test data of Example 1.37 (After Sabet, M. A.* Well Test Analysis *1991, Gulf Publishing Company).*

Example 1.37 The drawdown test data for an infinite conductivity fractured well is tabulated below:

t (hr)	p_{wf} (psi)	Δp (psi)	$\sqrt{t}$ ($hr^{1/2}$)
0.0833	3759.0	11.0	0.289
0.1670	3755.0	15.0	0.409
0.2500	3752.0	18.0	0.500
0.5000	3744.5	25.5	0.707
0.7500	3741.0	29.0	0.866
1.0000	3738.0	32.0	1.000
2.0000	3727.0	43.0	1.414
3.0000	3719.0	51.0	1.732
4.0000	3713.0	57.0	2.000
5.0000	3708.0	62.0	2.236
6.0000	3704.0	66.0	2.449
7.0000	3700.0	70.0	2.646
8.0000	3695.0	75.0	2.828
9.0000	3692.0	78.0	3.000
10.0000	3690.0	80.0	3.162
12.0000	3684.0	86.0	3.464
24.0000	3662.0	108.0	4.899
48.0000	3635.0	135.0	6.928
96.0000	3608.0	162.0	9.798
240.0000	3570.0	200.0	14.142

Additional reservoir parameters are:

$h = 82$ ft, $\phi = 0.12$

$c_t = 21 \times 10^{-6}$ psi^{-1}, $\mu = 0.65$ cp

$B_o = 1.26$ bbl/STB, $r_w = 0.28$ ft

$Q = 419$ STB/day, $p_i = 3770$ psi

Estimate:

- permeability, k;
- fracture half-length, x_f;
- skin factor, s.

Solution

Step 1. Plot:

- Δp vs. t on a log–log scale, as shown in Figure 1.77;
- Δp vs. $\sqrt{t}$ on a Cartesian scale, as shown in Figure 1.78;
- Δp vs. t on a semilog scale, as shown in Figure 1.79.

Step 2. Draw a straight line through the early points representing $\log(\Delta p)$ vs. $\log(t)$, as shown in Figure 1.77, and determine the slope of the line. Figure 1.77 shows a slope of $\frac{1}{2}$ (not 45° angle) indicating linear flow with no wellbore storage effects. This linear flow lasted for approximately 0.6 hours. That is:

$$t_{elf} = 0.6 \text{ hours}$$

$$\Delta p_{elf} = 30 \text{ psi}$$

and therefore the beginning of the infinite-acting pseudoradial flow can be approximated by the "double Δp rule" or "one log cycle rule," i.e., Equations 1.5.40 and 1.5.41, to give:

$$t_{bsf} \geq 10 t_{elf} \geq 6 \text{ hours}$$

$$\Delta p_{bsf} \geq 2\Delta p_{elf} \geq 60 \text{ psi}$$

Step 3. From the Cartesian scale plot of Δp vs. $\sqrt{t}$, draw a straight line through the early pressure data points representing the first 0.3 hours of the test (as shown

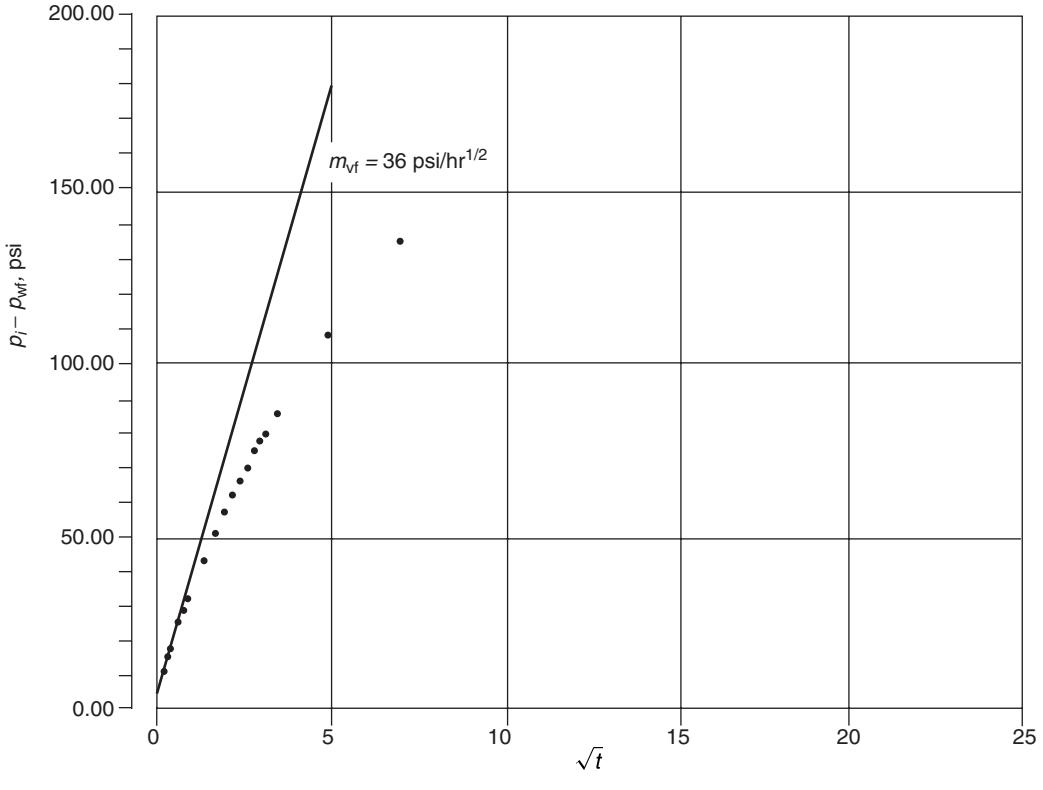

Figure 1.78 *Linear plot, drawdown test data of Example 1.37 (After Sabet, M. A.* Well Test Analysis *1991, Gulf Publishing Company).*

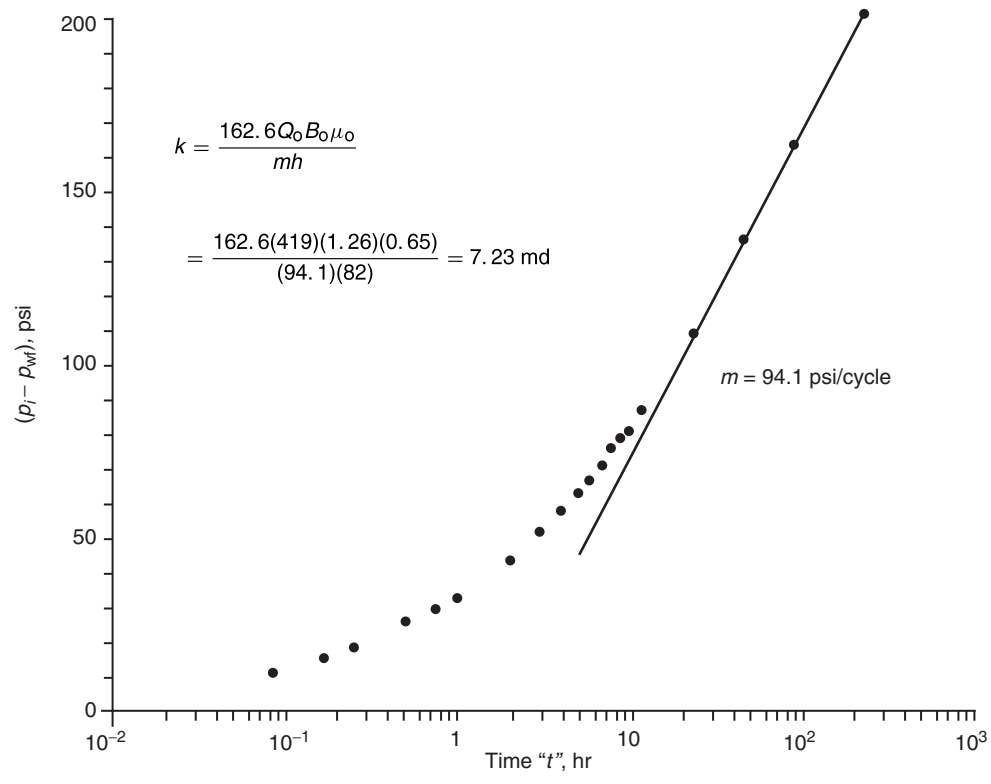

Figure 1.79 *Semilog plot, drawdown test data from Example 1.37.*

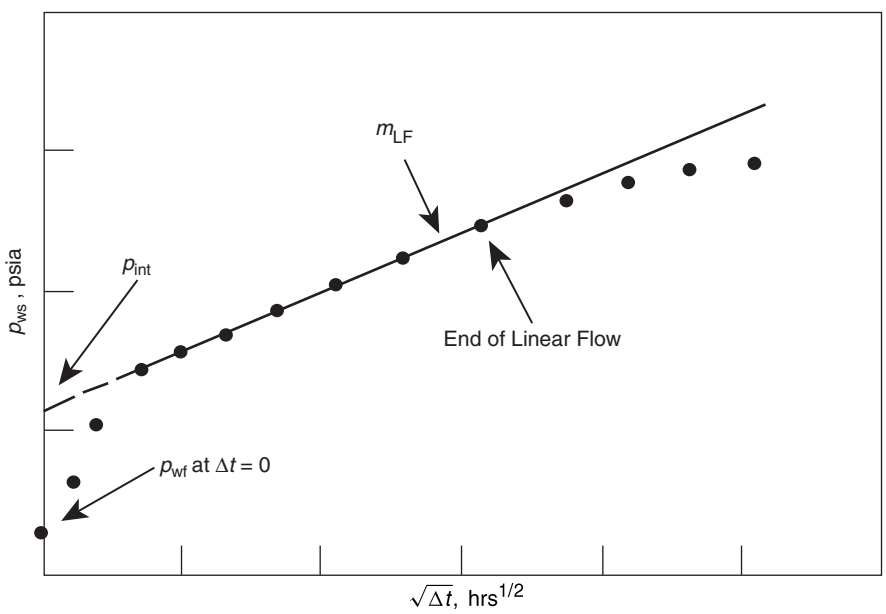

Figure 1.80 *Effect of skin on the square root plot.*

in Figure 1.79) and determine the slope of the line, to give:

$$m_{vf} = 36 \text{ psi/hr}^{1/2}$$

Step 4. Determine the slope of the semilog straight line representing the unsteady-state radial flow in Figure 1.79, to give:

$$m = 94.1 \text{ psi/cycle}$$

Step 5. Calculate the permeability k from the slope:

$$k = \frac{162.6 Q_o B_o \mu_o}{mh} = \frac{162.6(419)(1.26)(0.65)}{(94.1)(82)}$$

$$= 7.23 \text{ md}$$

Step 6. Estimate the length of the fracture half-length from Equation 1.5.37, to give:

$$x_f = \left[\frac{4.064QB}{m_{vf}h}\right]\sqrt{\frac{\mu}{k\phi c_t}}$$

$$= \left[\frac{4.064(419)(1.26)}{(36)(82)}\right]\sqrt{\frac{0.65}{(7.23)(0.12)(21\times 10^{-6})}}$$

$$= 137.3 \text{ ft}$$

Step 7. From the semilog straight line of Figure 1.78, determine Δp at $t = 10$ hours, to give:

$$\Delta p_{\text{at } \Delta t=10} = 71.7 \text{ psi}$$

Step 8. Calculate $\Delta p_{1 \text{ hr}}$ by applying Equation 1.5.39:

$$\Delta p_{1 \text{ hr}} = \Delta p_{\text{at } \Delta t=10} - m = 71.7 - 94.1 = -22.4 \text{ psi}$$

Step 9. Solve for the "total" skin factor s, to give

$$s = 1.151\left[\frac{\Delta p_{1 \text{ hr}}}{|m|} - \log\left(\frac{k}{\phi\mu c_t r_w^2}\right) + 3.23\right]$$

$$= 1.151\left[\frac{-22.4}{94.1}\right.$$

$$\left. - \log\left(\frac{7.23}{0.12(0.65)(21\times 10^{-6})(0.28)^2}\right) + 3.23\right]$$

$$= -5.5$$

with an apparent wellbore ratio of:

$$r_w^{\backslash} = r_w e^{-s} = 0.28e^{5.5} = 68.5 \text{ ft}$$

Notice that the "total" skin factor is a composite of effects that include:

$$s = s_d + s_f + s_t + s_p + s_{sw} + s_r$$

where:

s_d = skin due to formation and fracture damage
s_f = skin due to the fracture, large negative value $s_f \ll 0$
s_t = skin due to turbulence flow
s_p = skin due to perforations
s_w = skin due to slanted well
s_r = skin due to restricted flow

For fractured oil well systems, several of the skin components are negligible or cannot be applied, mainly s_t, s_p, s_{sw}, and s_r; therefore:

$$s = s_d + s_f$$

or:

$$s_d = s - s_f$$

Smith and Cobb (1979) suggested that the best approach to evaluate damage in a fractured well is to use the square root plot. In an ideal well without damage, the square root straight line will extrapolate to p_{wf} at $\Delta t = 0$, i.e, $p_{wf \text{ at } \Delta t=0}$, however, when a well is damaged the intercept pressure p_{int} will be greater than $p_{wf \text{ at } \Delta t=0}$, as illustrated in Figure 1.80. Note that the well shut-in pressure is described by Equation 1.5.35 as:

$$p_{ws} = p_{wf \text{ at } \Delta t=0} + m_{vf}\sqrt{t}$$

Smith and Cobb pointed out that the total skin factor exclusive of s_f, i.e., $s - s_f$, can be determined from the square root plot by extrapolating the straight line to $\Delta t = 0$ and an intercept pressure p_{int} to give the pressure loss due to skin damage, $(\Delta p_s)_d$, as:

$$(\Delta p_s)_d = p_{int} - p_{wf \text{ at } \Delta t=0} = \left[\frac{141.2QB\mu}{kh}\right]s_d$$

Equation 1.5.35 indicates that if $p_{int} = p_{wf \text{ at } \Delta t=0}$, then the skin due to fracture s_f is equal to the total skin.

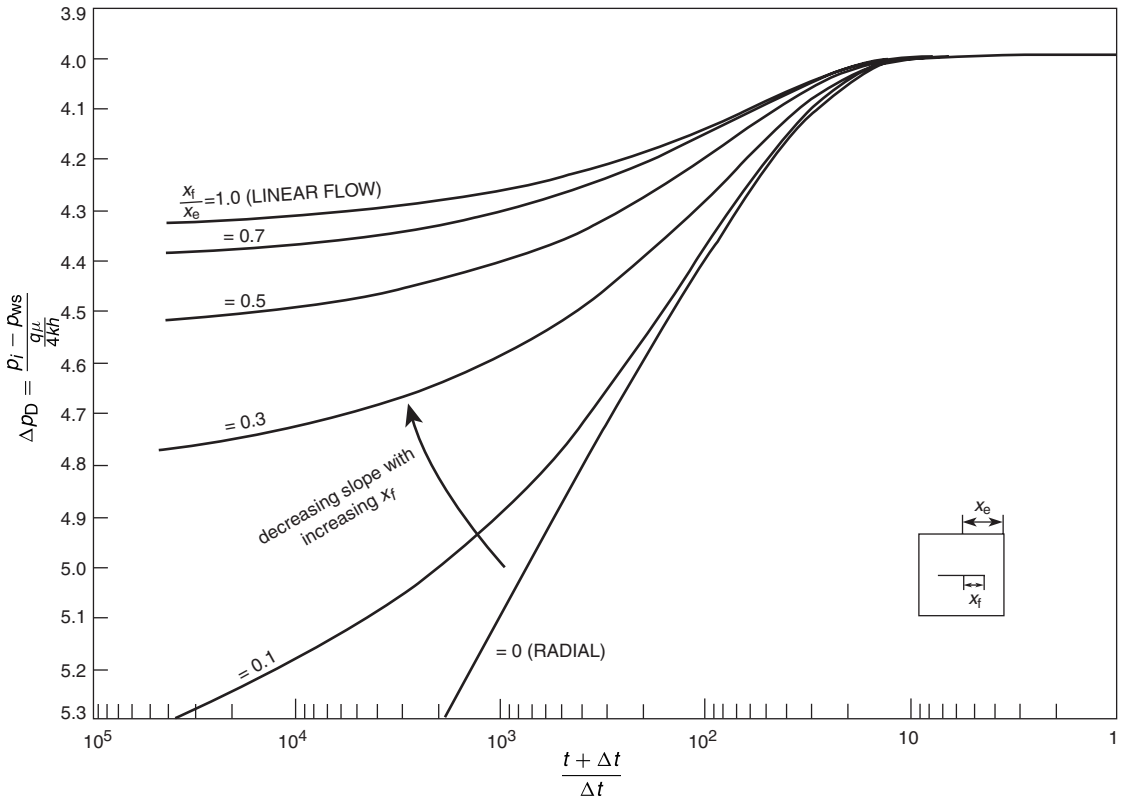

Figure 1.81 *Vertically fractured reservoir, calculated pressure buildup curves (After Russell and Truitt, 1964).*

It should be pointed out that the external boundary can distort the semilog straight line if the fracture half-length is greater than one-third of the drainage radius. The pressure behavior during this infinite-acting period is very dependent on the fracture length. For relatively short fractures, the flow is radial but becomes linear as the fracture length increases as it reaches the drainage radius. As noted by Russell and Truitt (1964), the slope obtained from the traditional well test analysis of a fractured well is erroneously too small and the calculated value of the slope progressively decreases with increasing fracture length. This dependency of the pressure response behavior on the fracture length is illustrated by the theoretical Horner buildup curves given by Russell and Truitt and shown in Figure 1.81. If the fracture penetration ratio x_f/x_e is defined as the ratio of the fracture half-length x_f to the half-length x_e of a closed square-drainage area, then Figure 1.81 shows the effects of fracture penetration on the slope of the buildup curve. For fractures of small penetration, the slope of the buildup curve is only slightly less than that for the unfractured "radial flow" case. However, the slope of the buildup curve becomes progressively smaller with increasing fracture penetrations. This will result in a calculated flow capacity kh which is too large, an erroneous average pressure, and a skin factor which is too small. Obviously a modified method for analyzing and interpreting the data must be employed to account for the effect of length of the fracture on the pressure response during the infinite-acting flow period. Most of the published correction techniques require the use of iterative procedures. The type curve matching approach and other specialized plotting techniques have been accepted by the oil industry as accurate and convenient approaches for analyzing pressure data from fractured wells, as briefly discussed below.

An alternative and convenient approach to analyzing fractured well transient test data is type curve matching. The type curve matching approach is based on plotting the pressure difference Δp versus time on the same scale as the selected type curve and matching one of the type curves. Gringarten et al. (1974) presented the type curves shown in Figures 1.82 and 1.83 for infinite conductivity vertical fracture and uniform flux vertical fracture, respectively, in a square well drainage area. Both figures present log–log plots of the dimensionless pressure drop p_d (equivalently referred to as dimensionless wellbore pressure p_{wd}) versus dimensionless time t_{Dx_f}. The fracture solutions show an initial period controlled by linear flow where the pressure is a function of the square root of time. In log–log coordinates, as indicated before, this flow period is characterized by a straight line with $\frac{1}{2}$ slope. The infinite-acting pseudoradial flow occurs at a t_{Dx_f} between 1 and 3. Finally, all solutions reach pseudosteady state.

During the matching process a match point is chosen; the dimensionless parameters on the axis of the type curve are used to estimate the formation permeability and fracture length from:

$$k = \frac{141.2QB\mu}{h}\left[\frac{p_D}{\Delta p}\right]_{MP} \qquad [1.5.43]$$

$$x_f = \sqrt{\frac{0.0002637k}{\phi\mu C_t}\left(\frac{\Delta t}{t_{Dx_f}}\right)_{MP}} \qquad [1.5.44]$$

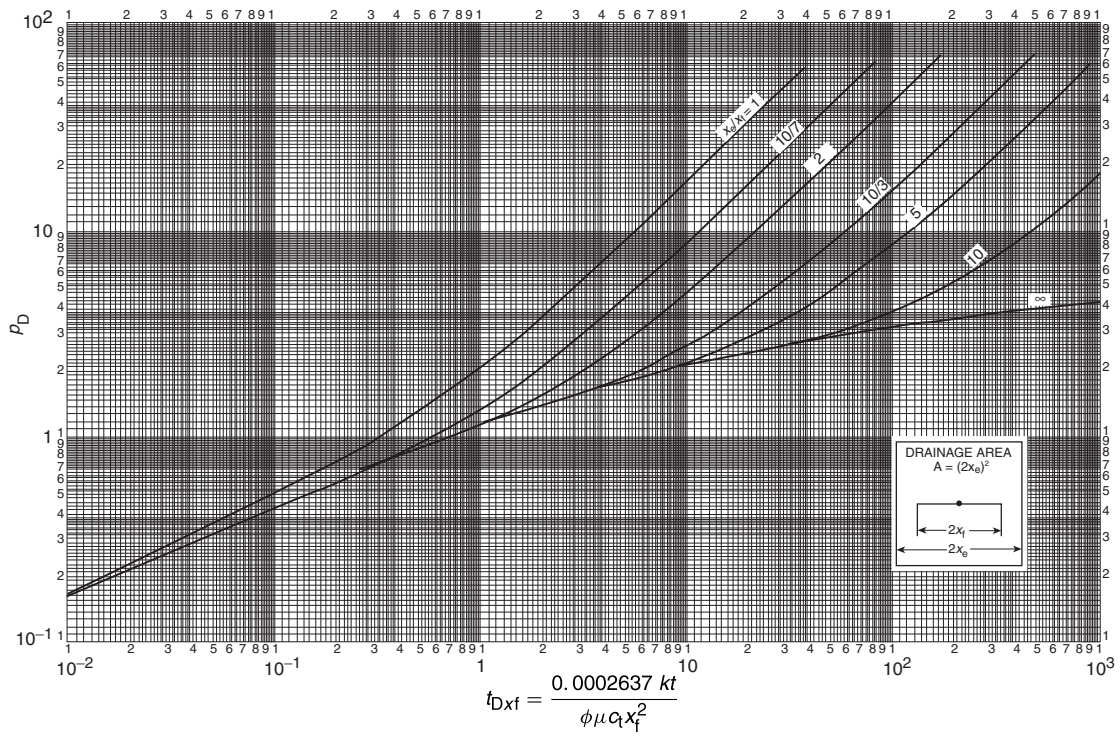

Figure 1.82 *Dimensionless pressure for vertically fractured well in the center of a closed square, no wellbore storage, infinite conductivity fracture (After Gringarten et al., 1974).*

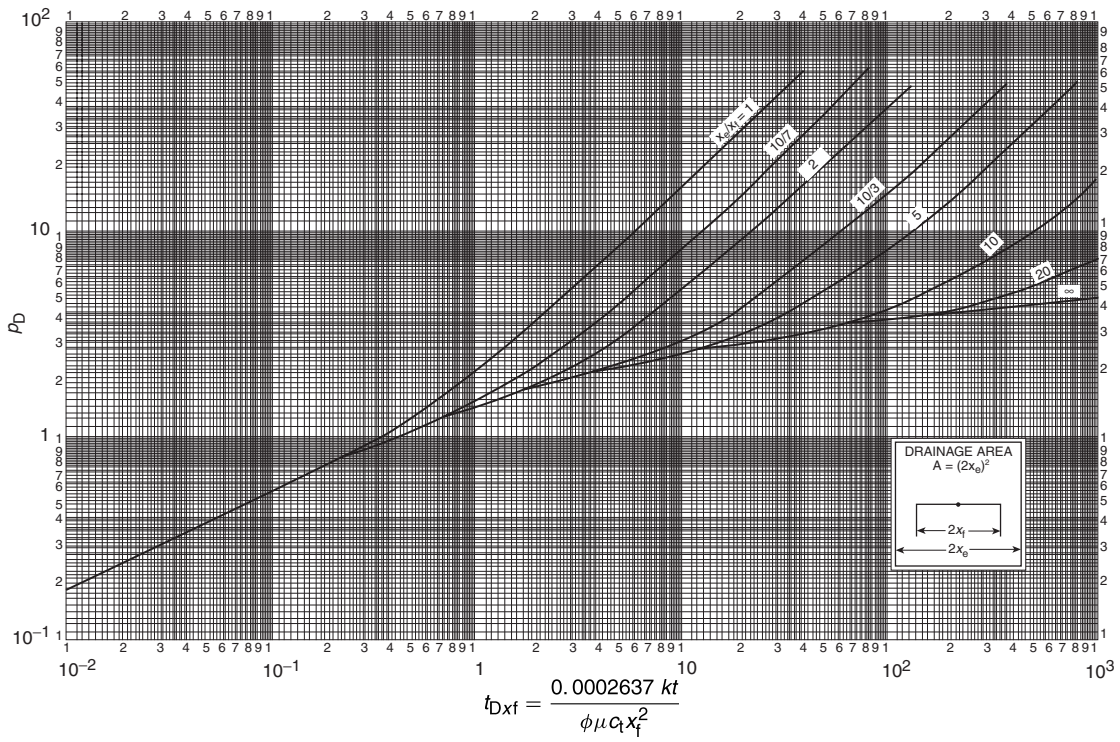

Figure 1.83 *Dimensionless pressure for vertically fractured well in the center of a closed square, no wellbore storage, uniform-flux fracture (After Gringarten et al., 1974).*

For large ratios of x_e/x_f, Gringarten and his co-authors suggested that the apparent wellbore radius $r_w^{\backslash}$ can be approximated from:

$$r_w^{\backslash} \approx \frac{x_f}{2} = r_w e^{-s}$$

Thus, the skin factor can be approximated from:

$$s = \ln\left(\frac{2r_w}{x_f}\right) \qquad [1.5.45]$$

Earlougher (1977) points out that if all the test data falls on the $\frac{1}{2}$-slope line on the log Δp vs. log(time) plot, i.e., the test is not long enough to reach the infinite-acting pseudo-radial flow period, then the *formation permeability k* cannot be estimated by either type curve matching or semilog plot. This situation often occurs in tight gas wells. However, the last point on the $\frac{1}{2}$ slope line, i.e., $(\Delta p)_{Last}$ and $(t)_{Last}$, may be used to estimate an upper limit of the permeability and a minimum fracture length from:

$$k \leq \frac{30.358QB\mu}{h(\Delta p)_{last}} \qquad [1.5.46]$$

$$x_f \geq \sqrt{\frac{0.01648k(t)_{last}}{\phi\mu c_t}} \qquad [1.5.47]$$

The above two approximations are only valid for $x_e/x_f \gg 1$ and for infinite conductivity fractures. For uniform-flux fracture, the constants 30.358 and 0.01648 become 107.312 and 0.001648.

To illustrate the use of the Gringarten type curves in analyzing well test data, the authors presented the following example:

Example 1.38 Tabulated below is the pressure buildup data for an infinite conductivity fractured well:

Δt (hr)	p_{ws} (psi)	$p_{ws} - p_{wf \text{ at } \Delta t=0}$ (psi)	$(t_p + \Delta t)\Delta t$
0.000	3420.0	0.0	0.0
0.083	3431.0	11.0	9 3600.0
0.167	3435.0	15.0	4 6700.0
0.250	3438.0	18.0	3 1200.0
0.500	3444.5	24.5	1 5600.0
0.750	3449.0	29.0	1 0400.0
1.000	3542.0	32.0	7800.0
2.000	3463.0	43.0	3900.0
3.000	3471.0	51.0	2600.0
4.000	3477.0	57.0	1950.0
5.000	3482.0	62.0	1560.0
6.000	3486.0	66.0	1300.0
7.000	3490.0	70.0	1120.0
8.000	3495.0	75.0	976.0
9.000	3498.0	78.0	868.0
10.000	3500.0	80.0	781.0
12.000	3506.0	86.0	651.0
24.000	3528.0	108.0	326.0
36.000	3544.0	124.0	218.0
48.000	3555.0	135.0	164.0
60.000	3563.0	143.0	131.0
72.000	3570.0	150.0	109.0
96.000	3582.0	162.0	82.3
120.000	3590.0	170.0	66.0
144.000	3600.0	180.0	55.2
192.000	3610.0	190.0	41.6
240.000	3620.0	200.0	33.5

Other available data:

$p_i = 3700$, $r_w = 0.28$ ft,
$\phi = 12\%$, $h = 82$ ft,
$c_t = 21 \times 10^{-6}$ psi^{-1}, $\mu = 0.65$ cp,
$B = 1.26$ bbl/STB, $Q = 419$ STB/day,
$t_p = 7800$ hours
drainage area = 1600 acres (not fully developed)

Calculate:

- permeability;
- fracture half-length, x_f;
- skin factor.

Solution

Step 1. Plot Δp vs. Δt on tracing paper with the same scale as the Gringarten type curve of Figure 1.82. Superimpose the tracing paper on the type curve, as shown in Figure 1.84, with the following match points:

$$(\Delta p)_{MP} = 100 \text{ psi}$$
$$(\Delta t)_{MP} = 10 \text{ hours}$$
$$(p_D)_{MP} = 1.22$$
$$(t_D)_{MP} = 0.68$$

Step 2. Calculate k and x_f by using Equations 1.5.43 and 1.5.44:

$$k = \frac{141.2QB\mu}{h}\left[\frac{p_D}{\Delta p}\right]_{MP}$$
$$= \frac{(141.2)(419)(1.26)(0.65)}{(82)}\left[\frac{1.22}{100}\right] = 7.21 \text{ md}$$

$$x_f = \sqrt{\frac{0.0002637k}{\phi\mu C_t}\left(\frac{\Delta t}{t_{Dxf}}\right)_{MP}}$$
$$= \sqrt{\frac{0.0002637(7.21)}{(0.12)(0.65)(21\times10^{-6})}\left(\frac{10}{0.68}\right)} = 131 \text{ ft}$$

Step 3. Calculate the skin factor by applying Equation 1.5.45:

$$s = \ln\left(\frac{2r_w}{x_f}\right)$$
$$\approx \ln\left[\frac{(2)(0.28)}{131}\right] = 5.46$$

Step 4. Approximate the time that marks the start of the semilog straight line based on the Gringarten et al. criterion. That is:

$$t_{Dx_f} = \left[\frac{0.0002637k}{\phi\mu c_t x_f^2}\right] t \geq 3$$

or:

$$t \geq \frac{(3)(0.12)(0.68)(21\times10^{-6})(131)^2}{(0.0002637)(7.21)} \geq 50 \text{ hours}$$

All the data beyond 50 hours can be used in the conventional Horner plot approach to estimate

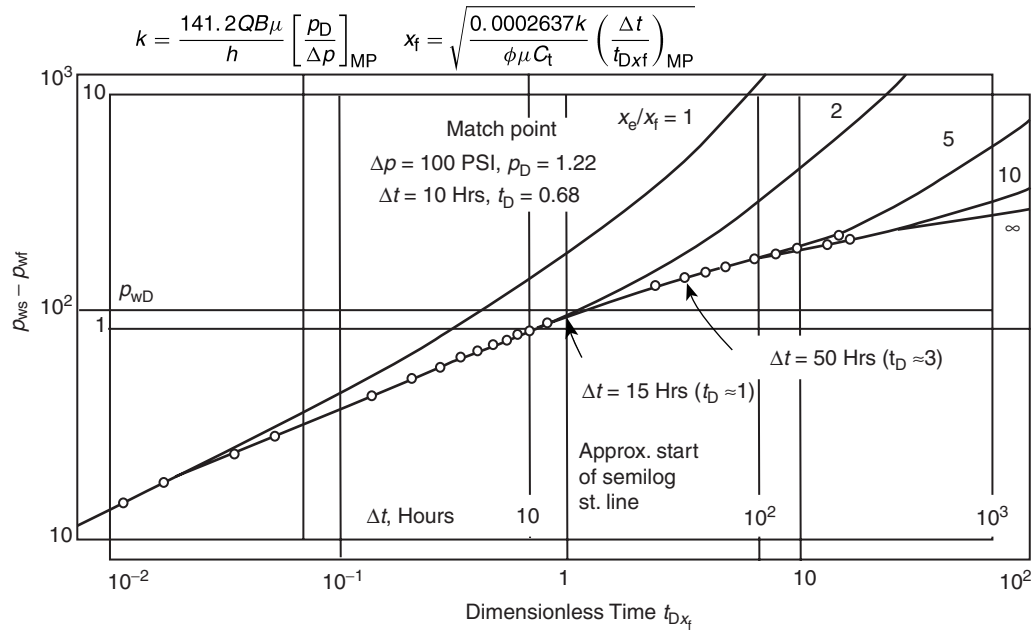

Figure 1.84 *Type curve matching. Data from Example 1.38 (Copyright ©1974 SPE, Gringarten et al., SPEJ, August 1974).*

permeability and skin factor. Figure 1.85 shows a Horner graph with the following results:

$$m = 95 \text{ psi/cycle}$$
$$p^* = 3764 \text{ psi}$$
$$p_{1\text{ hr}} = 3395 \text{ psi}$$
$$k = 7.16 \text{ md}$$
$$s = -5.5$$
$$x_f = 137 \text{ ft}$$

Cinco and Samaniego (1981) developed the type curves shown in Figure 1.86 for finite conductivity vertical fracture. The proposed type curve is based on the bilinear flow theory and presented in terms of $(p_D F_{CD})$ vs. $(t_{Dx_f} F_{CD}^2)$ on a log–log scale for various values of F_{CD} ranging from 0.1π to 1000π. The main feature of this graph is that for all values of F_{CD} the behavior of the bilinear flow ($\frac{1}{4}$ slope) and the formation linear flow ($\frac{1}{2}$ slope) is given by a single curve. Note that there is a transition period between the bilinear and linear flows. The dashed line in this figure indicates the approximate start of the infinite-acting pseudoradial flow.

The pressure data is plotted in terms of $\log(\Delta p)$ vs. $\log(t)$ and the resulting graph is matched to a type curve that is characterized by a dimensionless finite conductivity, $(F_{CD})_M$, with match points of:

- $(\Delta p)_{MP}$, $(p_D F_{CD})_{MP}$;
- $(t)_{MP}$, $(t_{Dx_f} F_{CD}^2)_{MP}$;
- end of bilinear flow $(t_{ebf})_{MP}$;
- beginning of formation linear flow $(t_{blf})_{MP}$;
- beginning of semilog straight line $(t_{bssl})_{MP}$.

From the above match F_{CD} and x_f can be calculated:

$$\text{For oil} \quad F_{CD} = \left[\frac{141.2QB\mu}{hk}\right]\frac{(p_D F_{CD})_{MP}}{(\Delta p)_{MP}} \qquad [1.5.48]$$

$$\text{For gas} \quad F_{CD} = \left[\frac{1424QT}{hk}\right]\frac{(p_D F_{CD})_{MP}}{(\Delta m(p))_{MP}} \qquad [1.5.49]$$

The fracture half-length is given by:

$$x_f = \left[\frac{0.0002637k}{\phi\mu c_t}\right]\frac{(t)_{MP}(F_{CD})_M^2}{(t_{Dx_f} F_{CD}^2)_{MP}} \qquad [1.5.50]$$

Defining the dimensionless effective wellbore radius $r_{wD}^{\backslash}$ as the ratio of the apparent wellbore radius $r_w^{\backslash}$ to the fracture half-length x_f, i.e., $r_{wD}^{\backslash} = r_w^{\backslash}/x_f$, Cinco and Samaniego correlated $r_{wD}^{\backslash}$ with the dimensionless fracture conductivity F_{CD} and presented the resulting correlation in graphical form, as shown in Figure 1.87.

Figure 1.87 indicates that when the dimensionless fracture conductivity is greater than 100, the dimensionless effective wellbore radius $r_{wD}^{\backslash}$ is independent of the fracture conductivity with a fixed value of 0.5, i.e., $r_{wD}^{\backslash} = 0.5$ for $F_{CD} > 100$. The apparent wellbore radius is expressed in terms of the fracture skin factor s_f by:

$$r_w^{\backslash} = r_w e^{-s_f}$$

Introducing $r_{wD}^{\backslash}$ into the above expression and solving for s_f gives:

$$s_f = \ln\left[\left(\frac{x_f}{r_w}\right) r_{wD}^{\backslash}\right]$$

For $F_{CD} > 100$, this gives:

$$s_f = -\ln\left(\frac{x_f}{2r_w}\right)$$

where:

s_f = skin due to fracture
r_w = wellbore radius, ft

It should be kept in mind that specific analysis graphs must be used for different flow regimes to obtain a better estimate of both fracture and reservoir parameters. Cinco and Samaniego used the following pressure buildup data to illustrate the use of their type curve to determine the fracture and reservoir parameters.

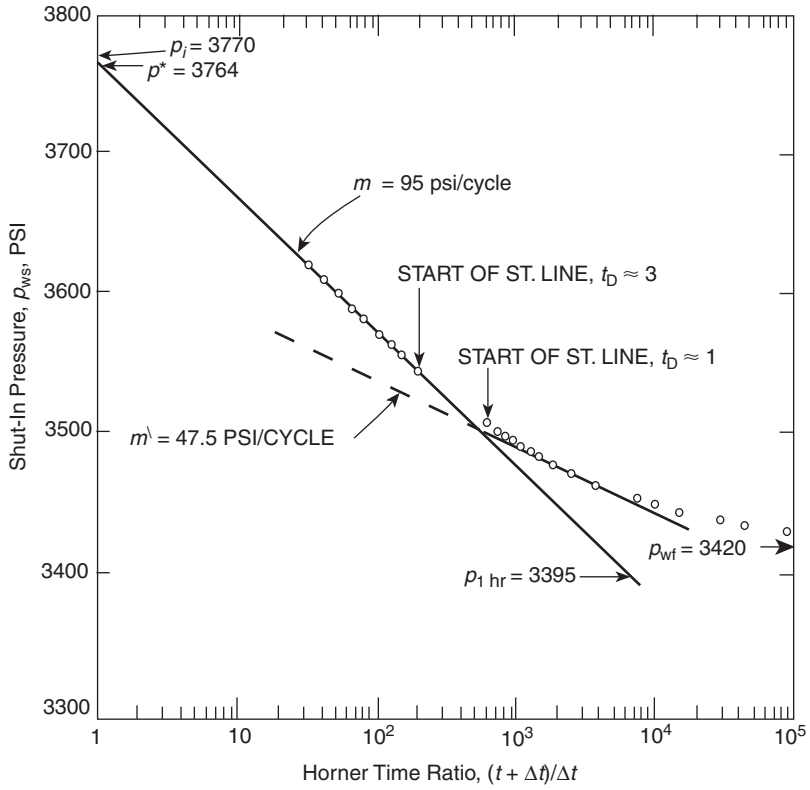

Figure 1.85 *Horner graph for a vertical fracture (infinite conductivity).*

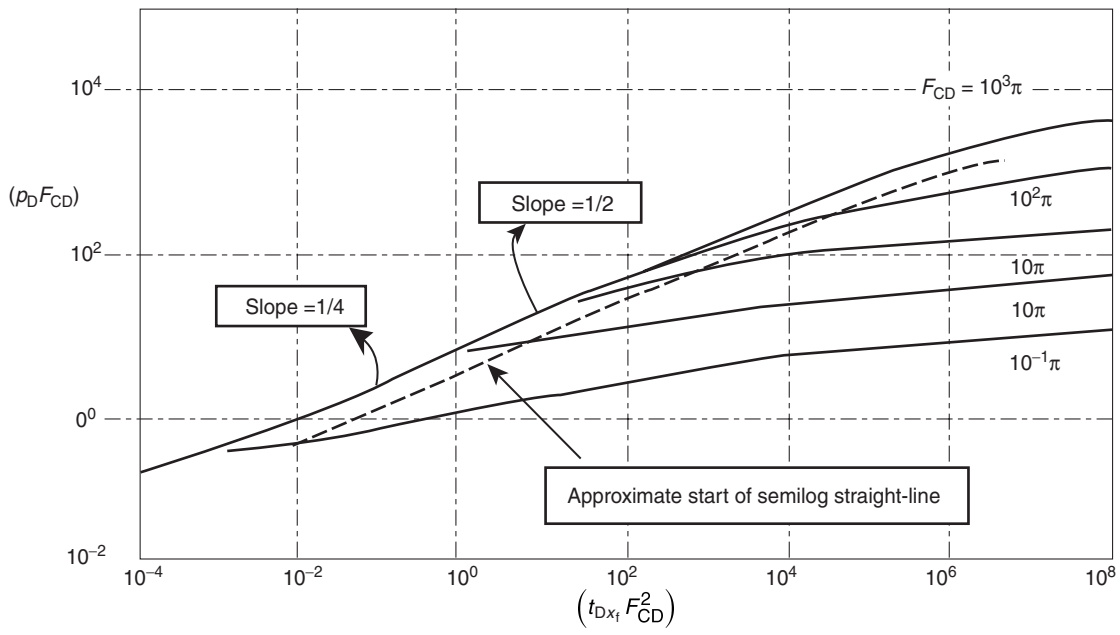

Figure 1.86 *Type curve for vertically fractured gas wells graph (After Cinco and Samaniego, 1981).*

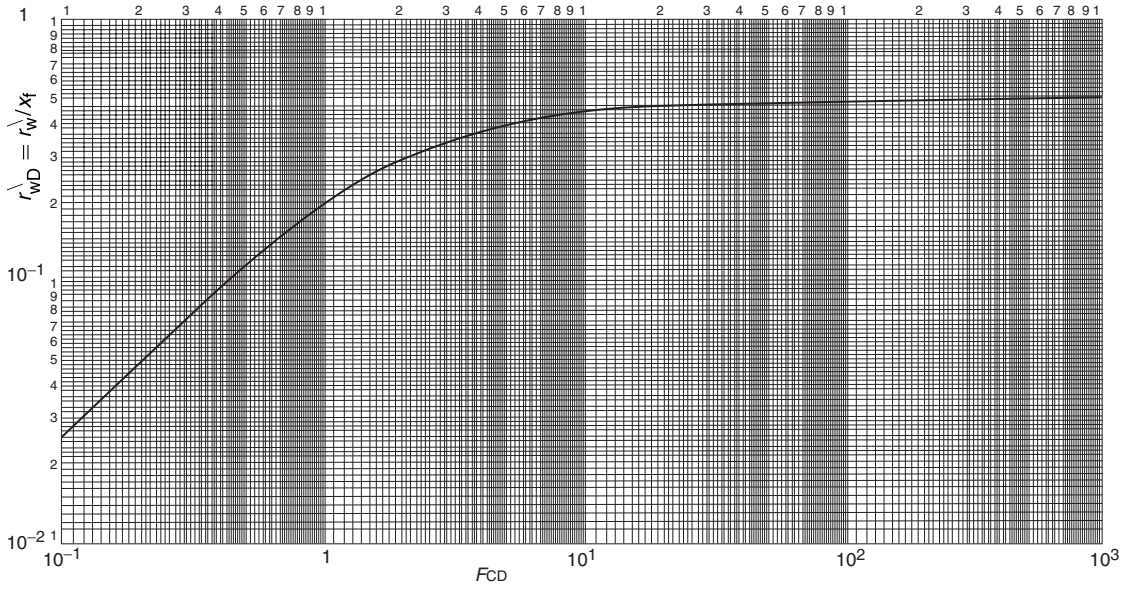

Figure 1.87 *Effective wellbore radius vs. dimensionless fracture conductivity for a vertical fracture graph (After Cinco and Samaniego, 1981).*

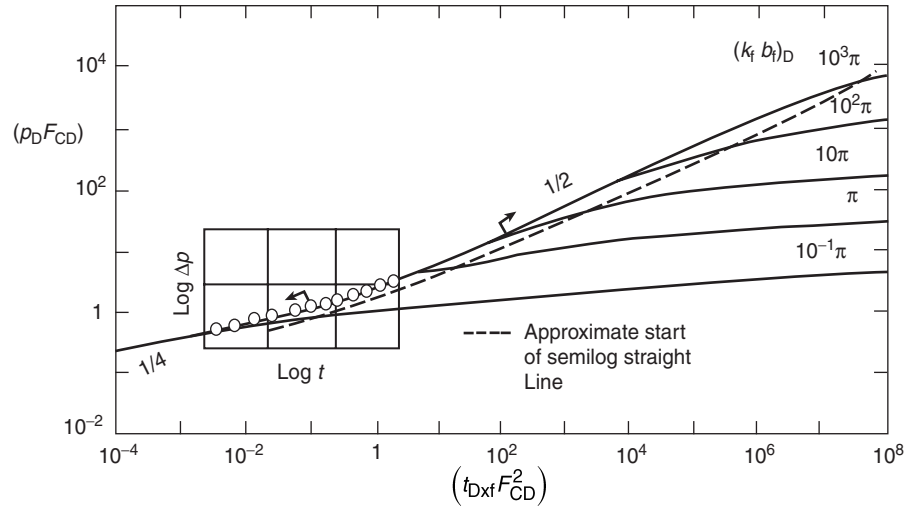

Figure 1.88 *Type curve matching for data in bilinear and transitional flow graph (After Cinco and Samaniego, 1981).*

Example 1.39 The buildup test data as given in Example 1.36 is given below for convenience:

$Q = 7350$ Mscf/day, $t_p = 2640$ hours

$h = 118$ ft, $\phi = 0.10$

$k = 0.025$ md, $\mu = 0.0252$

$T = 690°$R, $c_t = 0.129 \times 10^{-3}$ psi^{-1}

$p_{wf \text{ at } \Delta t=0} = 1320$ psia, $r_w = 0.28$ ft

The graphical presentation of the buildup data is given in the following two forms:

(1) The log–log plot of $\Delta m(p)$ vs. $(\Delta t)^{1/4}$, as shown earlier in Figure 1.73.

(2) The log–log plot of $\Delta m(p)$ vs. (Δt), on the type curve of Figure 1.86 with the resulting match as shown in Figure 1.88.

Calculate the fracture and reservoir parameters by performing conventional and type curve analysis. Compare the results.

Solution

Step 1. From the plot of $\Delta m(p)$ vs. $(\Delta t)^{1/4}$, in Figure 1.73, determine:

$m_{bf} = 1.6 \times 10^8$ psi^2/cphr$^{1/4}$

$t_{sbf} \approx 0.35$ hrs (start of bilinear flow)

$t_{ebf} \approx 2.5$ hrs (end of bilinear flow)

$\Delta m(p)_{ebf} \approx 2.05 \times 10^8$ psi^2/cp

Step 2. Perform the bilinear flow analysis, as follows:

- Using Equation 1.5.34, calculate fracture conductivity F_C:

$$F_C = \left[\frac{444.6QT}{m_{bf}h(\phi\mu c_t k)^{1/4}}\right]^2$$

$$= \left[\frac{444.6(7350)(690)}{(1.62\times10^8)(118)[(0.1)(0.0252)(0.129\times10^{-3})(0.025)]^{1/4}}\right]^2$$

$$= 154 \text{ md ft}$$

- Calculate the dimensionless conductivity F_{CD} by using Equation 1.5.36:

$$F_{CD} = \frac{1965.1QT}{kh\Delta m(p)_{ebf}}$$

$$= \frac{1965.1(7350)(690)}{(0.025)(118)(2.02\times10^8)} = 16.7$$

- Estimate the fracture half-length from Equation 1.5.21:

$$x_f = \frac{F_C}{F_{CD}k}$$

$$= \frac{154}{(16.7)(0.025)} = 368 \text{ ft}$$

- Estimate the dimensionless ratio $r_w^{\backslash}/x_f$ from Figure 1.86:

$$\frac{r_w^{\backslash}}{x_f} \approx 0.46$$

- Calculate the apparent wellbore radius $r_w^{\backslash}$:

$$r_w^{\backslash} = (0.46)(368) = 169 \text{ ft}$$

- Calculate the apparent skin factor

$$s = \ln\left(\frac{r_w}{r_w^{\backslash}}\right) = \ln\left(\frac{0.28}{169}\right) = -6.4$$

Step 3. Perform the type curve analysis as follows:

- Determine the match points from Figure 1.88, to give:

$$\Delta m(p)_{MP} = 10^9 \text{ psi}^2/\text{cp}$$

$$(p_D F_{CD})_{MP} = 6.5$$

$$(\Delta t)_{mp} = 1 \text{ hour}$$

$$[t_{Dx_f}(F_{CD})^2]_{MP} = 3.69\times10^{-2}$$

$$t_{sbf} \simeq 0.35 \text{ hour}$$

$$t_{ebf} = 2.5 \text{ hour}$$

- Calculate F_{CD} from Equation

$$F_{CD} = \left[\frac{1424(7350)(690)}{(118)(0.025)}\right]\frac{6.5}{(10^9)} = 15.9$$

- Calculate the fracture half-length from Equation 1.5.49:

$$x_f = \left[\frac{0.0002637(0.025)}{(0.1)(0.0252)(0.129\times10^{-3})}\frac{(1)(15.9)^2}{3.69\times10^{-2}}\right]^{1/2}$$

$$= 373 \text{ ft}$$

- Calculate F_C from Equation 1.5.21:

$$F_C = F_{CD}x_f k = (15.9)(373)(0.025) = 148 \text{ md ft}$$

- From Figure 1.86 :

$$r_w^{\backslash}/x_f = 0.46$$

$$r_w^{\backslash} = (373)(0.46) = 172 \text{ ft}$$

Test results	*Type curve analysis*	*Bilinear flow analysis*
F_C	148.0	154.0
x_f	373.0	368.0
F_{CD}	15.9	16.7
$r_w^{\backslash}$	172.0	169.0

The concept of the pressure derivative can be effectively employed to identify different flow regime periods associated with hydraulically fractured wells. As shown in Figure 1.89, a finite conductivity fracture shows a $\frac{1}{4}$ straight-line slope for both the pressure difference Δp and its derivative; however, the two parallel lines are separated by a factor of 4. Similarly, for an infinite conductivity fracture, two straight parallel lines represent Δp and its derivative with a $\frac{1}{2}$ slope and separation between the lines of a factor of 2 (as shown in Figure 1.90).

In tight reservoirs where the productivity of wells is enhanced by massive hydraulic fracturing (MHF), the resulting fractures are characterized as long vertical fractures with finite conductivities. These wells tend to produce at a constant and low bottom-hole flowing pressure, rather than constant flow rate. The diagnostic plots and the conventional analysis of bilinear flow data can be used when analyzing

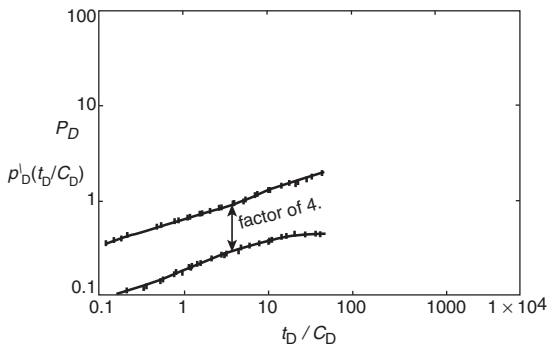

Figure 1.89 *Finite conductivity fracture shows as a $\frac{1}{4}$ slope line on a log–log plot, same on a derivative plot. Separation between pressure and derivative is a factor of 4.*

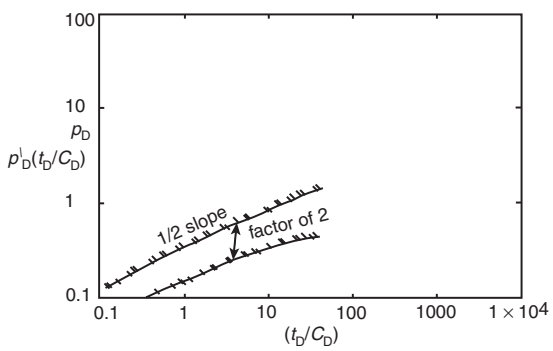

Figure 1.90 *Infinite conductivity fracture shows as a $\frac{1}{2}$ slope line on a log–log plot, same on a derivative plot. Separation between pressure and derivative is a factor of 2.*

well test data under constant flowing pressure. Equations 1.5.27 through 1.5.31 can be rearranged and expressed in the following forms.

For fractured oil wells

$$\frac{1}{Q} = \left[\frac{44.1B\mu}{h\sqrt{F_C}(\phi\mu c_t k)^{1/4}\Delta p}\right] t^{1/4}$$

or equivalently:

$$\frac{1}{Q} = m_{bf} t^{1/4}$$

and:

$$\log\left(\frac{1}{Q}\right) = \log(m_{bf}) + 1/4\log(t)$$

where:

$$m_{bf} = \frac{44.1B\mu}{h\sqrt{F_C}(\phi\mu c_t k)^{1/4}\Delta p}$$

$$F_C = k_f w_f = \left[\frac{44.1B\mu}{h m_{bf}(\phi\mu c_t k)^{1/2}\Delta p}\right]^2 \quad [1.5.51]$$

For fractured gas wells

$$\frac{1}{Q} = m_{bf} t^{1/4}$$

or:

$$\log\left(\frac{1}{Q}\right) = \log(m)$$

where:

$$m_{bf} = \frac{444.6T}{h\sqrt{F_C}(\phi\mu c_t k)^{1/4}\Delta m(p)}$$

Solving for F_C:

$$F_C = \left[\frac{444.6T}{h m_{bf}(\phi\mu c_t k)^{1/4}\Delta m(p)}\right]^2 \quad [1.5.52]$$

The following procedure can be used to analyze bilinear flow data under constant flow pressure:

Step 1. Plot $1/Q$ vs. t on a log–log scale and determine if any data falls on a straight line of a $\frac{1}{4}$ slope.
Step 2. If any data forms a $\frac{1}{4}$ slope in step 1, plot $1/Q$ vs. $t^{1/4}$ on a Cartesian role and determine the slope m_{bf}.
Step 3. Calculate the fracture conductivity F_C from Equation 1.5.51 or 1.5.52:

$$\text{For oil} \quad F_C = \left[\frac{44.1B\mu}{h m_{bf}(\phi\mu c_t k)^{1/4}(p_i - p_{wf})}\right]^2$$

$$\text{For gas} \quad F_C = \left[\frac{444.6T}{h m_{bf}(\phi\mu c_t k)^{1/4}[m(p_i) - m(p_{wf})]}\right]^2$$

Step 4. Determine the value of Q when the bilinear straight line ends and designate it as Q_{ebf}.
Step 5. Calculate F_{CD} from Equation 1.5.35 or 1.5.36:

$$\text{For oil} \quad F_{CD} = \frac{194.9Q_{ebf}B\mu}{kh(p_i - p_{wf})}$$

$$\text{For gas} \quad F_{CD} = \frac{1965.1Q_{ebf}T}{kh[m(p_i) - m(p_{wf})]}$$

Step 6. Estimate the fracture half-length from:

$$x_f = \frac{F_C}{F_{CD}k}$$

Agarwal et al. (1979) presented constant-pressure type curves for finite conductivity fractures, as shown in Figure 1.91. The reciprocal of the dimensionless rate $1/Q_D$ is expressed as a function of dimensionless time t_{Dx_f}, on log–log paper, with the dimensionless fracture conductivity F_{CD} as a correlating parameter. The reciprocal dimensionless rate $1/Q_D$ is given by:

$$\text{For oil wells} \quad \frac{1}{Q_D} = \frac{kh(p_i - p_{wf})}{141.2Q\mu B} \quad [1.5.53]$$

$$\text{For gas wells} \quad \frac{1}{Q_D} = \frac{kh[m(p_i) - m(p_{wf})]}{1424QT} \quad [1.5.54]$$

with:

$$t_{Dx_f} = \frac{0.0002637kt}{\phi(\mu c_t)_i x_f^2} \quad [1.5.55]$$

where:

p_{wf} = wellbore pressure, psi
Q = flow rate, STB/day or Mscf/day
T = temperature, °R
t = time, hours

subscripts:

i = initial
D = dimensionless

The following example, as adopted from Agarwal et al. (1979), illustrates the use of these type curves.

Example 1.40 A pre-frac buildup test was performed on a well producing from a tight gas reservoir, to give a formation permeability of 0.0081 md. Following an MHF treatment, the well produced at a constant pressure with recorded rate-time data as given below:

t (days)	Q (Mscf/day)	$1/Q$ (day/Mscf)
20	625	0.00160
35	476	0.00210
50	408	0.00245
100	308	0.00325
150	250	0.00400
250	208	0.00481
300	192	0.00521

The following additional data is available:

$p_i = 2394$ psi, $\Delta m(p) = 396 \times 10^6$ psi^2/cp
$h = 32$ ft, $\phi = 0.107$
$T = 720$°R, $c_{ti} = 2.34 \times 10^{-4}$ psi^{-1}
$\mu_i = 0.0176$ cp, $k = 0.0081$ md

Calculate:

- fracture half-length, x_f;
- fracture conductivity, F_C.

Solution

Step 1. Plot $1/Q$ vs. t on tracing paper, as shown in Figure 1.92, using the log–log scale of the type curves.
Step 2. We must make use of the available values of k, h, and $\Delta m(p)$ by arbitrarily choosing a convenient value of the flow rate and calculating the corresponding $1/Q_D$. Selecting $Q = 1000$ Mscf/day, calculate the corresponding value of $1/Q_D$ by applying Equation 1.5.54:

$$\frac{1}{Q_D} = \frac{kh\Delta m(p)}{1424QT} = \frac{(0.0081)(32)(396 \times 10^6)}{1424(1000)(720)} = 0.1$$

Step 3. Thus, the position of $1/Q = 10^{-3}$ on the y axis of the tracing paper is fixed in relation to $1/Q_D = 0.1$ on the y axis of the type curve graph paper; as shown in Figure 1.93.

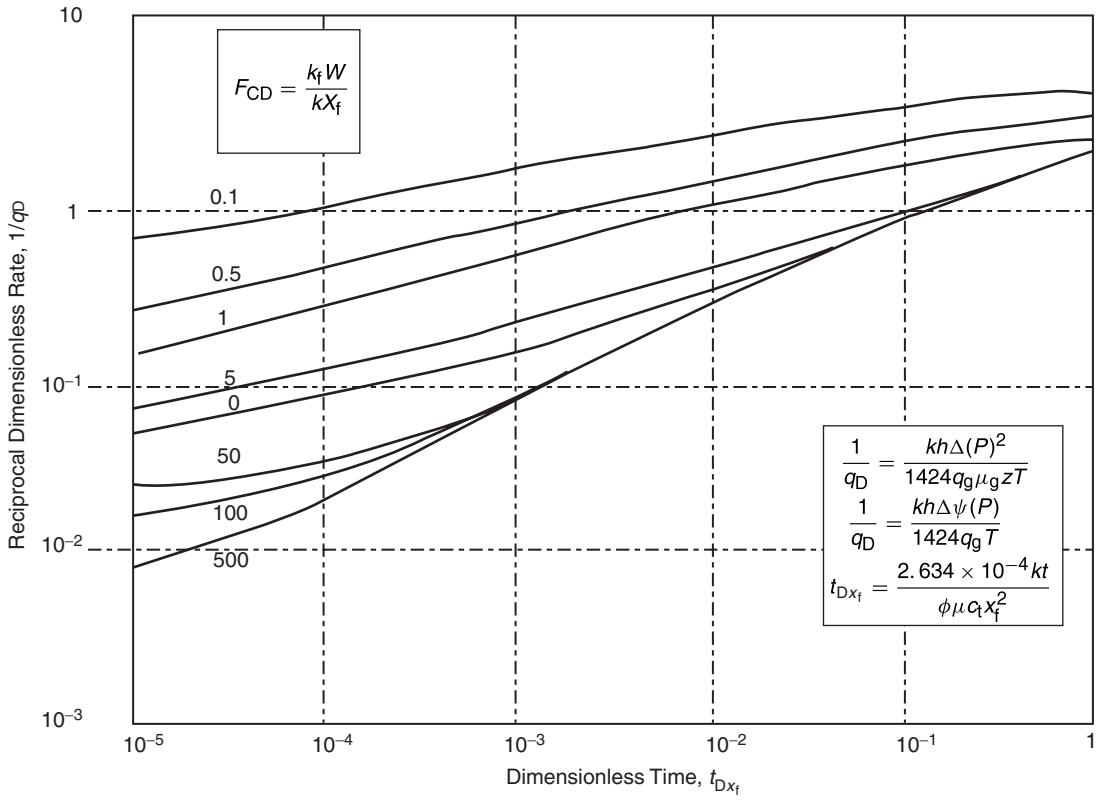

Figure 1.91 *Log–log type curves for finite capacity vertical fractures; constant wellbore pressure (After Agarwal et al., 1979).*

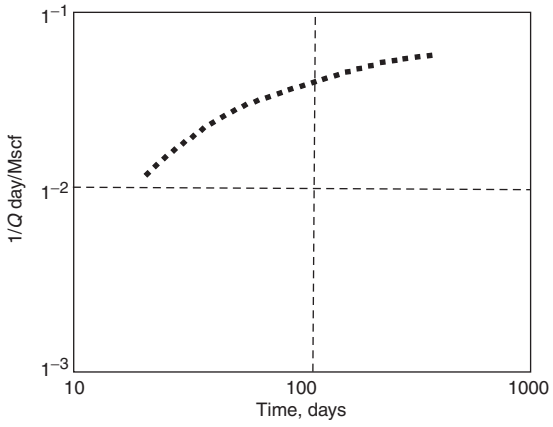

Figure 1.92 *Reciprocal smooth rate vs. time for MHF, Example 1.42.*

Step 4. Move the tracing paper horizontally along the x axis until a match is obtained, to give:

$$t = 100 \text{ days} = 2400 \text{ hours}$$
$$t_{Dx_f} = 2.2 \times 10^{-2}$$
$$F_{CD} = 50$$

Step 5. Calculate the fracture half-length from Equation 1.5.55:

$$x_f^2 = \left[\frac{0.0002637k}{\phi(\mu c_t)_i}\right]\left(\frac{t}{t_{Dx_f}}\right)_{MP}$$
$$= \left[\frac{0.0002637(0.0081)}{(0.107)(0.0176)(2.34 \times 10^{-4})}\right]\left(\frac{2400}{2.2 \times 10^{-2}}\right)$$
$$= 528\,174$$
$$x_f \approx 727 \text{ ft}$$

Thus the total fracture length is:

$$2x_f = 1454 \text{ ft}$$

Step 6. Calculate the fracture conductivity F_C from Equation 1.5.2:

$$F_C = F_{CD} k x_f = (50)(0.0081)(727) = 294 \text{ md ft}$$

It should be pointed out that if the pre-fracturing buildup test were not available, matching would require shifting the tracing paper along both the x and y axes to obtain the proper match. This emphasizes the need for determining kh from a pre-fracturing test.

Faults or impermeable barriers

One of the important applications of a pressure buildup test is analyzing the test data to detect or confirm the existence of faults and other flow barriers. When a sealing fault is located near a test well, it significantly affects the recorded well pressure behavior during the buildup test. This pressure

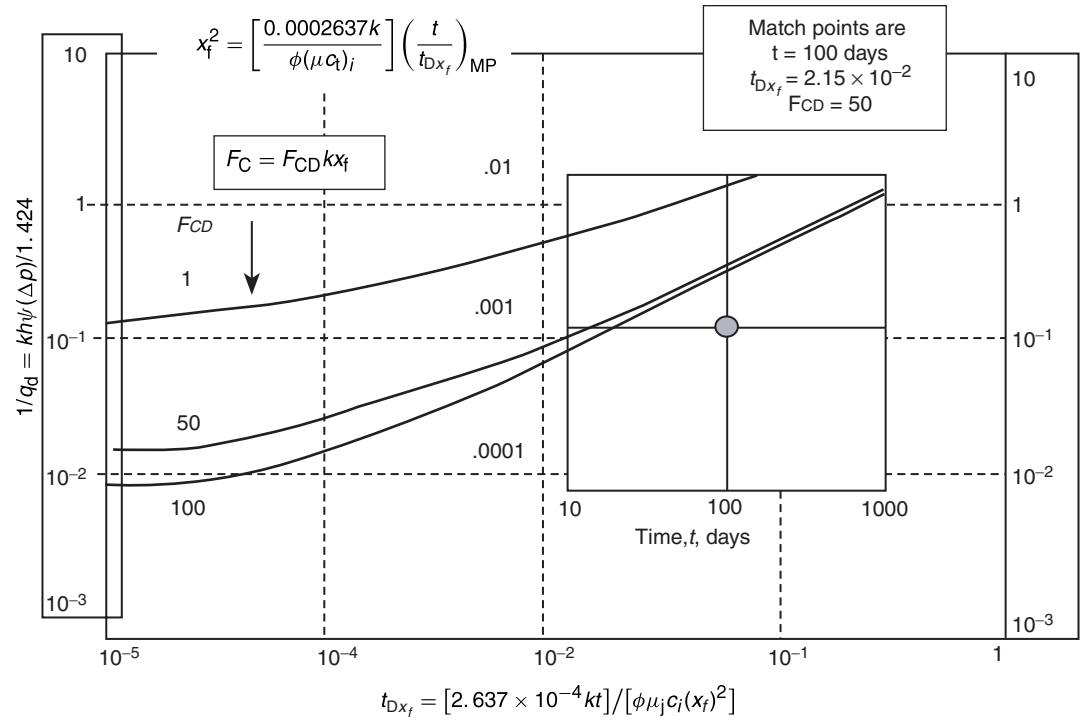

Figure 1.93 *Type curve matching for MHF gas well, Example 1.42.*

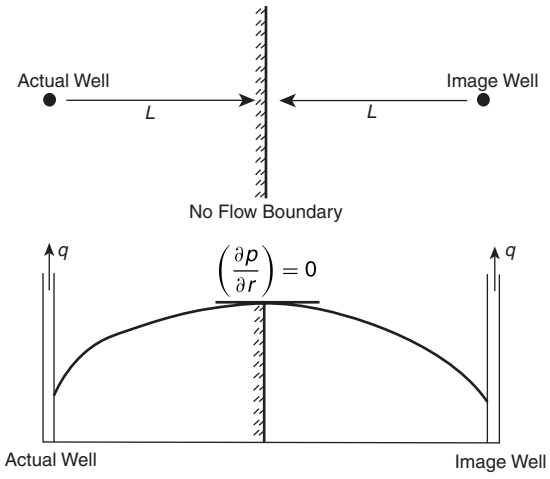

Figure 1.94 *Method of images in solving boundary problems.*

behavior can be described mathematically by applying the principle of superposition as given by the method of images. Figure 1.94 shows a test well that is located at a distance L from a sealing fault. Applying method images, as given Equation 1.2.157, the total pressure drop as a function of time t is:

$$(\Delta p)_{total} = \frac{162.6 Q_o B \mu}{kh}\left[\log\left(\frac{kt}{\phi\mu c_t r_w^2}\right) - 3.23 + 0.87s\right] - \left(\frac{70.6 Q_o B \mu}{kh}\right) \text{Ei}\left(-\frac{948\phi\mu c_t (2L)^2}{kt}\right)$$

When both the test well and image well are shut-in for a buildup test, the principle of superposition can be applied to Equation 1.2.57 to predict the buildup pressure at Δt as:

$$p_{ws} = p_i - \frac{162.6 Q_o B_o \mu_o}{kh}\left[\log\left(\frac{t_p + \Delta t}{\Delta t}\right)\right] - \left(\frac{70.6 Q_o B_o \mu_o}{kh}\right) \text{Ei}\left[\frac{-948\phi\mu c_t (2L)^2}{k(t_p + \Delta t)}\right] - \left(\frac{70.6(-Q_o) B_o \mu_o}{kh}\right) \text{Ei}\left[\frac{-948\phi\mu c_t (2L)^2}{k\Delta t}\right] \quad [1.5.56]$$

Recalling that the exponential integral $\text{Ei}(-x)$ can be approximated by Equation 1.2.68 when $x < 0.01$ as:

$$\text{Ei}(-x) = \ln(1.781x)$$

the value of the $\text{Ei}(-x)$ can be set equal to zero when x is greater than 10.9, i.e., $\text{Ei}(-x) = 0$ for $x > 10.9$. Notice that the value of $(2L)^2$ is large and for early buildup times, when Δt is small, the last two terms in can be set equal to zero, or:

$$p_{ws} = p_i - \frac{162.6 Q_o B_o \mu_o}{kh}\left[\log\left(\frac{t_p + \Delta t}{\Delta t}\right)\right] \quad [1.5.57]$$

which is essentially the regular Horner equation with a semilog straight-line slope of:

$$m = \frac{162.6 Q_o B_o \mu_o}{kh}$$

For a shut-in time sufficiently large that the *logarithmic approximation is accurate for the* Ei *functions*, Equation 1.5.56 becomes:

$$p_{ws} = p_i - \frac{162.6 Q_o B_o \mu_o}{kh}\left[\log\left(\frac{t_p + \Delta t}{\Delta t}\right)\right] - \frac{162.6 Q_o B_o \mu_o}{kh}\left[\log\left(\frac{t_p + \Delta t}{\Delta t}\right)\right]$$

Rearranging this equation by recombining terms gives:

$$p_{ws} = p_i - 2\left(\frac{162.6Q_oB_o\mu_o}{kh}\right)\left[\log\left(\frac{t_p + \Delta t}{\Delta t}\right)\right]$$

Simplifying:

$$p_{ws} = p_i - 2m\left[\log\left(\frac{t_p + \Delta t}{\Delta t}\right)\right] \qquad [1.5.58]$$

Three observations can be made by examining Equations 1.5.57 and 1.5.58:

(1) For early shut-in time buildup data, Equation 1.5.57 indicates that the data from the early shut-in times will form a straight line on the Horner plot with a slope that is identical to a reservoir without sealing fault.
(2) At longer shut-in times, the data will form a *second straight line* on the Horner plot with a slope that is twice that of the first line, i.e., second slope $= 2m$. The presence of the second straight line with a double slope of the first straight line provides a means of recognizing the presence of a fault from pressure buildup data.
(3) The shut-in time required for the slope to double can be approximated from the following expression:

$$\frac{948\phi\mu c_t(2L)^2}{k\Delta t} < 0.01$$

Solving for Δt gives:

$$\Delta t > \frac{380\,000\phi\mu c_t L^2}{k}$$

where:

Δt = minimum shut-in time, hours
k = permeability, md
L = distance between well and the sealing fault, ft

Notice that the value of p^* for use in calculating the average drainage region pressure $\bar{p}$ is obtained by extrapolating the *second straight line* to a unit-time ratio, i.e., to $(t_p + \Delta t)/\Delta t = 1.0$. The permeability and skin factor are calculated in the normal manner described before using the slope of the *first straight line*.

Gray (1965) suggested that for the case in which the slope of the buildup test has the time to double, as shown schematically in Figure 1.95, the distance L from the well to the fault can be calculated by finding the time Δt_x at which the two semilog straight lines intersect. That is:

$$L = \sqrt{\frac{0.000148k\Delta t_x}{\phi\mu c_t}} \qquad [1.5.59]$$

Lee (1982) illustrated Gray's method through the following examples.

Example 1.41 A pressure buildup test was conducted to confirm the existence of a sealing fault near a newly drilled well. Data from the test is given below:

Δt (hr)	p_{ws} (psi)	$(t_p + \Delta t)/\Delta t$
6	3996	47.5
8	4085	35.9
10	4172	28.9
12	4240	24.3
14	4298	20.9
16	4353	18.5
20	4435	15.0
24	4520	12.6

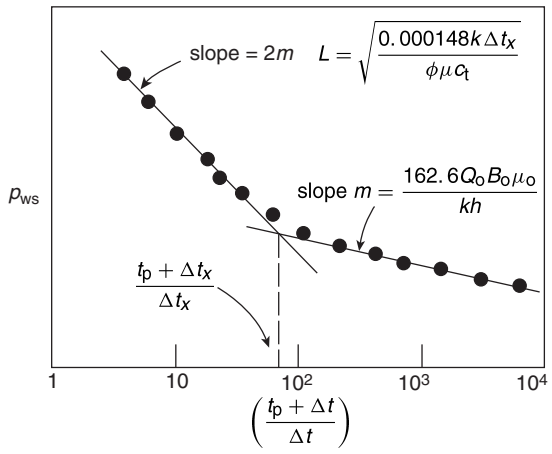

Figure 1.95 *Theoretical Horner plot for a faulted system.*

Δt (hr)	p_{ws} (psi)	$(t_p + \Delta t)/\Delta t$
30	4614	10.3
36	4700	8.76
42	4770	7.65
48	4827	6.82
54	4882	6.17
60	4931	5.65
66	4975	5.23

Other data include the following:

$\phi = 0.15$, $\mu_o = 0.6$ cp,
$c_t = 17 \times 10^{-6}$ psi^{-1} $r_w = 0.5$ ft,
$Q_o = 1221$ STB/day, $h = 8$ ft
$B_o = 1.31$ bbl/STB,

A total of 14 206 STB of oil had been produced before shut-in. Determine whether the sealing fault exists and the distance from the well to the fault.

Solution

Step 1. Calculate total production time t_p:

$$t_p = \frac{24N_p}{Q_o} = \frac{(24)(14206)}{1221} = 279.2 \text{ hours}$$

Step 2. Plot p_{ws} vs. $(t_p + \Delta t)/\Delta t$ as shown in Figure 1.96. The plot clearly shows two straight lines with the first slope of 650 psi/cycle and the second with 1300 psi/cycle. Notice that the second slope is twice that of the first slope indicating the existence of the sealing fault.

Step 3. Using the value of the *first slope*, calculate the permeability k:

$$k = \frac{162.6Q_oB_o\mu_o}{mh} = \frac{162.6(1221)(1.31)(0.6)}{(650)(8)}$$

$$= 30 \text{ md}$$

Step 4. Determine the value of Horner's time ratio at the intersection of the two semilog straight lines shown in Figure 1.96, to give:

$$\frac{t_p + \Delta t_x}{\Delta t_x} = 17$$

or:

$$\frac{279.2 + \Delta t_x}{\Delta t_x} = 17$$

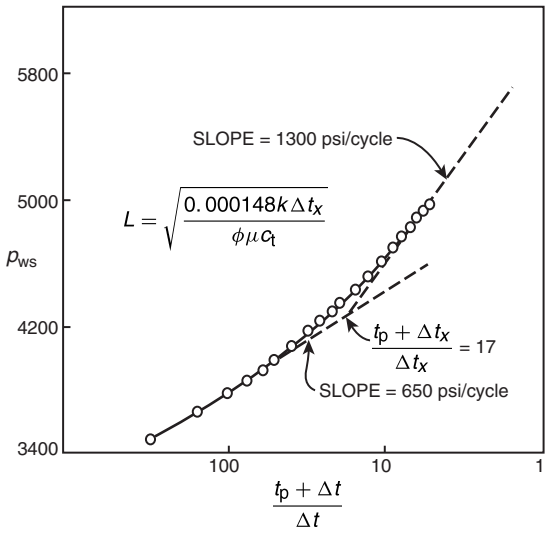

Figure 1.96 *Estimating distance to a no-flow boundary.*

from which:

$$\Delta t_x = 17.45 \text{ hours}$$

Step 5. Calculate the distance L from the well to the fault by applying Equation 1.5.59:

$$L = \sqrt{\frac{0.000148 k \Delta t_x}{\phi \mu c_t}}$$

$$= \sqrt{\frac{0.000148(30)(17.45)}{(0.15)(0.6)(17 \times 10^{-6})}} = 225 \text{ ft}$$

Qualitative interpretation of buildup curves

The Horner plot has been the most widely accepted means for analyzing pressure buildup data since its introduction in 1951. Another widely used aid in pressure transient analysis is the plot of change in pressure Δp versus time on a log–log scale. Economides (1988) pointed out that this log–log plot serves the following two purposes:

(1) the data can be matched to type curves;
(2) the type curves can illustrate the expected trends in pressure transient data for a large variety of well and reservoir systems.

The visual impression afforded by the log–log presentation has been greatly enhanced by the introduction of the pressure derivative which represents the changes of the slope of buildup data with respect to time. When the data produces a straight line on a semilog plot, the pressure derivative plot will, therefore, be constant. That means the pressure derivative plot will be flat for that portion of the data that can be correctly analyzed as a straight line on the Horner plot.

Many engineers rely on the log–log plot of Δp and its derivative versus time to diagnose and select the proper interpretation model for a given set of pressure transient data. Patterns visible in the log–log diagnostic and Horner plots for five frequently encountered reservoir systems are illustrated graphically by Economides as shown in Figure 1.97. The curves on the right represent buildup responses for five different patterns, a through e, with the curves on the left representing the corresponding responses when the data is plotted in the log–log format of Δp and $(\Delta t \Delta p\backslash)$ versus time.

The five different buildup examples shown in Figure 1.97 were presented by Economides (1988) and are briefly discussed below:

Example a illustrates the most common response—that of a homogeneous reservoir with wellbore storage and skin. Wellbore storage derivative transients are recognized as a "hump" in early time. The flat derivative portion in late time is easily analyzed as the Horner semilog straight line.

Example b shows the behavior of an infinite conductivity, which is characteristic of a well that penetrates a natural fracture. The $\frac{1}{2}$ slopes in both the pressure change and its derivative result in two parallel lines during the flow regime, representing linear flow to the fracture.

Example c shows the homogeneous reservoir with a single vertical planar barrier to flow or a fault. The level of the second-derivative plateau is twice the value of the level of the first-derivative plateau, and the Horner plot shows the familiar slope-doubling effect.

Example d illustrates the effect of a closed drainage volume. Unlike the drawdown pressure transient, this has a unit-slope line in late time that is indicative of pseudosteady-state flow; the buildup pressure derivative drops to zero. The permeability and skin cannot be determined from the Horner plot because no portion of the data exhibits a flat derivative for this example. When transient data resembles example d, the only way to determine the reservoir parameters is with a type curve match.

Example e exhibits a valley in the pressure derivative that is indicative of reservoir heterogeneity. In this case, the feature results from dual-porosity behavior, for the case of pseudosteady flow from matrix to fractures.

Figure 1.97 clearly shows the value of the pressure/pressure derivative presentation. An important advantage of the log–log presentation is that the transient patterns have a standard appearance as long as the data is plotted with square log cycles. The visual patterns in semilog plots are amplified by adjusting the range of the vertical axis. Without adjustment, many or all of the data may appear to lie on one line and subtle changes can be overlooked.

Some of the pressure derivative patterns shown are similar to those characteristics of other models. For example, the pressure derivative doubling associated with a fault (example c) can also indicate transient interporosity flow in a dual-porosity system. The sudden drop in the pressure derivative in buildup data can indicate either a closed outer boundary or constant-pressure outer boundary resulting from a gas cap, an aquifer, or pattern injection wells. The valley in the pressure derivative (example e) could indicate a layered system instead of dual porosity. For these cases and others, the analyst should consult geological, seismic, or core analysis data to decide which model to use in an interpretation. With additional data, a more conclusive interpretation for a given transient data set may be found.

An important place to use the pressure/pressure derivative diagnosis is on the well site. If the objective of the test is to determine permeability and skin, the test can be terminated once the derivative plateau is identified. If heterogeneities or boundary effects are detected in the transient, the test can be run longer to record the entire pressure/pressure derivative response pattern needed for the analysis.

1.6 Interference and Pulse Tests

When the flow rate is changed and the pressure response is recorded in the same well, the test is called a "single-well" test. Examples of single-well tests are drawdown, buildup, injectivity, falloff and step-rate tests. When the flow rate is changed in one well and the pressure response is recorded in another well, the test is called a "multiple-well" test.

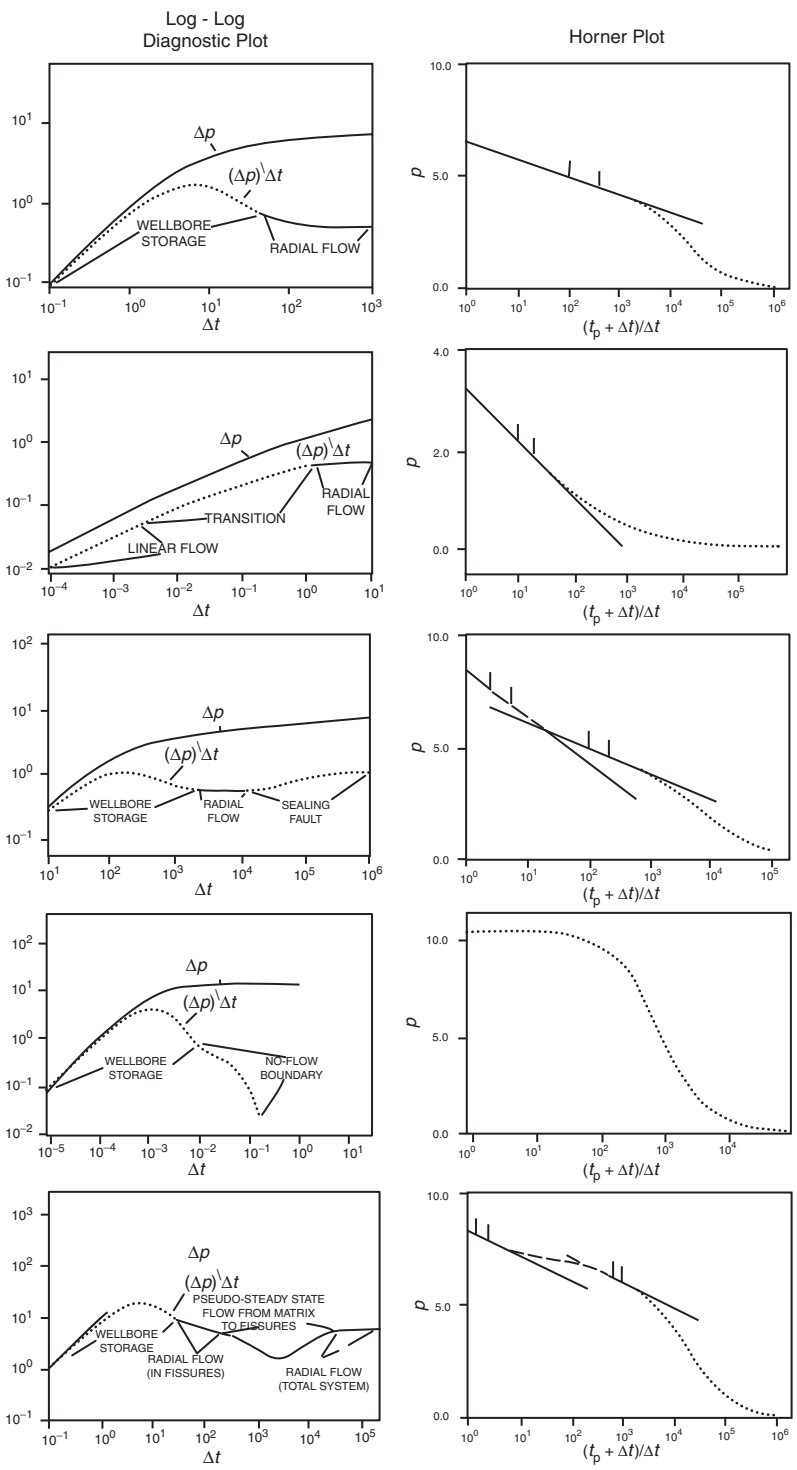

a

Well with Wellbore Storage and Skin in a Homogeneous Reservoir

b

Well with Infinite Conductivity Vertical Fracture in a Homogeneous Reservoir

c

Well with Wellbore Storage and skin in a Homogeneous Reservoir with One Sealing Fault

d

Well with Wellbore Storage and skin in a Homogeneous Reservoir with Closed Outer Boundary

e

Well with Wellbore Storage and skin in a Dual Porosity System with Pseudo-Steady State Flow from Matrix to Fractures

Figure 1.97 *Qualitative interpretation of buildup curves (After Economides, 1988).*

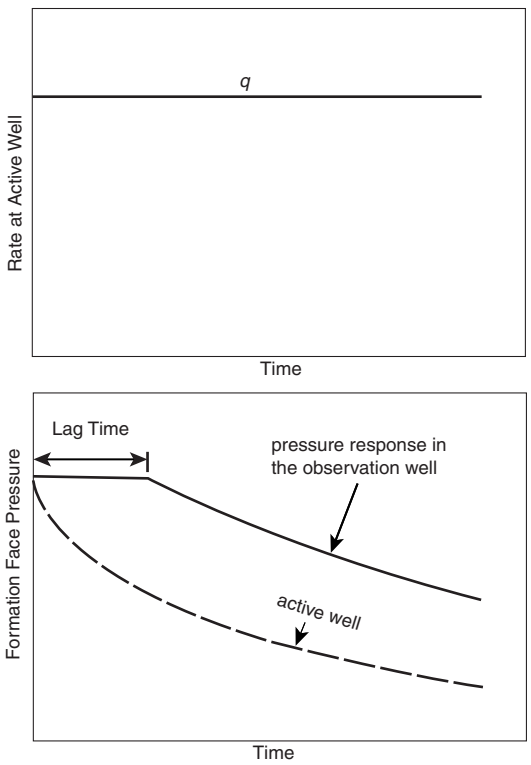

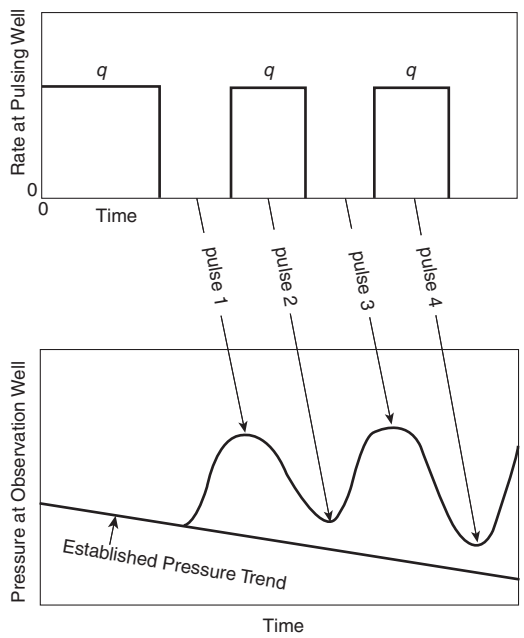

Figure 1.99 *Illustration of rate history and pressure response for a pulse test (After Earlougher, R. Advances in Well Test Analysis) (Permission to publish by the SPE, copyright SPE, 1977).*

Figure 1.98 *Rate history and pressure response of a two-well interference test conducted by placing the active well on production at constant rate.*

Examples of multiple-well tests are interference and pulse tests.

Single-well tests provide valuable reservoir and well characteristics that include flow capacity kh, wellbore conditions, and fracture length as examples of these important properties. However, these tests do not provide the directional nature of reservoir properties (such as permeability in the x, y, and z direction) and have inabilities to indicate the degree of communication between the test wells and adjacent wells. Multiple-well tests are run to determine:

- the presence or lack of communication between the test well and surrounding wells;
- the mobility–thickness product kh/μ;
- the porosity–compressibility–thickness product $\phi c_t h$;
- the fracture orientation if intersecting one of the test wells;
- the permeability in the direction of the major and minor axes.

The multiple-well test requires at least one active (producing or injecting) well and at least one pressure observation well, as shown schematically in Figure 1.98. In an interference test, all the test wells are shut-in until their wellbore pressures stabilize. The active well is then allowed to produce or inject at constant rate and the pressure response in the observation well(s) is observed. Figure 1.98 indicates this concept with one active well and one observation well. As the figure indicates, when the active well starts to produce, the pressure in the shut-in observation well begins to respond after some "time lag" that depends on the reservoir rock and fluid properties.

Pulse testing is a form of interference testing. The producer or injector is referred to as "the pulser or the active well" and the observation well is called "the responder." The tests are conducted by sending a series of short-rate pulses from the active well (producer or injector) to a shut-in observation well(s). Pulses generally are alternating periods of production (or injection) and shut-in, with the same rate during each production (injection) period, as illustrated in Figure 1.99 for a two-well system.

Kamal (1983) provided an excellent review of interference and pulse testing and summarized various methods that are used to analyze test data. These methods for analyzing interference and pulse tests are presented below.

1.6.1 Interference testing in homogeneous isotropic reservoirs

A reservoir is classified as "homogeneous" when the porosity and thickness do not change significantly with location. An "isotropic" reservoir indicates that the permeability is the same throughout the system. In these types of reservoirs, the type curve matching approach is perhaps the most convenient to use when analyzing interference test data in a homogeneous reservoir system. As given previously by Equation 1.2.66, the pressure drop at any distance r from an active well (i.e., distance between an active well and a shut-in observation well) is expressed as:

$$p_i - p(r,t) = \Delta p = \left[\frac{-70.6QB\mu}{kh}\right] \mathrm{Ei}\left[\frac{-948\phi c_t r^2}{kt}\right]$$

Earlougher (1977) expressed the above expression in a dimensionless form as:

$$\frac{p_i - p(r,t)}{\dfrac{141.2QB\mu}{kh}} = -\frac{1}{2}\mathrm{Ei}\left[\left(\frac{-1}{4}\right)\left(\frac{\phi\mu c_t r_w^2}{0.0002637kt}\right)\left(\frac{r}{r_w}\right)^2\right]$$

From the definitions of the dimensionless parameters p_D, t_D, and r_D, the above equations can be expressed in a

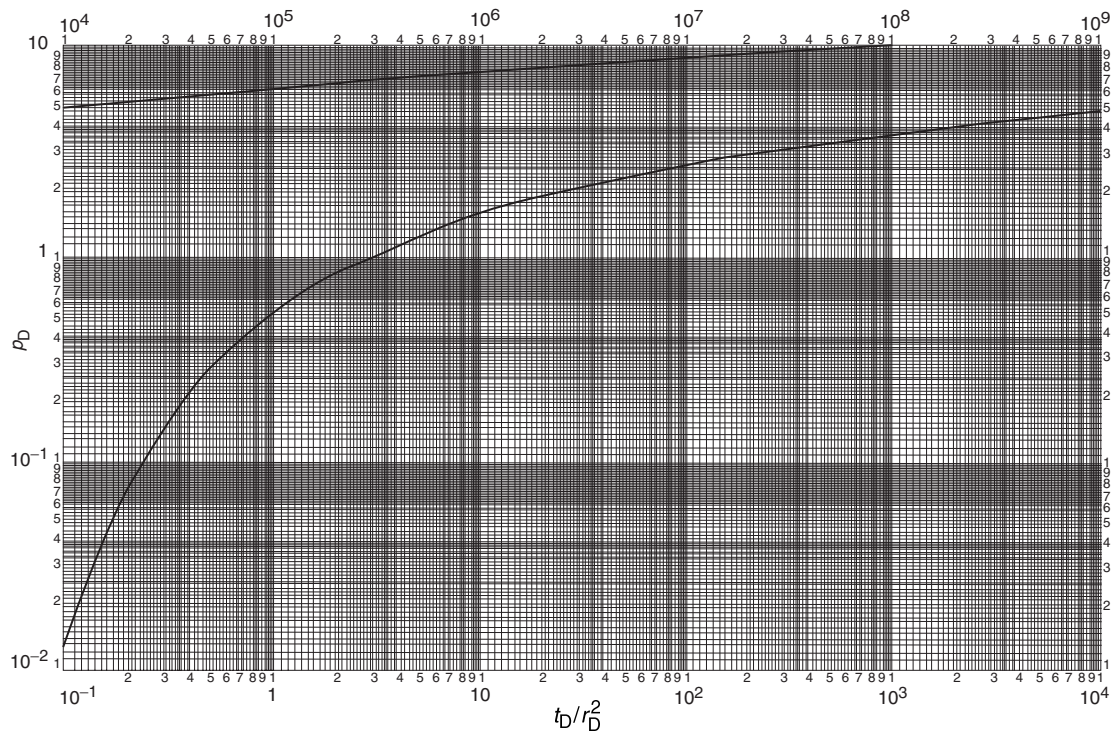

Figure 1.100 *Dimensionless pressure for a single well in an infinite system, no wellbore storage, no skin. Exponential–integral solution (After Earlougher, R. Advances in Well Test Analysis) (Permission to publish by the SPE, copyright SPE, 1977).*

dimensionless form as:

$$p_D = -\frac{1}{2}\text{Ei}\left[\frac{-r_D^2}{4t_D}\right] \qquad [1.6.1]$$

with the dimensionless parameters as defined by:

$$p_D = \frac{[p_i - p(r,t)]kh}{141.2QB\mu}$$

$$r_D = \frac{r}{r_w}$$

$$t_D = \frac{0.0002637kt}{\phi\mu c_t r_w^2}$$

where:

$p(r,t)$ = pressure at distance r and time t, psi
r = distance between the active well and a shut-in observation well
t = time, hours
p_i = reservoir pressure
k = permeability, md

Earlougher expressed in Equation 1.6.1 a type curve form as shown previously in Figure 1.47 and reproduced for convenience as Figure 1.100.

To analyze an interference test by type curve matching, plot the observation well(s) pressure change Δp versus time on tracing paper laid over Figure 1.100 using the matching procedure described previously. When the data is matched to the curve, any convenient match point is selected and match point values from the tracing paper and the underlying type curve grid are read. The following expressions can then be applied to estimate the average reservoir properties:

$$k = \left[\frac{141.2QB\mu}{h}\right]\left[\frac{p_D}{\Delta p}\right]_{MP} \qquad [1.6.2]$$

$$\phi = \frac{0.0002637}{c_t r^2}\left[\frac{k}{\mu}\right]\left[\frac{t}{t_D/r_D^2}\right]_{MP} \qquad [1.6.3]$$

where:

r = distance between the active and observation wells, ft
k = permeability, md

Sabet (1991) presented an excellent discussion on the use of the type curve approach in analyzing interference test data by making use of test data given by Strobel et al. (1976). The data, as given by Sabet, is used in the following example to illustrate the type curve matching procedure:

Example 1.42 An interference test was conducted in a dry gas reservoir using two observation wells, designated as Well 1 and Well 3, and an active well, designated as Well 2. The interference test data is listed below:

- Well 2 is the producer, $Q_g = 12.4$ MMscf/day;
- Well 1 is located 8 miles east of Well 2, i.e., $r_{12} = 8$ miles;
- Well 3 is located 2 miles west of Well 2, i.e., $r_{23} = 2$ miles.

Flow rate	*Time*	*Observed pressure* (psia)			
Q	t	*Well 1*		*Well 3*	
(MMscf/day)	(hr)	p_1	Δp_1	p_3	Δp_3
0.0	24	2912.045	0.000	2908.51	0.00
12.4	0	2912.045	0.000	2908.51	0.00

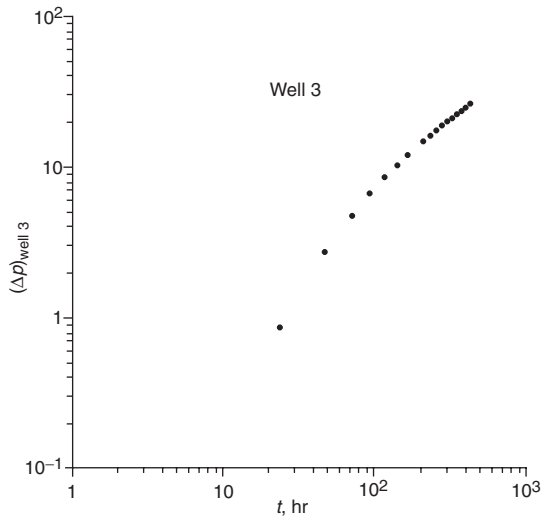

Figure 1.101 *Interference data of Well 3. (After Sabet, M. A. Well Test Analysis 1991, Gulf Publishing Company).*

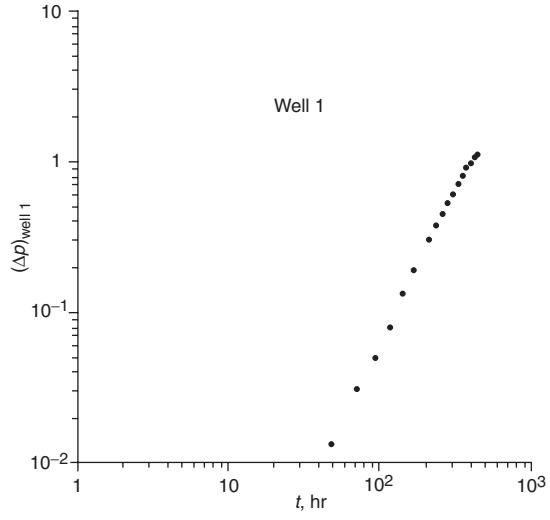

Figure 1.102 *Interference data of Well 1. (After Sabet, M. A. Well Test Analysis 1991, Gulf Publishing Company).*

Flow rate	*Time*	*Observed pressure* (psia)			
Q	t	*Well 1*		*Well 3*	
(MMscf/day)	(hr)	p_1	Δp_1	p_3	Δp_3
12.4	24	2912.035	0.010	2907.66	0.85
12.4	48	2912.032	0.013	2905.80	2.71
12.4	72	2912.015	0.030	2903.79	4.72
12.4	96	2911.997	0.048	2901.85	6.66
12.4	120	2911.969	0.076	2899.98	8.53
12.4	144	2911.918	0.127	2898.25	10.26
12.4	169	2911.864	0.181	2896.58	11.93
12.4	216	2911.755	0.290	2893.71	14.80
12.4	240	2911.685	0.360	2892.36	16.15
12.4	264	2911.612	0.433	2891.06	17.45
12.4	288	2911.533	0.512	2889.79	18.72
12.4	312	2911.456	0.589	2888.54	19.97
12.4	336	2911.362	0.683	2887.33	21.18
12.4	360	2911.282	0.763	2886.16	22.35
12.4	384	2911.176	0.869	2885.01	23.50
12.4	408	2911.108	0.937	2883.85	24.66
12.4	432	2911.030	1.015	2882.69	25.82
12.4	444	2910.999	1.046	2882.11	26.40
0.0	450	Well 2 shut-in			
0.0	480	2910.833	1.212	2881.45	27.06
0.0	504	2910.714	1.331	2882.39	26.12
0.0	528	2910.616	1.429	2883.52	24.99
0.0	552	2910.520	1.525	2884.64	23.87
0.0	576	2910.418	1.627	2885.67	22.84
0.0	600	2910.316	1.729	2886.61	21.90
0.0	624	2910.229	1.816	2887.46	21.05
0.0	648	2910.146	1.899	2888.24	20.27
0.0	672	2910.076	1.969	2888.96	19.55
0.0	696	2910.012	2.033	2889.60	18.91

The following additional reservoir data is available:

$T = 671.6°\text{R}$, $h = 75$ ft, $c_{\text{ti}} = 2.74 \times 10^{-4}$ psi^{-1}

$B_{\text{gi}} = 920.9$ bbl/MMscf, $r_{\text{w}} = 0.25$ ft, $Z_{\text{i}} = 0.868$,

$S_{\text{w}} = 0.21$, $\gamma_{\text{g}} = 0.62$, $\mu_{\text{gi}} = 0.0186$ cp

Using the type curve approach, characterize the reservoir in terms of permeability and porosity.

Solution

Step 1. Plot Δp vs. t on a log–log tracing paper with the same dimensions as those of Figure 1.100, as shown in Figures 1.101 and 1.102 for Wells 1 and 3, respectively.

Step 2. Figure 1.103 shows the match of interference data for Well 3, with the following matching points:

$$(p_{\text{D}})_{\text{MP}} = 0.1 \quad \text{and} \quad (\Delta p)_{\text{MP}} = 2 \text{ psi}$$

$$(t_{\text{D}}/r_{\text{D}}^2)_{\text{MP}} = 1 \quad \text{and} \quad (t)_{\text{MP}} = 159 \text{ hours}$$

Step 3. Solve for k and ϕ between Well 2 and Well 3 by applying Equations 1.6.2 and 1.6.3

$$k = \left[\frac{141.2QB\mu}{h}\right]\left[\frac{p_{\text{D}}}{\Delta p}\right]_{\text{MP}}$$

$$= \left[\frac{141.2(12.4)(920.9)(0.0186)}{75}\right]\left(\frac{0.1}{2}\right) = 19.7 \text{ md}$$

$$\phi = \frac{0.0002637}{c_{\text{t}} r^2}\left[\frac{k}{\mu}\right]\left[\frac{t}{t_{\text{D}}/r_{\text{D}}^2}\right]_{\text{MP}}$$

$$= \frac{0.0002637}{(2.74 \times 10^{-4})(2 \times 5280)^2}\left(\frac{19.7}{0.0186}\right)\left(\frac{159}{1}\right)$$

$$= 0.00144$$

Step 4. Figure 1.104 shows the match of the test data for Well 1 with the following matching points:

$$(p_{\text{D}})_{\text{MP}} = 1 \quad \text{and} \quad (\Delta p)_{\text{MP}} = 5.6 \text{ psi}$$

$$(t_{\text{D}}/r_{\text{D}}^2)_{\text{MP}} = 0.1 \quad \text{and} \quad (t)_{\text{MP}} = 125 \text{ hours}$$

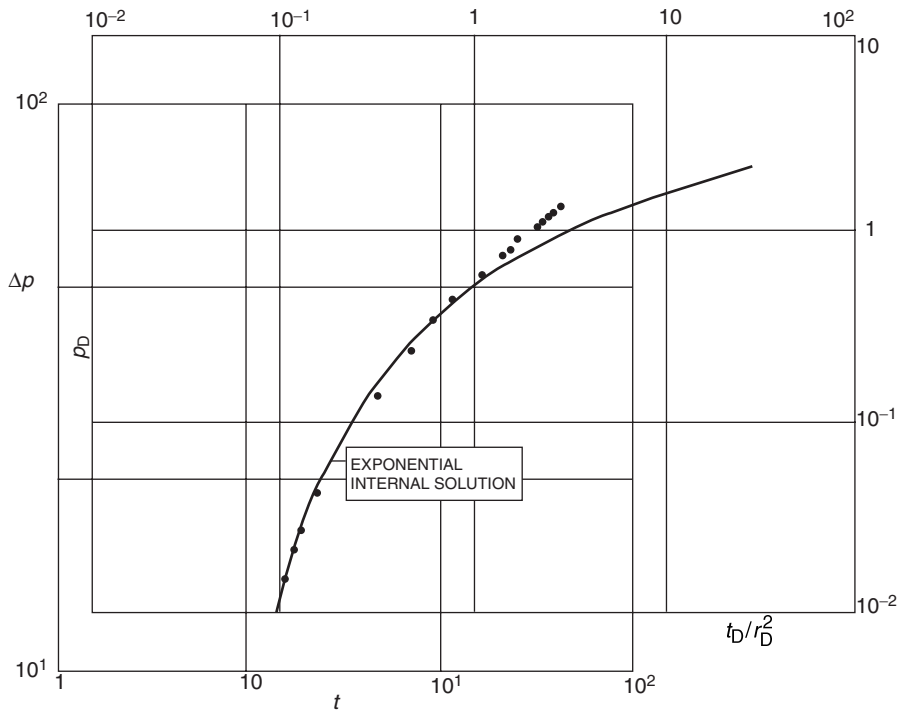

Figure 1.103 *Match of interference data of Well 3. (After Sabet, M. A. Well Test Analysis 1991, Gulf Publishing Company).*

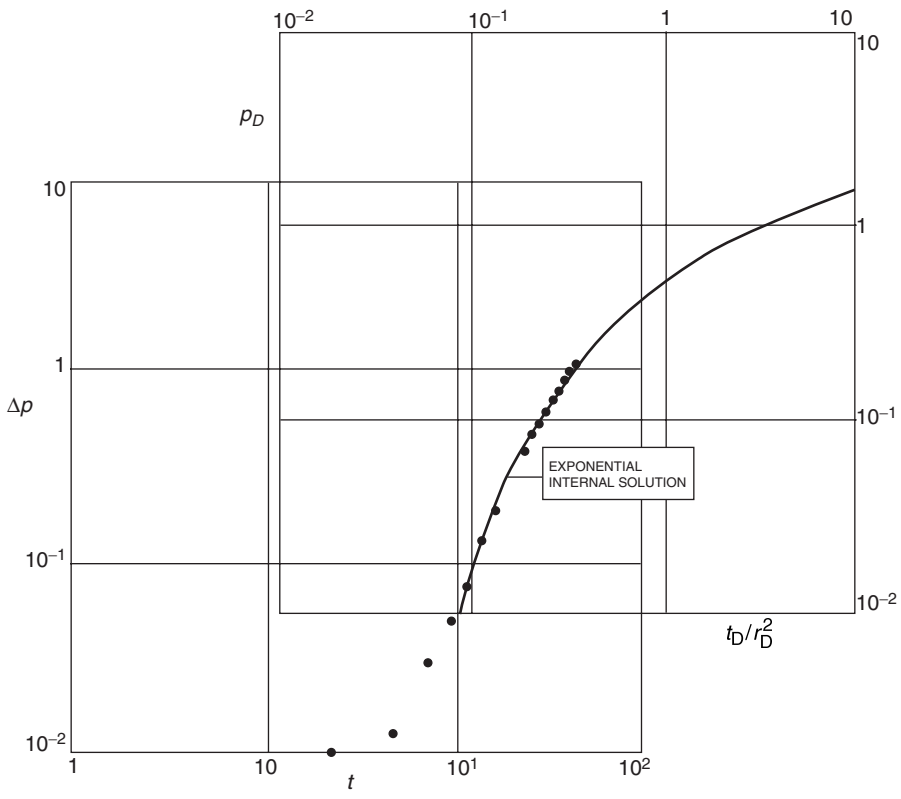

Figure 1.104 *Match of interference data of Well 1.*

Step 5. Calculate k and ϕ:

$$k = \left[\frac{141.2(12.4)(920.9)(0.0186)}{75}\right]\left(\frac{1}{5.6}\right)$$
$$= 71.8 \text{ md}$$
$$\phi = \frac{0.0002637}{(2.74\times10^{-4})(8\times5280)^2}\left(\frac{71.8}{0.0180}\right)\left(\frac{125}{0.1}\right)$$
$$= 0.0026$$

In a homogeneous and isotropic reservoir, i.e., permeability is the same throughout the reservoir, the minimum area of the reservoir investigated during an interference test between two wells located a distance r apart is obtained by drawing two circles of radius r centered at each well.

1.6.2 Interference testing in homogeneous anisotropic reservoirs

A homogeneous anisotropic reservoir is one in which the porosity ϕ and thickness h are the same throughout the system, but the permeability varies with direction. Using multiple observation wells when conducting an interference test in a homogeneous anisotropic reservoir, it is possible to determine the maximum and minimum permeabilities, i.e., k_{max} and k_{min}, and their directions relative to well locations. Based on the work of Papadopulos (1965), Ramey (1975) adopted the Papadopulos solution for estimating anisotropic reservoir properties from an interference test that requires at least three observation wells for analysis. Figure 1.105 defines the necessary nomenclature used in the analysis of interference data in a homogeneous anisotropic reservoir.

Figure 1.105 shows an active well, with its coordinates at the *origin*, and several observation wells are each located at coordinates defined by (x, y). Assuming that all the wells in the testing area have been shut in for a sufficient time to equalize the pressure to p_i, placing the active well on production (or injection) will cause a change in pressure of Δp, i.e., $\Delta p = p_i - p(x,y,t)$, at all observation wells. This change in the pressure will occur after a lag period with a length that depends, among other parameters, on:

- the distance between the active well and observation well;
- permeability;
- wellbore storage in the active well;
- the skin factor following a lag period.

Ramey (1975) showed that the change in pressure at an observation well with coordinates of (x,y) at any time t is given by the Ei function as:

$$p_D = -\frac{1}{2}\text{Ei}\left[\frac{-r_D^2}{4t_D}\right]$$

The dimensionless variables are defined by:

$$p_D = \frac{\bar{k}h[p_i - p(x,y,t)]}{141.2QB\mu} \quad [1.6.4]$$

$$\frac{t_D}{r_D^2} = \left[\frac{(\bar{k})^2}{y^2k_x + x^2k_y - 2xyk_{xy}}\right]\left(\frac{0.0002637t}{\phi\mu c_t}\right) \quad [1.6.5]$$

with:

$$\bar{k} = \sqrt{k_{max}k_{min}} = \sqrt{k_xk_y - k_{xy}^2} \quad [1.6.6]$$

Ramey also developed the following relationships:

$$k_{max} = \frac{1}{2}\left[(k_x + k_y) + \sqrt{(k_xk_y)^2 + 4k_{xy}^2}\right] \quad [1.6.7]$$

$$k_{min} = \frac{1}{2}\left[(k_x + k_y)^2 - \sqrt{(k_xk_y)^2 + 4k_{xy}^2}\right] \quad [1.6.8]$$

$$\theta_{max} = \arctan\left(\frac{k_{max} - k_x}{k_{xy}}\right) \quad [1.6.9]$$

$$\theta_{min} = \arctan\left(\frac{k_{min} - k_y}{k_{xy}}\right) \quad [1.6.10]$$

where:

k_x = permeability in x direction, md
k_y = permeability in y direction, md
k_{xy} = permeability in xy direction, md
k_{min} = minimum permeability, md
k_{max} = maximum permeability, md
$\bar{k}$ = average system permeability, md
θ_{max} = direction (angle) of k_{max} as measured from the $+x$ axis
θ_{min} = direction (angle) of k_{min} as measured from the $+y$ axis
x, y = coordinates, ft
t = time, hours

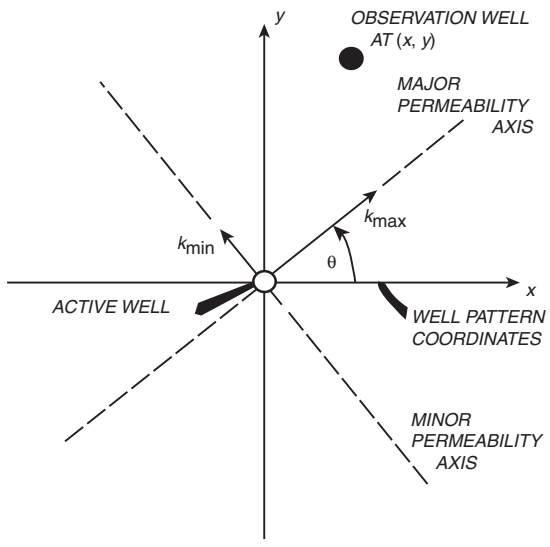

Figure 1.105 *Nomenclature for anisotropic permeability system (After Ramey, 1975).*

Ramey pointed out that if $\phi\mu c_t$ is not known, solution of the above equations will require that a minimum of three observation wells is used in the test, otherwise the required information can be obtained with only two observation wells. Type curve matching is the first step of the analysis technique. Observed pressure changes at each observation well, i.e., $\Delta p = p_i - p(x,y,t)$, are plotted on log–log paper and matched with the exponential–integral type curve shown in Figure 1.100. The associated specific steps of the methodology of using the type curve in determining the properties of a homogeneous anisotropic reservoir are summarized below:

Step 1. From at least three observation wells, plot the observed pressure change Δp versus time t for each well on the same size scale as the type curve given in Figure 1.100.

Step 2. Match each of the observation well data set to the type curve of Figure 1.100. Select a convenient match point for each data set so that the pressure match point $(\Delta p, p_D)_{MP}$ is the same for all observation well

responses, while the time match points $(t, t_D/r_D^2)_{MP}$ vary.

Step 3. From the pressure match point $(\Delta p, p_D)_{MP}$, calculate the average system permeability from:

$$\bar{k} = \sqrt{k_{min}k_{max}} = \left[\frac{141.2QB\mu}{h}\right]\left(\frac{p_D}{\Delta p}\right)_{MP} \quad [1.6.11]$$

Notice from Equation 1.6.6 that:

$$(\bar{k})^2 = k_{min}k_{max} = k_x k_y - k_{xy}^2 \quad [1.6.12]$$

Step 4. Assuming *three observation wells*, use the time match $[(t, (t_D/r_D^2)]_{MP}$ for each observation well to write:

Well 1:

$$\left[\frac{(t_D/r_D^2)}{t}\right]_{MP} = \left(\frac{0.0002637}{\phi\mu c_t}\right) \times \left(\frac{(\bar{k})^2}{y_1^2k_x + x_1^2k_y - 2x_1y_1k_{xy}}\right)$$

Rearranging gives:

$$y_1^2k_x + x_1^2k_y - 2x_1y_1k_{xy} = \left(\frac{0.0002637}{\phi\mu c_t}\right) \times \left(\frac{(\bar{k})^2}{\left[\frac{(t_D/r_D^2)}{t}\right]_{MP}}\right) \quad [1.6.13]$$

Well 2:

$$\left[\frac{(t_D/r_D^2)}{t}\right]_{MP} = \left(\frac{0.0002637}{\phi\mu c_t}\right) \times \left(\frac{(\bar{k})^2}{y_2^2k_x + x_2^2k_y - 2x_2y_2k_{xy}}\right)$$

$$y_2^2k_x + x_2^2k_y - 2x_2y_2k_{xy} = \left(\frac{0.0002637}{\phi\mu c_t}\right) \times \left(\frac{(\bar{k})^2}{\left[\frac{(t_D/r_D^2)}{t}\right]_{MP}}\right) \quad [1.6.14]$$

Well 3:

$$\left[\frac{(t_D/r_D^2)}{t}\right]_{MP} = \left(\frac{0.0002637}{\phi\mu c_t}\right) \times \left(\frac{(\bar{k})^2}{y_3^2k_x + x_3^2k_y - 2x_3y_3k_{xy}}\right)$$

$$y_3^2k_x + x_3^2k_y - 2x_3y_3k_{xy} = \left(\frac{0.0002637}{\phi\mu c_t}\right) \times \left(\frac{(\bar{k})^2}{\left[\frac{(t_D/r_D^2)}{t}\right]_{MP}}\right) \quad [1.6.15]$$

Equations 1.6.12 through 1.6.15 contain the following four unknowns:

k_x = permeability in x direction
k_y = permeability in y direction
k_{xy} = permeability in xy direction
$\phi\mu c_t$ = porosity group

These four equations can be solved simultaneously for the above four unknowns. The following example as given by Ramey (1975) and later by Earlougher (1977) is used to clarify the use of the proposed methodology for determining the properties of an anisotropic reservoir.

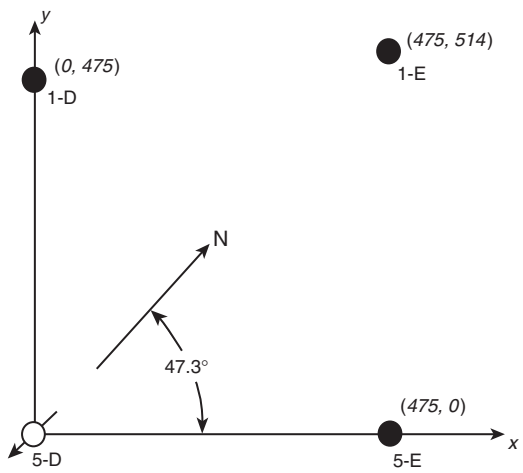

Figure 1.106 *Well locations for Example 1.43 (After Earlougher, R. Advances in Well Test Analysis) (Permission to publish by the SPE, copyright SPE, 1977).*

Example 1.43 The following data is for an interference test in a nine-spot pattern with one active well and eight observation wells. Before testing, all wells were shut in. The test was conducted by injecting at −115 STB/day and observing the fluid levels in the remaining eight shut-in wells. Figure 1.106 shows the well locations. For simplicity, only the recorded pressure data for three observation wells, as tabulated below, is used to illustrate the methodology. These selected wells are labeled Well 5-E, Well 1-D, and Well 1-E.

Well 1-D		*Well 5-E*		*Well 1-E*	
t (hr)	Δp (psi)	t (hr)	Δp (psi)	t (hr)	Δp (psi)
23.5	−6.7	21.0	−4.0	27.5	−3.0
28.5	−7.2	47.0	−11.0	47.0	−5.0
51.0	−15.0	72.0	−16.3	72.0	−11.0
77.0	−20.0	94.0	−21.2	95.0	−13.0
95.0	−25.0	115.0	−22.0	115.0	−16.0
			−25.0		

The well coordinates (x, y) are as follows:

	Well	x (ft)	y (ft)
1	1-D	0	475
2	5-E	475	0
3	1-E	475	514

$i_w = -115$ STB/day, $B_w = 1.0$ bbl/STB, $\mu_w = 1.0$ cp,
$\phi = 20\%$, $T = 75°$ F, $h = 25$ ft,
$c_o = 7.5 \times 10^{-6}$ psi^{-1}, $c_w = 3.3 \times 10^{-6}$ psi^{-1},
$c_f = 3.7 \times 10^{-6}$ psi^{-1}, $r_w = 0.563$ ft, $p_i = 240$ psi

Calculate k_{max}, k_{min}, and their directions relative to the x axis.

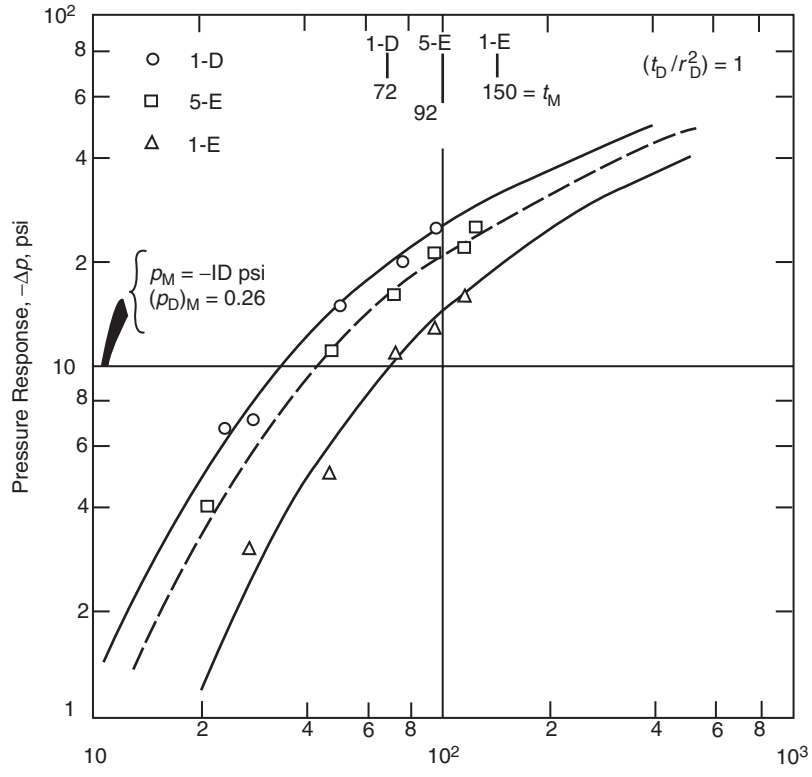

Figure 1.107 *Interference data of Example 1.6 matched to Figure 1.100. Pressure match is the same of all curves. (After Earlougher, R. Advances in Well Test Analysis). (Permission to publish by the SPE, copyright SPE, 1977).*

Solution

Step 1. Plot Δp versus time t for each of the three observation wells on a log–log plot of the same scale as that of Figure 1.100. The resulting plots with the associated match on the type curve are shown in Figure 1.107.

Step 2. Select the same pressure match point on the pressure scale for all the observation wells; however, the match point on the time scale is different for all wells:

Match point	*Well 1-D*	*Well 5-E*	*Well 1-E*
$(p_D)_{MP}$	0.26	0.26	0.26
$(t_D/r_D^2)_{MP}$	1.00	1.00	1.00
$(\Delta p)_{MP}$	−10.00	−10.00	−10.00
$(t)_{MP}$	72.00	92.00	150.00

Step 3. From the pressure match point, use Equation 1.6.11 to solve for $\bar{k}$:

$$\bar{k} = \sqrt{k_{min}k_{max}} = \left[\frac{141.2QB\mu}{h}\right]\left(\frac{p_D}{\Delta p}\right)_{MP}$$

$$= \sqrt{k_{min}k_{max}} = \left[\frac{141.2(-115)(1.0)(1.0)}{25}\right]\left(\frac{0.26}{-10}\right)$$

$$= 16.89 \text{ md}$$

or:

$$k_{min}k_{max} = (16.89)^2 = 285.3$$

Step 4. Using the time match point $(t, t_D/r_D^2)_{MP}$ for each observation well, apply Equations 1.6.13 through 1.6.15 to give:

For Well 1-D with $(x_1, y_1) = (0, 475)$:

$$y_1^2k_x + x_1^2k_y - 2x_1y_1k_{xy} = \left(\frac{0.0002637}{\phi\mu c_t}\right) \times \left(\frac{(\bar{k})^2}{\left[\frac{(t_D/r_D^2)}{t}\right]_{MP}}\right)$$

$$(475)^2k_x + (0)^2k_y - 2(0)(475) = \frac{0.0002637(285.3)}{\phi\mu c_t}\left(\frac{72}{1.0}\right)$$

Simplifying gives:

$$k_x = \frac{2.401 \times 10^{-5}}{\phi\mu c_t} \qquad \text{(A)}$$

For Well 5-E with $(x_2, y_2) = (475, 0)$:

$$(0)^2k_x + (475)^2k_y - 2(475)(0)k_{xy} = \frac{0.0002637(285.3)}{\phi\mu C_t}\left(\frac{92}{1.0}\right)$$

or:

$$k_y = \frac{3.068 \times 10^{-5}}{\phi \mu c_t} \quad \text{(B)}$$

For Well 1-E with $(x_3, y_3) = (475, 514)$:

$$(514)^2 k_x + (475)^2 k_y - 2(475)(514) k_{xy} = \frac{0.0002637(285.3)}{\phi \mu c_t} \left(\frac{150}{1.0}\right)$$

or:

$$0.5411 k_x + 0.4621 k_y - k_{xy} = \frac{2.311 \times 10^{-5}}{\phi \mu c_t} \quad \text{(C)}$$

Step 5. Combine Equations A through C to give:

$$k_{xy} = \frac{4.059 \times 10^{-6}}{\phi \mu c_t} \quad \text{(D)}$$

Step 6. Using Equations A, B, and D in Equation 1.6.12 gives:

$$[k_x k_y] - k_{xy}^2 = (\bar{k})^2$$

$$\left[\frac{(2.401 \times 10^{-5})}{(\phi \mu c_t)} \frac{(3.068 \times 10^{-5})}{(\phi \mu c_t)}\right] - \frac{(4.059 \times 10^{-6})^2}{(\phi \mu c_t)} = (16.89)^2 = 285.3$$

or:

$$\phi \mu c_t = \sqrt{\frac{(2.401 \times 10^{-5})(3.068 \times 10^{-5}) - (4.059 \times 10^{-6})^2}{285.3}}$$

$$= 1.589 \times 10^{-6} \text{ cp/psi}$$

Step 7. Solve for c_t:

$$c_t = \frac{1.589 \times 10^{-6}}{(0.20)(1.0)} = 7.95 \times 10^{-6} \text{ psi}^{-1}$$

Step 8. Using the calculated value of $\phi \mu c_t$ from step 6, i.e., $\phi \mu c_t = 1.589 \times 10^{-6}$, in Equations A, B, and D, solve for k_x, k_y, and k_{xy}:

$$k_x = \frac{2.401 \times 10^{-5}}{1.589 \times 10^{-6}} = 15.11 \text{ md}$$

$$k_y = \frac{3.068 \times 10^{-5}}{1.589 \times 10^{-6}} = 19.31 \text{ md}$$

$$k_{xy} = \frac{4.059 \times 10^{-6}}{1.589 \times 10^{-6}} = 2.55 \text{ md}$$

Step 9. Estimate the maximum permeability value by applying Equation 1.6.7, to give:

$$k_{max} = \frac{1}{2}\left[(k_x + k_y) + \sqrt{(k_x k_y)^2 + 4k_{xy}^2}\right]$$

$$= \frac{1}{2}\left[(15.11 + 19.31) + \sqrt{(15.11 - 19.31)^2 + 4(2.55)^2}\right] = 20.5 \text{ md}$$

Step 10. Estimate the minimum permeability value by applying Equation 1.6.8:

$$k_{min} = \frac{1}{2}\left[(k_x + k_y)^2 - \sqrt{(k_x k_y)^2 + 4k_{xy}^2}\right]$$

$$= \frac{1}{2}\left[(15.11 + 19.31) - \sqrt{(15.11 - 19.31)^2 + 4(2.55)^2}\right] = 13.9 \text{ md}$$

Step 11. Estimate the direction of k_{max} from Equation 1.6.9:

$$\theta_{max} = \arctan\left(\frac{k_{max} - k_x}{k_{xy}}\right) = \arctan\left(\frac{20.5 - 15.11}{2.55}\right) = 64.7^\circ \text{ as measured from the } +x \text{ axis}$$

1.6.3 Pulse testing in homogeneous isotropic reservoirs

Pulse tests have the same objectives as conventional interference tests, which include:

- estimation of permeability k;
- estimation of porosity–compressibility product ϕc_t;
- whether pressure communication exists between wells.

The tests are conducted by sending a sequence of flow disturbances "pulses" into the reservoir from an active well and monitoring the pressure responses to these signals at shut-in observation wells. The pulse sequence is created by producing from (or injecting into) the active well, then shutting it in, and repeating that sequence in a regular pattern, as depicted by Figure 1.108. The figure is for an active producing well that is pulsed by shutting in, continuing production, and repeating the cycle.

The production (or injection) rate should be the same during each period. The lengths of all production periods and all shut-in periods should be equal; however, production periods do not have to equal shut-in periods. These pulses create a very distinctive pressure response at the observation well which can be easily distinguished from any pre-existing trend in reservoir pressure, or random pressure perturbations "noise," which could otherwise be misinterpreted.

It should be noted that pulse testing offers several advantages over conventional interference tests:

- Because the pulse length used in a pulse test is short, ranging from a few hours to a few days, boundaries seldom affect the test data.
- Because of the distinctive pressure response, there are fewer interpretation problems caused by random "noise" and by trends in reservoir pressure at the observation well.
- Because of shorter test times, pulse tests cause less disruption of normal field operations than interference test.

For each pulse, the pressure response at the observation well is recorded (as illustrated in Figure 1.109) with a very sensitive pressure gauge. In pulse tests, pulse 1 and pulse 2 have characteristics that differ from those of all subsequent pulses. Following these pulses, all odd pulses have similar characteristics and all even pulses also have similar characteristics. Any one of the pulses can be analyzed for k and ϕc_t. Usually, several pulses are analyzed and compared.

Figure 1.109, which depicts the rate history of the active well and the pressure response at an observation well, illustrates the following five parameters which are required for the analysis of a pulse test:

(1) The "pulse period" Δt_p represents the length of the shut-in time.
(2) The "cycle period" Δt_C represents the total time length of a cycle, i.e., the shut-in period plus the flow or injection period.
(3) The "flowing or injection period" Δt_f represents the length of the flow or injection time.

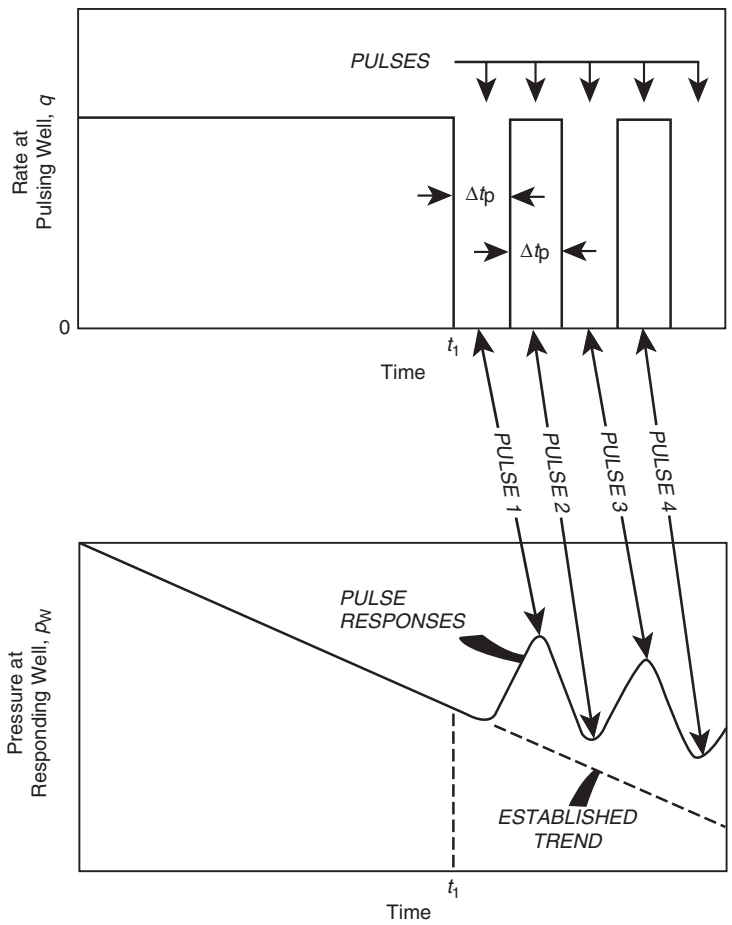

Figure 1.108 *Schematic illustration of rate (pulse) history and pressure response for a pulse test (After Earlougher, R. Advances in Well Test Analysis) (Permission to publish by the SPE, copyright SPE, 1977).*

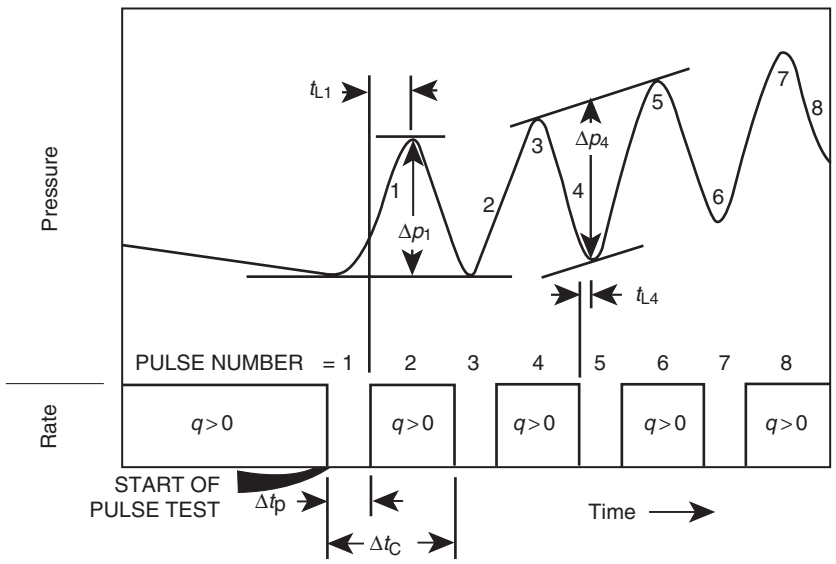

Figure 1.109 *Schematic pulse test rate and pressure history showing definition of time lag (t_L) and pulse response amplitude (Δ p) curves. (After Earlougher, R. Advances in Well Test Analysis) (Permission to publish by the SPE, copyright SPE, 1977).*

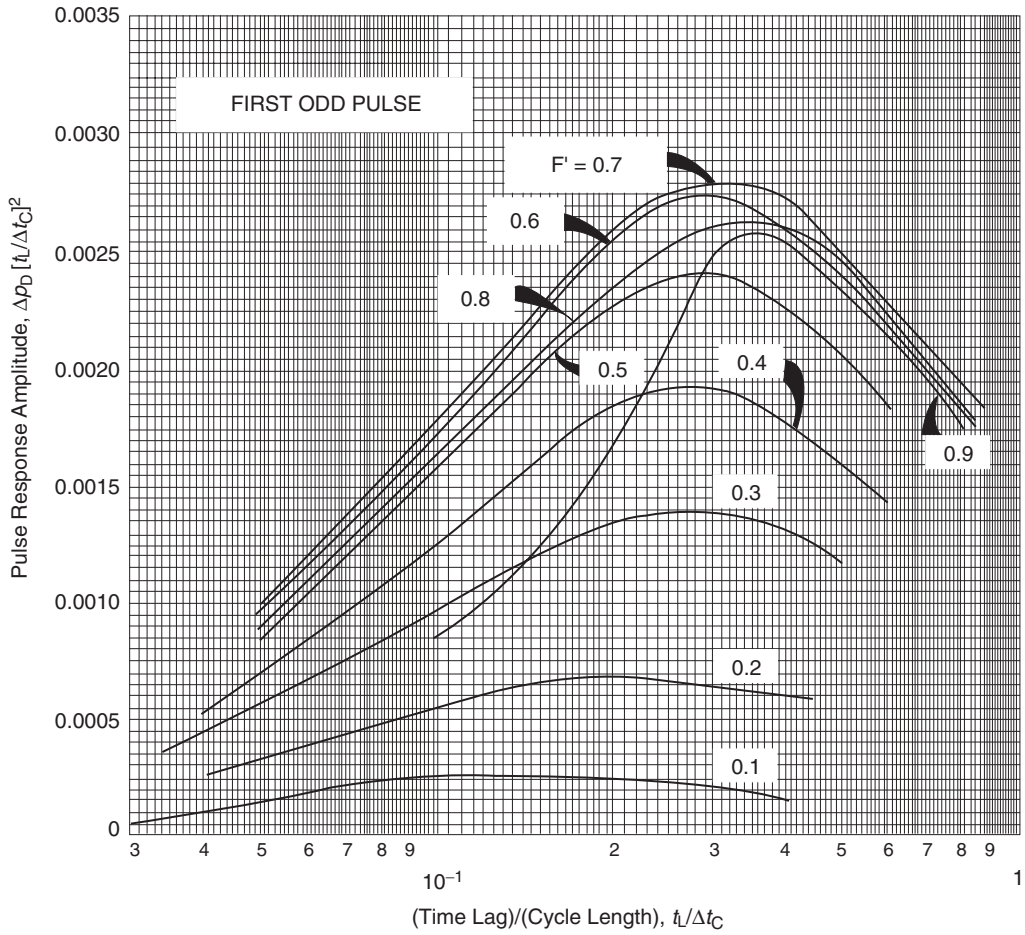

Figure 1.110 *Pulse testing: relation between time lag and response amplitude for first odd pulse. (After Kamal and Brigham, 1976).*

(4) The "time lag" t_L represents the elapsed time between the end of a pulse and the pressure peak caused by the pulse. This time lag t_L is associated with each pulse and essentially describes the time required for a pulse created when the rate is changed to move from the active well to the observation well. It should be pointed out that a flowing (or injecting) period is a "pulse" and a shut-in period is another pulse; the combined two pulses constitute a "cycle."

(5) The "pressure response amplitude" Δp is the vertical distance between two adjacent peaks (or valleys) and a line parallel to this through the valley (or peak), as illustrated in Figure 1.109. Analysis of simulated pulse tests show that pulse 1, i.e., the "first odd pulse," and pulse 2, i.e., the "first even pulse," have characteristics that differ from all subsequent pulses. Beyond these *initial pulses*, all odd pulses have similar characteristics, and all even pulses exhibit similar behavior.

Kamal and Brigham (1975) proposed a pulse test analysis technique that uses the following four dimensionless groups:

(1) Pulse ratio F', as defined by:

$$F' = \frac{\text{pulse period}}{\text{cycle period}} = \frac{\Delta t_p}{\Delta t_p + \Delta t_f} = \frac{\Delta t_p}{\Delta t_C} \qquad [1.6.16]$$

where the time is expressed in hours.

(2) Dimensionless time lag $(t_L)_D$, as given by:

$$(t_L)_D = \frac{t_L}{\Delta t_C} \qquad [1.6.17]$$

where:

$\bar{k}$ = average permeability, md

(3) Dimensionless distance (r_D) between the active and observation wells:

$$r_D = \frac{r}{r_w} \qquad [1.6.18]$$

where:

r = distance between the active well and the observation well, ft

(4) Dimensionless pressure response amplitude Δp_D:

$$\Delta p_D = \left[\frac{\bar{k}h}{141.2B\mu}\frac{\Delta p}{Q}\right] \qquad [1.6.19]$$

where Q is the rate at the active well while it is active, with the sign convention that $\Delta p/Q$ is always positive, i.e., the absolute value of $|\Delta p/Q|$.

Kamal and Brigham developed a family of curves, as shown in Figures 1.110 through 1.117, that correlates the

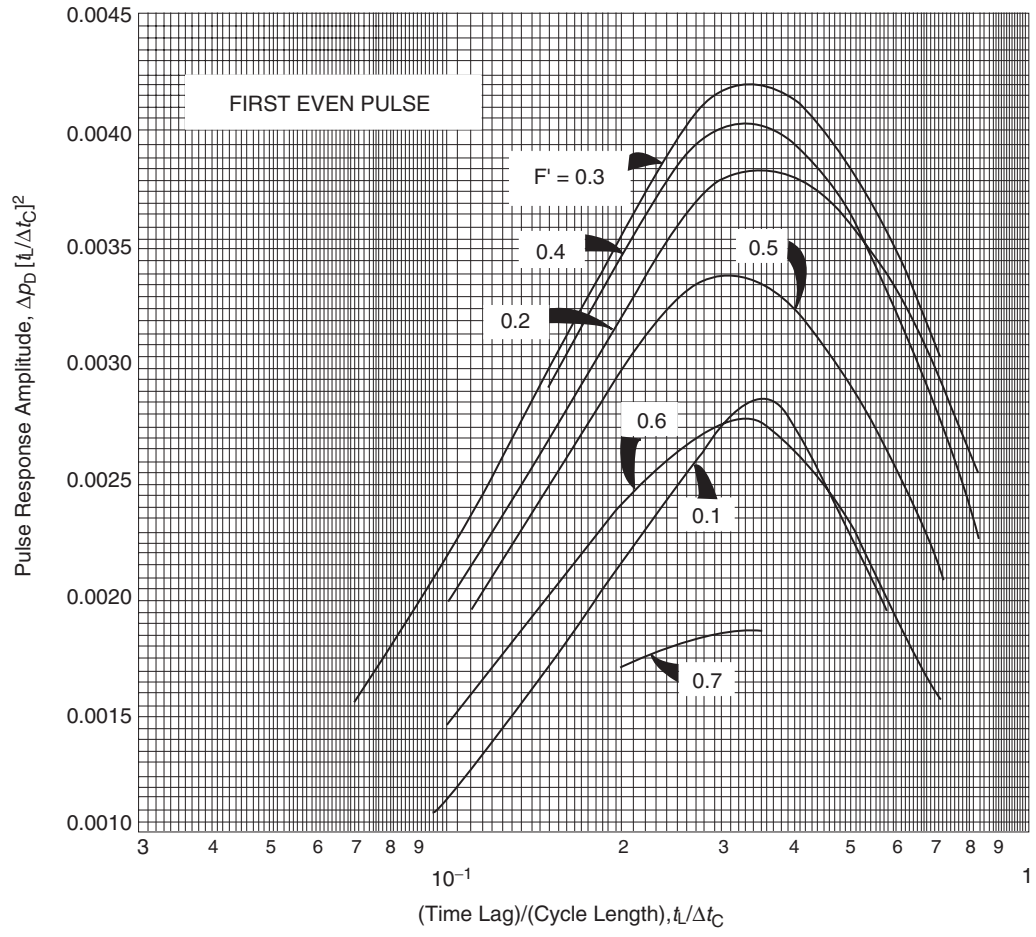

Figure 1.111 *Pulse testing: relation between time lag and response amplitude for first even pulse. (After Kamal and Brigham, 1976).*

pulse ratio $F\backslash$ and the dimensionless time lag $(t_L)_D$ to the dimensionless pressure Δp_D. These curves are specifically designated to analyze the pulse test data for the following conditions:

- *First* odd pulse: Figures 1.110 and 1.114.
- *First* even pulse: Figures 1.111 and 1.115.
- All the *remaining odd pulses* except the first: Figures 1.112 and 1.116.
- All the *remaining even pulses* except the first: Figures 1.113 and 1.117.

The time lag t_L and pressure response amplitude Δp from one or more pulse responses are used to estimate the average reservoir permeability from:

$$\bar{k} = \left[\frac{141.2QB\mu}{h\Delta p[(t_L)_D]^2}\right]\left[\Delta p_D (t_L/\Delta t_C)^2\right]_{Fig} \qquad [1.6.20]$$

The term $\left[\Delta p_D (t_L/\Delta t_C)^2\right]_{Fig}$ is determined from Figures 1.110, 1.111, 1.112, or 1.113 for the appropriate values of $t_L/\Delta t_C$ and $F\backslash$. The other parameters of Equation 1.6.20 are defined below:

Δp = amplitude of the pressure response from the observation well for the *pulse being analyzed*, psi
Δt_C = cycle length, hours
Q = production (injection) rate during active period, STB/day
$\bar{k}$ = average permeability, md

Once the permeability is estimated from Equation 1.6.20, the porosity–compressibility product can be estimated from:

$$\phi c_t = \left[\frac{0.0002637\bar{k}(t_L)}{\mu r^2}\right]\frac{1}{[(t_L)_D/r_D^2]_{Fig}} \qquad [1.6.21]$$

where:

t_L = time lag, hours
r = distance between the active well and observation well, ft

The term $\left[(t_L)_D/r_D^2\right]_{Fig}$ is determined from Figures 1.114, 1.115, 1.116, or 1.117. Again, the appropriate figure to be used in analyzing the pressure response data depends on whether the first-odd or fist-even pulse or one of the remaining pulses is being analyzed.

Example 1.44[a] In a pulse test following rate stabilization, the active well was shut in for 2 hours, then produced for 2 hours, and the sequence was repeated several times.

[a] After John Lee, *Well Testing* (1982).

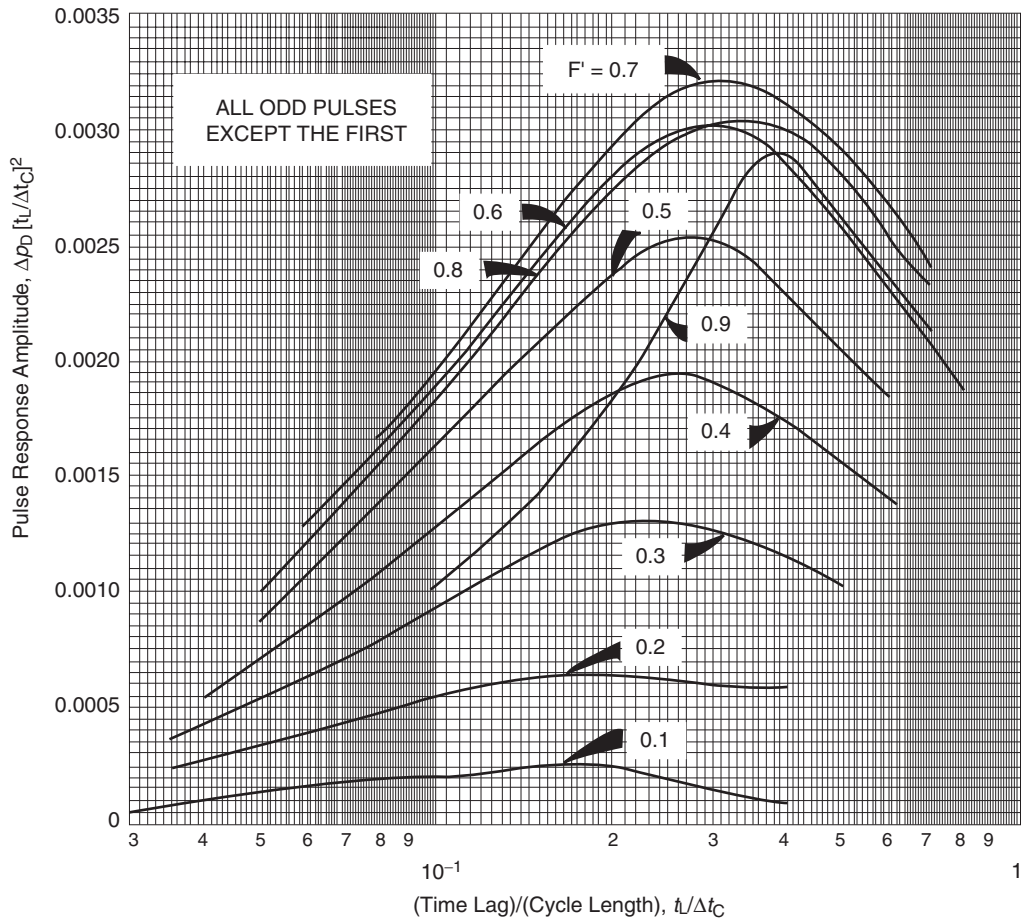

Figure 1.112 *Pulse testing: relation between time lag and response amplitude for all odd pulses after the first. (After Kamal and Brigham, 1976).*

An observation well at 933 ft from the active well recorded an amplitude pressure response of 0.639 psi during the *fourth* pulse and a time lag of 0.4 hours. The following additional data is also available:

$$Q = 425 \text{ STB/day}, \quad B = 1.26 \text{ bbl/STB},$$
$$r = 933 \text{ ft}, \quad h = 26 \text{ ft},$$
$$\mu = 0.8 \text{ cp}, \quad \phi = 0.08$$

Estimate $\bar{k}$ and ϕc_t.

Solution

Step 1. Calculate the pulse ratio $F\backslash$ from Equation 1.6.16, to give:

$$F\backslash = \frac{\Delta t_p}{\Delta t_C} = \frac{\Delta t_p}{\Delta t_p + \Delta t_f} = \frac{2}{2+2} = 0.5$$

Step 2. Calculate the dimensionless time lag $(t_L)_D$ by applying Equation 1.6.17:

$$(t_L)_D = \frac{t_L}{\Delta t_C} = \frac{0.4}{4} = 0.1$$

Step 3. Using the values of $(t_L)_D = 0.1$ and $F\backslash = 0.5$, use Figure 1.113 to get:

$$\left[\Delta p_D (t_L/\Delta t_C)^2\right]_{Fig} = 0.00221$$

Step 4. Estimate the average permeability from Equation 1.6.20, to give:

$$\bar{k} = \left[\frac{141.2QB\mu}{h\Delta p[(t_L)_D]^2}\right]\left[\Delta p_D (t_L/\Delta t_C)^2\right]_{Fig}$$
$$= \left[\frac{(141.2)(425)(1.26)(0.8)}{(26)(0.269)[0.1]^2}\right](0.00221) = 817 \text{ md}$$

Step 5. Using $(t_L)_D = 0.1$ and $F\backslash = 0.5$, use Figure 1.117 to get:

$$\left[(t_L)_D/r_D^2\right]_{Fig} = 0.091$$

Step 6. Estimate the product ϕc_t by applying Equation 1.6.21

$$\phi c_t = \left[\frac{0.0002637\bar{k}(t_L)}{\mu r^2}\right]\frac{1}{[(t_L)_D/r_D^2]_{Fig}}$$
$$= \left[\frac{0.0002637(817)(0.4)}{(0.8)(933)^2}\right]\frac{1}{(0.091)}$$
$$= 1.36 \times 10^{-6}$$

Step 7. Estimate c_t as:

$$c_t = \frac{1.36 \times 10^{-6}}{0.08} = 17 \times 10^{-6} \text{ psi}^{-1}$$

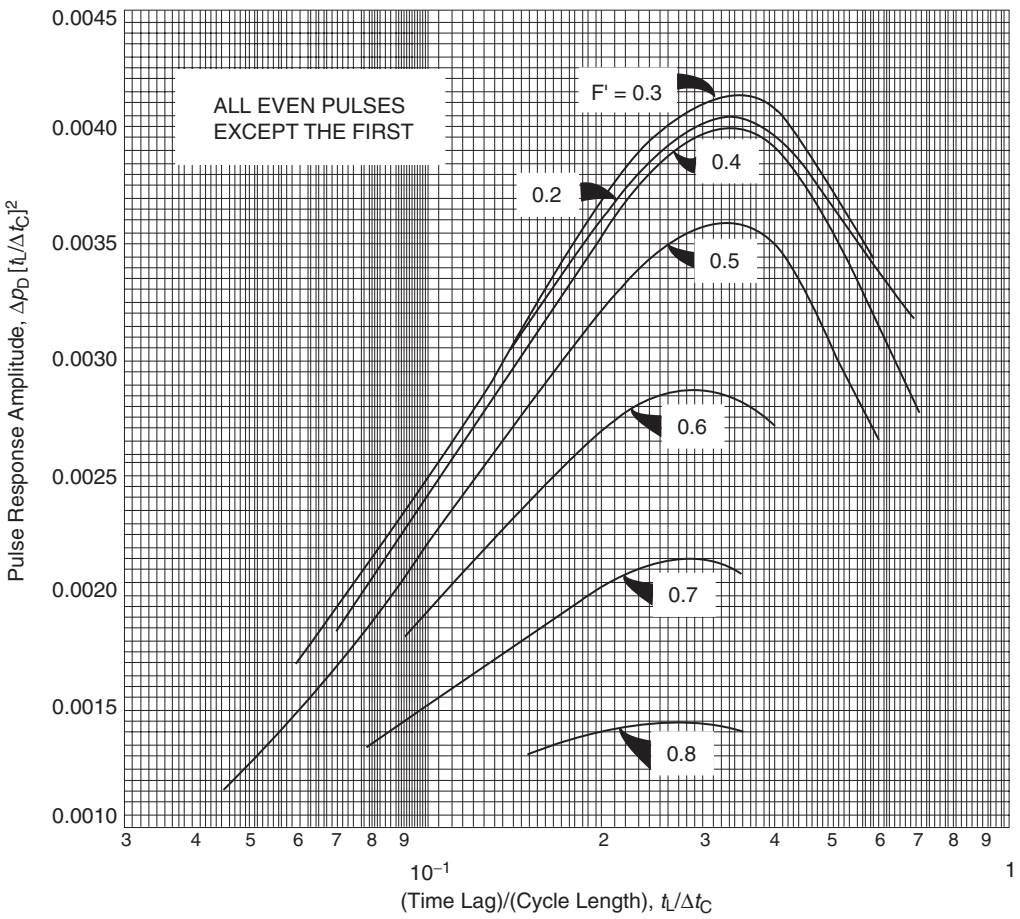

Figure 1.113 *Pulse testing: relation between time lag and response amplitude for all even pulses after the first. (After Kamal and Brigham, 1976).*

Example 1.45[a] A pulse test was conducted using an injection well as the pulsing well in a five-spot pattern with the four offsetting production wells as the responding wells. The reservoir was at its static pressure conditions when the first injection pulse was initiated at 9:40 a.m., with an injection rate of 700 bbl/day. The injection rate was maintained for 3 hours followed by a shut-in period for 3 hours. The injection shut-in periods were repeated several times and the results of pressure observation are given in Table 1.9. The following additional data is available:

$$\mu = 0.87 \text{ cp}, \quad c_t = 9.6 \times 10^{-6} \text{ psi}^{-1},$$
$$\phi = 16\%, \qquad r = 330 \text{ ft}$$

Calculate the permeability and average thickness.

Solution

Step 1. Plot the pressure response from one of the observations well as a function of time, as shown in Figure 1.118.
Analyzing first odd-pulse pressure data

Step 1. From Figure 1.118 determine the amplitude pressure response and time lag during the first pulse, to give:

$$\Delta p = 6.8 \text{ psi}$$
$$t_L = 0.9 \text{ hour}$$

Step 2. Calculate the pulse ratio $F\backslash$ from Equation 1.6.16, to give:

$$F\backslash = \frac{\Delta t_p}{\Delta t_C} = \frac{3}{3+3} = 0.5$$

Step 3. Calculate the dimensionless time lag $(t_L)_D$ by applying Equation 1.6.17:

$$(t_L)_D = \frac{t_L}{\Delta t_C} = \frac{0.9}{6} = 0.15$$

Step 4. Using the values of $(t_L)_D = 0.15$ and $F\backslash = 0.5$, use Figure 1.110 to get:

$$\left[\Delta p_D (t_L/\Delta t_C)^2\right]_{Fig} = 0.0025$$

Step 5. Estimate average hk from Equation 1.6.20, to give:

$$h\bar{k} = \left[\frac{141.2QB\mu}{\Delta p[(t_L)_D]^2}\right]\left[\Delta p_D (t_L/\Delta t_C)^2\right]_{Fig}$$
$$= \left[\frac{(141.2)(700)(1.0)(0.86)}{(6.8)[0.15]^2}\right](0.0025)$$
$$= 1387.9 \text{ md ft}$$

[a] Data reported by H. C. Slider, *Worldwide Practical Petroleum Reservoir Engineering Methods*, Penn Well Books, 1983.

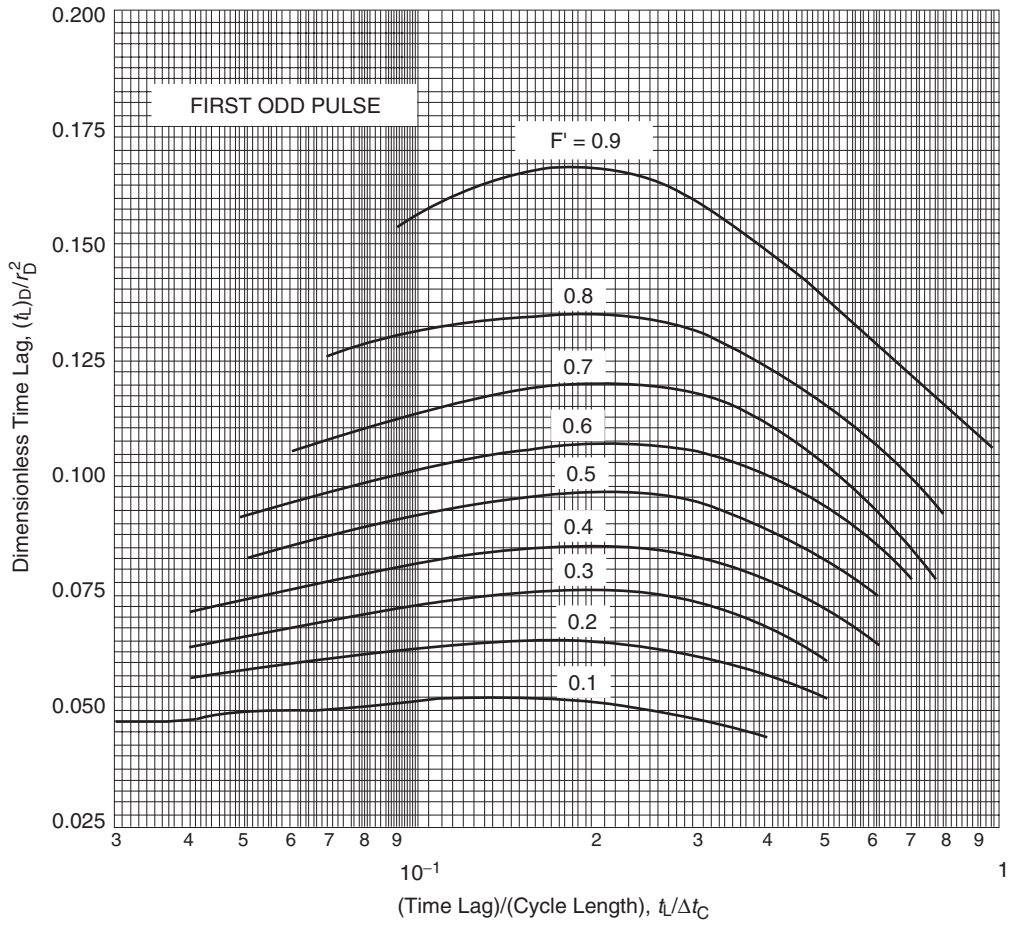

Figure 1.114 *Pulse testing: relation between time lag and cycle length for first odd pulse. (After Kamal and Brigham, 1976).*

Step 6. Using $(t_L)_D = 0.15$ and $F' = 0.5$, use Figure 1.114 to get:

$$\left[(t_L)_D/r_D^2\right]_{Fig} = 0.095$$

Step 7. Estimate the average permeability by rearranging Equation 1.6.21 as:

$$\bar{k} = \left[\frac{\phi c_t \mu r^2}{0.0002637(t_L)}\right]\left[(t_L)_D/r_D^2\right]_{Fig}$$

$$= \left[\frac{(0.16)(9.6\times10^{-6})(0.86)(330)^2}{0.0002637(0.9)}\right](0.095)$$

$$= 57.6 \text{ md}$$

Estimate the thickness h from the value of the product hk as calculated in step 5 and the above average permeability. That is:

$$\bar{k} = \left[\frac{h\bar{k}}{\bar{k}}\right] = \left[\frac{1387.9}{57.6}\right] = 24.1 \text{ ft}$$

Analyzing the fifth pulse pressure data

Step 1. From Figure 1.110 determine the amplitude pressure response and time lag during the fifth pulse, to give:

$\Delta p = 9.2$ psi

$t_L = 0.7$ hour

Step 2. Calculate the pulse ratio F' from Equation 1.6.16 to give:

$$F' = \frac{\Delta t_p}{\Delta t_C} = \frac{\Delta t_p}{\Delta t_p + \Delta t_f} = \frac{3}{3+3} = 0.5$$

Step 3. Calculate the dimensionless time lag $(t_L)_D$ by applying Equation 1.6.17:

$$(t_L)_D = \frac{t_L}{\Delta t_C} = \frac{0.7}{6} = 0.117$$

Step 4. Using the values of $(t_L)_D = 0.117$ and $F' = 0.5$, use Figure 1.111 to get:

$$\left[\Delta p_D (t_L/\Delta t_C)^2\right]_{Fig} = 0.0018$$

Step 5. Estimate average hk from equation 1.6.20, to give:

$$h\bar{k} = \left[\frac{141.2QB\mu}{\Delta p[(t_L)_D]^2}\right]\left[\Delta p_D (t_L/\Delta t_C)^2\right]_{Fig}$$

$$= \left[\frac{(141.2)(700)(1.0)(0.86)}{(9.2)[0.117]^2}\right](0.0018)$$

$$= 1213 \text{ md ft}$$

Step 6. Using $(t_L)_D = 0.117$ and $F' = 0.5$, use Figure 1.115 to get:

$$\left[(t_L)_D/r_D^2\right]_{Fig} = 0.093$$

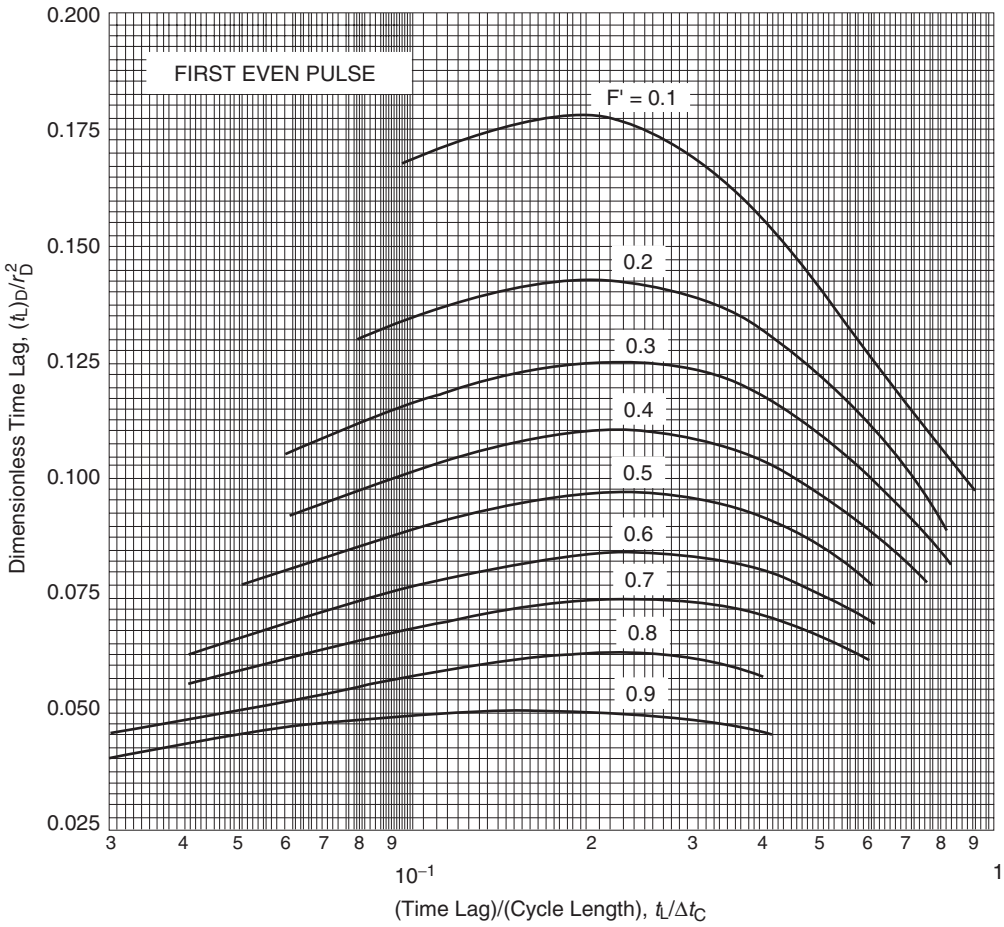

Figure 1.115 *Pulse testing: relation between time lag and cycle length for first even pulse. (After Kamal and Brigham, 1976).*

Step 7. Estimate the average permeability by rearranging Equation 1.6.21 as:

$$\bar{k} = \left[\frac{\phi c_t \mu r^2}{0.0002637(t_L)}\right][(t_L)_D/r_D^2]_{Fig}$$

$$= \left[\frac{(0.16)(9.6\times10^{-6})(0.86)(330)^2}{0.0002637(0.7)}\right](0.095)$$

$$= 72.5 \text{ md}$$

Estimate the thickness h from the value of the product hk as calculated in step 5 and the above average permeability. That is:

$$\bar{k} = \left[\frac{h\bar{k}}{\bar{k}}\right] = \left[\frac{1213}{72.5}\right] = 16.7 \text{ ft}$$

The above calculations should be repeated for all other pulses and the results should be compared with core and conventional well testing analysis to determine the best values that describe these properties.

1.6.4 Pulse testing in homogeneous anisotropic reservoirs

The analysis for the pulse test case is the same as that for the homogeneous isotropic case, except the average permeability $\bar{k}$ as defined by Equation 1.6.6 is introduced into 1.6.20 and 1.6.21, to give:

$$\bar{k} = \sqrt{k_x k_y - k_{xy}^2} = \left[\frac{141.2QB\mu}{h\Delta p[(t_L)_D]^2}\right][\Delta p_D (t_L/\Delta t_C)^2]_{Fig} \quad [1.6.22]$$

and:

$$\phi c_t = \left[\frac{0.0002637(t_L)}{\mu r^2}\right]\left[\frac{(\bar{k})^2}{y^2k_x + x^2k_y - 2xyk_{xy}}\right] \times \frac{1}{[(t_L)_D/r_D^2]_{Fig}} \quad [1.6.23]$$

The solution methodology outlined in analyzing interference test data in homogeneous anisotropic reservoirs can be employed when estimating various permeability parameters from pulse testing.

1.6.5 Pulse test design procedure

Prior knowledge of the expected pressure response is important so that the range and sensitivity of the pressure gauge

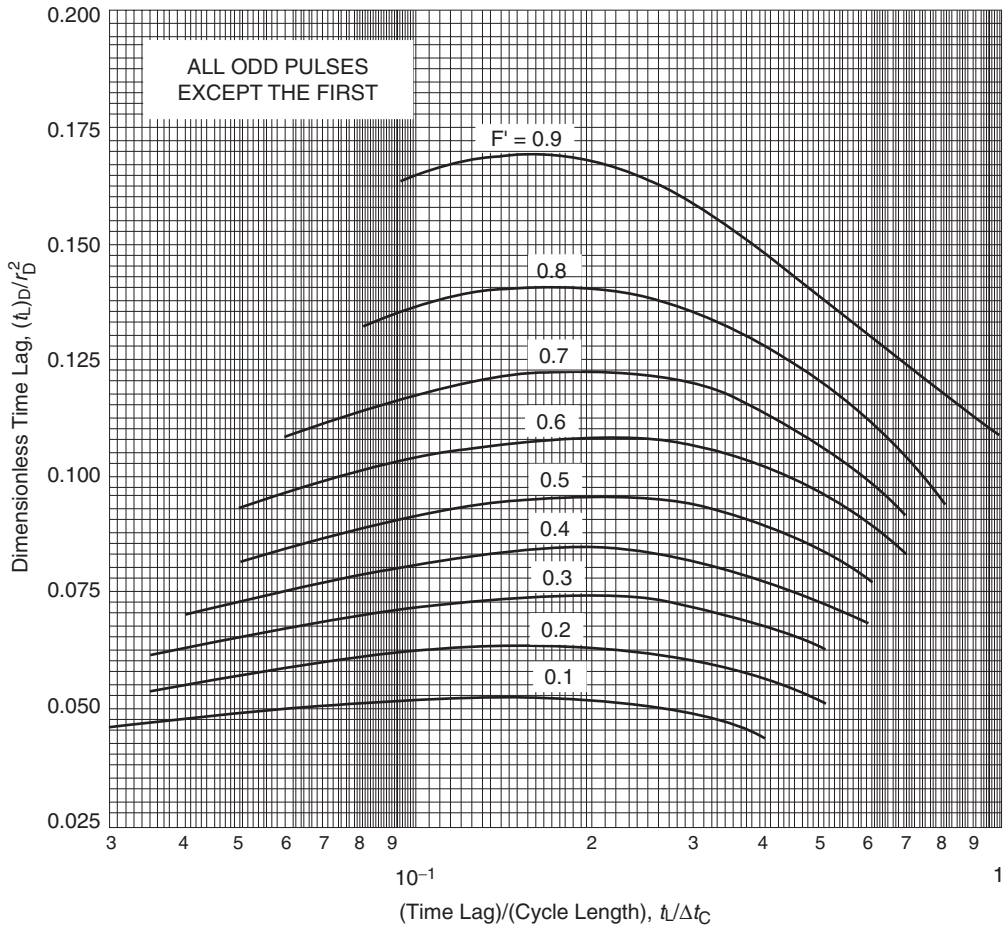

Figure 1.116 *Pulse testing: relation between time lag and cycle length for all odd pulses after the first. (After Kamal and Brigham, 1976).*

and length of time needed for the test can be predetermined. To design a pulse test, Kamal and Brigham (1975) recommend the following procedure:

Step 1. The first step in designing a pulse test is to select the appropriate pulse ratio F' as defined by Equation 1.6.16, i.e., pulse ratio = pulse period/cycle period. A pulse ratio near 0.7 is recommended if analyzing the odd pulses; and near 0.3 if analyzing the even pulses. It should be noted the F' should not exceed 0.8 or drop below 0.2.

Step 2. Calculate the dimensionless time lag from one of the following approximations:

For odd pulses $$(t_L)_D = 0.09 + 0.3F' \qquad [1.6.24]$$

For even pulses $$(t_L)_D = 0.027 - 0.027F' \qquad [1.6.25]$$

Step 3. Using the values of F' and $(t_L)_D$ from step 1 and step 2 respectively, determine the dimensionless parameter $\left[(t_L)_D/r_D^2\right]$ from Figure 1.114 or Figure 1.115.

Step 4. Using the values of F' and $(t_L)_D$, determine the dimensionless response amplitude $\left[\Delta p_D (t_L/\Delta t_C)^2\right]_{Fig}$ from the appropriate curve in Figure 1.110 or Figure 1.111.

Step 5. Using the following parameters:

- estimates of k, h, ϕ, μ, and c_t,
- values of $\left[(t_L)_D/r_D^2\right]_{Fig}$ and $\left[\Delta p_D (t_L/\Delta t_C)^2\right]_{Fig}$ from step 3 and 4, and
- Equations 1.6.1 and 1.6.2

calculate the cycle period (Δt_C) and the response amplitude Δp from:

$$t_L = \left[\frac{\phi \mu c_t r^2}{0.0002637\bar{k}}\right]\left[(t_L)_D/r_D^2\right]_{Fig} \qquad [1.6.26]$$

$$\Delta t_C = \frac{t_L}{(t_L)_D} \qquad [1.6.27]$$

$$\Delta p = \left[\frac{141.2QB\mu}{h\bar{k}\left[(t_L)_D\right]^2}\right]\left[\Delta p_D (t_L/\Delta t_C)^2\right]_{Fig} \qquad [1.6.28]$$

Step 6. Using the pulse ratio F' and cycle period Δt_C, calculate the pulsing (shut-in) period and flow period from:

Pulse (shut-in) period $$\Delta t_p = F'\Delta t_C$$

Flow period $$\Delta t_f = \Delta t_C - \Delta t_p$$

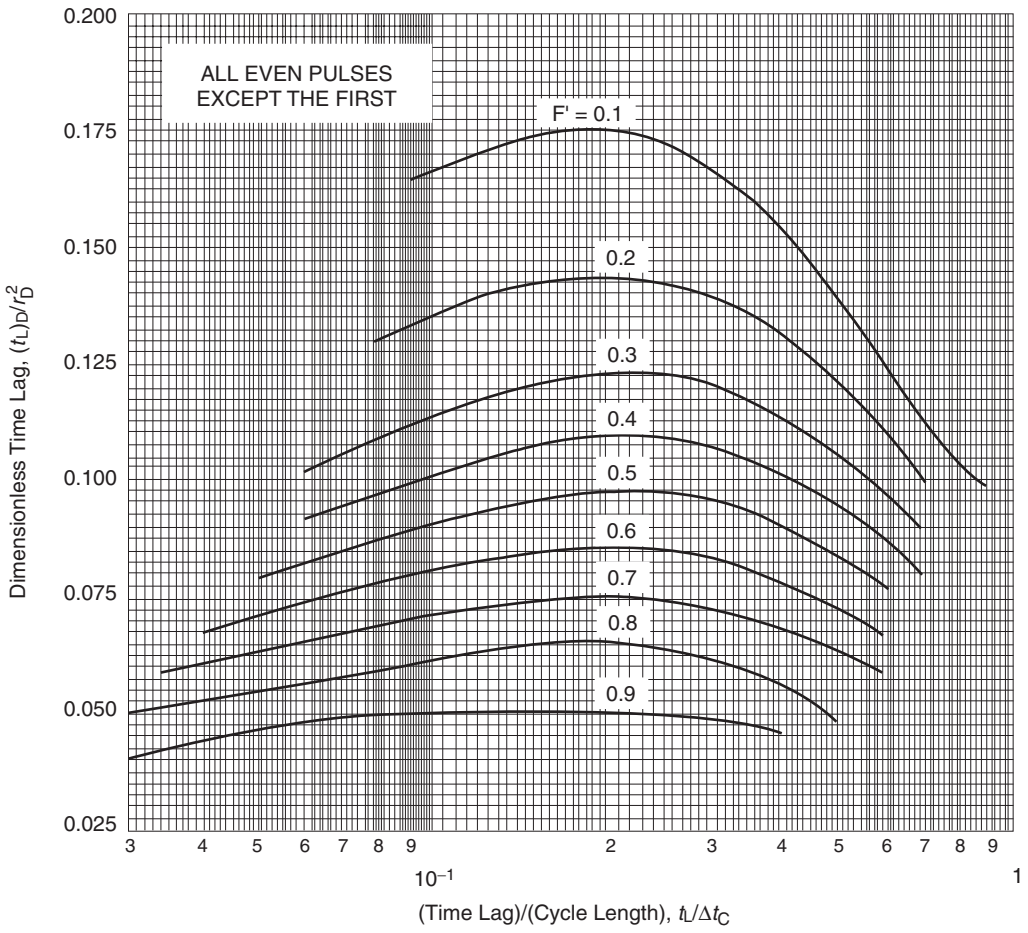

Figure 1.117 *Pulse testing: relation between time lag and cycle length for all even pulses after the first. (After Kamal and Brigham, 1976).*

Table 1.9 *Pressure behaviour of producing Well. After Slider, H. C., Worldwide Practical Petroleum Reservoir Engineering Methods, copyright ©1983, Penn Well Publishing*

Time	*Pressure* (psig)	*Time*	*Pressure* (psig)	*Time*	*Pressure* (psig)
9:40 a.m	390.1	2:23 p.m.	411.6	11:22 p.m.	425.1
10:10 a.m.	390.6	2:30 p.m.	411.6	12:13 a.m.	429.3
10:30 a.m.	392.0	2:45 p.m.	411.4	12:40 a.m.	431.3
10:40 a.m.	393.0	3:02 p.m.	411.3	1:21 a.m.	433.9
10:48 a.m.	393.8	3:30 p.m.	411.0	1:53 a.m.	433.6
11:05 a.m.	395.8	4:05 p.m	410.8	2:35 a.m.	432.0
11:15 a.m.	396.8	4:30 p.m.	412.0	3:15 a.m.	430.2
11:30 a.m.	398.6	5:00 p.m.	413.2	3:55 a.m.	428.5
11:45 a.m.	400.7	5:35 p.m.	416.4	4:32 a.m.	428.8
12:15 p.m.	403.8	6:00 p.m.	418.9	5:08 a.m.	430.6
12:30 p.m.	405.8	6:35 p.m.	422.3	5:53 a.m.	434.5
12:47 p.m.	407.8	7:05 p.m.	424.6	6:30 a.m.	437.4
1:00 p.m.	409.1	7:33 p.m.	425.3	6:58 a.m.	440.3
1:20 p.m.	410.7	7:59 p.m.	425.1	7:30 a.m.	440.9
1:32 p,m.	411.3	8:31 p.m.	423.9	7:58 a.m.	440.7
1:45 p.m.	411.7	9:01 p.m,	423.1	8:28 a.m.	439.6
2:00 p.m.	411.9	9:38 p.m.	421.8	8:57 a.m.	438.6
2:15 p.m.	411.9	10:26 p.m.	421.4	9:45 a.m.	437.0

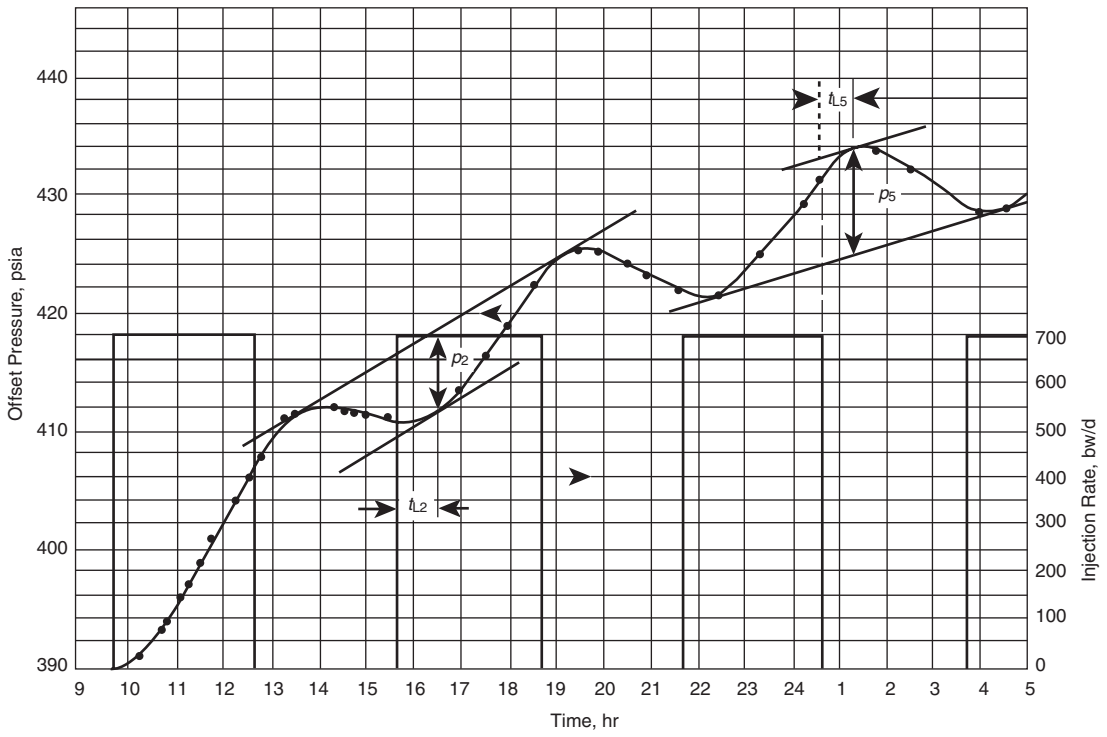

Figure 1.118 *Pulse pressure response for Example 1.45.*

Example 1.46 Design a pulse test using the following approximate properties:

$$\mu = 3 \text{ cp}, \quad \phi = 0.18, \quad k = 200 \text{ md}$$
$$h = 25 \text{ ft}, \quad r = 600 \text{ ft}, \quad c_t = 10 \times 10^{-6} \text{ psi}^{-1}$$
$$B = 1 \text{ bbl/STB}, \quad Q = 100 \text{ bbl/day}, \quad F\backslash = 0.6$$

Solution

Step 1. Calculate $(t_L)_D$ from Equation 1.6.24 or 1.6.25. Since $F\backslash$ is 0.6, the odd pulses should be used and therefore from Equation 1.6.24:

$$(t_L)_D = 0.09 + 0.3(0.6) = 0.27$$

Step 2. Selecting the first odd pulse, determine the dimensionless cycle period from Figure 1.114 to get:

$$\left[(t_L)_D / r_D^2\right]_{Fig} = 0.106$$

Step 3. Determine the dimensionless response amplitude from Figure 1.110 to get:

$$\left[\Delta p_D (t_L/\Delta t_C)^2\right]_{Fig} = 0.00275$$

Step 4. Solve for t_L, Δt_C, and Δp by applying Equations 1.6.26 through 1.6.28, to give:
Time lag:

$$t_L = \left[\frac{\phi \mu C_t r^2}{0.0002637\bar{k}}\right]\left[(t_L)_D / r_D^2\right]_{Fig}$$
$$= \left[\frac{(0.18)(3)(10 \times 10^{-6})(660)^2}{(0.0002637)(200)}\right](0.106)$$
$$= 4.7 \text{ hours}$$

Cycle time:

$$\Delta t_C = \frac{t_L}{(t_L)_D} = \frac{4.7}{0.27} = 17.5 \text{ hours}$$

Pulse length (shut-in):

$$\Delta t_P = \Delta t_C F\backslash = (17.5)(0.27) \approx 5 \text{ hours}$$

Flow period:

$$\Delta t_f = \Delta t_C - \Delta t_P = 17.5 - 4.7 \approx 13 \text{ hours}$$

Step 5. Estimate the pressure response from Equation 1.6.28:

$$\Delta p = \left[\frac{141.2QB\mu}{h\bar{k}\left[(t_L)_D\right]^2}\right]\left[\Delta p_D (t_L/\Delta t_C)^2\right]_{Fig}$$
$$= \left[\frac{(141.2)(100)(1)(3)}{(25)(200)(0.27)^2}\right](0.00275) = 0.32 \text{ psi}$$

This is the expected response amplitude for *odd-pulse* analysis. We shut in the well for 5 hours and produced for 13 hours and repeated each cycle with a period of 18 hours.

The above calculations can be repeated if we desire to analyze the first even-pulse response.

1.7 Injection Well Testing

Injectivity testing is a pressure transient test during injection into a well. Injection well testing and the associated analysis are essentially simple, as long as the mobility ratio between the injected fluid and the reservoir fluid is unity. Earlougher (1977) pointed out that the unit-mobility ratio is a reasonable approximation for many reservoirs under water floods. The objectives of injection tests are similar to those

of production tests, namely the determination of:

- permeability;
- skin;
- average pressure;
- reservoir heterogeneity;
- front tracking.

Injection well testing involves the application of one or more of the following approaches:

- injectivity test;
- pressure falloff test;
- step-rate injectivity test.

The above three analyses of injection well testing are briefly presented below.

1.7.1 Injectivity test analysis

In an injectivity test, the well is shut in until the pressure is stabilized at initial reservoir pressure p_i. At this time, the injection begins at a constant rate q_{inj}, as schematically illustrated in Figure 1.119, while recording the bottom-hole pressure p_{wf}. For a unit-mobility ratio system, the injectivity test would be identical to a pressure drawdown test except that the constant rate is negative with a value of q_{inj}. However, in all the preceding relationships, the injection rate will be treated as a positive value, i.e., $q_{inj} > 0$.

For a constant injection rate, the bottom-hole pressure is given by the linear form of Equation 1.3.1 as:

$$p_{wf} = p_{1\,hr} + m\log(t) \qquad [1.7.1]$$

The above relationship indicates that a plot of bottom-hole injection pressure versus the logarithm of injection time would produce a straight-line section as shown in Figure 1.119, with an intercept of $p_{1\,hr}$ and a slope m as defined by:

$$m = \frac{162.6 q_{inj} B\mu}{kh}$$

where:

q_{inj} = absolute value of injection rate, STB/day
m = slope, psi/cycle
k = permeability, md
h = thickness, ft

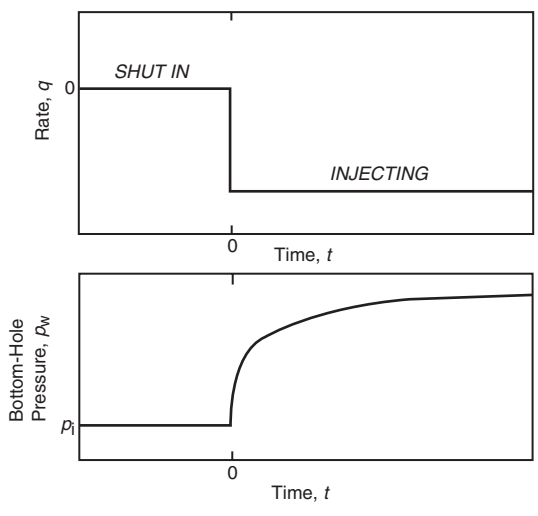

Figure 1.119 *Idealized rate schedule and pressure response for injectivity testing.*

Sabet (1991) pointed out that, depending on whether the density of the injected fluid is higher or lower than the reservoir fluid, the injected fluid will tend to override or underride the reservoir fluid and, therefore the net pay h which should be used in interpreting injectivity tests would not be the same as the net pay which is used in interpreting drawdown tests.

Earlougher (1977) pointed out that, as in drawdown testing, the wellbore storage has great effects on the recorded injectivity test data due to the expected large value of the wellbore storage coefficient. Earlougher recommended that all injectivity test analyses must include the log–log plot of $(p_{wf} - p_i)$ versus injection time with the objective of determining the duration of the wellbore storage effects. As defined previously, the beginning of the semilog straight line, i.e., the end of the wellbore storage effects, can be estimated from the following expression:

$$t > \frac{(200\,000 + 12\,000s)C}{kh/\mu} \qquad [1.7.2]$$

where:

t = time that marks the end of wellbore storage effects, hours
k = permeability, md
s = skin factor
C = wellbore storage coefficient, bbl/psi
μ = viscosity, cp

Once the semilog straight line is identified, the permeability and skin can be determined as outlined previously by:

$$k = \frac{162.6 q_{inj} B\mu}{mh} \qquad [1.7.3]$$

$$s = 1.1513\left[\frac{p_{1\,hr} - p_i}{m} - \log\left(\frac{k}{\phi\mu c_t r_w^2}\right) + 3.2275\right] \qquad [1.7.4]$$

The above relationships are valid as long as the mobility ratio is approximately equal to 1. If the reservoir is under water flood and a water injection well is used for the injectivity test, the following steps summarize the procedure of analyzing the test data assuming a unit-mobility ratio:

Step 1. Plot $(p_{wf} - p_i)$ versus injection time on a log–log scale.
Step 2. Determine the time at which the unit-slope line, i.e., 45° line, ends.
Step 3. Move $1\frac{1}{2}$ log cycles ahead of the observed time in step 2 and read the corresponding time which marks the start of the semilog straight line.
Step 4. Estimate the wellbore storage coefficient C by selecting any point on the unit-slope line and reading its coordinates, i.e., Δp and t, and applying the following expression:

$$C = \frac{q_{inj} Bt}{24\Delta p} \qquad [1.7.5]$$

Step 5. Plot p_{wf} vs. t on a semilog scale and determine the slope m of the straight line that represents the transient flow condition.
Step 6. Calculate the permeability k and skin factor from Equations 1.7.3 and 1.7.4 respectively.
Step 7. Calculate the radius of investigation r_{inv} at the end of injection time. That is:

$$r_{inv} = 0.0359\sqrt{\frac{kt}{\phi\mu c_t}} \qquad [1.7.6]$$

Step 8. Estimate the radius to the leading edge of the water bank r_{wb} before the initiation of the injectivity

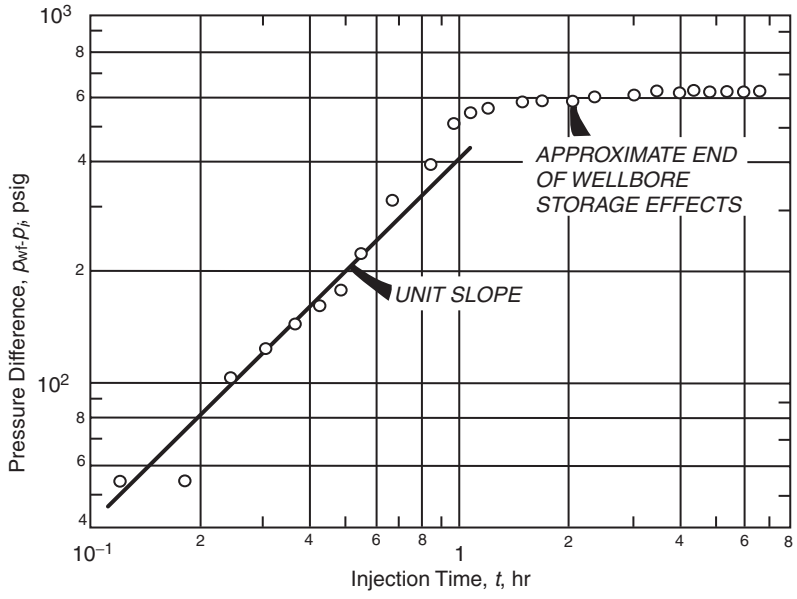

Figure 1.120 *Log–log data plot for the injectivity test of Example 1.47. Water injection into a reservoir at static conditions (After Earlougher, R. Advances in Well Test Analysis) (Permission to publish by the SPE, copyright SPE, 1977).*

test from:

$$r_{wb} = \sqrt{\frac{5.615 W_{inj}}{\pi h \phi (\bar{S}_w - S_{wi})}} = \sqrt{\frac{5.615 W_{inj}}{\pi h \phi (\Delta S_w)}} \qquad [1.7.7]$$

where:

r_{wb} = radius to the water bank, ft
W_{inj} = cumulative water injected at the start of the test, bbl
$\bar{S}_w$ = average water saturation at the start of the test
s_{wi} = initial water saturation

Step 9. Compare r_{wb} with r_{inv}: if $r_{inv} < r_{wb}$, the unit-mobility ratio assumption is justified.

Example 1.47[a] Figures 1.120 and 1.121 show pressure response data for a 7 hour injectivity test in a water-flooded reservoir in terms of $\log(p_{wf} - p_i)$ vs. $\log(t)$ and $\log(p_{wf})$ vs. $\log(t)$ respectively. Before the test, the reservoir had been under water flood for 2 years with a constant injection rate of 100 STB/day. The injectivity test was initiated after shutting in all wells for several weeks to stabilize the pressure at p_i. The following data is available:

$c_t = 6.67 \times 10^{-6}$ psi^{-1}

$B = 1.0$ bbl/STB, $\mu = 1.0$ cp

$S_w = 62.4$ lb/ft^3, $\phi = 0.15$, $q_{inj} = 100$ STB/day

$h = 16$ ft, $r_w = 0.25$ ft, $p_i = 194$ psig

$\Delta S_w = 0.4$, depth $= 1002$ ft, total test time $= 7$ hours

The well is completed with 2 inch tubing set on a packer. Estimate the reservoir permeability and skin factor.

[a]After Robert Earlougher, *Advances in Well Test Analysis*, 1977.

Solution

Step 1. The log–log data plot of Figure 1.120 indicates that the data begins to deviate from the unit-slope line at about 0.55 hours. Using the rule of thumb of moving 1 to $1\frac{1}{2}$ cycles in time after the data starts deviating from the unit-slope line, suggests that the start of the semilog straight line begins after 5 to 10 hours of testing. However, Figures 1.120 and 1.121 clearly show that the wellbore storage effects have ended after 2 to 3 hours.

Step 2. From the unit-slope portion of Figure 1.120, select the coordinates of a point (i.e. ,Δp and t) end calculate the wellbore storage coefficient C by applying Equation 1.7.5:

$$\Delta p = 408 \text{ psig}$$

$$t = 1 \text{ hour}$$

$$C = \frac{q_{inj} B t}{24 \Delta p}$$

$$= \frac{(100)(1.0)(1)}{(24)(408)} = 0.0102 \text{ bbl/psi}$$

Step 3. From the semilog plot in Figure 1.121, determine the slope of the straight line m to give:

$$m = 770 \text{ psig/cycle}$$

Step 4. Calculate the permeability and skin factor by using Equations 1.7.3 and 1.7.4:

$$k = \frac{162.6 q_{inj} B \mu}{mh}$$

$$= \frac{(162.6)(100)(1.0)(1.0)}{(80)(16)} - 12.7 \text{ md}$$

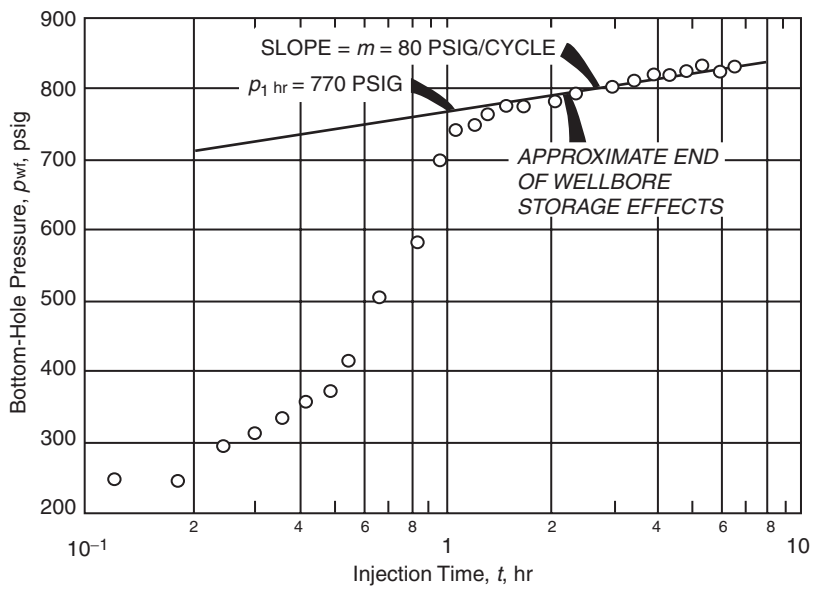

Figure 1.121 *Semilog plot for the injectivity test of Example 1.47. Water injection into a reservoir at static conditions (After Earlougher, R. Advances in Well Test Analysis) (Permission to publish by the SPE, copyright SPE, 1977).*

$$s = 1.1513\left[\frac{p_{1\ hr} - p_i}{m} - \log\left(\frac{k}{\phi\mu c_t r_w^2}\right) + 3.2275\right]$$

$$= 1.1513\left[\frac{770 - 194}{80} - \log\left(\frac{12.7}{(0.15)(1.0)(6.67\times10^{-6})(0.25)^2}\right) + 3.2275\right] = 2.4$$

Step 5. Calculate the radius of investigation after 7 hours by applying Equation 1.7.6:

$$r_{inv} = 0.0359\sqrt{\frac{kt}{\phi\mu c_t}}$$

$$= 0.0359\sqrt{\frac{(12.7)(7)}{(0.15)(1.0)(6.67\times10^{-6})}} \simeq 338\ \text{ft}$$

Step 6. Estimate the distance of the leading edge of the water bank before the start of the test from Equation 1.7.7:

$$W_{inj} \cong (2)(365)(100)(1.0) = 73\,000\ \text{bbl}$$

$$r_{wb} = \sqrt{\frac{5.615W_{inj}}{\pi h\phi(\Delta S_w)}}$$

$$= \sqrt{\frac{(5.615)(73\,000)}{\pi(16)(0.15)(0.4)}} \cong 369\ \text{ft}$$

Since $r_{inv} < r_{wb}$, the use of the unit-mobility ratio analysis is justified.

1.7.2 Pressure falloff test

A pressure falloff test is usually preceded by an injectivity test of a long duration. As illustrated schematically in Figure 1.122, falloff testing is analogous to pressure buildup testing in a production well. After the injectivity test that lasted for a total injection time of t_p at a constant injection rate of q_{inj}, the well is then shut in. The pressure data taken immediately before and during the shut in period is analyzed by the Horner plot method.

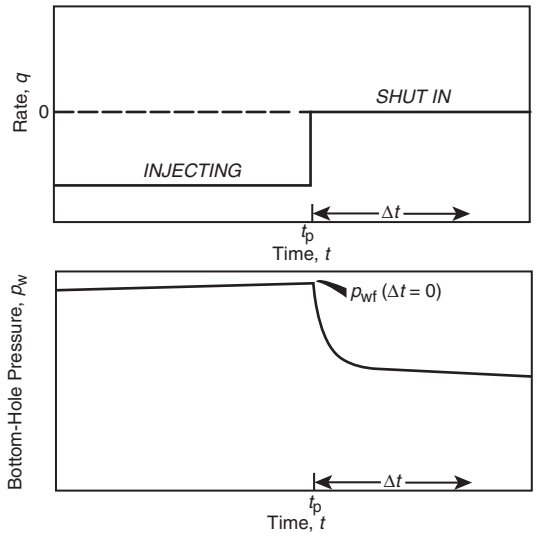

Figure 1.122 *Idealized rate schedule and pressure response for falloff testing.*

The recorded pressure falloff data can be represented by Equation 1.3.11, as:

$$p_{ws} = p^* + m\left[\log\left(\frac{t_p + \Delta t}{\Delta t}\right)\right]$$

with:

$$m = \left|\frac{162.6q_{inj}B\mu}{kh}\right|$$

where p^* is the false pressure that is only equal to the initial (original) reservoir pressure in a newly discovered field. As

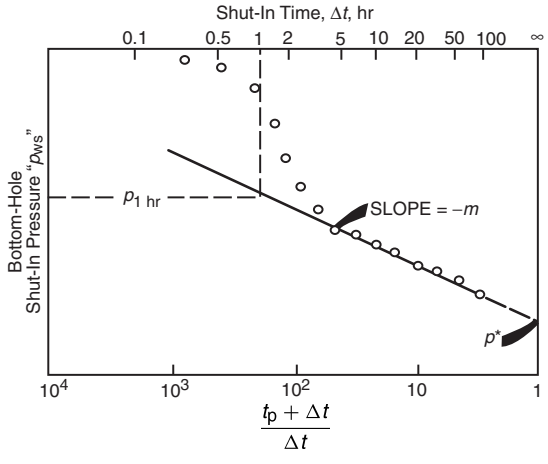

Figure 1.123 *Horner plot of a typical falloff test.*

shown in Figure 1.123, a plot of p_{ws} vs. $\log\left[\left(t_p + \Delta t\right)/\Delta t\right]$ would form a straight-line portion with an intercept of p^* at $\left(t_p + \Delta t\right)/\Delta t = 1$ and a negative slope of m.

It should be pointed out that the log–log data plot should be constructed to identify the end of the wellbore storage effects and beginning of the proper semilog straight line. The permeability and skin factor can be estimated as outlined previously by the expressions:

$$k = \frac{162.6 q_{inj} B\mu}{|m|\, h}$$

$$s = 1.513\left[\frac{p_{wf \text{ at } \Delta t=0} - p_{1\text{ hr}}}{|m|} - \log\left(\frac{k}{\phi\mu c_t r_w^2}\right) + 3.2275\right]$$

Earlougher (1977) indicated that if the injection rate varies before the falloff test, the equivalent injection time may be approximated by:

$$t_p = \frac{24 W_{inj}}{q_{inj}}$$

where W_{inj} is the cumulative volume injected since the last pressure equalization, i.e., last shut-in, and q_{inj} is the injection rate just before shut-in.

It is not uncommon for a falloff test to experience a change in wellbore storage after the test begins at the end of the injectivity test. This will occur in any well which goes on vacuum during the test. An injection well will go on vacuum when the bottom-hole pressure decreases to a value which is insufficient to support a column of water to the surface. Prior to going on vacuum, an injection well will experience storage due to water expansion; after going on vacuum, the storage will be due to a falling fluid level. This change in storage will generally exhibit itself as a decrease in the rate of pressure decline.

The falloff data can also be expressed in graphical form by plotting p_{ws} vs. $\log(\Delta t)$ as proposed by MDH (Miller–Dyes–Hutchinson). The mathematical expression for estimating the false pressure p^* from the MDH analysis is given by Equation 1.3.12 as:

$$p* = p_{1\text{ hr}} - |m| \log(t_p + 1) \qquad [1.7.8]$$

Earlougher pointed out that the MDH plot is more practical to use unless t_p is less than about twice the shut-in time.

The following example, as adopted from the work of McLeod and Coulter (1969) and Earlougher (1977), is used to illustrate the methodology of analyzing the falloff pressure data.

Example 1.48[a] During a stimulation treatment, brine was injected into a well and the falloff data, as reported by McLeod and Coulter (1969), is shown graphically in Figures 1.124 through 1.126. Other available data includes:

total injection time $t_p = 6.82$ hours,
total falloff time = 0.67 hours
$q_{inj} = 807$ STB/day, $B_w = 1.0$ bbl/STB,
$c_w = 3.0 \times 10^{-6}$ psi^{-1}
$\phi = 0.25$, $h = 28$ ft, $\mu_w = 1.0$ cp
$c_t = 1.0 \times 10^{-5}$ psi^{-1}, $r_w = 0.4$ ft, $S_w = 67.46$ lb/ft^3
depth = 4819 ft,
hydrostatic fluid gradient = 0.4685 psi/ft

The recorded shut-in pressures are expressed in terms of *wellhead pressures* p_{ts} with $p_{tf \text{ at } \Delta t=0} = 1310$ psig. Calculate:

- the wellbore storage coefficient;
- the permeability;
- the skin factor;
- the average pressure.

Solution

Step 1. From the log–log plot of Figure 1.124, the semilog straight line begins around 0.1 to 0.2 hours after shut-in. Using $\Delta p = 238$ psi at $\Delta t = 0.01$ hours as the selected coordinates of a point on the unit-slope straight line, calculate the wellbore storage coefficient from Equation 1.7.5, to give:

$$C = \frac{q_{inj} B t}{24 \Delta p}$$

$$= \frac{(807)(1.0)(0.01)}{(24)(238)} = 0.0014 \text{ bbl/psi}$$

Step 2. Figures 1.125 and 1.126 show the Horner plot, i.e., "wellhead pressures vs. $\log\left[\left(t_p + \Delta t\right)/\Delta t\right]$," and the MDH plot, i.e., "wellhead pressures vs. $\log(\Delta t)$, respectively, with both plots giving:

$$m = 270 \text{ psig/cycle}$$

$$p_{1\text{ hr}} = 85 \text{ psig}$$

Using these two values, calculate k and s:

$$k = \frac{162.6 q_{inj} B\mu}{|m|\, h}$$

$$= \frac{(162.6)(807)(1.0)(1.0)}{(270)(28)} = 17.4 \text{ md}$$

$$s = 1.513\left[\frac{p_{wf \text{ at } \Delta t=0} - p_{1\text{ hr}}}{|m|} - \log\left(\frac{k}{\phi\mu c_t r_w^2}\right) + 3.2275\right]$$

$$= 1.513\left[\frac{1310 - 85}{270} - \log\left(\frac{17.4}{(0.25)(1.0)(1.0\times 10^{-5})(0.4)^2}\right)\right]$$

$$+ 3.2275 = 0.15$$

Step 3. Determine p^* from the extrapolation of the Horner plot of Figure 1.125 to $(t_p + \Delta t)/\Delta t = 1$, to give:

$$p^*_{ts} = -151 \text{ psig}$$

Equation 1.7.8 can be used to approximate p^*:

$$p^* = p_{1\text{ hr}} - |m| \log(t_p + 1)$$

$$p^*_{ts} = 85 - (270)\log(6.82 + 1) = -156 \text{ psig}$$

[a] Robert Earlougher, *Advances in Well Test Analysis*, 1977.

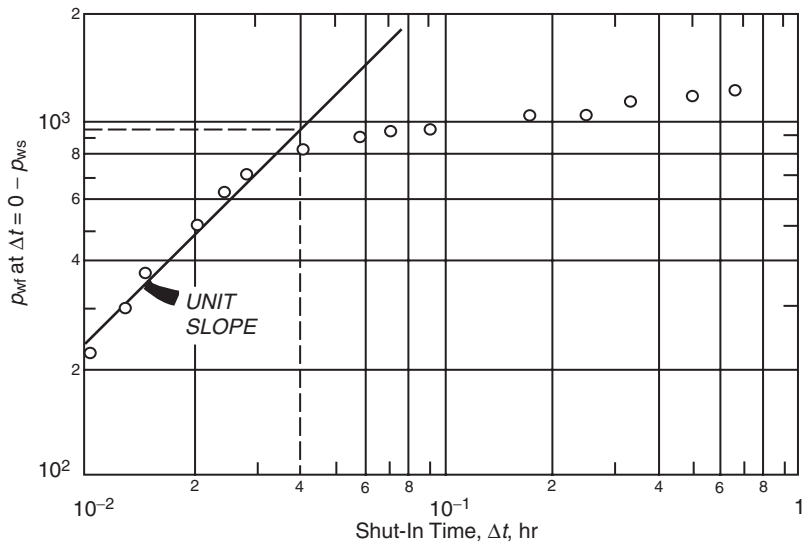

Figure 1.124 *Log–log data plot for a falloff test after brine injection, Example 1.48 (After Earlougher, R. Advances in Well Test Analysis) (Permission to publish by the SPE, copyright SPE, 1977).*

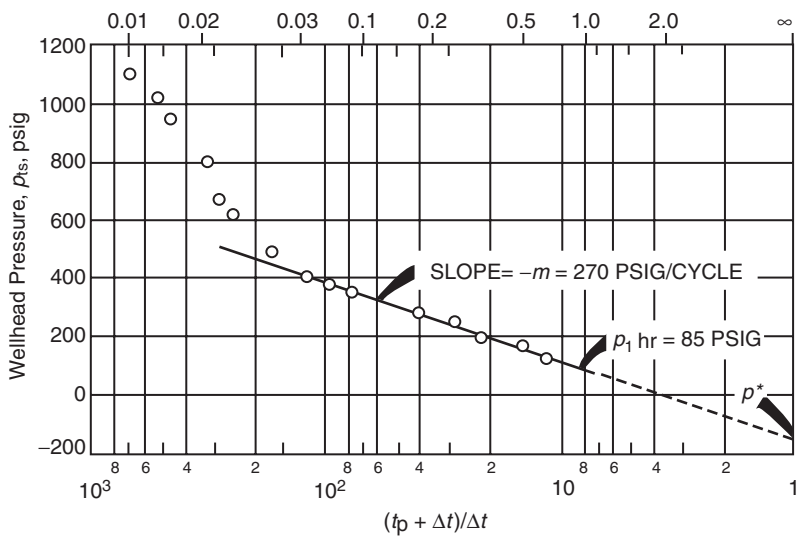

Figure 1.125 *Horner plot of pressure falloff after brine injection, Example 1.48.*

This is the false pressure at the wellhead, i.e., the surface. Using the hydrostatic gradient of 0.4685 psi/ft and the depth of 4819 ft, the reservoir false pressure is:

$$p^* = (4819)(0.4685) - 151 = 2107 \text{ psig}$$

and since injection time t_p is short compared with the shut-in time, we can assume that:

$$\bar{p} = p^* = 2107 \text{ psig}$$

Pressure falloff analysis in non-unit-mobility ratio systems

Figure 1.127 shows a plan view of the saturation distribution in the vicinity of an injection well. This figure shows two distinct zones.

Zone 1. represents the water bank with its leading edge at a distance of r_{f1} from the injection well. The mobility λ of the injected fluid in this zone, i.e., zone 1, is defined as the ratio of effective permeability of the injected fluid at its average saturation to its viscosity, or:

$$\lambda_1 = (k/\mu)_1$$

Zone 2. represents the oil bank with the leading edge at a distance of r_{f2} from the injection well. The mobility λ of the oil bank in this zone, i.e., zone 2, is defined as the ratio of oil effective permeability as evaluated at initial or connate water saturation to its viscosity, or:

$$\lambda_2 = (k/\mu)_2$$

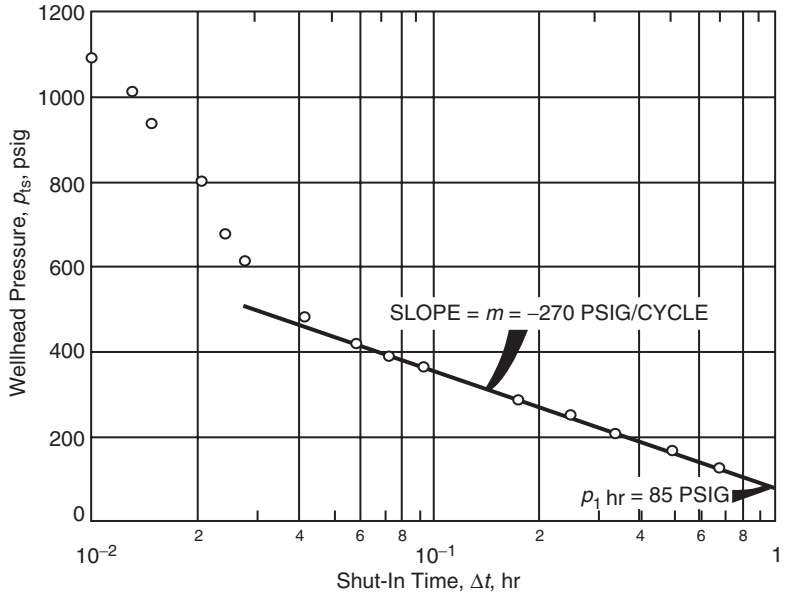

Figure 1.126 *Miller–Dyes–Hutchinson plot of pressure falloff after brine injection, Example 1.48.*

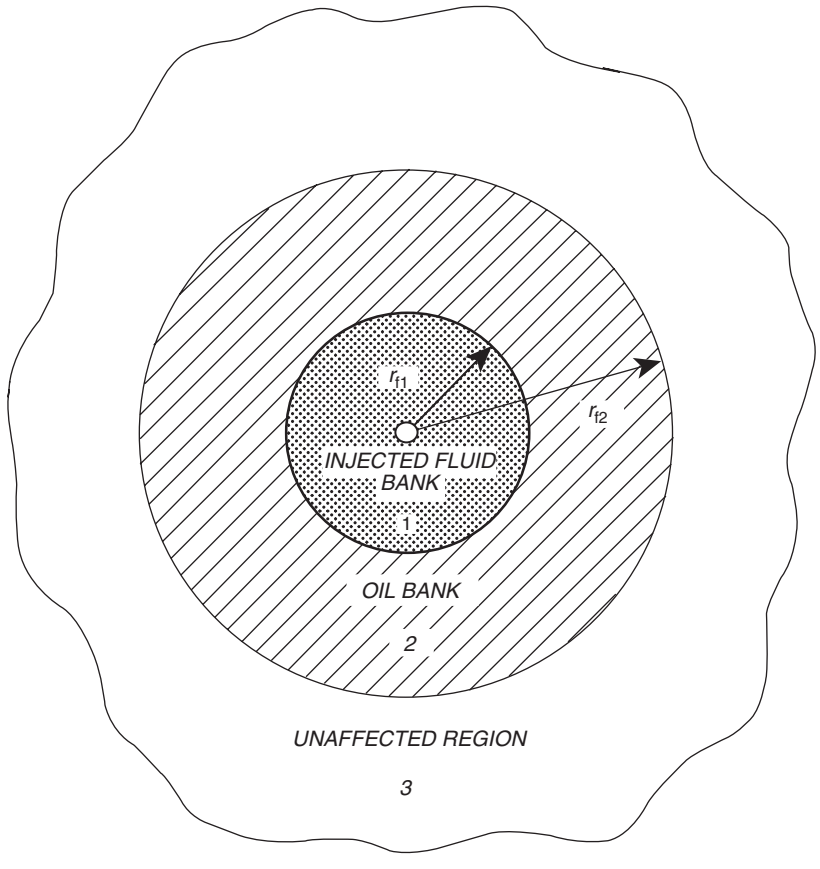

Figure 1.127 *Schematic diagram of fluid distribution around an injection well (composite reservoir).*

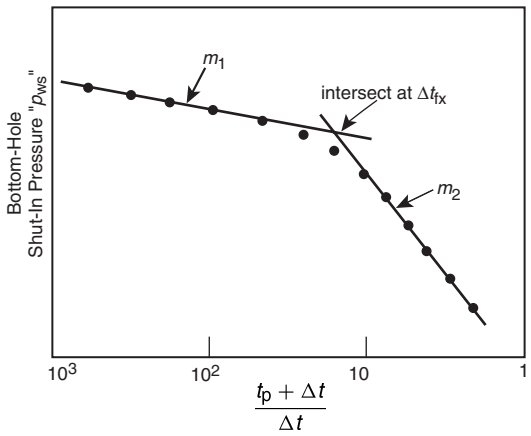

Figure 1.128 *Pressure falloff behavior in a two-bank system.*

The assumption of a two-bank system is applicable if the reservoir is filled with liquid or if the maximum shut-in time of the falloff test is such that the radius of investigation of the test does not exceed the outer radius of the oil bank. The ideal behavior of the falloff test in a two-bank system as expressed in terms of the Horner plot is illustrated in Figure 1.128.

Figure 1.128 shows two distinct straight lines with slopes of m_1 and m_2, that intersect at Δt_{fx}. The slope m_1 of the first line is used to estimate the effective permeability to water k_w in the flooded zone and the skin factor s. It is commonly believed that the slope of the second line m_2 will yield the mobility of the oil bank λ_o. However, Merrill et al. (1974) pointed out that the slope m_2 can be used only to determine the oil zone mobility if $r_{f2} > 10r_{f1}$ and $(\phi c_t)_1 = (\phi c_t)_2$, and developed a technique that can be used to determine the distance r_{f1} and mobility of each bank. The technique requires knowing the values of (ϕc_t) in the first and second zone, i.e., $(\phi c_t)_1$ and $(\phi c_t)_2$. The authors proposed the following expression:

$$\lambda = \frac{k}{\mu} = \frac{162.6QB}{m_2 h}$$

The authors also proposed two graphical correlations, as shown in Figures 1.129 and 1.130, that can be used with the Horner plot to analyze the pressure falloff data.

The proposed technique is summarized by the following:

Step 1. Plot Δp vs. Δt on a log–log scale and determine the end of the wellbore storage effect.

Step 2. Construct the Horner plot or the MDH plot and determine m_1, m_2, and Δt_{fx}.

Step 3. Estimate the effective permeability in the first zone, i.e., injected fluid invaded zone, "zone 1," and the skin factor from:

$$k_1 = \frac{162.6 q_{inj} B\mu}{|m_1| h} \qquad [1.7.9]$$

$$s = 1.513\left[\frac{p_{wf \text{ at } \Delta t=0} - p_{1 \text{ hr}}}{|m_1|} - \log\left(\frac{k_1}{\phi\mu_1 (c_t)_1 r_w^2}\right) + 3.2275\right]$$

where the subscript "1" denotes zone 1, the injected fluid zone.

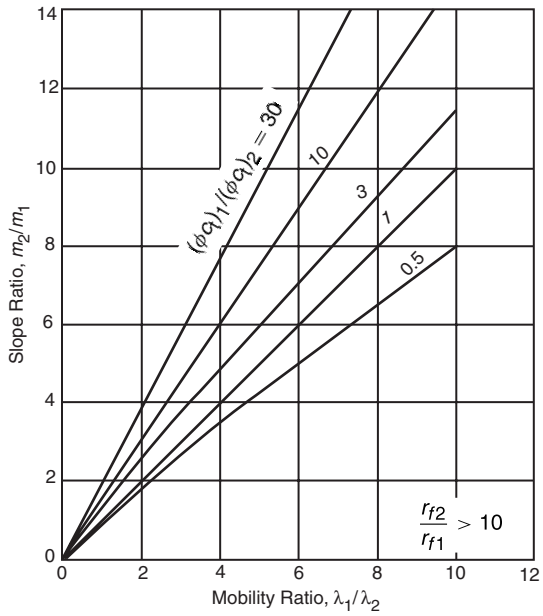

Figure 1.129 *Relationship between mobility ratio, slope ratio, and storage ratio. (After Merrill, et al. 1974).*

Step 4. Calculate the following dimensionless ratios:

$$\frac{m_2}{m_1} \quad \text{and} \quad \frac{(\phi c_t)_1}{(\phi c_t)_2}$$

with the subscripts "1" and "2" denoting zone 1 and zone 2 respectively.

Step 5. Use Figure 1.129 with the two dimensionless ratios of step 4 and read the mobility ratio λ_1/λ_2.

Step 6. Estimate the effective permeability in the second zone from the following expression:

$$k_2 = \left(\frac{\mu_2}{\mu_1}\right)\frac{k_1}{\lambda_1/\lambda_2} \qquad [1.7.10]$$

Step 7. Obtain the dimensionless time Δt_{Dfx} from Figure 1.130.

Step 8. Calculate the distance to the leading edge of the injected fluid bank r_{f1} from:

$$r_{f1} = \sqrt{\left[\frac{0.0002637(k/\mu)_1}{(\phi c_t)_1}\right]\left(\frac{\Delta t_{fx}}{\Delta t_{Dfx}}\right)} \qquad [1.7.11]$$

To illustrate the technique, Merrill et al. (1974) presented the following example.

Example 1.49 Figure 1.131 shows the MDH semilog plot of simulated falloff data for a two-zone water flood with no apparent wellbore storage effects. Data used in the simulation is given below:

$r_w = 0.25$ ft, $h = 20$ ft, $r_{f1} = 30$ ft

$r_{f2} = r_e = 3600$ ft, $(k/\mu)_1 = \eta_1 = 100$ md/cp

$(k/\mu)_2 = \eta_2 = 50$ md/cp, $(\phi c_t)_1 = 8.95 \times 10^{-7}$ psi^{-1}

$(\phi c_t)_2 = 1.54 \times 10^{-6}$ psi^{-1}, $q_{inj} = 400$ STB/day

$B_w = 1.0$ bbl/STB

Calculate λ_1, λ_2, and r_{f1} and compare with the simulation data.

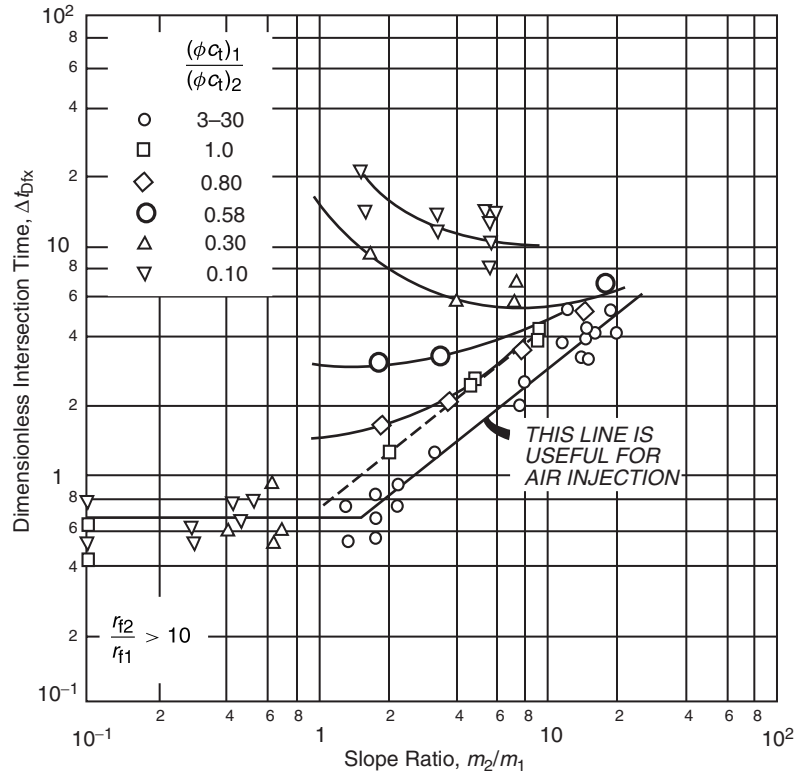

Figure 1.130 *Correlation of dimensionless intersection time, Δt_{Dfx}, for falloff data from a two-zone reservoir. (After Merrill et al.1974).*

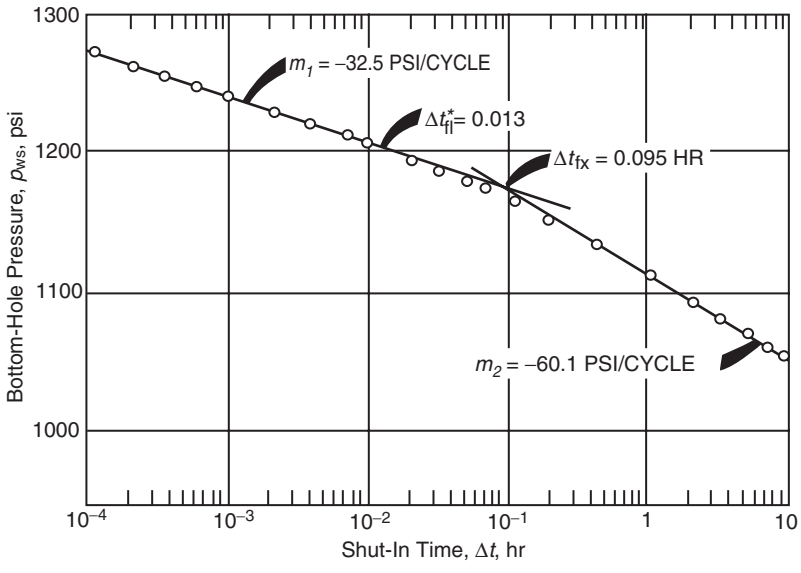

Figure 1.131 *Falloff test data for Example 1.49. (After Merrill et al. 1974).*

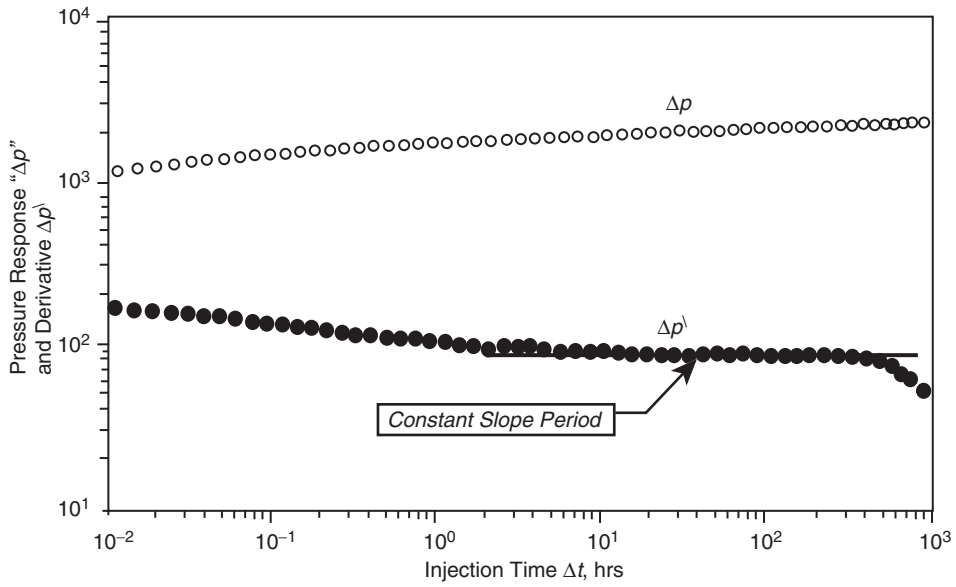

Figure 1.132 *Injection pressure response and derivative (base case).*

Solution

Step 1. From Figure 1.131, determine m_1, m_2, and Δt_{fx} to give:

$$m_1 = 32.5 \text{ psi/cycle}$$

$$m_2 = 60.1 \text{ psi/cycle}$$

$$\Delta t_{fx} = 0.095 \text{ hour}$$

Step 2. Estimate $(k/\mu)_1$, i.e., mobility of water bank, from Equation 1.7.9:

$$\left(\frac{k}{\mu}\right)_1 = \frac{162.6 q_{inj} B}{|m_1| h} = \frac{162.6(400)(1.0)}{(32.5)(20)}$$

$$= 100 \text{ md/cp}$$

The value matches the value used in the simulation.

Step 3. Calculate the following dimensionless ratios:

$$\frac{m_2}{m_1} = \frac{-60.1}{-32.5} = 1.85$$

$$\frac{(\phi c_t)_1}{(\phi c_t)_2} = \frac{8.95 \times 10^{-7}}{1.54 \times 10^{-6}} = 0.581$$

Step 4. Using the two dimensionless ratios as calculated in step 4, determine the ratio λ_1/λ_2 from Figure 1.129:

$$\frac{\lambda_1}{\lambda_2} = 2.0$$

Step 5. Calculate the mobility in the second zone, i.e., oil bank mobility $\lambda_2 = (k/\mu)_2$, from Equation 1.7.10:

$$\left(\frac{k}{\mu}\right)_2 = \frac{(k/\mu)_1}{(\lambda_1/\lambda_2)} = \frac{100}{2.0} = 50 \text{ md/cp}$$

with the exact match of the input data.

Step 6. Determine Δt_{Dfx} from Figure 1.130:

$$\Delta t_{Dfx} = 3.05$$

Step 7. Calculate r_{f1} from Equation 1.7.11:

$$r_{f1} = \sqrt{\frac{(0.0002637)(100)(0.095)}{(8.95 \times 10^{-7})(3.05)}} = 30 \text{ ft}$$

Yeh and Agarwal (1989) presented a different approach of analyzing the recorded data from the injectivity and falloff tests. Their methodology uses the pressure derivate $\Delta p'$ and Agarwal equivalent time Δt_e (see Equation 1.4.16) in performing the analysis. The authors defined the following nomenclature:

During the injectivity test period:

$$\Delta p_{wf} = p_{wf} - p_i$$

$$\Delta p'_{wf} = \frac{d(\Delta p_{wf})}{d(\ln t)}$$

where:

p_{wf} = bottom-hole pressure at time t during injection, psi
t = injection time, hours
$\ln t$ = natural logarithm of t

During the falloff test period:

$$\Delta p_{ws} = p_{wf \text{ at } \Delta t=0} - p_{ws}$$

$$\Delta p'_{ws} = \frac{d(\Delta p_{ws})}{d(\ln \Delta te)}$$

with:

$$\Delta t_e = \frac{t_p \Delta t}{t_p + \Delta t}$$

where:

Δt = shut-in time, hours
t_p = injection time, hours

Through the use of a numerical simulator, Yeh and Agarwal simulated a large number of injectivity and falloff tests and made the following observations for both tests:

Pressure behavior during injectivity tests

(1) A log–log plot of the injection pressure difference Δp_{wf} and its derivative $\Delta p'_{wf}$ versus injection time will exhibit a constant-slope period, as shown in Figure 1.132, and designated as $(\Delta p'_{wf})_{const}$. The water mobility λ_1 in

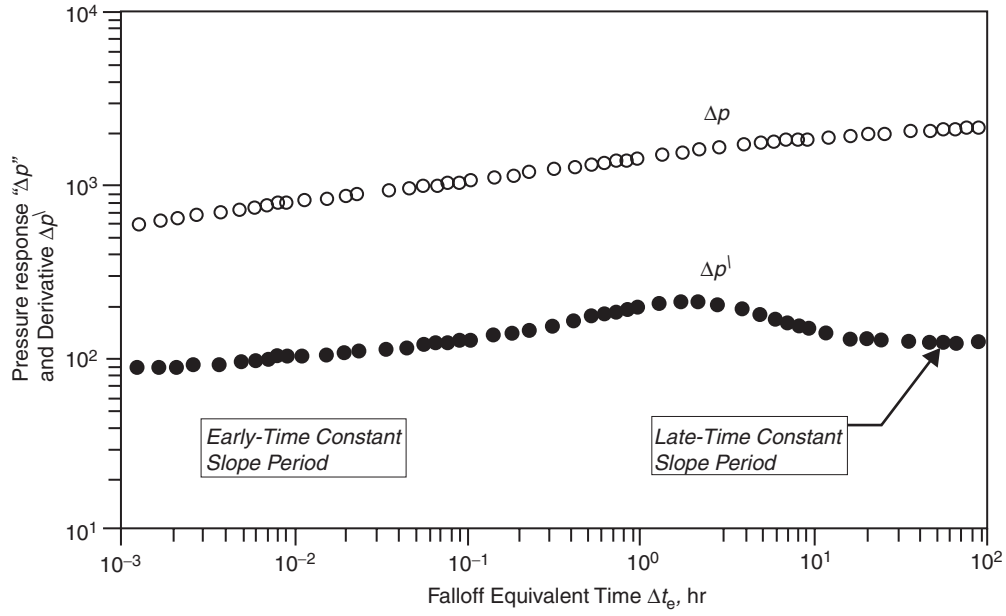

Figure 1.133 *Falloff pressure response and derivative (base case).*

the floodout zone, i.e., water bank, can be estimated from:

$$\lambda_1 = \left(\frac{k}{\mu}\right)_1 = \frac{70.62 q_{inj} B}{h(\Delta p'_{wf})_{const}}$$

Notice that the constant 70.62 is used instead of 162.6 because the pressure derivative is calculated with respect to the natural logarithm of time.

(2) The skin factor as calculated from the semilog analysis method is usually in excess of its true value because of the contrast between injected and reservoir fluid properties.

Pressure behavior during falloff tests

(1) The log–log plot of the pressure falloff response in terms of Δp and its derivative as a function of the falloff equivalent time Δt_e is shown in Figure 1.133. The resulting derivative curve shows two constant-slope periods, $(\Delta p'_{ws})_1$ and $(\Delta p'_{ws})_2$, which reflect the radial flow in the floodout zone, i.e., water bank, and, the radial flow in the unflooded zone, i.e., oil bank.

These two derivative constants can be used to estimate the mobility of the water bank λ_1 and the oil bank λ_2 from:

$$\lambda_1 = \frac{70.62 q_{inj} B}{h(\Delta p'_{ws})_1}$$

$$\lambda_2 = \frac{70.62 q_{inj} B}{h(\Delta p'_{ws})_2}$$

(2) The skin factor can be estimated from the first semilog straight line and closely represents the actual mechanical skin on the wellbore.

1.7.3 Step-rate test

Step-rate injectivity tests are specifically designed to determine the pressure at which fracturing could be induced in the reservoir rock. In this test, water is injected at a constant rate for about 30 minutes before the rate is increased and maintained for successive periods, each of which also lasts for 30 minutes. The pressure observed at the end of each injection rate is plotted versus the rate. This plot usually shows two straight lines which intersect at the fracture pressure of the formation, as shown schematically in Figure 1.134. The suggested procedure is summarized below:

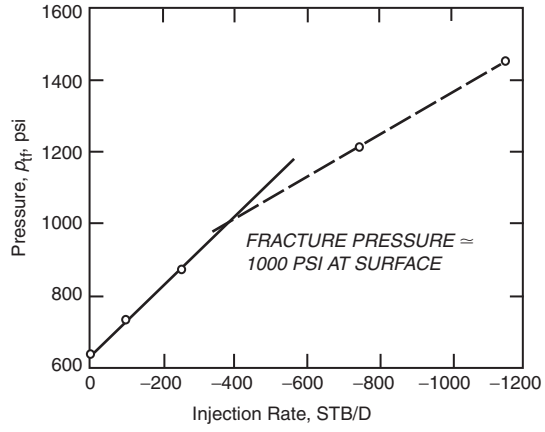

Figure 1.134 *Step-rate injectivity data plot.*

Step 1. Shut in the well and allow the bottom-hole pressure to stabilize (if shutting in the well is not possible, or not practical, stabilize the well at a low flow rate). Measure the stabilized pressure.

Step 2. Open the well at a low injection rate and maintain this rate for a preset time. Record the pressure at the end of the flow period.

Step 3. Increase the rate, and at the end of an interval of time equal to that used in step 2, again record the pressure.

Step 4. Repeat step 3 for a number of increasing rates until the parting pressure is noted on the step-rate plot depicted by Figure 1.134.

As pointed out by Horn (1995), data presented in graphical form is much easier to understand than a single table of numbers. Horn proposed the following "toolbox" of graphing functions that is considered an essential part of computer-aided well test interpretation system:

Flow period	*Characteristic*	*Plot used*
Infinite-acting radial flow drawdown)	Semilog straight line	p vs. log Δt (semilog plot, sometimes called MDH plot)
Infinite-acting radial flow (buildup)	Horner straight line	p vs. $\log(t_p + \Delta t)/\Delta t$ (Horner plot)
Wellbore storage	Straight line p vs. t, or unit-slope log Δp vs. log Δt	log Δp vs. log Δt (log–log plot, type curve)
Finite conductivity fracture	Straight-line slope $\frac{1}{4}$, log Δp vs. log Δt plot	log Δp vs. log Δt, or Δp vs. $\Delta t^{1/4}$
Infinite conductivity fracture	Straight-line slope $\frac{1}{2}$, log Δp vs. log Δt plot	log Δp vs. log Δt, or Δp vs. $\Delta t^{1/2}$
Dual-porosity behavior	S-shaped transition between parallel semilog straight lines	p vs. log Δt (semilog plot)
Closed boundary	Pseudosteady state, pressure linear with time	p vs. Δt (Cartesian plot)
Impermeable fault	Doubling of slope on semilog straight line	p vs. log Δt (semilog plot)
Constant-pressure boundary	Constant pressure, flat line on all p, t plots	Any

Chaudhry (2003) presented another useful "toolbox" that summarizes the pressure derivative trends for common flow regimes that have been presented in this chapter, as shown in Table 1-10.

Kamal et al. (1995) conveniently summarized; in tabulated form, various plots and flow regimes most commonly used in transient tests and the information obtained from each test as shown in Tables 1-11 and 1-12.

Table 1.10 *Pressure Derivative Trends for Common Flow Regimes.*

Wellbore storage dual-porosity matrix to fissure flow	Semilog straight lines with slope 1.151 Parallel straight-line responses are characteristics of naturally fractured reservoirs
Dual porosity with pseudosteady-state interporosity flow	Pressure change slope → increasing, leveling off, increasing Pressure derivative slope = 0, valley = 0 Additional distinguishing characteristic is middle-time valley trend during more than 1 log cycle
Dual porosity with transient interporosity flow	Pressure change slope → steepening Pressure derivative slope = 0, upward trend = 0 Additional distinguishing characteristic → middle-time slope doubles
Pseudosteady state	Pressure change slope → for drawdown and zero for buildup Pressure derivative slope → for drawdown and steeply descending for buildup Additional distinguishing characteristic → late time drawdown pressure change and derivative are overlain; slope of 1 occurs much earlier in the derivative
Constant-pressure boundary (steady state)	Pressure change slope → 0 Pressure derivative slope → steeply descending Additional distinguishing characteristic → cannot be distinguished from psuedosteady state in pressure buildup test
Single sealing fault (pseudoradial flow)	Pressure change slope → steeping Pressure derivative slope → 0, upward trend → 0 Additional distinguishing characteristic → late-time slope doubles
Elongated reservoir linear flow	Pressure change slope → 0.5 Pressure derivative slope → 0.5 Additional distinguishing characteristic → late-time pressure change and derivative are offset by factor of 2; slope of 0.5 occurs much earlier in the derivative
Wellbore storage infinite-acting radial flow	Pressure change slope = 1, pressure derivative slope = 1 Additional distinguishing characteristics are: early time pressure change, and derivative are overlain
Wellbore storage, partial penetration, infinite-acting radial flow	Pressure change increases and pressure derivative slope = 0 Additional distinguishing characteristic is: middile-time flat derivative
Linear flow in an infinite conductivity vertical fracture	$K(x_f)^2$ → calculate from specialized plot Pressure slope = 0.5 and pressure derivative slope = 0.5 Additional distinguishing characteristics are: early-time pressure change and the derivative are offset by a factor of 2
Bilinear flow to an infinite conductivity vertical fracture	$K_f w$ → calculate from specialized plot Pressure slope = 0.25 and pressure derivative slope = 0.25 Additional distinguishing characteristic are: early-time pressure change and derivative are offset by factor of 4

(continued)

Table 1.10 *Pressure Derivative Trends for Common Flow Regimes (continued)*

Wellbore storage infinite acting radial flow	Sealing fault
Wellbore storage	No flow boundary
Wellbore storage linear flow	$Kb^2 \rightarrow$ calculate from specialized plot

Table 1.11 *Reservoir properties obtainable from various transient tests (After Kamal et al. 1995).*

Drill item tests	Reservoir behavior	Step-rate tests	Formation parting pressure
	Permeability		Permeability
	Skin		Skin
	Fracture length	Falloff tests	Mobility in various banks
	Reservoir pressure		Skin
	Reservoir limit		Reservoir pressure
	Boundaries		Fracture length
Repeat/multiple-formation tests	Pressure profile		Location of front
			Boundaries
Drawdown tests	Reservoir behavior	Interference and pulse tests	Communication between wells
	Permeability		
	Skin		Reservoir type behavior
	Fracture length		Porosity
	Reservoir limit		Interwell permeability
	Boundaries		Vertical permeability
Buildup tests	Reservoir behavior	Layered reservoir tests	Properties of individual layers
	Permeability		Horizontal permeability
	Skin		Vertical permeability
	Fracture length		Skin
	Reservoir pressure		Average layer pressure
	Boundaries		Outer Boundaries

Table 1.12 *Plots and flow regimes of transient tests (After Kamal et al. 1995)*

	Plot				
Flow regime	*Cartesian*	$\sqrt{\Delta t}$	$\sqrt[4]{\Delta t}$	*Log–log*	*Semilog*
Wellbore storage	Straight line Slope $\rightarrow C$ Intercept $\rightarrow \Delta t_c$ Δp_c			Unit slope on Δp and $p\backslash$ Δp and $p\backslash$ coincide	Positive s Negative s
Linear flow		Straight line Slope $= m_f \rightarrow l_f$ Intercept = fracture damage		Slope $= \frac{1}{2}$ on $p\backslash$ and on Δp if $s = 0$ Slope $< \frac{1}{2}$ on Δp if $s \neq 0$ $p\backslash$ at half the level of Δp	
Bilinear flow			Straight line Slope $= m_{bf} \rightarrow C_{fd}$	Slope $= \frac{1}{4}$ $p\backslash$ at $\frac{1}{4}$ level of Δp	
First IARF [a] (high-k layer, fractures)	Decreasing slope			$p\backslash$ horizontal at $p\backslash_D = 0.5$	Straight line Slope $= m \rightarrow kh$ $\Delta p_{1\ hr} \rightarrow s$
Transition	More decreasing slope			$\Delta p = \lambda e^{-2s}$ or $B\backslash$ $p\backslash_D = 0.25$ (transition) $=< 0.25$ (pseudo-steady state)	Straight line Slope $= m/2$ (transition) $= 0$ (pseudo-steady state)
Second IARF (total system)	Similar slope to first IARF			$p\backslash$ horizontal at $p\backslash_D = 0.5$	Straight line Slope $= m \rightarrow kh, p^*$ $\Delta p_{1\ hr} \rightarrow s$
Single no-flow boundary				$p\backslash$ horizontal at $p\backslash_D = 1.0$	Straight line Slope $= 2m$ Intersection with IARF$\rightarrow$distance to boundary
Outer no-flow boundaries (drawdown test only)	Straight line Slope $= m^* \rightarrow \phi Ah$ $p_{int} \rightarrow C_A$			Unit slope for Δp and $p\backslash$ Δp and $p\backslash$ coincide	Increasing slope

[a] IARF = Infinite-Acting Radial Flow.

Problems

1. An incompressible fluid flows in a linear porous media with the following properties.

   $L = 2500$ ft, $h = 30$ ft, width $= 500$ ft, $k = 50$ md,
   $\phi = 17\%$, $\mu = 2$ cp, inlet pressure $= 2100$ psi,
   $Q = 4$ bbl/day, $\rho = 45$ lb/ft^3

   Calculate and plot the pressure profile throughout the linear system.
2. Assume the reservoir linear system as described in problem 1 is tilted with a dip angle of 7°. Calculate the fluid potential through the linear system.
3. A gas of 0.7 specific gravity is flowing in a linear reservoir system at 150°F. The upstream and downstream pressures are 2000 and 1800 psi, respectively. The system has the following properties:

   $L = 2000$ ft, $W = 300$ ft, $h = 15$ ft
   $k = 40$ md, $\phi = 15\%$

   Calculate the gas flow rate.
4. An oil well is producing a crude oil system at 1000 STB/day and 2000 psi of bottom-hole flowing pressure. The pay zone and the producing well have the following characteristics.

   $h = 35$ ft, $r_w = 0.25$ ft, drainage area $= 40$ acres
   API $= 45°$, $\gamma_g = 0.72$, $R_s = 700$ scf/STB
   $k = 80$ md

   Assuming steady-state flowing conditions, calculate and plot the pressure profile around the wellbore.
5. Assuming steady-state flow and an incompressible fluid, calculate the oil flow rate under the following conditions:

   $p_e = 2500$ psi, $p_{wf} = 2000$ psi, $r_e = 745$ ft
   $r_w = 0.3$ ft, $\mu_o = 2$ cp, $B_o = 1.4$ bbl/STB
   $h = 30$ ft, $k = 60$ md

6. A gas well is flowing under a bottom-hole flowing pressure of 900 psi. The current reservoir pressure is 1300 psi. The following additional data is available:

   $T = 140°$F, $\gamma_g = 0.65$, $r_w = 0.3$ ft
   $k = 60$ md, $h = 40$ ft, $r_e = 1000$ ft

   Calculate the gas flow rate by using

   (a) the real-gas pseudopressure approach;
   (b) the pressure-squared method.
7. After a period of shut-in of an oil well, the reservoir pressure has stabilized at 3200 psi. The well is allowed to flow at a constant flow rate of 500 STB/day under a transient flow condition. Given:

   $B_o = 1.1$ bbl/STB, $\mu_o = 2$ cp, $c_t = 15 \times 10^{-6}$ psi^{-1}
   $k = 50$ md, $h = 20$ ft, $\phi = 20\%$
   $r_w = 0.3$ ft, $p_i = 3200$ psi

   calculate and plot the pressure profile after 1, 5, 10, 15, and 20 hours.
8. An oil well is producing at a constant flow rate of 800 STB/day under a transient flow condition. The following data is available:

   $B_o = 1.2$ bbl/STB, $\mu_o = 3$ cp, $c_t = 15 \times 10^{-6}$ psi^{-1}
   $k = 100$ md, $h = 25$ ft, $\phi = 15\%$
   $r_w = 0.5$, $p_i = 4000$ psi,

   Using the Ei function approach and the p_D method, calculate the bottom-hole flowing pressure after 1, 2, 3, 5, and 10 hours. Plot the results on a semilog scale and Cartesian scale.
9. A well is flowing under a drawdown pressure of 350 psi and produces at a constant flow rate of 300 STB/day. The net thickness is 25 ft. Given:

   $r_e = 660$ ft, $r_w = 0.25$ ft
   $\mu_o = 1.2$ cp, $B_o = 1.25$ bbl/STB

   calculate:

   (a) the average permeability;
   (b) the capacity of the formation.
10. An oil well is producing from the center of a 40 acre square drilling pattern. Given:

    $\phi = 20\%$, $h = 15ft$, $k = 60$ md
    $\mu_o = 1.5$ cp, $B_o = 1.4$ bbl/STB, $r_w = 0.25$ ft
    $p_i = 2000$ psi, $p_{wf} = 1500$ psi

    calculate the oil flow rate.
11. A shut-in well is located at a distance of 700 ft from one well and 1100 ft from a second well. The first well flows for 5 days at 180 STB/day, at which time the second well begins to flow at 280 STB/day. Calculate the pressure drop in the shut-in well when the second well has been flowing for 7 days. The following additional data is given:

    $p_i = 3000$ psi, $B_o = 1.3$ bbl/STB, $\mu_o = 1.2$ cp,
    $h = 60$ ft, $c_t = 15 \times 10^{-6}$ psi^{-1}, $\phi = 15\%$, $k = 45$ md
12. A well is opened to flow at 150 STB/day for 24 hours. The flow rate is then increased to 360 STB/day and lasts for another 24 hours. The well flow rate is then reduced to 310 STB/day for 16 hours. Calculate the pressure drop in a shut-in well 700 ft away from the well, given:

    $\phi = 15\%$, $h = 20$ ft, $k = 100$ md
    $\mu_o = 2$ cp, $B_o = 1.2$ bbl/STB, $r_w = 0.25$ ft
    $p_i = 3000$ psi, $c_t = 12 \times 10^{-6}$ psi^{-1}

13. A well is flowing under unsteady-state flowing conditions for 5 days at 300 STB/day. The well is located at 350 ft and 420 ft distance from two sealing faults. Given:

    $\phi = 17\%$, $c_t = 16 \times 10^{-6}$ psi^{-1}, $k = 80$ md
    $p_i = 3000$ psi, $B_o = 1.3$ bbl/STB, $\mu_o = 1.1$ cp
    $r_w = 0.25$ ft, $h = 25$ ft

    calculate the pressure in the well after 5 days.
14. A drawdown test was conducted on a new well with results as given below:

t (hr)	p_{wf} (psi)
1.50	2978
3.75	2949
7.50	2927
15.00	2904
37.50	2876
56.25	2863
75.00	2848
112.50	2810
150.00	2790
225.00	2763

Given:

$p_i = 3400$ psi, $h = 25$ ft, $Q = 300$ STB/day
$c_t = 18 \times 10^{-6}$ psi^{-1}, $\mu_o = 1.8$ cp,
$B_o = 1.1$ bbl/STB, $r_w = 0.25$ ft, $\phi = 12\%$,

and assuming no wellbore storage, calculate:

(a) the average permeability;
(b) the skin factor.

15. A drawdown test was conducted on a discovery well. The well was allowed to flow at a constant flow rate of 175 STB/day. The fluid and reservoir data is given below:

$S_{wi} = 25\%$, $\phi = 15\%$, $h = 30$ ft, $c_t = 18 \times 10^{-6}$ psi^{-1}
$r_w = 0.25$ ft, $p_i = 4680$ psi, $\mu_o = 1.5$ cp,
$B_o = 1.25$ bbl/STB

The drawdown test data is given below:

t (hr)	p_{wf} (psi)
0.6	4388
1.2	4367
1.8	4355
2.4	4344
3.6	4334
6.0	4318
8.4	4309
12.0	4300
24.0	4278
36.0	4261
48.0	4258
60.0	4253
72.0	4249
84.0	4244
96.0	4240
108.0	4235
120.0	4230
144.0	4222
180.0	4206

Calculate:

(a) the drainage area;
(b) the skin factor;
(C) the oil flow rate at a bottom-hole flowing pressure of 4300 psi, assuming a semisteady-state flowing conditions.

16. A pressure buildup test was conducted on a well that had been producing at 146 STB/day for 53 hours. The reservoir and fluid data is given below.

$B_o = 1.29$ bbl/STB, $\mu_o = 0.85$ cp,
$c_t = 12 \times 10^{-6}$ psi^{-1}, $\phi = 10\%$, $p_{wf} = 1426.9$ psig,
$A = 20$ acres

The buildup data is as follows:

Time	p_{ws} (psig)
0.167	1451.5
0.333	1476.0
0.500	1498.6
0.667	1520.1
0.833	1541.5
1.000	1561.3
1.167	1581.9
1.333	1599.7
1.500	1617.9
1.667	1635.3
2.000	1665.7
2.333	1691.8
2.667	1715.3
3.000	1736.3
3.333	1754.7
3.667	1770.1
4.000	1783.5
4.500	1800.7
5.000	1812.8
5.500	1822.4
6.000	1830.7
6.500	1837.2
7.000	1841.1
7.500	1844.5
8.000	1846.7
8.500	1849.6
9.000	1850.4
10.000	1852.7
11.000	1853.5
12.000	1854.0
12.667	1854.0
14.620	1855.0

Calculate:

(a) the average reservoir pressure;
(b) the skin factor;
(c) the formation capacity;
(d) an estimate of the drainage area and compare with the given value.